AD-A018 844

NON-DESTRUCTIVE INSPECTION PRACTICES. VOLUME II

Enrico Bolis

Advisory Group for Aerospace Research and Development

Prepared for:

North Atlantic Treaty Organization

October 1975

AGARD-AG-201-VOL.II

AGARD-AG-201-VOL.II

ADVISORY GROUP FOR AEROSPACE RESEARCH & DEVELOPMENT

AGARDograph No 201

on

Non-Destructive Inspection Practices

Edited by
E Bolis

Volume II

NORTH ATLANTIC TREATY ORGANIZATION

AGARD-AG-201
Volume II

NORTH ATLANTIC TREATY ORGANISATION

ADVISORY GROUP FOR AEROSPACE RESEARCH AND DEVELOPMENT

(ORGANISATION DU TRAITE DE L'ATLANTIQUE NORD)

AGARDograph No.201

NON-DESTRUCTIVE INSPECTION PRACTICES

Edited by

Enrico Bolis

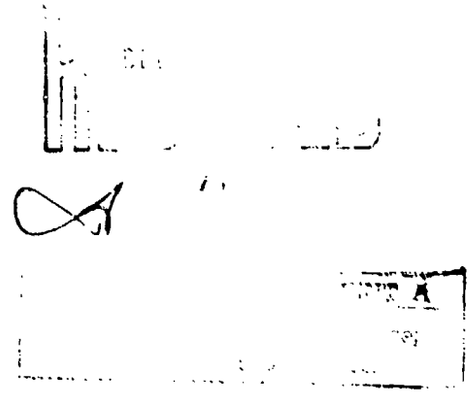

Published in two volumes

VOLUME II

This AGARDograph was sponsored by the Structures and Materials Panel of AGARD.

THE MISSION OF AGARD

The mission of AGARD is to bring together the leading personalities of the NATO nations in the fields of science and technology relating to aerospace for the following purposes:

Exchanging of scientific and technical information;

Continuously stimulating advances in the aerospace sciences relevant to strengthening the common defence posture;

Improving the co-operation among member nations in aerospace research and development;

Providing scientific and technical advice and assistance to the North Atlantic Military Committee in the field of aerospace research and development;

Rendering scientific and technical assistance, as requested, to other NATO bodies and to member nations in connection with research and development problems in the aerospace field;

Providing assistance to member nations for the purpose of increasing their scientific and technical potential;

Recommending effective ways for the member nations to use their research and development capabilities for the common benefit of the NATO community.

The highest authority within AGARD is the National Delegates Board consisting of officially appointed senior representatives from each member nation. The mission of AGARD is carried out through the Panels which are composed of experts appointed by the National Delegates, the Consultant and Exchange Program and the Aerospace Applications Studies Program. The results of AGARD work are reported to the member nations and the NATO Authorities through the AGARD series of publications of which this is one.

Participation in AGARD activities is by invitation only and is normally limited to citizens of the NATO nations.

Published October 1975

620.179.1:629.73.083.02

Set and printed by Technical Editing and Reproduction Ltd
Harford House, 7–9 Charlotte St, London, W1P 1HD

CONTENTS

VOLUME I

		Page / Reference
PREFACE		iii
LIST OF CONTRIBUTORS		iv
FOREWORD		vi
1. INTRODUCTION		
Chapter 1.1	PHILOSOPHY OF NON-DESTRUCTIVE INSPECTION by E.Bolis	1
Chapter 1.2	BASIC CONCEPTS IN FRACTURE MECHANICS by J.Eftis, D.L.Jones and H.Liebowitz)	11
Chapter 1.3	DESIGN FOR INSPECTION AND PLANNING FOR MAINTENANCE OF STRUCTURAL INTEGRITY by H.Tyrer	27
Chapter 1.4	STANDARDS OF ACCEPTANCE BY NON-DESTRUCTIVE INSPECTION FOR RAW MATERIALS AND COMPONENTS by H.F.Campbell	55
2. GENERAL TOPICS		
Chapter 2.1	SURVEY OF PROBLEMS by R.J.Schliekelmann	83
Chapter 2.2	CRITICAL SURVEY OF METHODS by E.J. Van der Schee and P.F.A.Bijlmer	91
Chapter 2.3	QUALIFICATION OF PERSONNEL by R.Hilverdink	129
3. METHODS		
Chapter 3.1	3.1.1 MAGNETIC PARTICLE INSPECTION 3.1.2 LIQUID PENETRANT INSPECTION by G.Magistrali	141 169
Chapter 3.2	EDDY CURRENT NDI IN AIRLINE MAINTENANCE by M. Van Averbeke	181
Chapter 3.3	X-RADIOGRAPHY by A. De Sterke ANNEX: RADIATION SAFETY by A.H.A.M.Röpke	229 260
Chapter 3.4	X-RAY DIFFRACTION by A.Tronca	269
Chapter 3.5	GAMMAGRAPHY IN AIRLINE MAINTENANCE by M. Van Averbeke	293
Chapter 3.6	ULTRASONIC AND ACOUSTIC METHODS by K.G.Walther	331

		Reference
Chapter 3.7	DETECTION AND DETERMINATION OF FLAW SIZE BY ACOUSTIC EMISSION by C.E.Hartbower	387
Chapter 3.8	LIQUID CRYSTAL AND NEUTRON RADIOGRAPHY METHODS by S.P.Brown	449
Chapter 3.9	HOLOGRAPHIC METHODS by E.Maddux	459

VOLUME II

4. PROBLEMS

Chapter 4.1	THE NON-DESTRUCTIVE MEASUREMENT OF RESIDUAL STRESS by F.Rotvel	471
Chapter 4.2	NDI OF WELDING by G.Fenoglio and G.Magistrali	507
Chapter 4.3	NDI OF BONDED STRUCTURES by M.Tréca	529
Chapter 4.4	NDI OF COMPOSITE MATERIALS by W.L.Shelton	579
Chapter 4.5	DETECTION AND MEASUREMENT OF CORROSION BY NDI by A.R.Bond	593

5. APPENDIX

Chapter 5.1	SUBJECT INDEX	611
Chapter 5.2	CROSS REFERENCE TABLE SHOWING WHICH NDI METHODS MAY BE USED FOR INVESTIGATING VARIOUS TYPES OF DEFECTS	621
Chapter 5.3	NON-DESTRUCTIVE INSPECTION PROCEDURES, USAF (T.O. 1F 104A 36S 4/5)	625
Chapter 5.4	NON-DESTRUCTIVE TEST MANUAL, BOEING DOCUMENT D6 7170 REV. 14 MAR 15/74 (PART 4, 55-10-07; PART 6, 55-00-00)	643

CHAPTER 4.1

THE NON-DESTRUCTIVE MEASUREMENT OF RESIDUAL STRESSES

by

F.Rotvel

The Technical University of Denmark
Department of Solid Mechanics
Building 404
DK 2800 Lyngby, Denmark

CONTENTS

4.1.1 RESIDUAL STRESSES AND THEIR IMPORTANCE
- 4.1.1.1 Definition of Residual Stresses
- 4.1.1.2 Effect of Mean Stress on Fatigue Strength
- 4.1.1.3 Effect of Mean Stress on Stress Corrosion

4.1.2 PRINCIPLES OF RESIDUAL STRESS FORMATION
- 4.1.2.1 Plastic Deformation in Regions with Stress Gradients
- 4.1.2.2 Temperature Gradients
- 4.1.2.3 Chemical Expansion or Contraction of Surface Material
- 4.1.2.4 Electroplating

4.1.3 STABILITY OF RESIDUAL STRESSES IN SERVICE

4.1.4 MEASUREMENT OF STRESS BY X-RAYS
- 4.1.4.1 The Characteristics of the X-Ray Stress Measurement
- 4.1.4.2 The Physical Principle of the X-Ray Stress Measuring Method
- 4.1.4.3 The Film Method
- 4.1.4.4 The Diffractometer Method
- 4.1.4.5 Comparisons Between the Film and the Diffractometer Method
- 4.1.4.6 Experimental Factors Affecting Measuring Accuracy
- 4.1.4.7 The Measurement of Stress Versus Depth

4.1.5 SOME FUTURE NON-DESTRUCTIVE STRESS MEASURING METHODS
- 4.1.5.1 The Ultrasonic Stress Measuring Method
- 4.1.5.2 The Knoop Hardness Stress Measuring Method

THE NON-DESTRUCTIVE MEASUREMENT OF RESIDUAL STRESSES

F.Rotvel

4.1.1 RESIDUAL STRESSES AND THEIR IMPORTANCE

4.1.1.1 Definition of Residual Stresses

Residual stresses are defined as all stresses acting in a body when all surfaces are unloaded and body forces are absent. Resulting forces and moments on the body from residual stresses are zero. Residual stresses are divided into classes according to the range over which they are in equilibrium. In English literature it is a common practice to divide residual stresses into microstresses and macrostresses, microstresses being defined as stress systems which are in equilibrium over distances of the order of several grain diameters and down to atomic distances, while macro-stresses are in equilibrium over macroscopic distances. In German literature it has been common practice to use a still finer division for microstresses, as illustrated in Figure 1 (taken from Reference 1). Stresses which are in equilibrium over several grain diameters are called stresses of the 2nd kind. Stresses which are in equilibrium within the grains are called stresses of the 3rd kind, and stresses which are in equilibrium over atomic distances are called stresses of the 4th kind. However, the trend is to drop this fine division because of the difficulties involved in the definition and separate measurement of different kinds of microstresses.

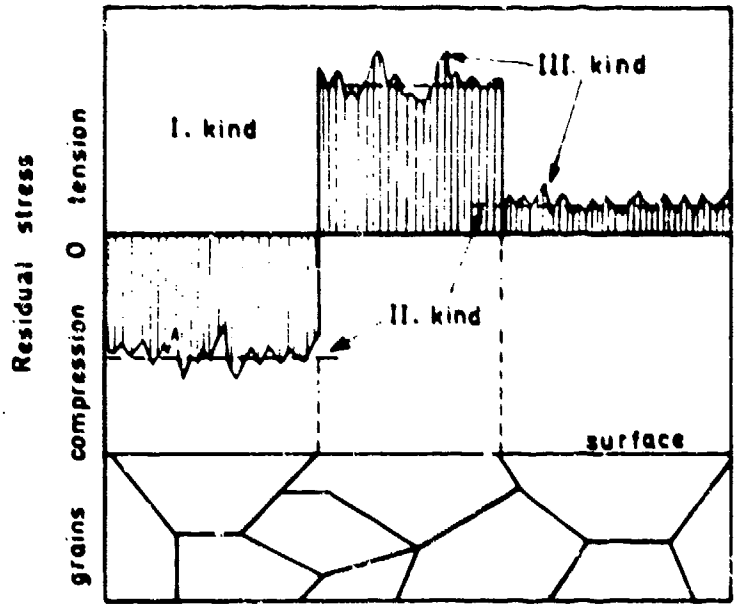

Fig.1 Definition of residual stresses of different kinds. After Peiter[1]

The present chapter treats only the non-destructive measurement of macro-residual stresses. Microstresses are only considered in so far they cause errors in the measurement of macro-residual stress.

At the beginning of the present century, all residual stresses were considered to be dangerous to the material and were avoided where possible by stress relieving heat treatment. Nowadays it is recognized that residual stresses may be either beneficial or detrimental, depending on their sign and distribution and it has become common industrial practice to induce beneficial residual stresses in the surfaces of highly loaded members.

In many ways macro-residual stresses influence material properties in the same way as the mean value of a loading stress. There is no difference in the nature of residual stress and mean stress and their effects on material properties are additive. However, there may be a difference in stability during the lifetime of a specimen because the residual stresses may fade. This problem will be returned to later.

The effect of micro-residual stresses on material properties has not yet been solved. This is because microstresses are created in processes which also work harden the material, making it impossible to separate the effects.

The non-destructive detection and measurement of residual stresses is almost exclusively done by the x-ray diffraction method, which therefore will dominate this chapter. However, some progress has recently been made in an ultrasonic residual stress measuring method and in the Knoop-diamond indentation method. The principles of the latter two methods will therefore be outlined and the experimental difficulties will be discussed.

4.1.1.2 Effect of Mean Stress on Fatigue Strength

For over 100 years it has been well known that variable stresses may cause cracks in a structure, even if the stresses are well below the yield point. This phenomenon was termed fatigue. Since then there has been an ever increasing effort to prevent failures by fatigue. One of the successful ways of increasing fatigue strength has been found to be the introduction of compressive residual stresses in surfaces of highly loaded members. To understand why compressive residual stresses are beneficial let us study the effect of mean stresses on fatigue.

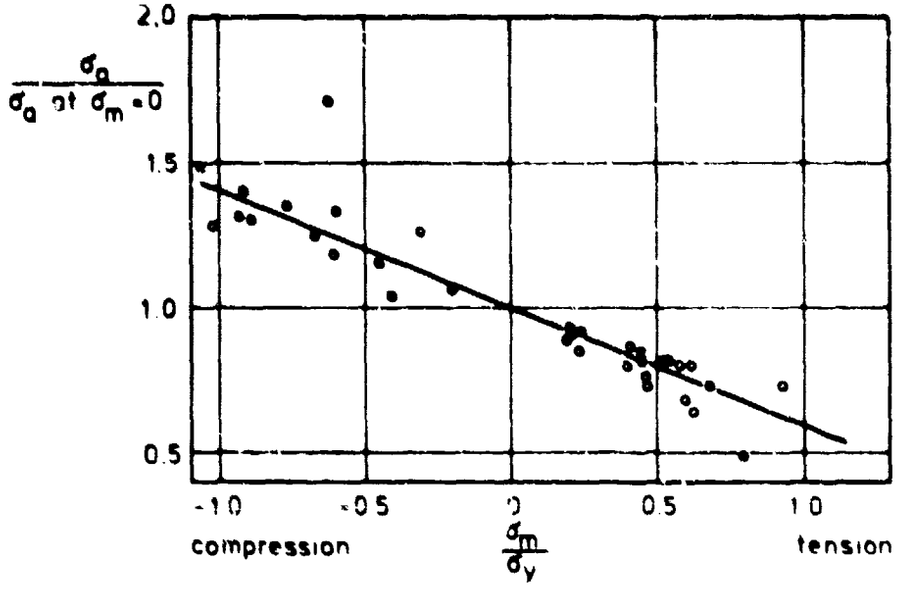

Fig. 2 The effect of mean stress on the fatigue limit of various steels and aluminium alloys. After Forrest[3]

In Figure 2 results from tests on steels and aluminium alloys with different mean stresses are plotted. The data have been collected by Forrest[3] from different sources. σ_a is the stress amplitude at the fatigue limit, σ_m is the mean stress and σ_y is the yield stress. The figure clearly shows how a compressive mean stress increases the permissible stress amplitude, while a tensile mean stress lowers the fatigue strength. The stress conditions for the tests shown in Figure 2 were uniaxial and the specimens were unnotched.

4.1.1.3 Effect of Mean Stress on Stress Corrosion

Stress corrosion is the accelerated formation of cracks when a material is loaded with static tensile stresses and at the same time is attacked by a corrosive medium. According to Champion[3] susceptibility of a metal to stress corrosion implies a greater deterioration in the mechanical properties of the material through the simultaneous action of a static tensile stress and exposure to a corrosive environment than would occur by the separate but additive action of those agencies. Most metals and alloys are susceptible to this form of corrosion. Stress corrosion cracks make the material fatigue damage sensitive because of the stress concentration factor at the crack tip.

Figure 3 shows typical results from stress corrosion tests on an aluminium alloy in NaCl solution found by Helfrich[4]. The abscissa in Figure 3 is the time to total failure. It is evident that a threshold stress exists below which stress corrosion cracking does not take place. Below the threshold stress normal corrosion occurs. The threshold stress is temperature dependent and dependent on material and corrosive medium. So far, correlation between laboratory tests and service life has not been good. Threshold values determined in the laboratory are therefore not likely to be useful as guidelines for the inspector. However, whenever a tensile residual stress is measured in the surface of a material that is known to be stress corrosion susceptible, the risk of stress corrosion cracks should be considered.

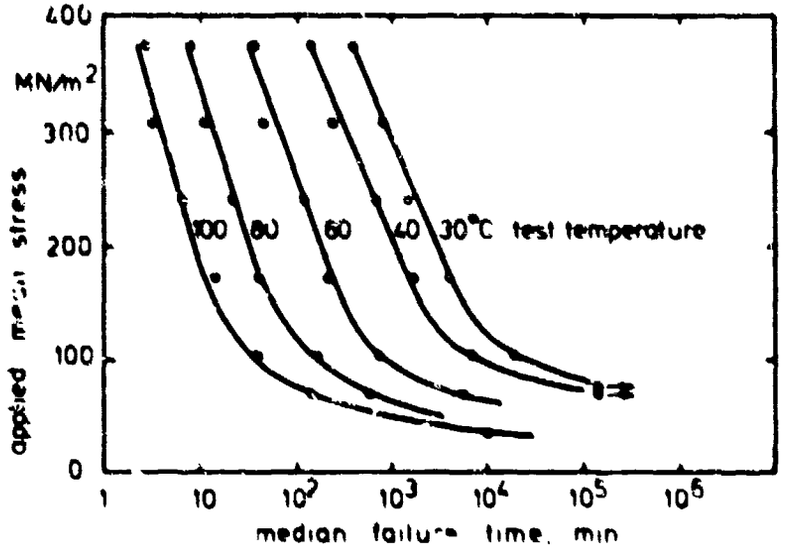

Fig.3 The effect of mean stress on corrosion life. After Heltrich[4]

4.1.2 PRINCIPLES OF RESIDUAL STRESS FORMATION

This section describes processes by which residual stresses are created. It is thus also a list of processes whose presence is to be sought, and may be detected by residual stress measuring methods.

4.1.2.1 Plastic Deformation in Regions with Stress Gradients

As an illustrative example of how residual stresses are formed by plastic deformation, let us look at an initially stress free beam loaded in bending and let us suppose the material has the working curve of Figure 4. When the moment is small the stress distribution is linear as shown in Figure 5(a). With increasing moment the stresses in the upper and the lower surfaces reach the tensile and the compressive yield stress respectively (on the tensile side the stress is now at point A in Figure 4). At a still larger moment the material yields at the surfaces, and the deformation is governed by the conditions that plane cross sections remain plane and there is equilibrium of moments and stresses. At the largest bending moment, M_y, applied, the stress distribution may be like the fully drawn line in Figure 5. If we look at Figure 4, the material in the tensile surface may now have reached point B. The dashed line in Figure 5(b) indicates the stress distribution if the material had behaved elastically. During unloading the material behaves elastically, following the line BC in Figure 4. Thus, to obtain the resulting residual stress distribution, shown in Figure 5(c), we have to subtract the dashed line from the fully drawn line of Figure 5(b). After unloading, the upper and the lower surface contain compressive and tensile residual stresses, respectively, i.e. the residual stresses created by plastic bending are of opposite sign to the loading stresses. This result is generally valid also for other kinds of plastic loading.

The important thing to notice here is that if the beam later is fatigue loaded with moments smaller than and in the same direction as the largest preload moment, then the maximum stresses in the surfaces will be smaller than if no preload had been applied, because the residual stresses subtract from the loading stresses. This leads to an improvement in fatigue strength. Conversely, a fatigue loading moment directed opposite to the preload moment will show a lower fatigue strength, because the residual stresses add to the loading stresses.

The principle of applying a static overload when the fatigue loading is unidirectional is used in processes like stretching of notched details and presetting of springs. Besides introducing compressive residual stresses in highly loaded areas, a further advantage is obtained compared to a non-treated specimen if the specimen contained tensile residual stresses in the as-fabricated state. Such tensile stresses disappear when yielding take place.

So far, only static overloads with essentially the same kind of loading as the fatigue load have been considered. As the fatigue process is usually concentrated in the surface, various methods have been adopted which introduce compressive residual stresses locally at highly loaded areas of the surface. Among these methods may be mentioned (1) Shot-peening, in which the surface is bombarded with small pieces of steel, (2) Strain peening, where the specimen surface is loaded in tension while a shot-peening treatment is carried out, so that higher compressive residual stresses are obtainable in the direction of the tensile load; (3) Cold rolling, in which a roller under pressure is forced over the surface, and (4) Stress coining, which is a method of plastic cold working the material around holes in a structure[5].

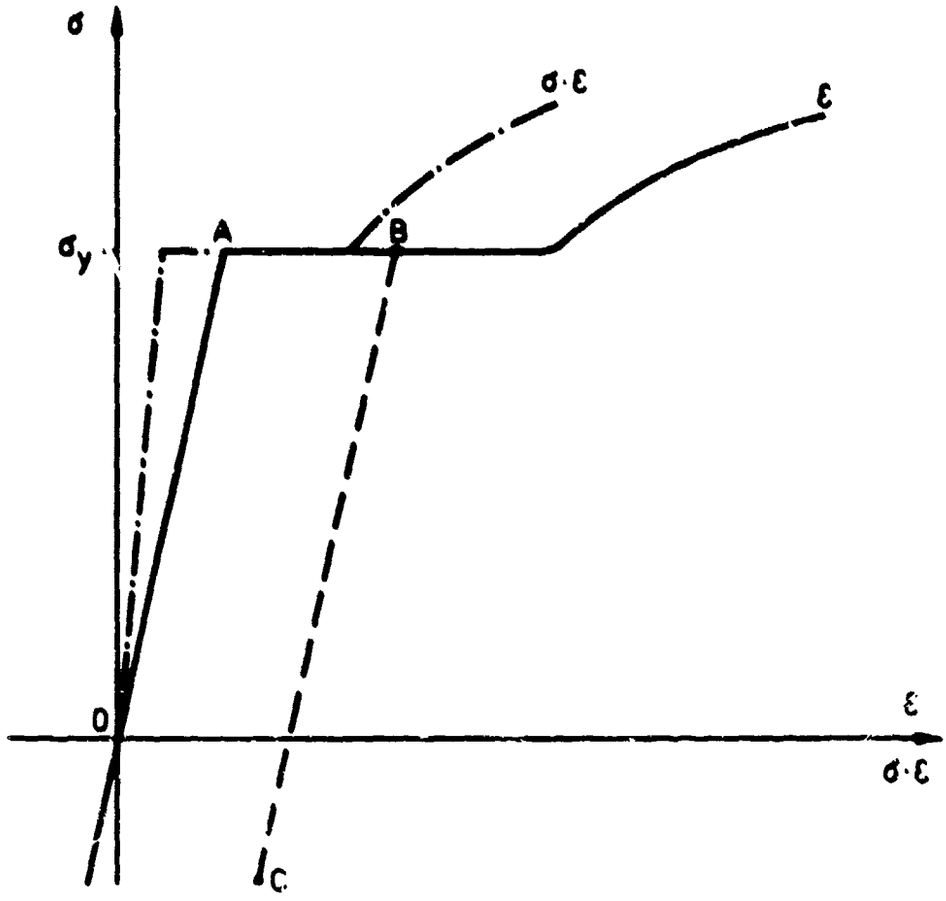

Fig.4 Example of stress-strain curve and the stress-stress strain curve

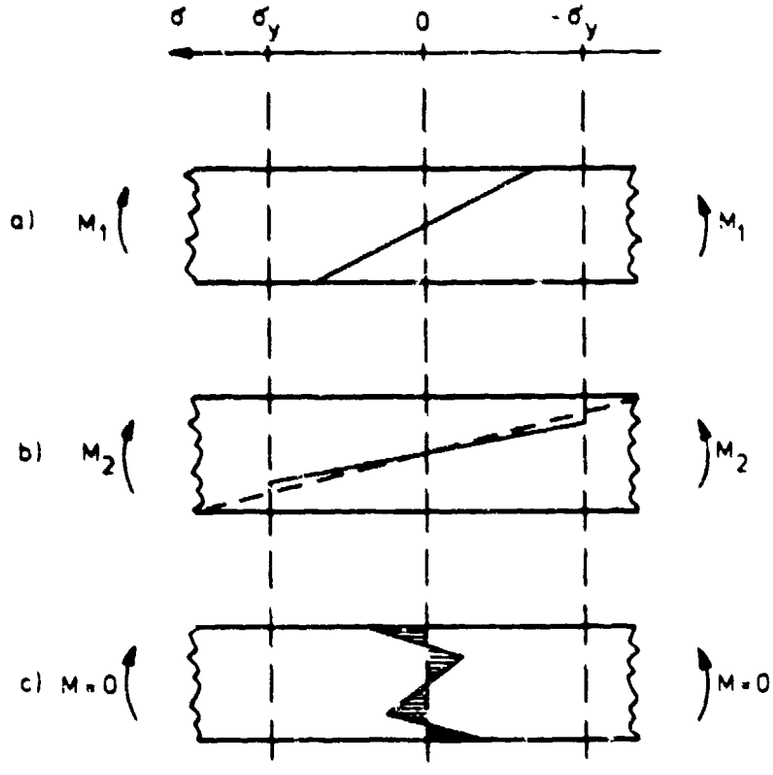

Fig.5 The creation of residual stresses in a beam when loading with moments exceeding the yield moment

In each of these methods the surface material is loaded locally beyond the tri-axial yield stress. Unloading takes place elastically in the same way as the stresses on the tensile side of the bending example (Fig.5), and a compressive residual stress results. Figure 9 shows the residual stress distribution after shot-peening and strain-peening measured by Mattson and Roberts[6] on SAE 5160 spring steel. A static tensile load of 60% of the yield stress in the strain-peening treatment doubles the residual stress compared to conventional shot-peening..

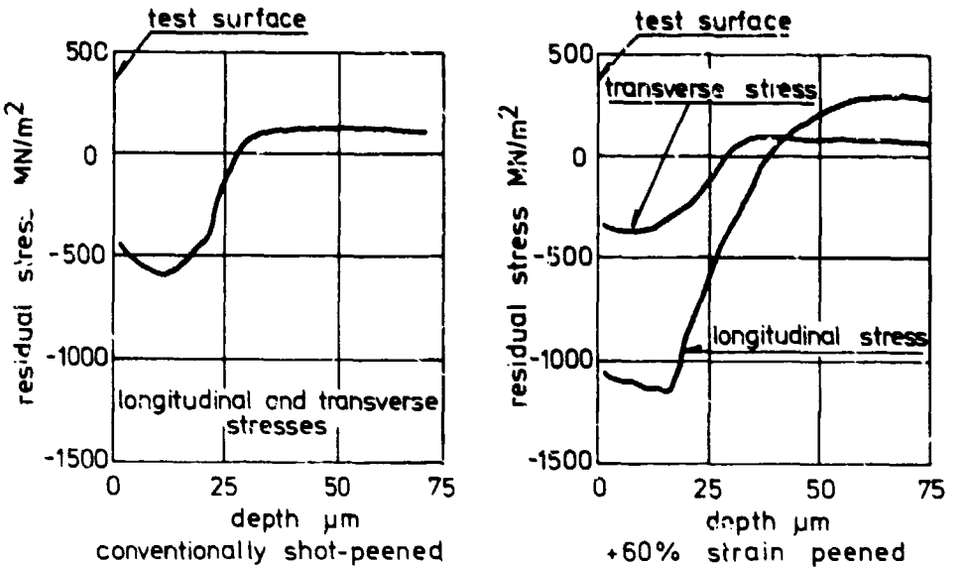

Fig.6 Residual stress distribution below the surface of shot-peened and strain-peened specimens. After Mattson and Roberts[6]

Fabrication processes like machining, grinding, polishing and cold drawing produce residual stresses in essentially the same way. From the scant data available it seems that shapering, lathe machining, griding and cold drawing are processes that may produce tensile residual stresses at or near the surface. Figures 7–10 show examples of such dangerous tensile residual stresses taken from the literature. These residual stress distributions should only be taken as guide lines. Large variations occur, depending on the degree of cold work and depth of cold-worked material.

4.1.2.2 Temperature Gradients

If the cooling rates of surface material are sufficiently higher than that of the center material, residual stresses build up after heat treatments. Figure 11 shows schematically changes in the longitudinal residual stress during symmetrical cooling of a long cylindrical rod. It is assumed that no phase changes take place, the residual stresses therefore being a result only of uneven thermal contraction. First the surface cools off, while the center is still hot. This creates tensile stresses in the surface balanced by compressive stresses in the center (the stress distribution at time t_1 in Figure 11). When the center starts cooling off, the stress difference between surface and center decreases and then changes sign, because the cold surface hinders the thermal contraction of the center. Finally a stress state as shown for time t_2 is reached. The maximum stresses will usually be somewhat less than the yield stress.

At welds, residual stresses are created by the same mechanism. Figure 12 shows residual stresses around a butt weld. The stress parallel to the weld is tensile in the weld and in the material immediately adjacent to it. This tensile stress is balanced by compressive stresses away from the weld. Near the edges the parallel stresses obviously reduce to zero. The transverse stress in the weld is tensile near the center and compressive near the weld ends.

Spot heating is a method of improving fatigue strength which relies on the residual stresses created during cooling. If a structure, preferably a plate, is heated locally and then allowed to cool, a residual stress distribution around the center of heating develops. Figure 13 (taken from Reference 11) shows schematically the resulting stress pattern. The idea is to make use of the balancing compressive tangential stress which is created a small distance away from the center. Figure 14 show the correct position for spot heating and the effect on fatigue life.

The Gunnert method is another means of introducing residual stresses to improve fatigue strength. Here the place to be treated is heated for a longer period than in spot heating in order to get high temperature also in the underlying layers. The surface is then quenched by a jet of water. Compression stresses are created in the surface, balanced by tensile stresses in the slower cooling volume.

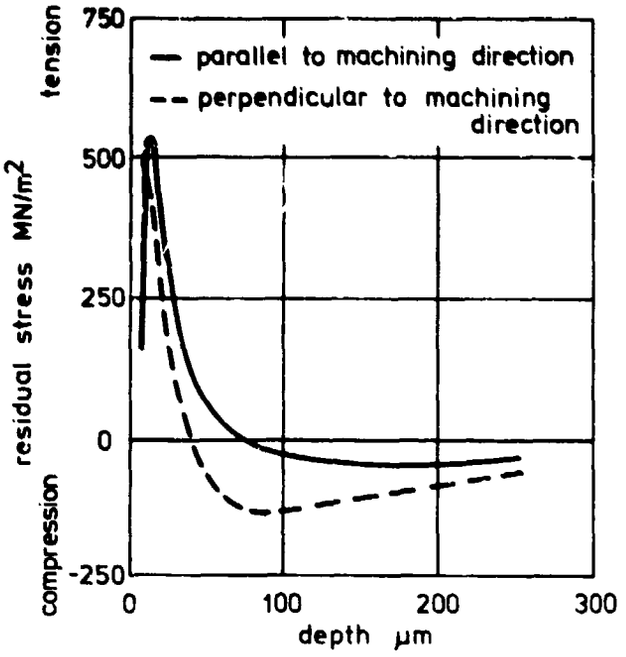

Fig.7 Residual stress distribution below the surface after shaper finish machining. After Winter and McDonald[7]

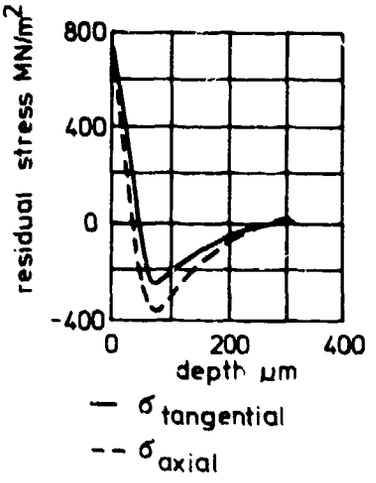

Fig.8 Residual stress distribution below the surface after lathe machining without water cooling. After Bühler and Tönshoff[8]

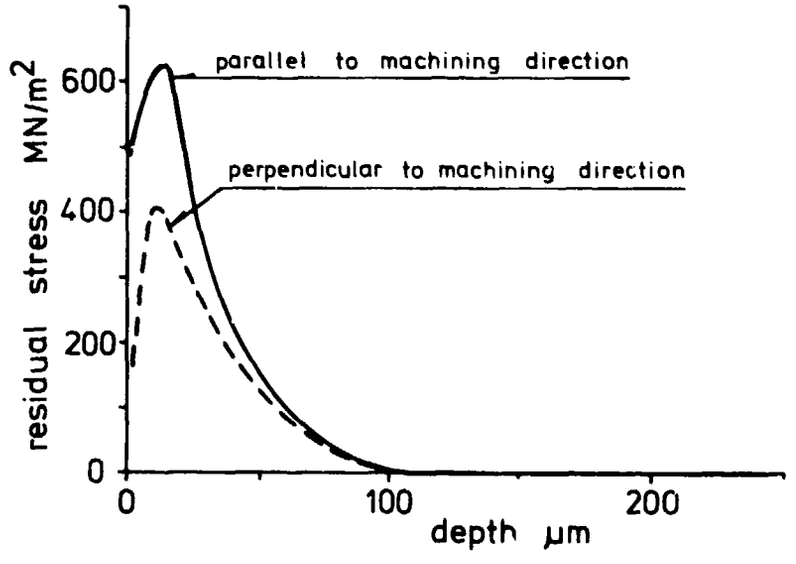

Fig.9 Residual stress distribution below the surface after grinding. Example from Letner[9]

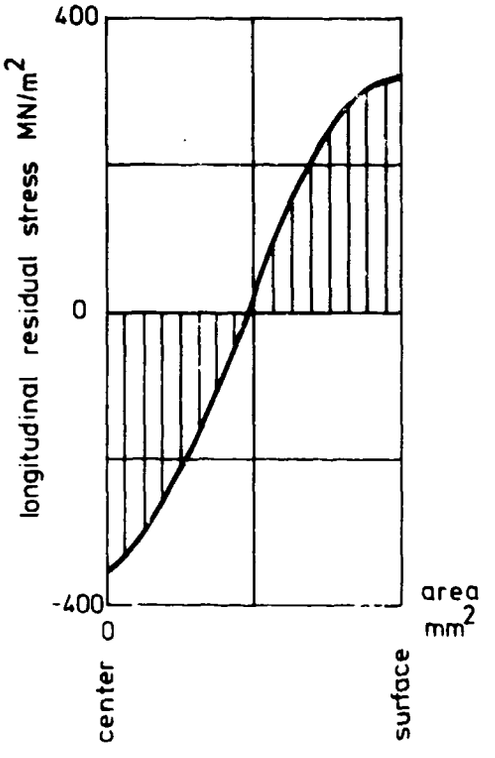

Fig.10 Residual stress distribution over the cross-section of a cold-drawn rod. After Peiter[10]

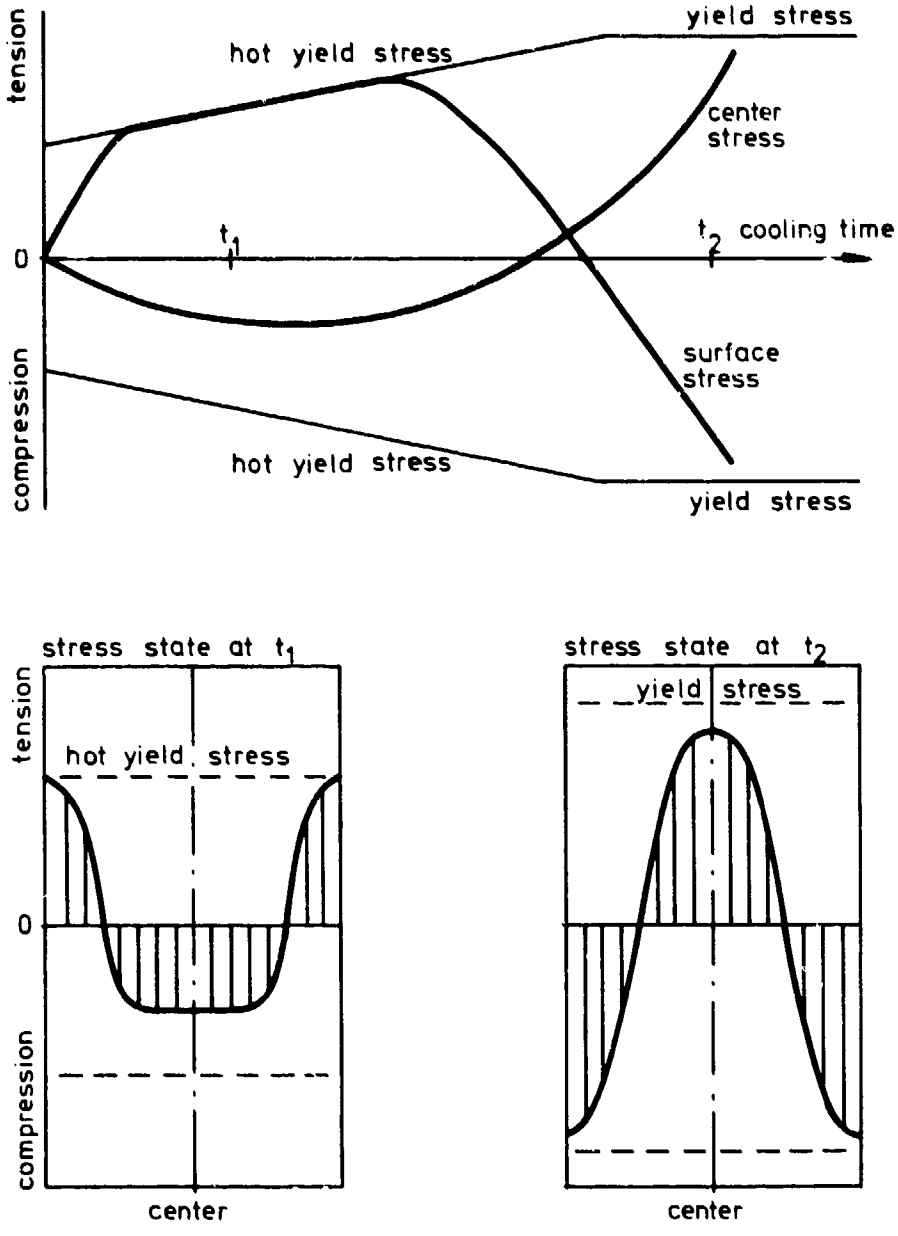

Fig.11 The creation of residual stresses in a rod during cooling. After Peiter[1]

It is characteristic of all residual stress distributions caused by uneven cooling rates that tensile stresses develop in that part of the body which cools last.

4.1.2.3 Chemical Expansion or Contraction of Surface Material

Many metals and alloys may exist in both stable and metastable phases at the same temperature. The metastable phase transform to the stable phases if the rate of diffusion is high enough. At normal operating temperatures the rate of diffusion will often be low, making the metastable phases stable enough for engineering purposes. Usually phase transformations involve a change in volume whereby tensile residual stresses are created in the more close-packed phases balanced by compressive stresses in the less close-packed phases. This section describes briefly some processes which make use of this principle of residual stress formation and gives some examples of the stress distributions obtainable.

Induction hardening, case hardening and flame hardening create metastable martensite in the surface. Martensite being less close-packed than the base material, the resulting residual stress is compressive in the surface.

Carburizing is a process where carbon atoms are diffused into a steel that is not in itself fully hardenable. Carburizing improves the properties of the surface material and introduces some compressive residual stresses. Usually carburizing is followed by a hardening treatment which creates martensite in the surface. Figure 15 (taken from Reference 12) shows the resulting residual stress distribution.

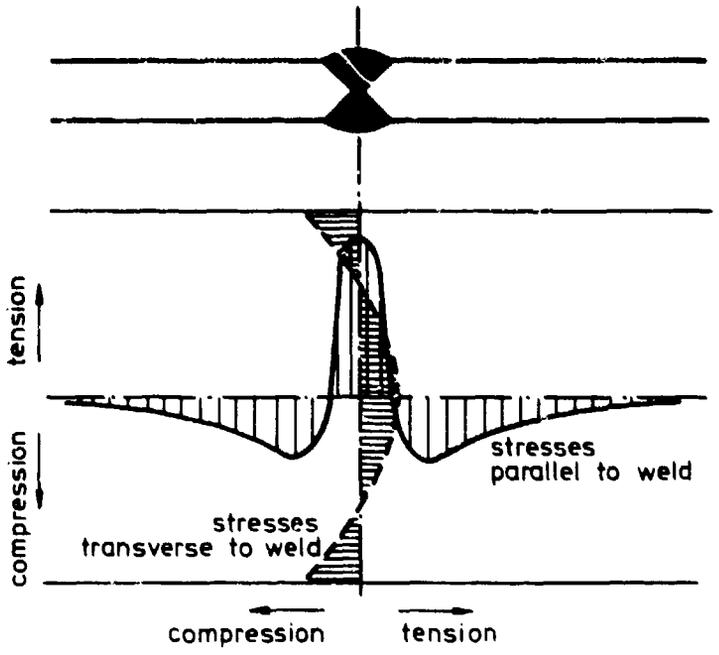

Fig.12 The residual stress distribution in the vicinity of a butt weld

Decarburizing is an unintentional removal of carbon atoms from the surface. Decarburizing leads to tensile residual stresses, increased surface roughness, and lower mechanical strength of the surface material.

Nitriding consists of heating steels of special composition to temperatures about 500°C in contact with a nitrogen-containing medium. Nitriding gives very hard and fatigue resistant surfaces when used on special steels.

Cyaniding is a process in which the steel is in contact with molten cyanide. Both carbon and nitrogen diffuse into the metal.

Anodic treatment of aluminium alloys in chromic or sulphuric acid electrolytes produces a hard, shallow film on the surface with good abrasion resistance and increased protection against corrosive attack.

With the exception of the anodic treatment, all the methods mentioned above create a surface layer with compressive residual stresses balanced by tensile stresses in the interphase and the base metal. It is therefore often observed that cracks start below the surface. The anodic treatment of aluminium alloys decreases the fatigue strength because of high tensile stresses. When a shot-peening treatment is carried out either before or after the anodic treatment, the fatigue strength equals that of the non-treated metal.

4.1.2.4 Electroplating

Electrodeposition of one metal on another is extensively used in industry for corrosion protection, wear resistance, and salvage of worn components. The fatigue strength of some of these metal combinations has been found to be much lower than that of the base material. The deleterious effect is attributed to three main problems created by the electrodeposition process[13]:

(1) Hydrogen embrittlement when the base material is steel.

(2) Development of fine cracks in the electrodeposit (especially if chromium is used).

(3) High tensile stresses in the deposit.

Hothersall measured residual stresses in various electrodeposited steels. His results were summarized by Harris[13] and Table 1 shows results from tests with conventional electrolytes, indicating large variations in sign and magnitude.

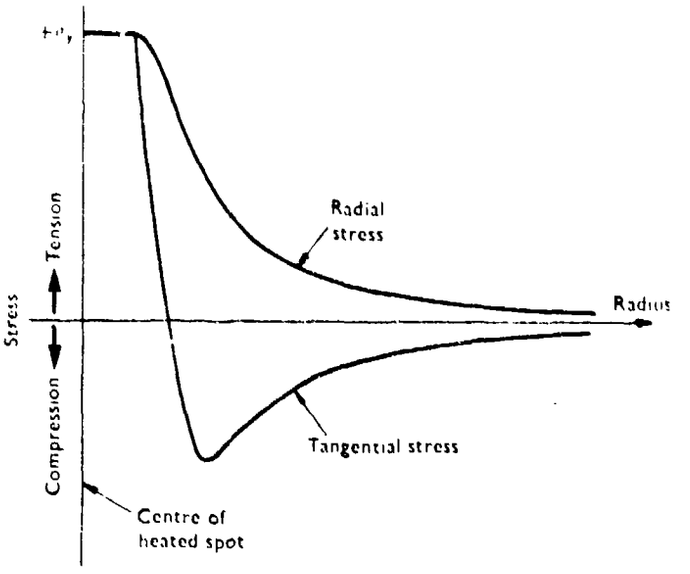

Fig.13 The residual stress distribution around the center of a heated spot. After Gurney[11]

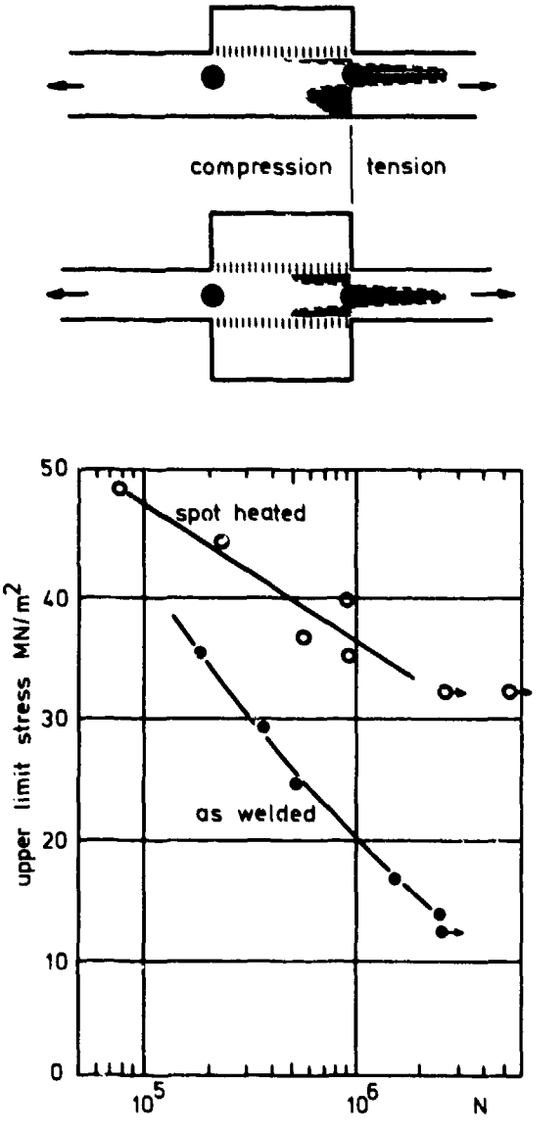

Fig.14 The correct position to spot heat and the effect of spot-heating on fatigue strength. After Gurney[11]

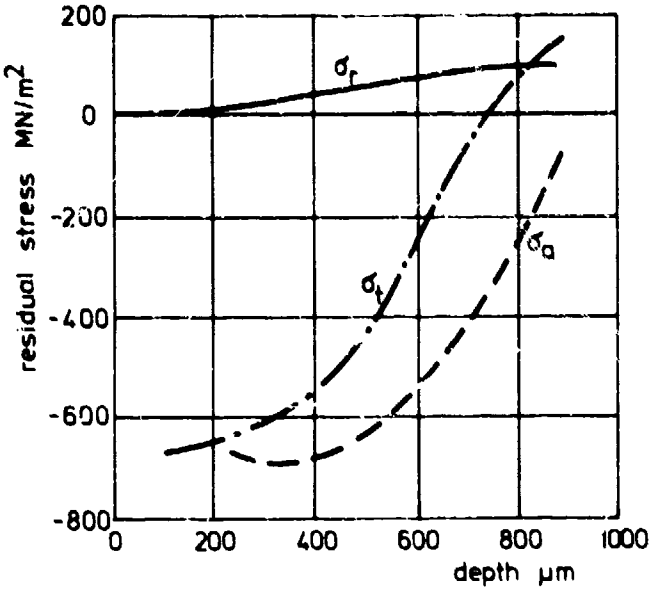

Fig.15 The residual stress distribution below the surface after carburizing and hardening. After Hammer[12]

TABLE 1

Electrodeposited metal	*Residual stress*
Cadmium	Compressive (slight)
Chromium	Tensile (0–400 MN/m²)
Cobalt	Tensile (marked)
Copper	Tensile or compressive (0–15 MN/m²)
Iron	Tensile
Lead	Compressive (30 MN/m²)
Nickel	Normally tensile (0–300 MN/m²)
Silver	Tensile (slight)
Zinc	Compressive (0–30 MN/m²)

4.1.3 STABILITY OF RESIDUAL STRESSES IN SERVICE

Residual stresses are not necessarily constant during the lifetime of a component. The more important causes of changing residual stresses are:

(1) Positive or negative peaks in the loading,

(2) Cyclic creep, and

(3) High temperatures.

Rosenthal[14] collected data on residual stress relief by uniaxial loading from various sources and suggested a simple relation to explain the data. Using as a yield criterion the simple maximum-shear-stress, which may be written as

$$\max\left\{\frac{|\sigma_1|}{2}, \frac{|\sigma_2|}{2}, \frac{|\sigma_3|}{2}, \frac{|\sigma_1-\sigma_2|}{2}, \frac{|\sigma_2-\sigma_3|}{2}, \frac{|\sigma_3-\sigma_1|}{2}\right\} = \frac{\sigma_y}{2} \quad (1)$$

the residual maximum shear stress [i.e. the left hand side of Equation (1)] measured after application of the load was plotted as function of load maximum shear stress (Fig.16). The resulting test points lie close to straight line within the scatter of experimental data. However, fatigue stressing generally seems to reduce residual stresses more than the application of a single load. This phenomenon is due to cyclic creep.

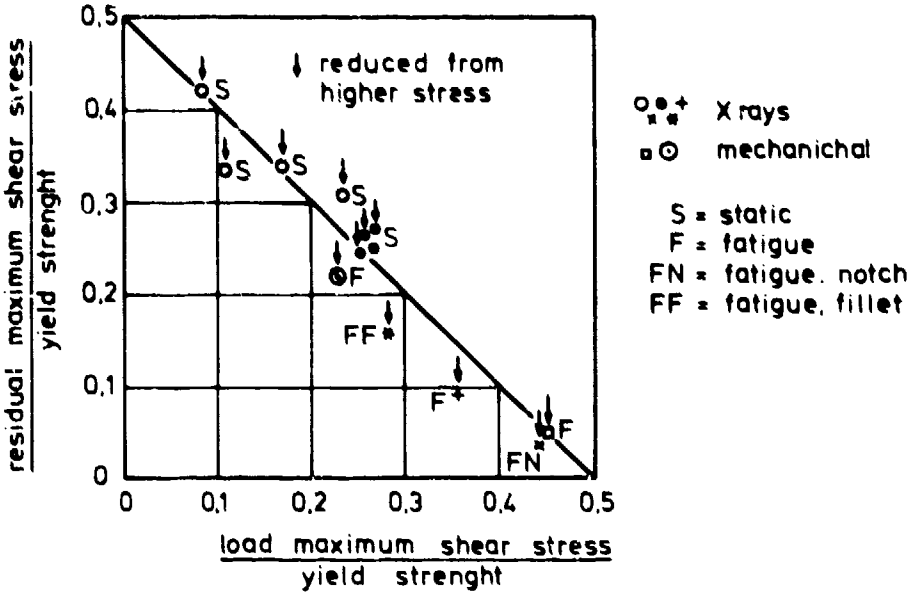

Fig.16 Relief of residual stresses due to single static and alternating loads compared with Equation (1). After Rosenthal[14]

Morrow[15] studied cyclic creep on 4340 steel at different hardnesses. Specimens were loaded with constant amplitude and mean value of deflection and the mean load was recorded. Some of his results for the soft condition of the steel are shown in Figure 17. It is observed that the mean stress gradually approaches zero during fatigue loading and that the rate of change increases with increasing amplitude. Morrow termed the phenomenon cycle-dependent stress relaxation, but the term cyclic creep can be used equally well.

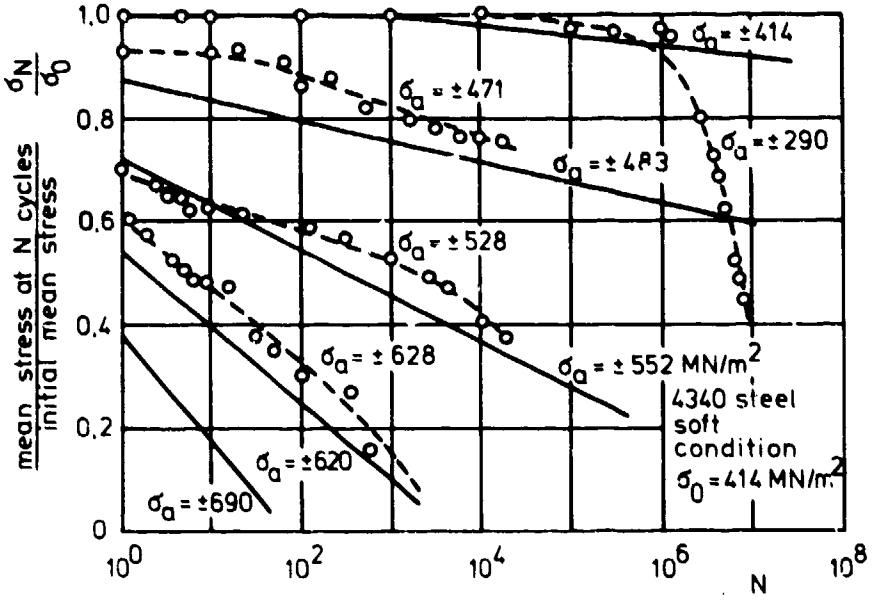

Fig.17 Relief of mean stress during fatigue life under constant deformation loading. After Morrow and Sinclair[15]

In notched specimens, cyclic creep alters the residual stresses because the creep relieves the stresses in the notch.

Compressive residual stresses are also sensitive to high temperatures, especially if the heating time is short and the cooling time long. During heating the surface material wants to expand but is hindered by the cool layers beneath the surface. High compressive thermal stresses result, which add to the residual stresses. The compressive yield stress is easily exceeded, especially since the yield stress is lower at high temperatures. If the cooling time is long only small thermal stresses will be introduced, so the final result is a decrease of residual stress.

4.1.4 MEASUREMENT OF STRESS BY X-RAYS

4.1.4.1 The Characteristics of the X-Ray Stress Measurement

As is the case for all other stress measuring methods, the x-ray method is really a strain measurement. Strain is defined as change of length divided by original length. For x-ray measurements the length in question is the distance between the reflecting lattice planes of the crystals. Compared to other stress measuring methods the x-ray method has the following unique characteristics (summarized by Glocker et al.[16]):

(1) The x-ray method is only applicable on crystalline materials.

(2) The measurement is truly non-destructive. The measurement leaves no surface markings and the state of the material is completely unchanged.

(3) Only elastic strains are measured. Elastic strains may be related to the sum of residual stresses and load stresses using the expanded Hooke's law.

(4) The measurement is selective. The measured strains are the average strains in a small proportion of the crystallites in the irradiated volume.

(5) The measured strains are perpendicular to the reflecting planes.

(6) The x-rays used are soft. The stress measurement is therefore restricted to a thin surface layer of the order of 0.01 mm in which the stress state is biaxial.

It follows from property (6) that mill-scale, rust, paint, etc. should be removed and the surface roughness should be low before attempting to measure stress by x-rays. The best way of achieving this is to use electrolytic polishing. Mechanical polishing or grinding introduces residual stresses detectable by x-rays, no matter how carefully these treatments are carried out.

4.1.4.2 The Physical Principle of the X-Ray Stress Measuring Method

The x-ray stress measuring method builds on the principle of Bragg reflection. A crystallite only reflects x-rays if the Bragg equation is fulfilled,

$$n\lambda = 2d \sin\theta , \tag{2}$$

and if the reflection planes lie in reflection position (as shown in Figure 18). In Equation (2), n is an integer, λ is the wavelength of the x-rays, d is the distance between reflecting lattice planes, and the angle θ is defined in Figure 18. In x-ray diffraction, very intensive, monochromatic K_α-radiation is used and the superimposed white radiation is filtered out as completely as possible. K_α-radiation consists of two radiations with slightly different wavelength, called $K_{\alpha 1}$ and $K_{\alpha 2}$. The $K_{\alpha 1}$ is approximately twice as intense as the $K_{\alpha 2}$, with small variations from metal to metal. It is not possible to separate $K_{\alpha 1}$ and $K_{\alpha 2}$ by the use of filters or electronic discriminators. In stress work the intensity lines therefore appear as two neighboring lines. In hardened or plastically deformed steel the two lines may overlap due to the line broadening.

For given values of n, λ and d, a given crystal either reflects x-rays at the angle θ or does not reflect at all, depending on the orientation of the crystal. In a polycrystalline material, generally only few crystals will satisfy the reflection condition, as stated under property (4) in Section 4.1. Strains in a polycrystalline material change the value of d in different directions in the material. Equation (2) shows that a change in d will shift the angle θ. These angle shifts are measured and used to compute the stresses.

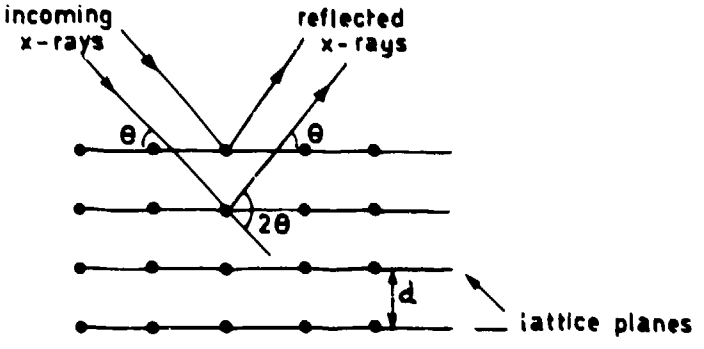

Fig.18 Reflection of x-rays from a set of lattice planes

To increase the sensitivity of the stress measurement, it is desirable to increase the angle shifts as much as possible for given values of strain. From Equation (2)

$$\theta = \arcsin\left(\frac{n\lambda}{2d}\right) . \tag{3}$$

Expanding θ in a Taylor-series in variable d from the stress free lattice plane distance d_0, the following relation is obtained.

$$\theta - \theta_0 = -\tan\theta_0 \frac{d - d_0}{d_0} . \tag{4}$$

Here it is evident that a large angle shift is obtained when θ_0 approaches 90° i.e. reflection lines in the back reflection region should be used. Table II lists some intensity lines suitable for stress measurement.

TABLE II

Intensity Lines for X-Ray Stress Measurements

Metal	K_α-*radiation*	*Filter*	*Reflecting planes*	*Bragg-angle* θ
Aluminium	Cu	Ni	(511)/(333)	81.24
	Co	Fe	(420)	81.04
	Cr	V	(222)	78.32
Brass 68% Cu	Co	Fe	(400)	75.50
Cartridge	Ni	Co	(331)	79
Chromium	Cu	Ni	(213)	87.66
	Co	Fe	(310)	78.70
	Cr	V	(211)	76.46
Copper	Cu	Ni	(420)	72.34
	Co	Fe	(400)	81.78
Germanium	Cu	Ni	(515)/(711)	76.48
Gold	Cu	Ni	(511)/(333)	78.93
	Co	Fe	(420)	78.77
	Cr	V	(400)	76.51
Magnesium	Fe	Mn	(105)	83
Nickel	Cu	Ni	(420)	77.83
	Cu	Ni	(313)	72.32
Silver	Cu	Ni	(511)/(333)	78.35
	Co	Fe	(420)	78.20
	Cr	V	(222)	76.03
Steel α	Mo	Zr	(651)/732)	76.98
α	Co	Fe	(310)	80.63
α	Cr	V	(211)	78.01
austenitic	Cr	V	(220)	64
Tungsten	Mo	Zr	(626)	77.72
	Cu	Ni	(400)	76.84
	Co	Fe	(222)	78.31

Figure 19 shows a surface segment with principal stress directions 1 and 2 and the normal 3. In the theory of elasticity it is proved that the normal strain at the surface in the direction (φ, ψ) is determined by

$$\epsilon_{\varphi,\psi} = \tfrac{1}{2}s_2(\sigma_1 \cos^2\varphi + \sigma_2 \sin^2\varphi)\sin^2\psi + s_1(\sigma_1 + \sigma_2) . \tag{5}$$

The constants of elasticity $\frac{1}{2}s_2$ and s_1 are connected with the normally used elastic modulus E and Poisson ratio ν by the formulas

$$s_1 = -\frac{\nu}{E} \quad \text{and} \quad \tfrac{1}{2}s_2 = \frac{1+\nu}{E} . \tag{6}$$

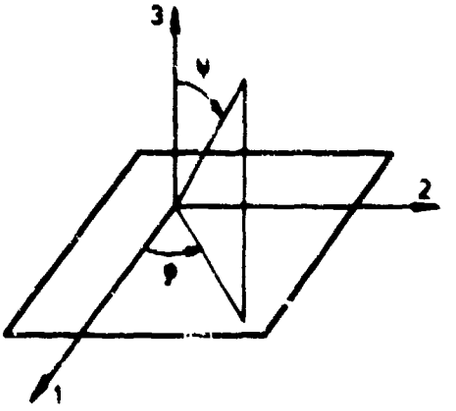

Fig.19 A sketch of a surface segment defining the angles ψ and φ

From the theory of elasticity we also know the normal stress in the direction (φ, $\psi = 0$):

$$\sigma_\varphi = \sigma_1 \cos^2\varphi + \sigma_2 \sin^2\varphi . \tag{7}$$

Substituting Equation (7) into Equation (5) gives

$$\epsilon_{\varphi,\psi} = \tfrac{1}{2}s_2\, \sigma_\varphi \sin^2\psi + s_1(\sigma_1 + \sigma_2) . \tag{8}$$

Differentiating with respect to $\sin^2\psi$ yields

$$\frac{\partial \epsilon_{\varphi,\psi}}{\partial \sin^2\psi} = \tfrac{1}{2}s_2\, \sigma_\varphi = m_\varphi . \tag{9}$$

The important step to be taken now is to equate the lattice strain

$$\frac{d - d_0}{d_0} \tag{10}$$

and the elasticity theory strain defined by Equation (8). To measure σ_φ, the lattice distance d is measured at several ψ-values in the φ-plane, the lattice strains as defined by Equation (10) are plotted as a function of $\sin^2\psi$ (as shown in Figure 20) and the stress is computed from the slope of the straight line connecting the test points. This so-called $\sin^2\psi$-method is due to Macherauch and Müller[17].

It is not necessary to know the stress-free lattice plane distance d_0 when computing the lattice strains, because only the slope of the straight line in Figure 20 is used to compute the stress. The lattice distance measured at $\psi = 0$ could be used just as well, the only effect being to shift the line without changing the slope. It is advisable to measure d at least at four different ψ-values when a new material or a new material treatment is measured. When it has been established that the plot is linear within the measuring accuracy, two measurements of d suffice to determine the stress in one direction. To measure both principal stresses in the surface, when the principal stress directions are known, requires at least three d measurements (one at $\psi = 0$, and two at $\psi \neq 0$ and $\varphi = 0$ and $\varphi = 90°$ respectively). In this way the principal stresses are measured directly. If it is not experimentally possible to carry out measurements at $\varphi = 0$ and 90°, the formulas given below for unknown principal stress directions may be used to compute the principal stresses. Only then is the angle φ_a known. If the principal stress directions are unknown, at least four d measurements are necessary (one at $\psi = 0$, and three at $\psi \neq 0$ in three different φ-directions). In this case the φ-values, φ_a, φ_b and φ_c (see Figure 21) are unknown, but we know the differences between the φ-values,

$$\Delta_b = \varphi_b - \varphi_a \tag{11}$$

and

$$\Delta_c = \varphi_c - \varphi_a \,, \tag{12}$$

and we can measure the stress values σ_a, σ_b and σ_c in the φ-directions (Fig.21). From the known quantities we first compute φ_a from

$$\varphi_a = \frac{1}{2} \arctan \left| \frac{2[\sin^2\Delta_b(\sigma_a - \sigma_c) - \sin^2\Delta_c(\sigma_a - \sigma_b)]}{\sin^2 2\Delta_c)(\sigma_a - \sigma_b) - \sin(2\Delta_b)(\sigma_a - \sigma_c)} \right| . \tag{13}$$

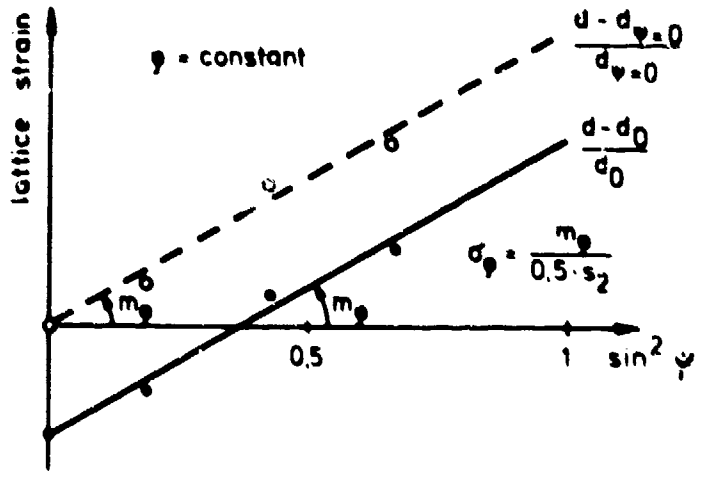

Fig.20 Computation of the stress from the lattice strains at different ψ-angles

Then the principal stresses may be computed using Equations (14) and (15)

$$\sigma_1 = \frac{-\sigma_a \sin^2(\varphi_a + \Delta_b) + \sigma_b \sin^2\varphi_a}{\cos^2(\varphi_a + \Delta_b) - \cos^2\varphi_a} \tag{14}$$

$$\sigma_2 = \frac{\sigma_a \cos^2(\varphi_a + \Delta_b) - \sigma_b \cos^2\varphi_a}{\cos^2(\varphi_a + \Delta_b) - \cos^2\varphi_a} \,. \tag{15}$$

Recommended values of Δ_b and Δ_c are either 45° and 90° or 60° and 120°.

4.1.4.3 The Film Method

In the film method, the x-rays coming from the x-ray tube pass through the aperture in the center of the film, go on to the component and are finally reflected and detected on the film (Fig.22). If the lattice distances d_1 and d_2 are different because of stresses in the material the diffraction ring deforms because the Bragg angle changes. On the film the radii r_1 and r_2 are not readily measured, because the center of the film is not known with accuracy. This difficulty is overcome by measuring instead the distance, Δ, from the specimen diffraction ring to the diffraction ring of a stress relieved powder of some reference material. Common reference materials are gold, silver and chromium. The choice of reference materials is dictated by the position of its diffraction ring relative to the specimen diffraction ring. The diffraction rings should be close, but must not overlap on the film. Suitable reference materials may be found from the Bragg angles given in Table II for various combinations of material and K_α-radiation. The reference material may either be used as a thin foil which is attached to the surface (this necessitates two exposures on the same film; one without and one with the reference material) or reference powder may be painted on the surface in such a thin layer that simultaneous recording of both diffraction rings is possible.

The following quantities on the film are measured: $2r_f$, $\Delta_1 = r_f - r_1$, and $\Delta_2 = r_f - r_2$. The sequence of equations below shows how to compute the lattice strain for $\psi = \psi_1$.

(1) Compute the material to film distance from

$$D = \frac{2r_f}{2 \tan(2\theta_f)} \,. \tag{16}$$

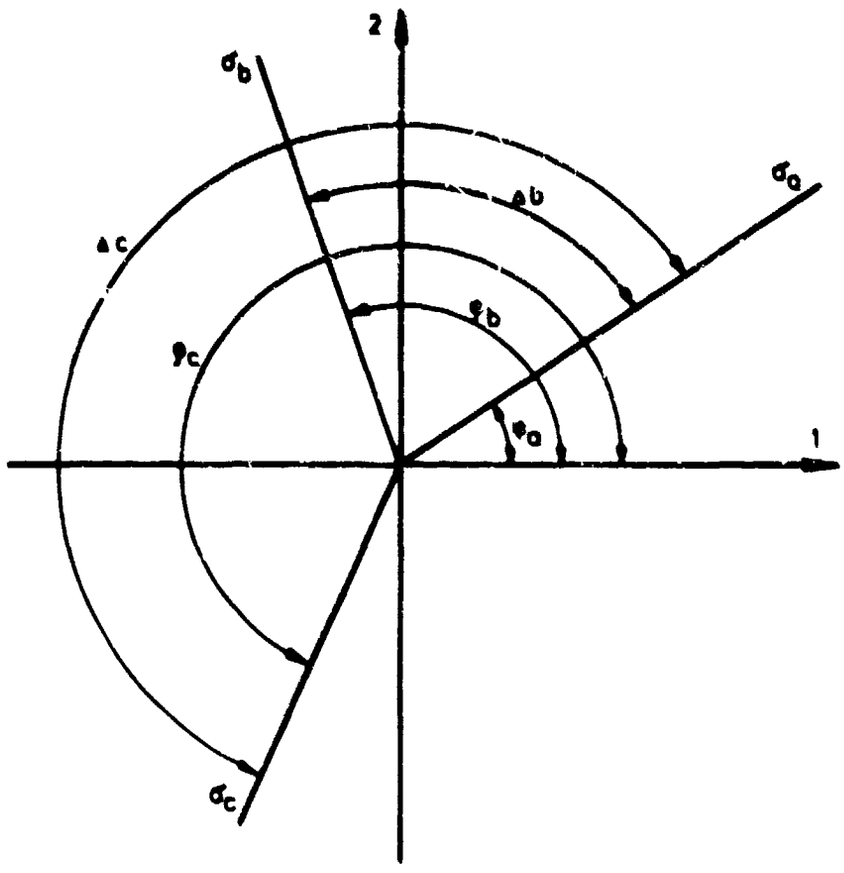

Fig.21 Definition of the angles when the principal stress directions are unknown

(2) Compute the radius of the diffraction ring for the specimen material

$$r_1 = \frac{2r_f}{2} - \Delta_1 \,. \tag{17}$$

(3) Compute the Bragg angle θ_1 by

$$\theta_1 = \tfrac{1}{2} \arctan\left(\frac{r_1}{D}\right). \tag{18}$$

(4) Compute lattice strain using

$$\frac{d_1 - d_0}{d_0} = \frac{\dfrac{n\lambda}{2 \sin \theta_1} - \dfrac{n\lambda}{2 \sin \theta_0}}{\dfrac{n\lambda}{2 \sin \theta_0}} = \frac{\sin \theta_0}{\sin \theta_1} - 1 \,. \tag{19}$$

It may again be mentioned that in Equation (19), instead of using d_0 and the equivalent θ_0, it is possible to use any of the θ-values computed by Equation (18) for the same stress measurement. Points (1) to (4) are repeated for each ψ-value. Suitable angles of incidence ψ_0 have been recommended by Macherauch and Müller[17] (Table III). The lattice strains are then plotted as shown in Figure 20 and the stress σ_φ is computed from the slope of the line. Equations (16), (17), (18) and (19) are well suited for work with a small, programmable table-top computer.

To obtain sharp and clear intensity lines on the film, a filter is necessary (see Table II for correct choice of filter). Most often the filter is placed in the incident beam because a small filter area suffices there. Now that large filters have become available, it is possible to place the filter directly over the film i.e. in the reflected beam. Sharper pictures are thus obtained, because the filter also absorbs fluorescent radiation from the material of the component. A course grained material gives diffraction rings with a spotty appearance that are difficult to measure. To improve the measuring accuracy the film may be oscillated a few degrees.

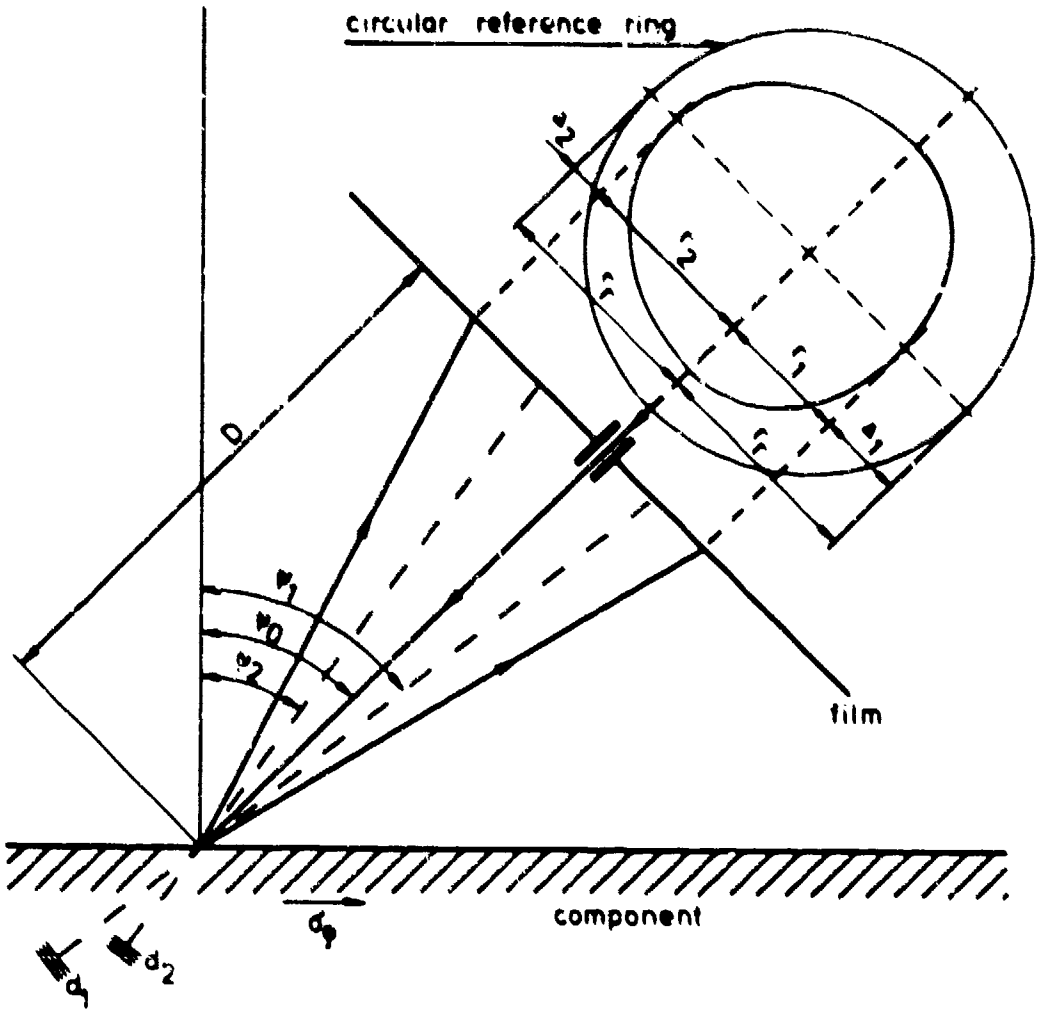

Fig.22 Schematic set-up for the film method showing the x-ray paths and the diffraction rings on the film

TABLE III

Recommended Angles of Incidence ψ_0 and Corresponding Values of ψ for the Film Method (Macherauch and Müller[17])

Bragg angle θ	*Angle between surface normal and primary beam* ψ_0		*Measuring angles* ψ (and $\sin^2\psi$)			
78	33	45	21 (0.128)	33 (0.296)	45 (0.500)	57 (0.702)
79	33	45	22 (0.140)	34 (0.313)	44 (0.482)	56 (0.688)
80	35	45	25 (0.178)	35 (0.329)	45 (0.500)	55 (0.670)
81	18	45	9 (0.024)	27 (0.206)	36 (0.345)	54 (0.652)
82	16	45	8 (0.019)	24 (0.166)	37 (0.362)	53 (0.638)

The film method requires only simple instrumentation. The high voltage supply for the x-ray tube may be of a simple type. High stabilization is not necessary. The x-ray tube should be of high output to minimize the exposure time. Usually a square anode window is used in film work. The film camera should be of the flat plate back reflection type with provisions for oscillation of the film. Cameras used for stress work are open on one side. Great care should therefore be taken to ensure that no person enters into the primary beam with any part of his body. The film characteristics should include high sensitivity, fine grain, low fogging, low and uniform expansion due to changes in temperature and humidity, and wide exposure range. The diffraction rings on the film may be measured either with a glass measuring scale or with a photometer.

4.1.4.4 The Diffractometer Method

In the diffractometer stress measuring technique the reflected intensity is detected by either a proportional or a scintillation counter. Geiger Müller counters are not used because of their low counting speed. The electrical impulses from the detector are counted or time-averaged in associated counting electronics.

One advantage of the diffractometer technique compared to the film technique is the higher peak-to-background ratio obtainable because of the combined effects of filtering and electronic discrimination. Another advantage is that the intensity is measured directly as a function of 2θ. Corrections for θ- and ψ-dependent intensity factors which affect the position and contour of the line can easily be made.

Diffractometers usually employ Bragg-Brentano focusing in measurements with $\psi = 0$, as shown in Figure 23. Bragg-Brentano focusing is characterized by the condition that the x-ray source, the sample surface and the receiving slit all lie on the arc of a circle. Normally the surface is not curved as shown in Figure 23, but flat. This results in a loss of sharpness in the diffracted line, and necessitates the use of smaller divergence slits. When the sample is rotated by the angle ψ, the focusing point of the diffracted beam is moved from A to B in Figure 23. Defining ψ as positive when directed as shown, the distance AB is given by

$$AB = R_0 \left[1 - \frac{\cos\left(\psi + \frac{\pi}{2} - \theta\right)}{\cos\left(\psi - \frac{\pi}{2} + \theta\right)} \right], \qquad (20)$$

On existing diffractometers the problem associated with the movement of the focusing point is handled in two different ways. One way is to move the detector slit to point B, where the intensity is higher. A relatively small detector is used. The other way is to keep the detector slit fixed and use a relatively large detector slit. The first method leads to greater intensities and is in theory able to resolve finer details in the line shape, but in the high-angle range used in stress work there exist no fine details, because even the K_α-doublet is widely dispersed. Also, the intensity lines of materials where stress measurements are wanted are generally broad because of cold work or hardening, so that even the K_α-doublet disappears. Kirk[18] states that the detector slit movement should be very carefully adjusted because an error of 1 μm when moving the detector slit 100 mm toward the center (corresponding to $\psi = 60°$ when $R_0 = 180$ mm) introduces an error of 0.001° 2θ in the line position. The shorter measuring time obtained when moving the detector is thus compensated by a longer adjustment time.

4.1.4.4.1 Practical Diffractometers for Stress Measurement

Any normal diffractometer may be used to measure stress, provided the specimen holder allows the ψ-rotation. Diffractometers are classified as vertical or horizontal, depending on the orientation of the plane defined by the primary and the reflected beams. Larger specimens may be mounted on horizontal diffractometers. Properties to look for in diffractometers from the user's point of view are: accuracy and repeatability of 2θ-setting, maximum 2θ-angle that can be measured, maximum specimen size allowed, and how fast and how accurate are the alignment procedures.

Because normal diffractometers accommodate specimens of limited size only, special open diffractometers have been developed which measure intensity lines in the back-reflection region only. Figure 24 shows an example. Small specimens may be mounted on the little column. When measuring stress on larger structures the diffractometer is turned 180° on the ground plate, after which it may be brought close to the spot of interest. Figure 25 shows a schematic lay-out of the diffractometer. The x-ray tube with focus F and the tube carriage 24 are locked in some position on the circular rail 23. This position determines the angle ψ_0 of the incident ray (the same angle as ψ_0 in Figure 22). ψ_0 may be varied between − 10° and + 60°. In contrast to normal diffractometers, the angle ψ is therefore not constant when scanning through a diffraction line. This may lead to difficulties on broad lines when using the ψ-dependent absorption factor. During measurement the detector 64 and the detector carriage 28 scan through the intensity line. The diffractometer is aligned such that the specimen surface normal coincides with the φ-axis of rotation, and the surface is in the center of the circular rail. The φ-value is changed by rotating the circular rail around the φ-axis. With this arrangement all necessary movements are done by the diffractometer itself, while the specimen position is fixed.

The use of x-ray stress measurement as a production control requires high speed and involves increased safety demands. Therefore, there has been an increasing effort toward automation of stress measurement. The first step in this direction was the automatic recording of line profiles in step-scanning and the automatic computation of line profile and position (Koves and Hy[19]).

An interesting approach to the rapid measurement of residual stresses is presented by Weinmann et al.[20]. Using an x-ray apparatus equipped with two independent x-ray tubes and two independent dual detectors operating simultaneously, they obtained repeatabilities of ± 20 MN m^{-2} for measuring times of only 3 minutes. At only 20 seconds measuring time, the repeatability decreased to ± 200 MN m^{-2}. Figure 26 shows schematically the set-up. The x-ray tubes and the specimen are fixed in relation to each other. The two outputs from each dual detector drive a

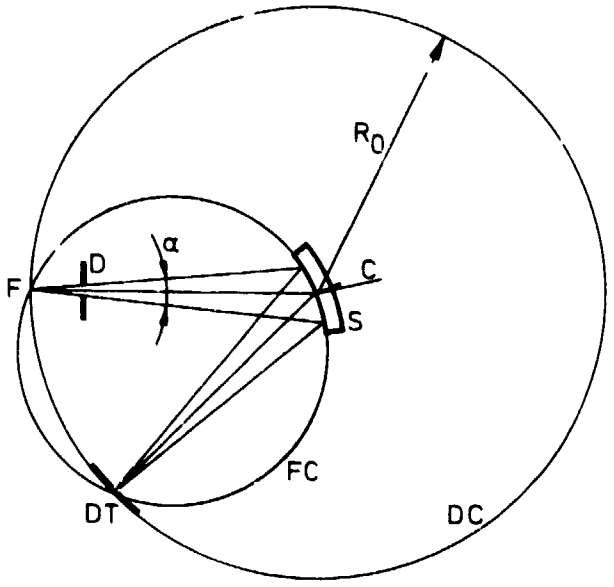

F focus
FC focussing circle
DC diffractometer circle
D divergence slit
DT detector slit
S specimen
C center of diffractometer
α divergence

Ideal Bragg-Brentano focussing at $\psi = 0$

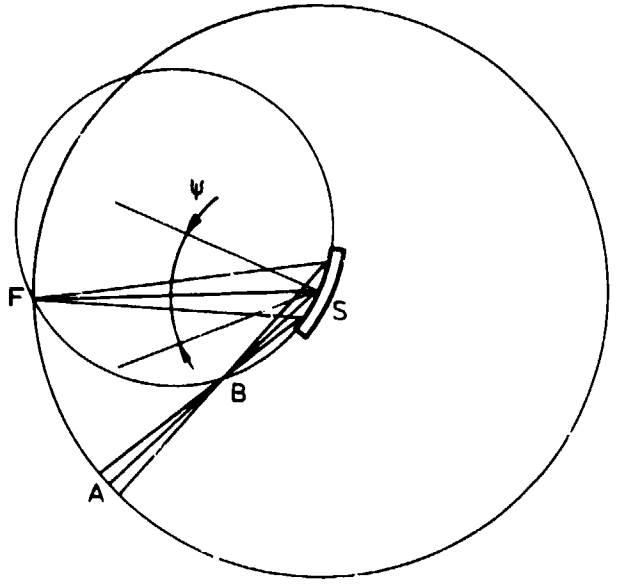

Focussing at $\psi \neq 0$

Fig.23 The focussing conditions for the diffractometer method

null-seeking mechanism which moves the detector arm until the outputs are equal. Potentiometers are driven by a gear mechanism at the end of the detector arms and the voltage difference developed between the potentiometers is calibrated to be proportional to the stress in the specimen and is plotted to give an immediate indication of the stress value.

Commercial diffractometers have now become available which permit the automatic measurement of all intensity lines for one stress measurement using the $\sin^2\psi$-method . The necessary input data for the intensity lines are punched on a card which is read by the diffractometer control box.

4.1.4.4.2 Intensity Line Measurements

Diffractometer measurements may be taken and data obtained in two different ways: continuous scan and step-scan.

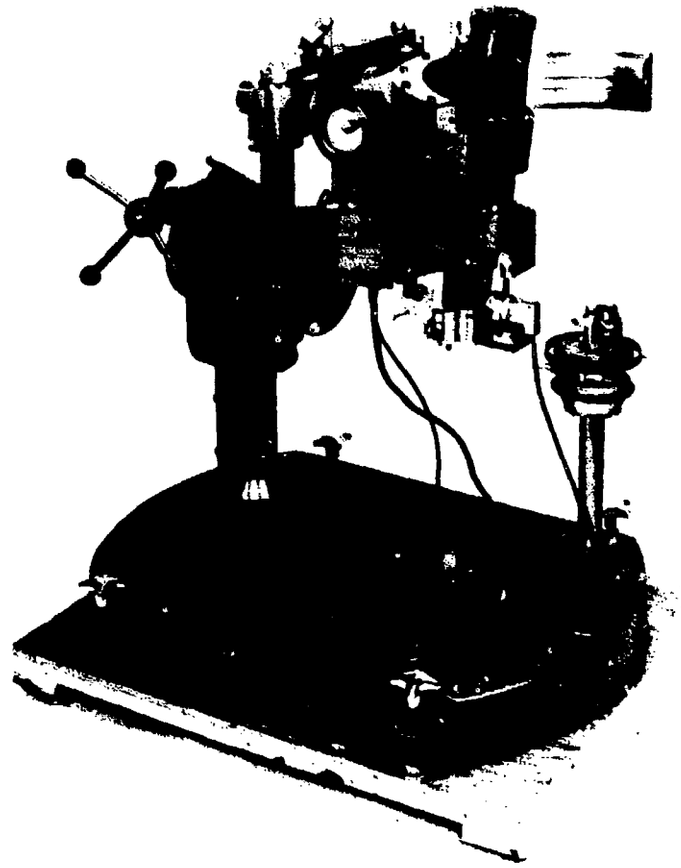

Fig.24 An open back-reflection diffractometer (courtesy of Siemens)

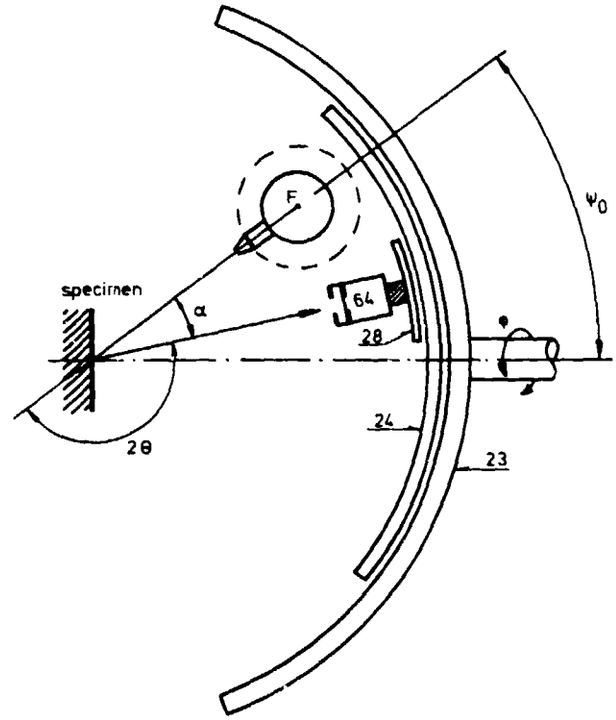

Fig.25 The principle of the back-reflection diffractometer

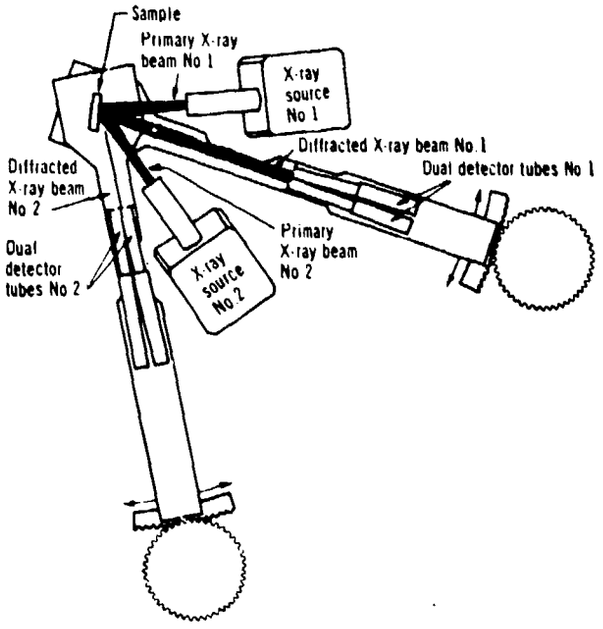

Fig.26 The principal lay-out of a special diffractometer for fast stress measurement. After Weinmann et al.[20]

In the continuous scan mode the intensity line is plotted and some graphical procedure is used to determine line position. Continuous scanning gives recordings as shown in Figure 27. To determine the line position, the line sides may be extrapolated and the crossing point used as a measure of the position. This method requires that the sides are reasonably linear, which is not the case when the lines are broad or when the K_α-lines partly overlap. A second method is to construct a middle line to the two sides and let the crossing between the middle line and the top of the diffraction line represent the line position. On broad lines this method is too inaccurate for stress measurement. A third method is to use the mid-point between the line sides at a given proportion (usually 1/2 or 1/3) of the maximum intensity. While they fail on broad lines, on narrow lines the graphical methods are accurate enough.

It is important to note that although different measuring techniques and different computing procedures yield different absolute angle positions, the necessary requirement for a good technique is that the line shift with change in ψ is proportional to stress. This requirement is not fulfilled for all combinations of computing methods and line shapes because the line profile may change with ψ.

In the step-scanning mode the reflected intensity is measured at fixed angle intervals through the diffraction line, and some computing procedure is used to establish the line position. For stress measurements the step-scan method is generally favored because correction factors are easily applied and because it may yield higher accuracy. The proper choice of number of steps and number of counts in each step depends on the computing procedure to be used. Line location estimates may be obtained as the 2θ-angle of either the centroid of the line profile or the maximum of the line profile.

Determination of the centroid is a slow procedure because the tails of the diffraction lines must be included in the measurements. On broad lines some part of the high angle tail may fall outside the measuring range of the diffractometer. Available diffractometers have an upper limit for 2θ between 160° and 165°, the limitation being caused by mechanical interference between the detector and the top of the x-ray tube. It is found that on broad lines, determination of the centroid does not lead to greater accuracy in stress than the simpler determination of the angle of the line maximum. The centroid is therefore seldom used in practical stress work.

The angle of line maximum may be determined either by approximating the top of the line with a parabola or by approximating larger parts of the line with some curve approximation. The parabola method is well established and has found general acceptance in the case of broad lines also.

Before attempting to compute the line positions, the measured intensities should be corrected for certain θ- and ψ-dependent intensity factors which influence the shape of the line profile. These are:

The polarization factor $\quad \frac{1}{2}(1 + \cos^2 2\theta)$.

The Lorentz factor $\quad \dfrac{1}{4 \sin^2\theta \cos\theta}$.

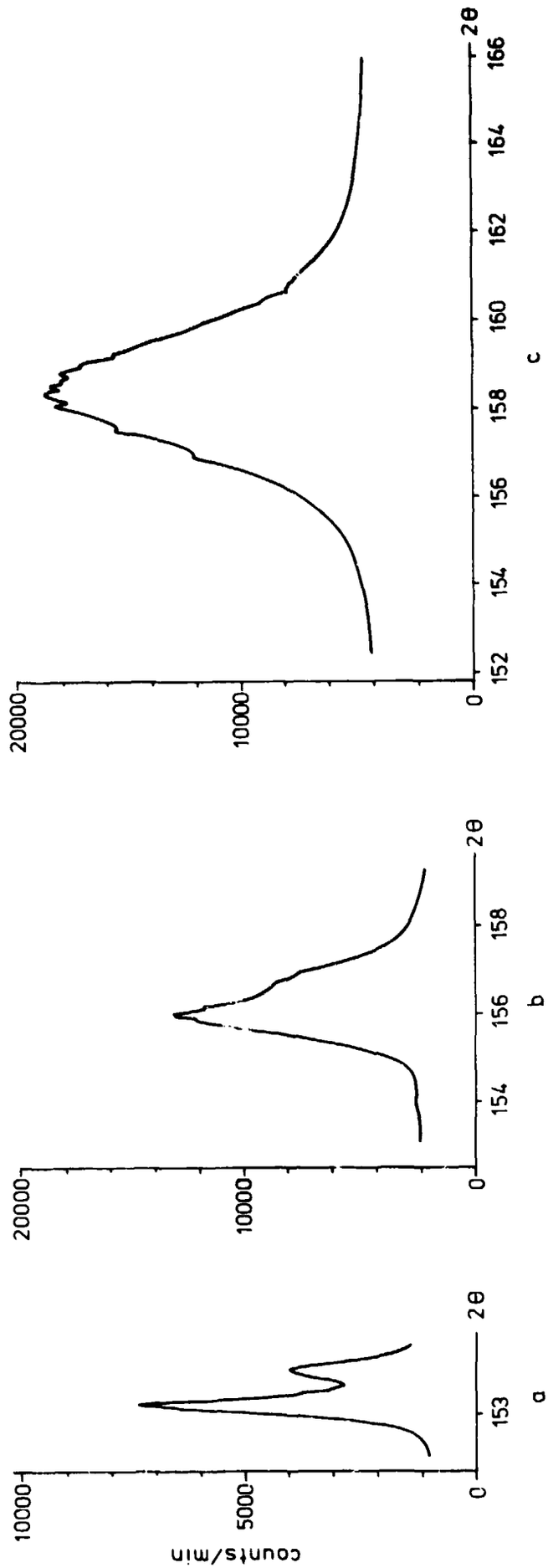

Fig.27 Examples of line profiles using Cr–K_α radiation. (a) Stress free gold powder. (b) Normalized steel. (c) Hardened steel

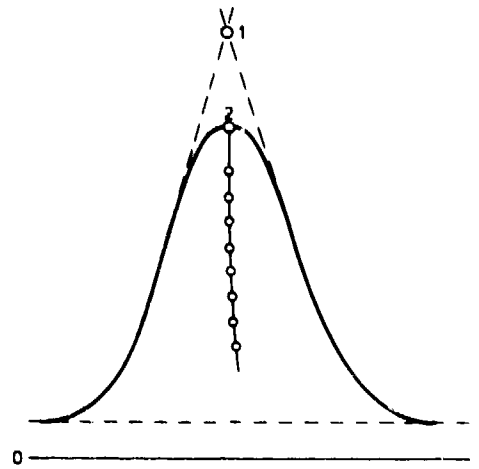

Fig.28 Two ways of estimating the line position: (1) The crossing point of the tangents. (2) The crossing point between the diffraction line and the middle line

The absorption factor $1 - \tan \psi \cot \theta$.

The polarization and the Lorentz factors are well treated in ordinary textbooks on x-ray diffraction. The absorption factor, which was derived by Koistinen and Marburger[21], is the only ψ-dependent factor. All these factors are usually combined in one

$$\text{PLA} = \frac{1}{8} \frac{(1 + \cos^2 2\theta)(1 - \tan \psi \cot \theta)}{\sin^2 \theta \cos(\theta)} . \qquad (21)$$

Intensities measured in counts per unit time are corrected by division with PLA. The correction is only necessary on broad lines, where it has the effect of improving line symmetry. This is most desirable, because most curve approximations assume the line shape to be symmetrical.

In principle, the measured intensities should be corrected for the background because the gradient of the background intensity (the change in background per degree 2θ) depends on the angle ψ, and because line symmetry is improved. However, using a wrong background gradient only leads to small errors in stress. This is fortunate because determination of the background on broad lines may be impossible on the high 2θ side of the line and the variation of background intensity beneath the diffraction line is unknown. Christenson[22] suggests that the background for the martensite line of hardened steel is that of a pure austenitic steel. The importance of the background correction increases with decreasing ratio of line intensity to background intensity and increasing line width.

4.1.4.4.3 The Three-Point Parabola Method

The line is step-scanned with low accuracy, i.e. with a small number of counts in each step (below 10,000 counts). Three points are chosen which are equally spaced on the 2θ-axis, which straddle the peak, and where the intensities in the outer points after correction by the PLA factor are approximately 85% of the peak intensity. The intensity is then measured with great accuracy at the three points (approximately 100,000 counts) and the intensities are corrected for PLA and background (Fig.29). A parabola is fitted to the measured points, and the 2θ-angle of the peak of the parabola is computed from

$$2\theta_{\text{peak}} = 2\theta_0 + \frac{3a + b}{a + b} \frac{\Delta 2\theta}{2} . \qquad (22)$$

Here $2\theta_0$, a, b, and 2θ are all defined in Figure 29.

The parabola method is the most accurate for very narrow lines or very broad lines. In both these cases the lines will be nearly symmetric after correction. In the intermediate width range, where the K_α-lines partly overlap, the resulting line profile is skewed and the parabola is not a good approximation. This would not matter if the line profile were independent of ψ-angle, because only relative changes of 2θ with change in ψ are necessary in stress measurement. However, some experimental factors lead to ψ-dependent line-broadening, thus changing the skewness of the line profile in the case of partly overlapping K_α-lines. One remedy would be to remove the $K_{\alpha 2}$-radiation with a crystal monochromator, but this generally decreases the intensity to an extent that makes this solution impractical. Another remedy is to use better line profile approximations than the simple parabola, as described in the next section.

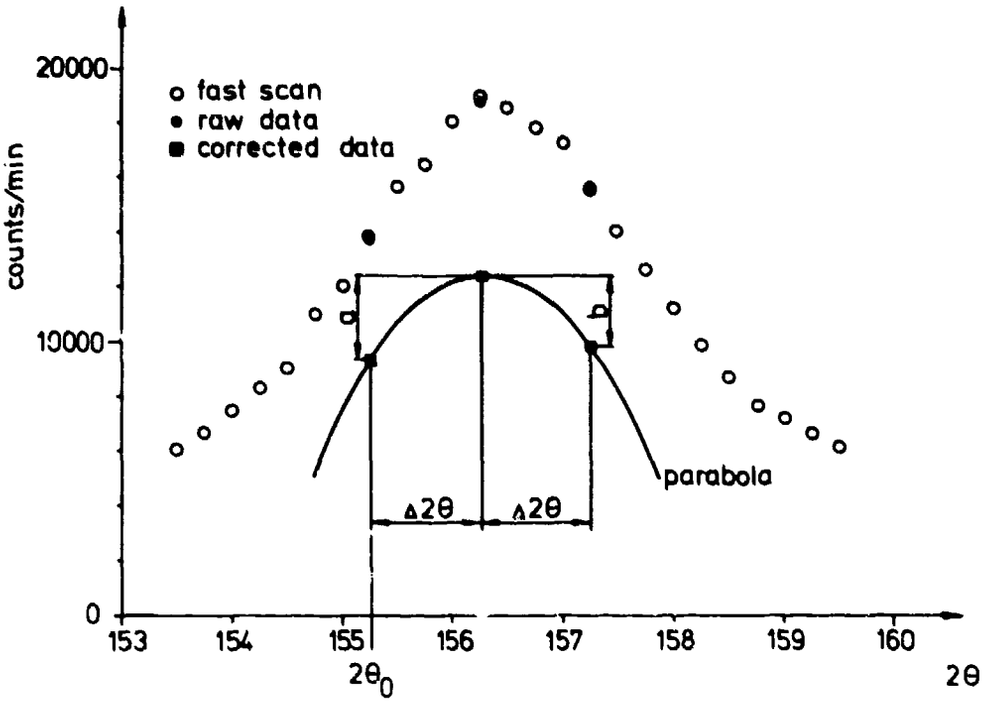

Fig.29 Illustration of the three-point parabola method

4.1.4.4.4 The Curve-Fitting Method

The most accurate way of determining intensity line positions is to approximate the line profile with a curve which has the same general shape. A good curve approximation has the following properties:

(1) It has the form

$$I = A\left[F\left(\frac{2\theta - E}{C}\right) + BF\left(\frac{2\theta - E - D}{C}\right)\right] . \tag{23}$$

This is because the intensity line profile is composed of two superimposed intensity lines due to $K_{\alpha 1}$ and $K_{\alpha 2}$ radiation. The shapes of these intensity lines (defined by the function F) are assumed to be identical except that the $K_{\alpha 2}$ radiation is approximately half as intense as the $K_{\alpha 1}$. The accurate value B of the intensity ratio depends on anode material and may be taken from tables[23], but generally B may be set equal to $\frac{1}{2}$. E is the 2θ-angle of the maximum of the $K_{\alpha 1}$-line. C is a measure of the line width. C gives information on microstrains and on the size of the crystallites. D is the 2θ-angle difference between the K_α-lines. D may be computed from the tabulated wavelengths $\lambda_{\alpha 1}$ and $\lambda_{\alpha 2}$ by the formula

$$D = 2\frac{\lambda_{\alpha 2} - \lambda_{\alpha 1}}{\lambda_{\alpha 1}} \tan\left(\frac{2\theta_{\alpha 1}}{2}\right) . \tag{24}$$

In Equation (24) the angle $2\theta_{\alpha 1}$ is determined with sufficient accuracy as the angle of the greatest measured intensity after correction for PLA and background.

(2) The function $F = F(z)$ in Equation (23) is symmetrical about $z = 0$.

(3) $F(z)$ approaches zero as z approaches $\pm$ infinity.

The following types of curves all have the required properties and have been found useful for stress work.

$$F_1(z) = \exp(-z^2) \tag{25}$$

$$F_2(z) = (1 + z^2)^{-1} \tag{26}$$

$$F_3(z) = (1 + z^2)^{-2} . \tag{27}$$

That these curves are useful does not imply that the line profiles have precisely the same shape as any of the

Equations (25) to (27). Many experimental conditions influence the line profile. The more important conditions and their effect on the line profile are listed below:

(1) The detector slit yields a rectangular intensity profile of the same width as the slit.

(2) The intensity distribution over the anode of the x-ray tube (an example of which is shown in Figure 30 taken from Wilson[24]) yields intensity lines with the same profile.

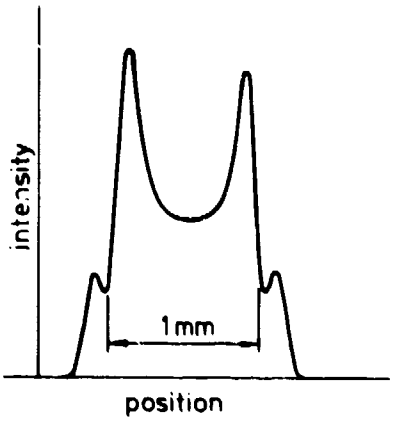

Fig.30 Intensity distribution over the anode of an x-ray tube. After Wilson[24]

(3) The K_α-radiations are not strictly monochromatic. The distribution of wavelength is approximately gaussian [curve F_1, Equation (25)] around the mean value.

(4) The size distribution of the crystallites in a polycrystalline material becomes important when the crystallites are small, because small crystallites broaden the diffraction lines. The size distribution is approximately of Cauchy type [curve F_2, Equation (26)] (Ref.25).

(5) The distribution of microstrains is approximately gaussian [curve F_1, Equation (25)] (Ref.25).

In Equation (23) the parameters A, C and E are preferably determined such that the sum S of squares of the normalized errors is minimized. This sum may be written

$$S = \sum_{i=1}^{m} \left(\frac{I_i - I_{curve,i}}{s(I_i)} \right)^2 , \tag{28}$$

where m is the number of steps, I_i are the measured intensities, I_{curve} are computed from the curve approximation formula at the same 2θ-value, and $s(I_i)$ are the standard deviations of the measured intensities.

$$s(I_i) = \frac{I_i}{\sqrt{(N_i)}} , \tag{29}$$

where N_i is the number of counts in the intensity measurement. The computing procedure is too cumbersome to be made manually, so a computer program has to be used. For the computing procedure to be effective, the lines should be step-scanned at least for intensities down to one half the maximum intensity, and the number of steps should be much greater than the number of parameters (i.e. greater than 3) to be determined.

Although so many experimental factors contribute in different ways to the shape of the line profile, quite close agreement between measured and computed intensities may be obtained as shown in Figure 31. The vertical lines at the measured intensities indicate the uncertainty ranges defined as two times the standard deviation on each side of the points. Equally good agreement was obtained for $\psi \neq 0$ and for the narrow gold line.

4.1.4.5 Comparisons Between the Film and the Diffractometer Method

The equipment for the film method is cheaper because the high voltage source does not have to be highly stabilized and because sophisticated electronics are not needed.

With the film method it is easy to get access to large structures of complicated shape.

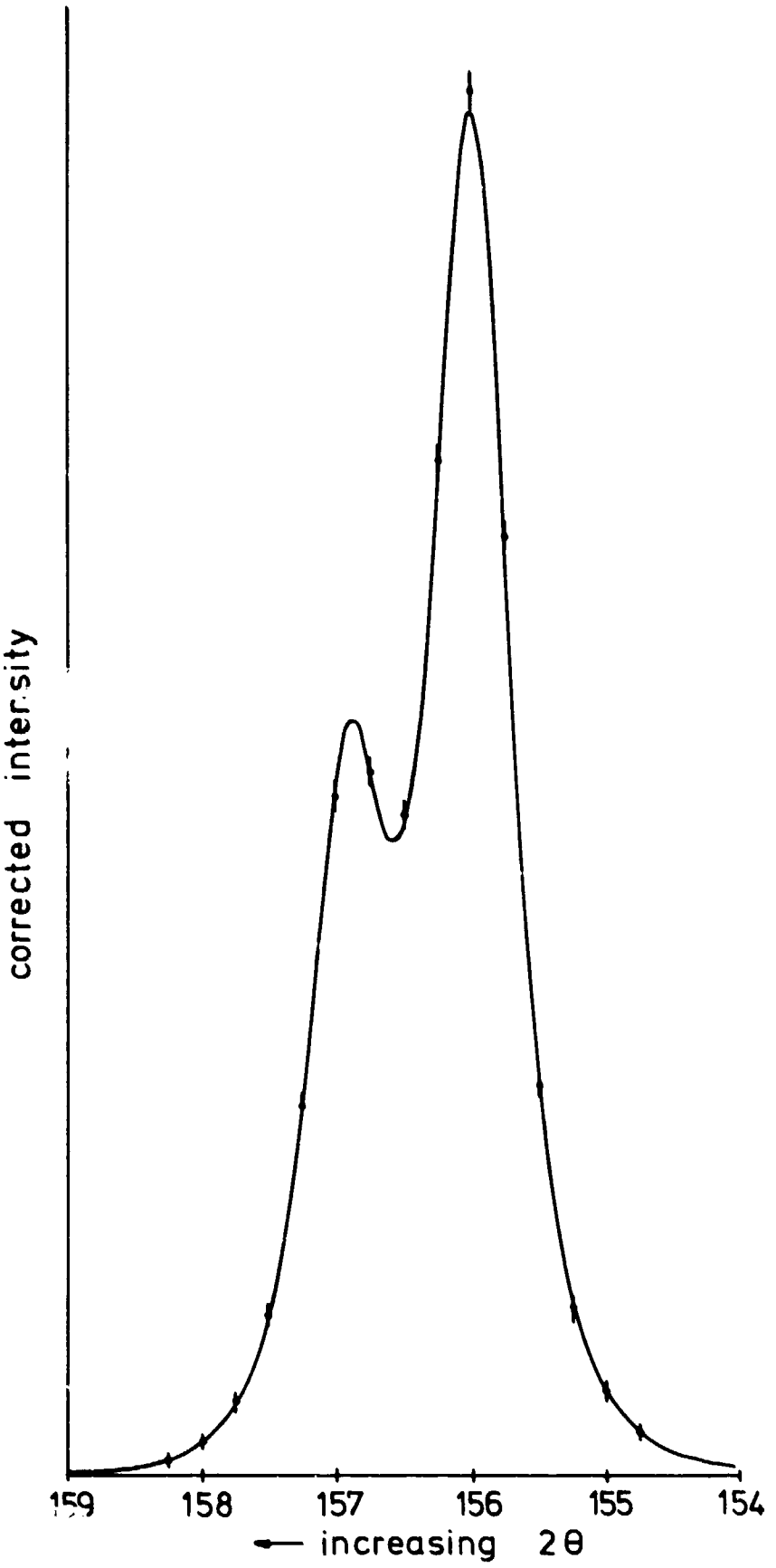

Fig.31 Example of agreement between line profile approximation and measured and corrected intensities. Measuring conditions were: Cr-K_α, normalized carbon steel, $\frac{1}{2}°$ divergence slit, 1 mm receiving slit, $\psi = 0$, discrimination with filter and electronically, line profile approximation using Equation (27)

The diffractometer method is faster for the same accuracy.

Generally the diffractometer method is the more accurate, because increased ratios of line intensity to background intensity can be obtained.

On broad lines that result after hardening or large plastic deformation of inhomogeneous materials, only the diffractometer method may be used because the measurement of the line position on the film becomes too inaccurate.

4.1.4.6 Experimental Factors Affecting Measuring Accuracy

4.1.4.6.1 X-Ray Elastic Constants

The elastic constant $\frac{1}{2}s_2$ used in Equation (9) to compute stress cannot generally be computed from Equation (6) using the bulk values of the elastic moduli E and ν. The value of $\frac{1}{2}s_2$ depends on many factors: x-ray radiation, the set of reflecting planes, grain size, degree of cold work, composition of material etc. For the case of steel, values of $\frac{1}{2}s_2$ reported in the literature vary between 3.8×10^{-6} and 8.6×10^{-6} m²/MN depending on the combination of the above-mentioned factors. Using the bulk values of E and ν, $\frac{1}{2}s_2$ would be computed to be 6.4×10^{-6} m²/MN. The effect of some influencing factors on the value of $\frac{1}{2}s_2$ are treated, for example, by Prümmer[26], Faninger[27] and Taira et al.[28]. For accurate stress work the value of $\frac{1}{2}s_2$ must therefore be determined experimentally using known load stresses. When measuring $\frac{1}{2}s_2$, the applied stresses may not be increased past the x-ray yield stress, i.e. the yield stress of the surface material. This is generally lower than the yield stress of the bulk material.

4.1.4.6.2 Misaligned Diffractometer

Correct stress measurement is, in principle, only possible with a correctly adjusted diffractometer. Some misalignments lead to ψ-dependent changes of 2θ which cannot be distinguished from the changes caused by stresses. The alignment is correct when the anode, the center line of the divergence slit, the diffractometer axis of rotation, and the centerline of the detector slit all lie in the same plane when the detector is in position 0°. When measuring stress, the surface of the specimen must be tangential to the center axis of the diffractometer. However, the requirements for the adjustments when measuring stress are not severe, because only differences in 2θ-angles at different ψ-angles are used to compute the stresses. On one occasion, deliberate misadjustment of the specimen surface 1 mm behind the center produced an error in the stress of only 40 MN/m² (the conditions were: Cr K_α, $2\theta = 156°$, normalized carbon steel, measurement at $\psi = 0$ and 60°). This error vanished within the measuring accuracy when the measured line shifts were corrected using the line shifts of the gold line at $2\theta = 153°$ measured at the same ψ-angles. Other tests have shown that the errors in stress produced by misadjustments of anode and divergence slit up to 0.1 mm can also be completely corrected using a suitable stress free powder.

4.1.4.6.3 Surface Roughness

Surface roughness may cause errors in stress measurement because of the small penetration of the x-rays. When using Cr–K_α radiation on a steel specimen at $\psi = 0$, 50% of the measured intensity is reflected from layers less than 3.8 μm from the surface and 95% of the measured intensity is reflected from layers less than 16 μm from the surface. At $\psi = 60°$ the corresponding depths decrease to 1.6 μm and 7 μm. Taira and Arima[29] investigated the effect of surface roughness on x-ray stress measurement on a 0.17% carbon steel. The x-ray stress was determined from diffraction line measurements at $\psi = 0°$ and 45°. They found that surface scratches parallel to the applied stress had no effect on the value of stress. The effect of scratches perpendicular to the applied stress is shown in Figure 32. The effect of the roughness is explained by noting that with increasing roughness an increasing part of the reflected intensity comes from the mountains on the surface where the stresses are smaller than in the valleys.

4.1.4.6.4 Microstresses

Microstresses may affect the measured stress values. Experience has shown that not only do microstresses broaden the diffraction lines, but they may also shift the diffraction lines in the same way as macrostresses. This is in contrast to what might be expected, because the microstresses are in equilibrium over distances much smaller than the irradiated area. The effect of microstresses is illustrated by tests made by Kolb[30] (Fig.33). Steel specimens were deformed plastically in tension and the resulting residual stress distributions in depth were found by removing material layers by electropolishing. The measured stress values do not converge to zero when almost all material is removed, as would have been the case if the measured stresses were macrostresses. The measured stress distribution is not in equilibrium over the cross section, so part of the measured stresses must be ascribed to the mean value of microstresses. The apparent lack of equilibrium of the microstresses is caused by the selective character of the x-ray measuring method. Only crystals with their reflecting plares oriented in a small angle range in the specimen reflect x-rays. In uniaxial tension the dislocations move preferentially in an angle range where the shear stress is largest. The microstresses created, therefore, show a direction dependency which is detected by the x-ray method.

The value of the microstresses depends on the plastic deformation and on the degree of heterogeneity in the material. In carbon steels the value increases with increasing carbon content. Kolb and Macherauch[31] found that

microstresses were not created in steels with carbon content less than 0.4%. This is however in contrast with the test results of Taira and Yoshioka[28], who found microstresses in steels with 0.14% carbon.

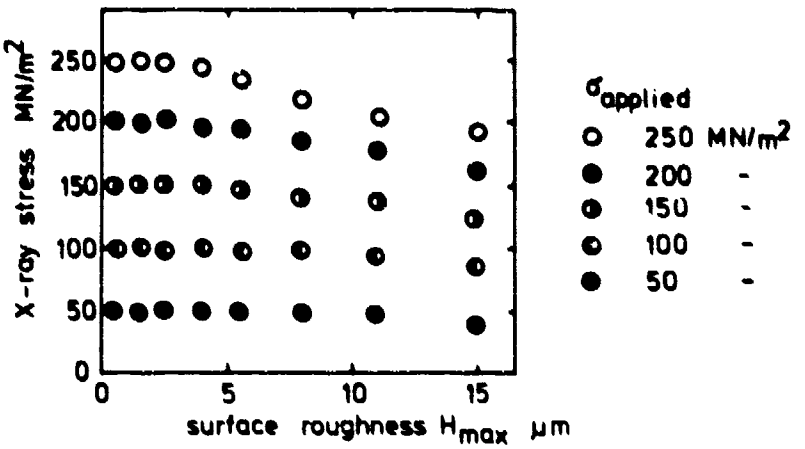

Fig.32 The effect of surface roughness on the measured stress value. The scratches were perpendicular to the stress. After Taira and Arima[29]

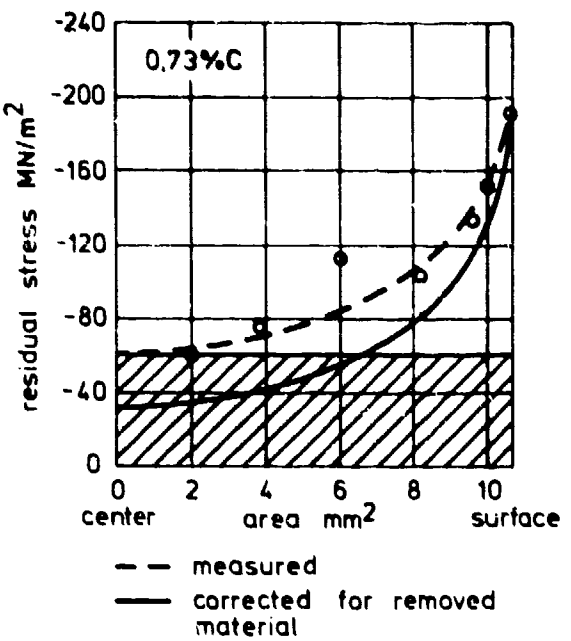

Fig.33 Residual stress distribution over the cross section after plastic tensile deformation. After Kolb[30]

If it is known that the material of the component to be measured has been deformed plastically, it is thus necessary to consider the possibility of erroneous stress values caused by superimposed microstresses.

4.1.4.6.5 Change in Temperature During Measurement

Stresses are computed from two or more diffraction line measurements carried out at different times. A change of material temperature between the measurements shifts the diffraction lines because of the thermal expansion, and an error results. The temperature sensitivity of diffraction lines may be computed from

$$\frac{\Delta 2\theta}{\Delta T} = -2 \tan \theta \, \alpha_T \, . \qquad (30)$$

Here ΔT is the change in temperature and α_T is the thermal expansion coefficient for the material. Strictly speaking, α_T should be the expansion coefficient for the reflecting set of crystallographic planes, but the bulk value is a useful approximation. For the commonly used combination of Cr K_α radiation on steel ($2\theta = 156°$), a $\Delta T = 1°C$ causes a line shift of $-0.007°2\theta$. If the stress measurement is carried out at $\psi = 0$ and 45° and the shift occurs between the two measurements, an error of approximately 4 MN/m² is introduced. This value is of the same order of magnitude as the stress measuring accuracy using the best methods available today. The temperature should therefore be kept as constant as possible during measurement.

4.1.4.6.6 Errors Caused by the Grain Structure of the Materials

In a polycrystalline material loaded with homogeneous macrostresses, the strains are not homogeneous on a microscale. The strains in a grain depend on its orientation in relation to the neighbouring grains and on the orientation of the crystal planes in relation to the principal stress directions. Therefore, the strains vary from grain to grain and only statistical descriptions of the strains are possible. If the irradiated number of grains is sufficiently large, the mean strain will be proportional to the applied stress. The factor of proportionality depends on the set of crystal planes used in the measurement.

When irradiating a polycrystalline material with x-rays, only a small number of the grains contribute to the reflected intensity (only those which lie in a small angle range around the correct reflecting position). From a statistical point of view the reflecting grains may be considered as a random sample from a large population. If the mean strain in the sample differs from the mean strain in the population, erroneous stress values will be computed. The errors become important when the grains are large or when a small area (i.e. the bottom of a notch) is irradiated.

4.1.4.7 The Measurement of Stress Versus Depth

In some cases the surface stress alone does not give all the necessary information, but the stress versus depth curve must also be known. To measure the stress distribution below the surface, the non-destructivity of the measurement must be sacrificed. The measurement is carried out by electropolishing off layers of the material and measuring the stress on the new surfaces. Mechanical removal of material is not recommended because residual stresses are introduced no matter how carefully the surface is machined.

When measuring stresses versus depth, the problem is that the measured stresses must be corrected for the forces exerted by the stresses in the removed material. The correction depends both on the original shape of the specimen and on the place on the specimen where the material is removed. Correction methods have only been developed for the case of cylindrical specimens etched axisymmetrically and for the case of flat plates etched on one side.

For cylindrical specimens it may be shown (e.g. Ref.33) that if x-ray stresses, $\sigma_{x\text{-ray},i}$, are measured at decreasing cross-section areas, f_i, the stress, σ_n, in the undisturbed specimen at cross section area f_n is given by

$$\sigma_n = \sigma_{x\text{-ray},n} + \sum_{i=1}^{n-1} \sigma_{x\text{-ray},i} \frac{f_{i+1} - f_i}{f_i} \quad (31)$$

The formula is approximate because the x-ray stress is measured in discrete steps and not continuously. Figure 34 shows an example of the application of Equation (31).

Doi and Sato[34] derived a relationship between measured stresses and the stresses in the undisturbed specimen for the case of a flat plate etched on one side. When the stresses were measured on the etched surfaces they found an integral equation which, using summations instead of integrals, may be written

$$\sigma_n = \sigma_{x\text{-ray},n} + 2\sum_{i=1}^{n}\left(\sigma_{x\text{-ray},i}\frac{z_{i+1} - z_i}{h - z_i}\right) - 6(h - z_n)\sum_{i=1}^{n}\left(\sigma_{x\text{-ray},i}\frac{z_{i+1} - z_i}{(h - z_i)^2}\right). \quad (32)$$

In Equation (32), z is the thickness of the removed material layer and h is the original thickness of the plate. The first summation sign is due to the normal force exerted by the removed material, and the second summation is due to bending moments. Equation (32) may be used for both principal stress directions of the plate. A similar equation was derived for the case where the x-ray stress measurement and the polishing occurred on the two opposite faces of a plate.

4.1.5 SOME FUTURE NON-DESTRUCTIVE STRESS MEASURING METHODS

4.1.5.1 The Ultrasonic Stress Measuring Method (See Chapter 3.6)

Ultrasonic wave velocities depend on the state of stress. This well-known fact is now in the early stages of development as a means of measuring both loading stresses and residual stresses[35,36]. Ultrasonic waves are either

longitudinal or shear waves, i.e. the particle motions are parallel or perpendicular respectively to the direction of the wave propagation. Ultrasonic shear waves have the same polarization property as light waves, such that all particle motions lie in the same plane. The velocity of both longitudinal and shear waves depend on the stress, but in stress work only polarized shear waves are used, because the change in velocity of a polarized shear wave depends on the angle between the principal stress directions and the direction of polarization. Using shear waves thus gives information both on the direction and the difference of the principal stresses, while the use of longitudinal waves gives information only on the sum of the principal stresses and not their direction.

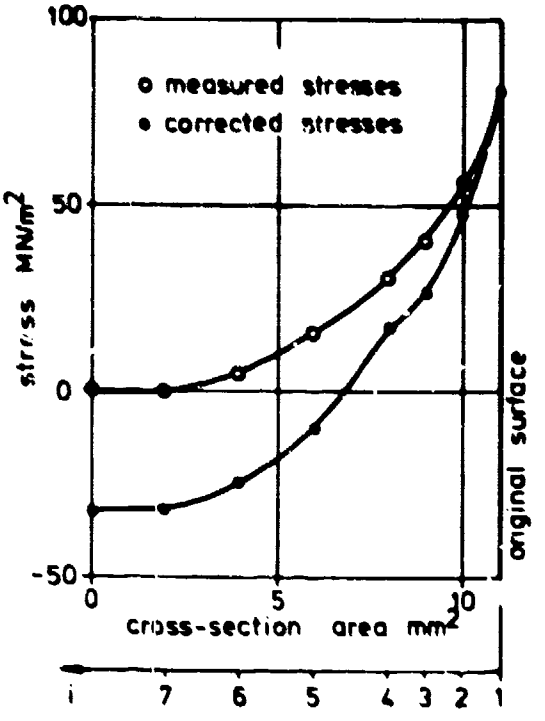

Fig.34 Illustration of the use of Equation (31)

The velocity of shear waves is determined by

$$V_s = \sqrt{(\mu/\rho)}\,, \tag{33}$$

where μ is the shear modulus and ρ is the density. The ultrasonic method exploits the fact that the stress-strain curve is not exactly linear (as is conventionally postulated in Hooke's law of the theory of elasticity), i.e. the shear modulus and hence, according to Equation (33), also the velocity, is dependent on stress. The change in velocity is found to be proportional to the stress in the material (Figure 35 from Reference 35).

Before the ultrasonic stress measuring method may be used as a standard measuring method, several difficulties have to be solved. The first problem is that of actually getting shear waves into the material. The normally used coupling oil-film cannot transmit shear waves, so either a very viscous coupling medium must be used or the transducer may be cemented to the surface.

A second problem is caused by preferred orientation in the material, which also changes the velocity of shear waves. Preferred orientations of one or more per cent, which are often encountered in practice, may completely hinder residual stress measurements. However, it is still possible to measure loading stresses, because the velocity change may be referred to the velocity at zero loading stress.

The measurement gives an average stress value in the material volume traversed by the ultrasonic beam. The minimum length of the path is of the order of 10 mm, and the minimum width of the ultrasonic beam is possibly of the order of 5 mm.

4.1.5.2 The Knoop Hardness Stress Measuring Method

It is an old observation that the hardness is dependent on the state of stress in the material. The normal hardness testing methods are however not sensitive to the direction of the stresses. In 1964 Oppel[37] showed that

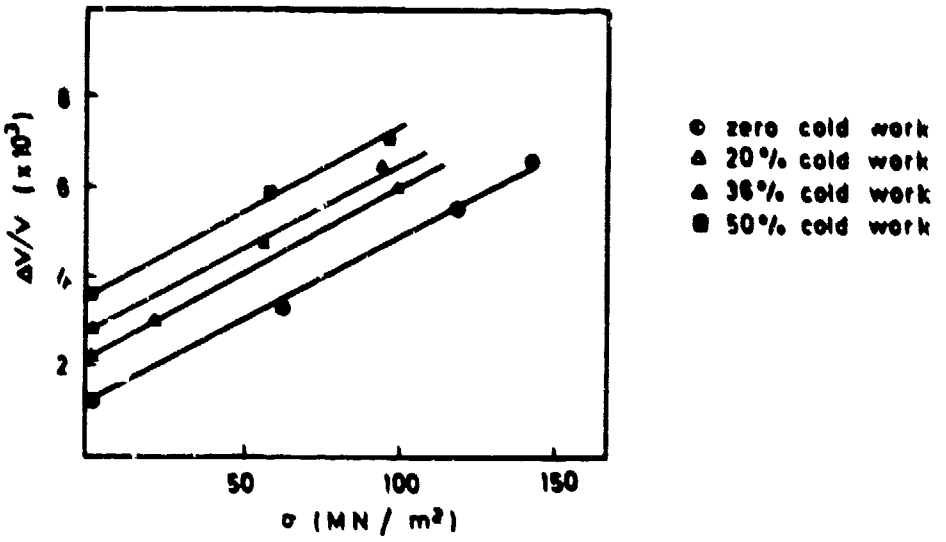

Fig.35 Relative change in ultrasonic velocity as function of stress and cold work. After Gause[35]

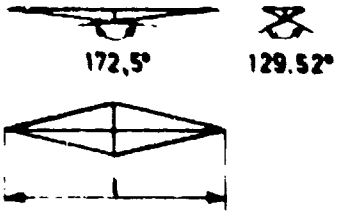

Fig.36 Impression mark of the Knoop diamond

indentations of the Knoop diamond (Fig.36) are sensitive both to the direction and the size of the residual stresses. The Knoop hardness is computed from

$$H_{Knoop} = 14.23 \cdot P/l^2 \quad (kp/mm^2) \tag{34}$$

where P is the force in kp and l is the length of the long diagonal of the indentation in mm. Oppel showed the following equations to be valid in a linear range

$$\sigma_x + \sigma_y = Ea(\Delta H_x + \Delta H_y) \tag{35}$$

$$\sigma_x - \sigma_y = Eb(\Delta H_x + \Delta H_y) . \tag{36}$$

In these formulas ΔH_x and ΔH_y are defined by

$$\Delta H_x = \frac{H_x - H_0}{H_0} \quad \text{and} \quad \Delta H_y = \frac{H_y - H_0}{H_0} . \tag{37}$$

H_x and H_y are the Knoop hardness with the long diagonal in the direction of the subscript. The coefficients a and b may be determined from a loading test with known uniaxial stress. Both a and b are negative. H_0 is the hardness in the stress-free state. Thus, by measuring the Knoop hardness in two perpendicular directions x and y, the stresses in these directions may be found. If the principal stress directions are unknown, the hardness must also be measured in the directions x + 45° and y + 45° and the stresses in these directions computed. The principal stresses and their direction in relation to the x and y directions may then be computed from formulas analogous to Equations (13), (14) and (15).

The Knoop stress measuring method has the following characteristics:

(1) The measured stress values are average stresses over depth of approximately 10 μm (assuming a load P = 1 kp on steel specimens)

(2) The spread in hardness measurements is rather large. Therefore, to obtain acceptable stress accuracies a large number of hardness measurements have to be carried out in the surface region of interest (about 10 in each direction).

(3) The indentation mark in the surface makes this method semi-nondestructive, because the fatigue strength of the member is reduced. The defect may however be repaired by pressing a Brinell ball over the Knoop indentation. In this way the stress concentration is reduced and high local compressive residual stresses are introduced at the tip of the indentation.

(4) The Knoop method is also applicable on materials other than metals. Racké and Fett[38] demonstrated its use on different polymers as well.

Stengel and Gaymann[39] discussed the difficulties of the Knoop method and gave the following main causes of uncertainty:

(1) Determination of the reference hardness H_0. H_0 must be measured at a stress free spot which has the same basic hardness. If it is not possible to measure H_0, then only the difference between the principal stresses can be measured (by using H_1 or H_2 instead of H_0 in Equation (37)). A uniaxial stress state may be measured using the same approximation.

(2) Scatter of hardnesses. The inevitable scatter of the hardness measurements causes a corresponding scatter in the measured stress. It is claimed that the 95% error limits are 35 MN/m² when measuring uniaxial stress on polished 2024 aluminium alloy. For steel the corresponding values are ± 100 MN/m².

(3) Inclination of the test surface. The measured stresses are very sensitive to the angle of inclination. An angle of 0.5° produces a stress error of 40 MN/m² in aluminium and 130 MN/m² in steel. Reference 39 gives a correction curve for inclination errors.

(4) Curvature of the test surface. The Knoop hardness is very sensitive to curvatures. Even a small curvature of 50 mm radius causes an error in stress of 400 MN/m². Curved surfaces should therefore be machined flat, but it is doubtful whether this can be done without introducing additional disturbing residual stresses.

(5) Other effects which influence the residual stresses but which are difficult to evaluate quantitatively are texture, plated surfaces, plastic deformation (work hardening), and uneven quenching effects.

REFERENCES

1. Peiter, A. — *Eigenspannungen I.* Art. Michael Triltsch 1966.
2. Forrest, P.G. — *Fatigue of Metals*, Pergamon Press, 1962.
3. Champion, F.A. — *Corrosion Testing Procedures*, Wiley, 1965.
4. Helfrich, W.J. — ASTM STP 425, pp.21-30, 1967.
5. Speakman, E.R. — ASTM STP 46., pp.209-25, 1970.
6. Mattson, R.L. Roberts, J.G. — p.337 in Rassweiler and Grube: *Internal Stresses and Fatigue of Metals*, Elsevier, 1959.
7. Winter, P.M. McDonald, W.J. — Journ. of Basic Engineering 91 Series D, pp.15-22.
8. Bühler, H. Tönshoff, H.K. — *Werkstatt und Betrieb* 100, pp.211-18, 1967.
9. Letner, H.R. — Trans. of the ASME 77, pp.1089-98, 1955.
10. Peiter, A. — *Zeitschr. für Metallkunde* 57, pp.1-8, 1966.
11. Gurney, T.R. — *Fatigue of Welded Structures*, Cambridge University Press, 1968.
12. Hammer, K. — *Härterei-Technische Mitt.* 22, pp.160-65, 1967.
13. Harris W.J. — *Metallic Fatigue*, Pergamon Press, 1961.
14. Rosenthal, — Chapter in *Metal Fatigue* (G.Sines and J.L.Waisman) McGraw-Hill, 1959.

15. Morrow, JoDean; Sinclair, G.M. — ASTM STP 237, pp.83-109, 1959.

16. Glocker, R. — *Materia prüfung mit Röntgenstrahlen*, Springer Verlag, 1971.

17. Macherauch, E.; Müller, P. — *Zeitschr für Angewandte Physik* 13, p.305, 1961.

18. Kirk, D. — *Strain* 7, pp.7-14, 1971.

19. Koves, G.; Ho, C.Y. — Norelco Reporter 11, pp.99-102, 1964.

20. Weinmann, E.W.; Hunter, J.E.; McCormack, D.D. — *Metal Progress* 96, pp.88-90, 1969.

21. Koistinen, D.P.; Marburger, R.E. — Trans. of the ASM 51, p.537, 195º

22. Christenson, A.L. et al. — *The Measurement of Stress by X-Ray*, SAE Information Report TR 182, 1960.

23. Lonsdale, K. — *International Tables for Crystallography*, The Kynoch Press, 1968.

24. Wilson, A.J.C. — *Mathematical Theory of X-Ray Powder Diffractometry*, Philips Technical Library, 1963.

25. Warren, B.E. — *Progress in Metal Physics* 8, pp.147-202, 1959.

26. Prümmer, R. — Doctor Dissertation, Universität Karlsruhe, 1967.

27. Faninger, G. — *Härterei Technische Mitt.* 22, pp.26-36, 1967.

28. Taira, S.; Hayashi, K.; Watase, Z. — The Twelfth Japan Congress on Materials Research, pp.1-7, 1969.

29. Taira, S.; Arima, J. — Proc. 7th Japan Congress on Testing Materials, Kyoto, pp.21-25, 1964.

30. Kolb, K. — *Härterei Technische Mitt.* 20, pp.228-37, 1965.

31. Kolb, K.; Macherauch, E. — *Zeitschr. Metallkunde* 58, pp.238-42, 1967.

32. Taira, S.; Yoshioko, Y — Proc. 7th Japan Congress on Testing Materials, Kyoto, pp.31-37, 1964.

33. Christian, H. — *Härterei-Technische Mitt.* 26, pp.180-98, 1971.

34. Doi, O.; Sato, Y. — Bulletin of the Japan Soc. Mech Engrs 14, pp.383-91, 1971.

35. Gause, R.L. — *Ultrasonic Analysis of Cold-Rolled Aluminium*, NASA-SP-5082, pp.31-42, October 1966.

36. Crecraft, D.I. — *Strain* 1, pp.4-8, 1965.

37. Oppel, G.U. — *Experimental Mechanics* 21, pp.135-40, 1964.

38. Racké, H.H.; Fett, T. — *Materialprüfung*, pp.37-42, 1971.

39. Stengel, B.; Gaymann, T. — *Determination of Residual Stresses by Indentation Hardness Testing*, Paper 16, AGARD Symp. on Stress Corrosion, 1972.

CHAPTER 4.2

NDI OF WELDING

by

G.Fenoglio and G.Magistrali

Laboratori Centrali FIAT
Strada Torino, 50
10043 Orbassano, Torino
Italy

CONTENTS

4.2.1 INTRODUCTION

4.2.2 WELDING IN THE AERONAUTICAL INDUSTRY

4.2.3 INERT-GAS TUNGSTEN-ARC WELDING (T.I.G.)

4.2.4 SHIELDED METAL-ARC WELDING

4.2.5 GAS METAL-ARC WELDING

4.2.6 GAS WELDING

4.2.7 ARC-SPOT WELDING

4.2.8 STUD WELDING

4.2.9 PLASMA ARC WELDING

4.2.10 ELECTRON-BEAM WELDING

4.2.11 SPOT, SEAM AND STITCH WELDING

4.2.12 FLASH WELDING

4.2.13 WELDING OF MATERIALS USED IN THE AERONAUTICAL INDUSTRY

4.2.14 ALUMINIUM AND ALUMINIUM ALLOYS

4.2.15 WELDABILITY OF ALUMINIUM AND ITS ALLOWS: WELDING DEFECTS
- 4.2.15.1 Inclusions, Accretion of Foreign Particles and Fracture
- 4.2.15.2 Blowholes and Porosity
- 4.2.15.3 Tendency to Cracking

4.2.16 TITANIUM AND TITANIUM ALLOYS

4.2.17 WELDABILITY OF TITANIUM AND ITS ALLOYS. WELDING DEFECTS
- 4.2.17.1 Porosity
- 4.2.17.2 Tendency to Cracking

4.2.18 STAINLESS STEELS

4.2.19 WELDABILITY OF AUSTENITIC STAINLESS STEELS. WELD DEFECTS
- 4.2.19.1 Tendency to Cracking
- 4.2.19.2 Porosity and Inclusions

4.2.20 NICKEL AND NICKEL ALLOYS

4.2.21 WELDABILITY OF NICKEL AND ITS ALLOYS. WELDING DEFECTS
- 4.2.21.1 Incomplete Root Penetration. Blowholes
- 4.2.21.2 Slag Inclusions
- 4.2.21.3 Oxide Inclusions. Lack of Fusion
- 4.2.21.4 Tendency to Cracking

4.2.22 TYPICAL WELDING DEFECTS AND THEIR DETECTION BY NON-DESTRUCTIVE TESTING

4.2.23 DANGER OF DEFECTS AND ACCEPTABILITY CRITERIA

FIGURES

NDI OF WELDING

G.Fenoglio and G.Magistrali

4.2.1 INTRODUCTION

Welding is a method of joining parts which maintains the continuity of the material between the two sections joined. When applied to metal parts it provides continuity of the metal surface and from this viewpoint it is entirely different from other types of permanent joint, such as riveting or gluing.

This achievement of metal continuity through the welded joint involves the fusion of certain amounts of the parent metal and the filler metal.

Fusion implies the action of special thermal and chemico-metallurgical factors in the welded material. The thermal conditions occurring are the attainment of a temperature higher than the melting point of the parent metal in the fusion zone and the achievement of a thermal gradient transverse to the axis of the weld, such as to cause, in the fusion zone, thermal changes in the parent metal.

Concerning the chemico-metallurgical factors, it is well known that the solidification of any alloy occurs within a certain range of temperature and, in the cooling phase which follows, structural modifications may take place in the alloy.

Correct welding procedure calls for strict compliance with the thermal and chemico-metallurgical conditions required. When perfect conditions, depending on the parent metal to be welded and on the welding process adopted, are not achieved, the metal continuity through the weld shows areas of discontinuity (spots) known as welding flaws.

4.2.2 WELDING IN THE AERONAUTICAL INDUSTRY

The aeronautical industry has universally accepted welding as a working process of joining metals in aircraft manufacture. The advent of supersonic aircraft has brought with it ever-increasing operational temperatures and more severe service conditions; these new factors have further emphasized the importance of this technology and demand continuous refinement of the various welding processes, as well as the development of new techniques.

The processes of autogenous welding by fusion or pressure (resistance welding) are the most interesting. The choice of process may sometimes be difficult since it requires a thorough analysis by means of destructive and non-destructive corrosion, impact and fatigue tests and is always conditioned by the following factors:

(a) in-service conditions of the product,
(b) geometry of the joint,
(c) structure of the parent metal,
(d) characteristics inherent in the various welding processes,
(e) characteristics of the welds made by the various welding processes,
(f) economic considerations.

4.2.3 INERT-GAS TUNGSTEN-ARC WELDING (T.I.G.)

The process of welding with a gas shield and a non-consumable electrode of tungsten is the most widespread, and it can be either manual or automatic. Manual welding is preferable when the part to be welded is of irregular shape with variable section (e.g., pipes, accessories, cowlings and cowling components). The automatic process is preferable for longitudinal welds when a minimum of distortion and the smallest possible extent of the heat-affected zone are required. Automatic welding also has the advantages of a high-speed process.

For thicknesses up to 0.020 inch it is not practicable to add metal in filler rod form. In such cases, on each part to be welded, a flange twice as high as the thickness of the metal sheet must be obtained by folding. The flange is melted and so provides the filler metal for the weld. For thicknesses above 0.020 inch it may be necessary to add metal in the form of filler rod.

4.2.4 SHIELDED METAL-ARC WELDING

Welding with a covered electrode is a manual process of welding suitable for thicknesses of 0.125 inch or more. If compared to gas tungsten-arc welding, which has replaced it in recent years in many fields, the process of welding with a covered electrode gives rise to smaller distortions and limits the formation of hot cracks on those alloys which exhibit this phenomenon during welding. The aeronautical industry usually prefers welding with a covered electrode in the manufacture of structural components of a low-carbon steel or low-alloy steel.

4.2.5 GAS METAL-ARC WELDING

The process of welding with a gas shield and with a consumable electrode is generally used on steel and aluminium alloys of considerable thickness. It limits to the minimum the distortions due to welding and the enormous advantages of this amply justify its widespread use. A typical application of this process is in the manufacture of in-flight refuelling tanks for jet aircraft.

The automatic process is the most common; the manual process is generally restricted to the manufacture of non-critical components, tooling and ground-support equipment.

4.2.6 GAS WELDING

Oxy-acetylene welding has been entirely replaced by the gas-shielded process with consumable and non-consumable electrodes. The disadvantages inherent in this process are mainly the atmospheric reaction of the welded zone and excessive heating.

4.2.7 ARC-SPOT WELDING

The aeronautical industry employs two types of electric arc spot-welding: with gas shield and non-consumable tungsten electrode and with gas shield and consumable electrode. One application of this process is in the spot welding of undulating sections extruded from honeycomb panels.

4.2.8 STUD WELDING

Even if only to a limited degree, the aeronautical industry uses the processes of percussion stud welding and arc stud welding. These processes are essentially utilized for anchorage points of components and structures that form equipment mountings. The choice of welding process depends on the thickness of the material to be welded and on the required diameter of the stud.

4.2.9 PLASMA ARC WELDING

The process of plasma arc welding is spreading fast. Thank to its effectiveness and simplicity, it is rapidly replacing the T.I.G. process in many applications. By comparison with the T.I.G. process, plasma arc welding does not require precise control of the distance between the parent metal and the electrode and enables welds to be obtained that are much narrower (about half) and of as good, if not better, quality.

4.2.10 ELECTRON-BEAM WELDING

The process of welding with electron beams is chiefly used to obtain a weld of high purity on reactive and refractory metals. The advantages of electron-beam welding partly arise from the high vacuum and are partly the direct result of the process itself. They are: high purity of the welding atmosphere, a limited heat-affected zone, strict control of the welding heat, high operational speed, good efficiency of the joint and the minimum of distortion due to shrinkage.

4.2.11 SPOT, SEAM AND STITCH WELDING

These welding processes involve melting and their use is common in the aeronautical industry. They are used especially on alloys and stainless steels employed in the manufacture of both structures and critical components.

4.2.12 FLASH WELDING

Machines for flash welding ranging from 20 kVA to more than 1000 kVA are commonly used. The applications of this process are numerous, ranging from landing gear components like the struts, bracing and retraction mechanisms, to the various connecting rods of the engine. The materials most often used in flash welding are the low-alloy steels susceptible to heat treatment. In some instances it is possible to utilize stainless austenitic steels and titanium alloys and the use of flash welding on aluminium alloys is becoming very popular.

4.2.13 WELDING OF MATERIALS USED IN THE AERONAUTICAL INDUSTRY

Materials with high strength/weight ratios are the most important for the aeronautical industry. Aluminium and magnesium alloys possess this characteristic and are the most used structural materials. Where special ambient conditions require their use, low-alloy steels, stainless, corrosion-proof steels, titanium, nickel and cobalt alloys are employed.

4.2.14 ALUMINIUM AND ALUMINIUM ALLOYS

The properties of pure aluminium are such that only in particular applications is it used on its own. More often it is advisable to use alloys that, maintaining aluminium as a prominent element, have an extremely low specific weight (≤ 3 g/m^3). The alloy elements most frequently used are Cu, Si, Mn, Mg, Zn, and Ni. They can form, with aluminium, binary, ternary, quaternary, and sometimes even more complicated alloys. A list of the weldable aluminium alloys used in the aeronautical industry is shown in Table I. The commonest welding processes are: gas welding, gas tungsten-arc welding, gas metal-arc welding and resistance welding.

4.2.15 WELDABILITY OF ALUMINIUM AND ITS ALLOYS: WELDING DEFECTS

4.2.15.1 Inclusions, Accretion of Foreign Particles and Fracture

One of the first chemico-physical factors which hamper the welding of aluminium and its alloys is the tendency of aluminium to oxidation. As the parent metal heats up during welding, it is reoxidized progressively, even if previously pickled, and when the fusion zone shows refractory qualities and specific weight of oxide higher than the metal, can easily cause inclusions and accretion of foreign particles. The defects increase particularly with alloys embodying magnesium, because of its strong tendency to oxidation. Further difficulties in welding are caused by high thermal conductivity of the aluminium alloys which leads to significant heat absorption on the part of the parent metal, with consequent changes in metallurgical properties extending over a wide zone. The high thermal factor necessary to avoid incomplete fusion and accretion of foreign matter can bring about the opposite defect, i.e., fracture of the joint, because the strong thermal conductivity tends to enlarge rapidly the area affected by the fusion zone once this has appeared.

Welding of aluminium and its alloys therefore demands the use of welding processes that are characterized by powerful sources of heat that are so concentrated that extension of the heat-affected zone may be eliminated altogether and, with it, the defects just mentioned. From this point of view gas tungsten-arc welding is the most suitable process for obtaining welds which are exempt from, or have limited, oxide inclusion and accretion of foreign particles.

4.2.15.2 Blowholes and Porosity

A phenomenon which often occurs in welding aluminium alloys and which affects their weldability in many ways is the appearance of blowholes and porosity. The problem is not important with pure aluminium but it is serious for its alloys, especially those based on magnesium. Blowholes are mainly attributable to hydrogen, whose solubility in aluminium is very much restricted in the solid state but increases to very high values in the liquid state and decreases markedly with temperature. Hydrogen can arise in welded joints from various sources:

- From the atmosphere surrounding the fusion zone during welding.
- From atmospheric humidity and from air or steam jets used in scorifying.
- From crystallization of water that can mix with the oxygen on the surface and which can always be found in the parent metal or in the filler rods.

The heat-affected zone, especially in the transitional area from the fusion zone, is generally the most given to blowholes. They can appear as general porosity or as large cavities. Blowholes are disadvantageous especially near the surface of material overheated by the proximity of the heat source, and can burst externally, giving the two strips on either side of the weld a pitted look, ugly and unsuitable for corrosion resistance.

Blowholes may also be found in the fusion zone, especially if the welding process is characterized by a very rapid cooling of the fusion zone, as occurs in gas metal-arc welding. Gas tungsten-arc welding is the most suitable

manual process for achieving welds without, or with very limited, porosity: the operator can, in fact, maintain the fusion zone under control long enough to dispel the gases that try to escape in the fusion zone during the solidification phase. The advantages offered by gas tungsten-arc welding may also include the fact that it is always easier to peel off mechanically the thin film of hydroxide from the surface of the filler metal used in gas tungsten-arc welding than from a filler wire, as used in gas metal-arc welding.

If, for reasons depending on the possibility of cracking, for reduction of the heat-affected zone or the welding speed, it is necessary to employ gas metal-arc welding, it is preferable to use larger electrode-wire diameters, i.e. wires with a smaller surface/volume ratio.

Suitable remedies for limiting blowholes and porosity are as follows:

- Choose a well-degasified metal, rapidly solidified and hot-rolled immediately after solidification.
- Use a dry and clean filler metal.
- Avoid, as far as possible, the use of flux mixed with water.
- Choose root-preparation and welding techniques which give a high ratio of the free surface to the volume of the fusion zone, in order to facilitate the release of gases during the solidification phase.

4.2.15.3 Tendency to Cracking

During welding many aluminium alloys show a tendency, to a greater or lesser degree, to cracking, under high temperature conditions near to those of "solidus" and in the last stages of cooling. Hot cracks are the most common and are characteristic of alloys having large solidification times. When one of these alloys solidifies, the dendrites that form in the liquid begin, at a certain stage, to encroach on each other, giving rise to a regular lattice of grains between whose interstices some liquid still remains. The limited section between grains can yield under shrinkage due to decrease in temperature and can then give rise to cracks that the remaining liquid, through its reduced volume or viscosity, is not able to fill up. There is thus a "hot fragility interval" during which cracks may appear; it is between the temperature of solidus and the temperature at which the alloy begins to take on cohesion. Considering purely binary alloys and very slow cooling, their crack sensitivity is greatest at their highest degree of solubility in the solid phase and at eutectic temperature. It is obvious that the presence of other alloys or a very high rate of cooling can affect this to a greater or lesser degree.

The rate of cooling tends to shift maximum crack sensitivity towards lower alloy values. For pure aluminium and for alloys of composition identical or similar to the eutectic (also for the Al-Mn alloys whose solidification time is always very short) the interval of fragility is practically null and the risk of formation of hot cracks is also at its lowest. In order to restrict cracking, the choice of filler metal is of primary importance: its composition must be such that, after dilution with the parent metal, alloys of minimum tendency to cracking result. In normal industrial practice, aluminium alloys are usually used as filler metal in welding processes:

- Pure aluminium.
- Alloys Al-Si at 4 to 12% Si.
- Alloys of composition similar to that of the parent metal.

It may be noted, however, that:

- Pure aluminium, although reducing liability to cracking, is deficient from the point of view of mechanical properties.
- Al-Si alloys are successfully used to weld alloys of the same composition and offer also the advantage of limiting hot-cracking; if used on alloys of different composition, they have the disadvantage of inadequate mechanical properties and of corrosion sensitivity.
- The use of filler metal identical to the parent metal represents the best solution for the welding of alloys not liable to cracking; for alloys liable to cracking it is advisable to choose as filler metal an alloy of the same type but richer in alloy elements. For instance an Al-Cu 4% alloy which tends to crack if welded with filler metal of the same composition, reacts much better if welded with 6 10% Cu alloy.

Similar considerations affect the Al-Mg alloys.

It is possible to reduce hot-cracking by resorting to additive elements such as titanium, zirconium and niobium which are in a condition to refine the grains. Rate of cooling also plays an important part in grain refining and therefore welding processes of the shortest duration, like gas metal-arc welding, are preferable.

TABLE I

Aluminium and Aluminium Alloys Commonly Used in the Aircraft Industry*†

Description	*Government Specifications Pertaining to Materials*	*Spot and Seam Welding***	*Gas Metal and Gas Tungsten-Arc*	*Gas Welding*
Clad plate, sheet, strip:				
2014	QQ-A-255	S	L	U
2024	QQ-A-362	S	U	U
7075	QQ-A-287	S	U	U
7178	MIL-A-9183	S	L	U
Rolled bars, rods and shapes:				
2014	QQ-A-266	L	L	U
2017	QQ-A-351	L	L	U
2024	QQ-A-268	L	U	U
6061	QQ-A-325	S	S	S
7075	QQ-A-282	L	U	U
1100	QQ-A-411	L	S	S
Extruded bars, rods and shapes:				
2014	QQ-A-261	S	L	U
2024	QQ-A-267	S	U	U
6061	QQ-A-270	S	S	S
7075	QQ-A-[illegible]	S	U	U
1100	MIL-[illegible]45	S	S	S
3003	QQ-A-357	S	S	S
Forgings:				
2014	QQ-A-367	L	L	U
2219	QQ-A-367	L	S	U
7075	QQ-A-367	L	U	U
Sheet and plate:				
1100	QQ-A-561	S	S	S
3003	QQ-A-359	S	S	S
2014	AMS-4[illegible]	L	L	U
2024	QQ-A-355	L	U	U
2219	MIL-A-8920	S	S	S
5052	QQ-A-318	S	S	S
5083	MIL-A-17358	S	S	S
5086	MIL-A-19070	S	S	S
5456	MIL-A-79842	S	S	S
6061	QQ-A-327	S	S	S
7075	QQ-A-283	L	U	U
Tubing:				
1100	WW-T-783	S	S	S
3003	WW-T-788	S	S	S
2024	WW-T-785	L	L	U
5052	WW-T-787	S	S	S
6061	WW-T-789	S	S	S

Code:

S Satisfactory.
U Unsatisfactory.
L limited weldability (crack sensitivity, loss in corrosion resistance or poor weld properties).

* Applications: general airframe structure, cowlings, fairings ducts, tanks, etc.

** Owing to the possibility of corrosion, restrictions have been placed on the spot welding of bars of 7075, 2024 and 2014 alloys to themselves or to each other (see MIL-W-6858).

† From Welding Handbook, Section Five, fifth edition (Chapter 91), published by the American Welding Society.

(Continued)

TABLE I (Continued)

Description	*Government Specification Pertaining to Materials*	*Spot and Seam Welding***	*Gas Metal and Gas Tungsten-Arc*	*Gas Welding*
Castings:				
356 Perm. mold.	QQ-A-596	S	S	S
356 Sand	QQ-A-601	S	S	S
355 Perm. mold	QQ-A-596	S	S	S
355 Sand	QQ-A-601	S	S	S
195 Sand	QQ-A-601	L	L	L
220 Sand	QQ-A-601	U	U	U
43 Perm. mold.	QQ-A-596	S	S	S
43 Die	QQ-A-591	S	S	S
13 Die	QQ-A-596	..	..	..

Codes:

S - Satisfactory.
U – Unsatisfactory.
L - Limited weldability (crack sensitivity, loss in corrosion resistance or poor weld properties).

** Owing to the possibility of corrosion, restrictions have been placed on the spot welding of bars of 7075, 2024 and 2014 alloys to themselves or to each other (see MIL-W-6858).

4.2.16 TITANIUM AND TITANIUM ALLOYS

The aeronautical industry uses either commercially pure titanium or its alloys for the construction of structural components with particular mechanical and technical requirements. A list of the titanium alloys used, indicating their relevant degree of weldability, is given in Table II. The strong reactivity that titanium possesses, if compared to air and to most elements and their compounds (except the inert gases), and the high embrittlement it experiences when contaminated by N, O, C and H, even in relatively low quantities, advise decidedly against welding processes using flux, such as oxy-acetylene welding with covered electrodes. The most common welding processes used on titanium and its alloys are gas tungsten-arc welding, gas metal-arc welding and resistance welding.

4.2.17 WELDABILITY OF TITANIUM AND ITS ALLOYS. WELDING DEFECTS

4.2.17.1 Porosity

In welding titanium and its alloys porosity is at present a persistent defect. The techniques and process of welding can affect the extent of this defect but no procedure yet exists which can guarantee freedom from porosity. The main cause of porosity in welding titanium and its alloys are gases, and particularly hydrogen, which are trapped in the fusion zone during solidification. The hydrogen that remains trapped in the fusion zone may originate in the following ways:

- From the parent metal itself, in which it can preexist in solution as an impurity. Welding of parent metal with hydrogen content of 100 p.p.m. tends to show porosity.

  From the filler metal. Filler metal with hydrogen content in 100 p.p.m. proportion can be critical for porosity in welding.

- From humidity in the parts to be welded. In this connection mild preheating of the parent metal is helpful.

The possibility of obtainaing a weld without porosity must be related to the degree of cleanness of the parent metal in the area of the weld.

Particles resulting from grinding, spattering, grease and finger-marks are all possible causes of porosity. Light, superficial oxidation is not a serious problem in relation to porosity. Superficial oxidation of the parent metal, like the presence of sulphur or air in the fusion zone, may cause embrittlement in the welded joint but does not increase the porosity appreciably. Similarly, the dew-point of the shielding gas, although it can affect the hydrogen content in the weld and consequently its embrittlement, does not seem to affect the porosity significantly.

An appreciable effect on the porosity of the weld is also due to the welding parameters. Even if the available data are conflicting, it is possible that the temperature of the fusion zone and its cooling time are able to limit the extent of this defect. In many instances a marked reduction of the welding speed, causing a lower rate of cooling of the fusion zone, has proved useful in containing the formation of porosity. From this point of view gas metal-arc

welding is less suitable than gas tungsten-arc welding. It must be noted that, because there are many parameters affecting the temperature of the fusion zone, it is not always possible to obtain the desired result by altering only one of them. Generally speaking it is true that the so-called "cold welding" causes porosity.

4.2.17.2 Tendency to Cracking

Titanium possesses a high yield stress and a small interval between yield stress and ultimate stress. As a result the relatively high residual welding stresses are not compensated by sufficient deformation of the cracks. Of particular importance are cracks due to stress corrosion. In certain ambient conditions, the residual welding stress may be strong enough to supply the energy necessary to initiate cracks due to stress corrosion phenomena. Finger-marks, salts, grease and sulphur components in the welding zone, before welding takes place, can all create the environmental conditions which may facilitate the appearance of stress-corrosion cracks. It is then of great importance that the parent metal is carefully cleaned before welding. However, it is necessary to take special precautions in this operation also. The solvents used must not leave residue behind, particularly chlorinates. Solvents such as trichloroethylene and methylenechloride must never be used. Acetone, alcohol and methyl ketone should be used instead.

TABLE II

Titanium and Titanium Alloys Commonly Used in the Aircraft Industry*

Nominal Composition (per cent)	*Other Designations*		*Spot, Seam and Flash Welding*	*Gas Metal and Gas Tungsten-Arc Welding*	*Gas and Shielded Metal-Arc Welding*
	AMS No.	*Military No. (a)*			
99.5	4902		S	S	U
99.2	4941 4951	T-9047B-1	S	S	U
99.0	4900A	T-7993B	S	S	U
99.0	4901B		S	S	U
98.9	4921		S	S	U
		Alpha alloy grades			
5Al-2.5Sn	4910 4926 4953 4966		S	S	U
8Al-1Mo-1V	In prepar.	In prepar.	S	S	U
8Al-2Cb-1Ta(b)		In prepar.	S	S	U
		Alpha – beta alloy grades			
8Mn	4908A		U	U	U
4Al-3Mo-1V	4912 4913		U	U	U
2.5Al-16V		T-8884(1)	U	U	U
5Al-1.25Fe-2.75Cr			U	U	U
2Fe-2Cr-2Mo	4923 4911		U	U	U
6Al-4V	4928A 4935	OS-10737 OS-10740	S	S	S
		Beta alloy grades			
13V-11Cr-3Al	4917		S	S	U

Code:

S Satisfactory.
U Unsatisfactory.
(a) Other numbers, T-12117 and WA-PD-76C (1), apply to all grades and all products; T-14557, T-14558, T-9046C and T-9047C apply to all grades; and T-8884 (ASG) applies to various grades.
(b) Formerly Al-Cb-1TA. All data given are for the 8-2-1 composition.

* From Welding Handbook, Section Five, fifth edition (Chapter 91) and Welding Handbook, Section Four, fifth edition (Chapter 73), published by the American Welding Society.

4.2.18 STAINLESS STEELS

For the manufacture of components which operate in particularly corrosive atmospheres, the aeronautical industry mainly uses austenitic chrome-nickel stainless steels. Martensitic and ferritic stainless steels are rarely used.

The most common welding processes are: gas-shielded arc welding, shielded metal-arc welding and resistance welding. A list of the stainless steels with chrome-nickel composition most commonly used, with indications of their degree of weldability, is given in Table III.

4.2.19 WELDABILITY OF AUSTENITIC STAINLESS STEELS. WELD DEFECTS

4.2.19.1 Tendency to Cracking

Defects often found in joints made by the action of heat on chrome-nickel stainless steels are cracks of "hot" type, that is, defects of metallurgical origin which may occur during the first stages of solidification of the weld metal. Macroscopic cracks may appear also and usually have a tendency to form between dendrites in the fusion zone. These macroscopic cracks may reach the surface and their direction may be longitudinal or transverse to that of the weld and may even be branched when they start from the crater which forms at the toe of the weld.

Tendency to cracking has been found more frequently in steel of "stabilized" type, for instance AISI-347, that is used under heavy duty conditions and at high temperature. Welds on this type of steel have shown a tendency to hot cracks in the heat-affected zone of the weld, although it is not clear whether such cracks appear during the welding process or whether they originate or develop after heat treatments, which are sometimes applied in order to keep the ferrite content low in the filler metal or for expansion purposes in view of stress-corrosion phenomena.

In order to keep hot cracks to a minimum, a wise general precaution is to make the weld rapidly and with as little overheating as possible; this limits the size of the fusion zone and speeds up solidification. For this purpose, processes are preferable that utilize very concentrated heat sources and so permit fast and localized fusion with a small increase of heat (for instance, the gas-shielded arc welding and the shielded metal-arc welding processes). Small and undisturbed fusion zones help to protect the fusion zone itself against oxidation from the atmosphere. In relation to the formation of hot cracks in the shielded metal-arc welding process, basic covered electrodes give higher reliability than electrodes covered with the so-called "neutral" (rutile-basic) covering. This fact is attributable both to the higher Si content of the rutile electrode and to the shape of the resistant section of the weld: with the "neutral" electrode the section is at the same layer and sharper than the one obtained with basic electrodes, and is thus less resistant and a source of more consistent shrinkage effect. In accordance with the need to limit the size of the fusion zone and the overheating of the parent metal, it is also preferable to use covered electrodes of smaller diameter and it is advisable, when welding by multiple runs, to check the weld temperature (as a general rule, temperatures not greater than 110 - 150°C are indicated).

It is furthermore preferable to utilize a root-preparation technique which involves the minimum volume of fusion metal and a shorter total heating time of the joint, because fewer runs are required. From this point of view X type preparation is preferable to V type.

In relation to hot cracks, it must be borne in mind that a completely austenitic deposit is more easily given to crack formation than one with mixed austenitic-ferritic structure. Compositions of the type 25% Cr - 20% Ni or 18% Cr - 8% Ni (when it is completely austenitic) are more liable to crack than compositions of the type 18% Cr 8% Ni with low carbon, the type 18% Cr - 8% Ni - 2% Mo, or the type 24% Cr - 12% Ni - 2% Mo that deposit a certain amount of ferrite. Because of this, when technical requirements for special types of construction do not prohibit the use of it, it is preferable to employ filler materials able to deposit 2 - 8% of ferrite in a structure prevalently austenitic. Also, with a correct welding procedure, hot cracks, on austenitic stainless steel can sometimes occur in the craters at the end of the weld. This possible defect is practically eliminated by feeding more filler material onto the shrinking end crater before switching off the arc, utilizing current generators which allow a progressive, steady reduction of the welding current at switch-off point, or else forming the end crater on a separate metal plate that is not part of the joint itself. It is also good practice to remove the seam point or, at least, to melt it accurately in order to incorporate it into the joint itself.

4.2.19.2 Porosity and Inclusions

The defects of porosity and inclusions are mainly attributable to defective cleanness of the root of the joint. Cleaning is a very important factor in the achievement of strong welds on austenitic stainless steel welding: lack of cleaning favour not only porosity and inclusions but also the formation of hot cracks. Grease smears, oil, powder and foreign particles (like Fe, Zn, Cu, slags or oxides arising from previous welding runs) must be completely eliminated from the roots. In this respect pollutions of S and C are particularly dangerous and are always possible if the joint contains paint stains, chalk, thermocolour, lubricant or liquid used, for instance, in non-destructive testing. It is good practice to clean mechanically, with a metallic brush, or chemically, with a pickling solution, using, in the first instance, brand new tools or at least tools reserved for stainless steel and not contaminated by use on other types of steel. It must be remembered that clean conditions are especially important with modern welding processes using

gas shielding, where good protection against atmospheric agents is possible but it is not always possible to scorify the after-effects of impurities.

TABLE III

Austenitic Chrome–Nickel Stainless Steel Commonly Used in Aircraft Applications*(a)

Description; AISI Designation	*Projection Spot and Seam Welding*	*Flash Welding*	*Gas-Shielded Metal-Arc Welding*	*Gas Welding*
Sheet:				
301	S	L[b,c]	L[b]	L[b]
302	S	L[b,c]	L[b]	L[b]
321	S	L[c]	S	S
347	S	L[c]	S	S
Bar:				
302[d]	S[e]	L[b,c]	L[b]	L[b]
304 Grade 1A	S[e]	L[b,c]	L[b]	L[b]
321 Class B	S[e]	S	S	S
347 Class B	S[e]	S	S	S
Tubing:				
302	S[f]	L[b,c]	L[b]	L[b]
321	S[f]	L[c]	S	S
347	S[f]	L[c]	S	S

Code:

S Satisfactory

L Limited weldability (crack sensitivity or loss in corrosion resistance or poor weld properties).

* From Welding Handbook, Section Five, fifth edition (Chapter 91), published by American Welding Society.

(a) Corrosion-resistant and heat-resistant applications; exhaust stacks, fire walls and seals, surfaces exposed to exhaust gases, high-pressure lines, lavatory equipment and miscellaneous furniture.

(b) Solution annealing post-heat treatment required to dissolve precipitated carbides unless reduced corrosion resistance is acceptable.

(c) Requires specialized techniques.

(d) Except free machining bar.

(e) May be satisfactorily welded in thin, smooth sections.

(f) Poor accessibility and fit-up restrict the use of tubular forms.

4.2.20 NICKEL AND NICKEL ALLOYS

For the construction of welded structures characterized by high resistance to corrosion and high mechanical resistance under heat, nickel alloys, of the solid-solution-strengthened type and of the precipitation-hardenable type are largely used. In particular, the solid-solution-strengthened types are generally used when there is a demand for moderate mechanical strength at high temperature combined with excellent characteristics of resistance to corrosion and oxidation, while the precipitation-hardenable alloys are mainly used for components where high strength weight ratios and excellent resistance to "creep" are required. A list of nickel alloys used in the aeronautical industry, with indications of the welding processes applicable to them, is given in Table IV.

In general, on the nickel alloys, the same welding processes, by fusion and resistance, as for chrome-nickel stainless steel, are applicable. The prevalent use of thin materials favours, in particular, welding processes by fusion, such as shielded metal-arc welding and gas tungsten-arc welding; different types of resistance welding are also frequently used, especially spot welding and roll welding. Among more advanced welding processes by fusion applicable to nickel alloys, gas metal-arc welding is of particular interest, especially in relation to the current need to weld thin metal sheets in every position; the so-called "thin thread" version of this process which involves transfer of the filler metal is of the type known as "gas shorting-arc". An ever-increasing interest is also evident in electron-beam welding and submerged arc welding.

4.2.21 WELDABILITY OF NICKEL AND ITS ALLOYS. WELDING DEFECTS

The welding of nickel and its alloys does not generally present greater difficulties than the welding of chrome-nickel stainless steels of similar austenitic structure. However, the severity of the working conditions that a nickel alloy must normally bear result in a requirement for perfection of the weld (not merely an absence of the traditional geometrical discontinuities called welding defects); to obtain this perfection it is necessary to comply strictly with the precautions recommended by good workshop practice for stainless steels. Such precautions concern essentially the need to avoid pollution by foreign particles that can produce not only weld defects but can also be potential causes of serious deterioration of the mechanical and anti-corrosion properties of the joint under service conditions.

4.2.21.1 Incomplete Root Penetration. Blowholes

Some nickel alloys exhibit a reduced fluidity of the fusion zone, which can cause difficulty in achieving the first welding run and bring about defective root penetration. The defect can occur especially in welding processes using shielded gas. To compensate for the reduced fluidity of the fusion zone one generally resorts to *ad hoc* re-touching in preparing the roots of the joint, for instance on the "shoulder" and at the ends in V welds, and to a light pre-heating (of 50° to 150°C).

Preheating favours, amongst other things, the expulsion from the fusion zone of the gases (H, N) that tend otherwise, especially with pure nickel and nickel-copper alloys, to give rise to blowholes.

However, in order to facilitate penetration and dispel the tendency of gas-inclusion, a mixture of argon and hydrogen is sometimes used as the gas shield, instead of pure argon; this allows more heat to be conveyed into the fusion zone, raising its temperature because of dissociation and reassociation of the molecules of hydrogen according to the equilibrium $H_2 \rightleftharpoons 2H \pm Q$. The most appropriate percentage of hydrogen employed does not exceed 10%. The danger of blowholes is also reduced by the presence in the filler metal of deoxidating and gas-fixing elements such as aluminium and titanium. With the aim of avoiding increase in the loss of deoxidising properties it may help to prevent turbulence of the fusion zone, which can be caused by excessive speed of release of the gas shield and by movement of the welding flash or the rod of filler metal. Absolute cleanness of the surface under treatment is always extremely important.

4.2.21.2 Slag Inclusions

In using the covered-electrode process, it is possible that slag inclusions appear in the weld metal. This defect is more a characteristic of the particular welding process chosen than a property of nickel alloys, and it is mentioned here in order to emphasize how important it is, on parent metals, to take great care to remove the slag completely after a welding run with a covered electrode. Residual slag is particularly dangerous in welds destined to operate at high temperature: surface residual slag may encourage the absorption of sulphur from corrosive atmospheres and so induce embrittlement from sulphur, while in alloys containing chrome and operating in oxidising atmospheres the slag, which melts at a lower temperature than the metal, can remove the surface film of chrome-oxide and lead to corrosive attack underneath.

4.2.21.3 Oxide Inclusions. Lack of Fusion

Nickel alloys of the precipitation-hardenable type contain elements which can produce, during welding, refractory oxides and therefore oxide inclusions and lack of fusion. The danger of these defects makes indispensable proper action between one welding run and the next in order to remove the existing oxides completely. The most efficient cleaning method consists of sand-blasting and grinding after each run; the use of a normal metallic brush is not considered sufficient. A gas shield reversed is deemed indispensable when the weld alloy has a high aluminium and titanium content.

4.2.21.4 Tendency to Cracking

The solubility of silicon in nickel may seem high enough to limit the formation of dangerous eutectics with low melting point and consequently the possibility of hot cracks forming in those nickel alloys which contain it to a certain degree. It decreases, however, with the addition of copper and chrome, and the alloys of nickel-chrome, nickel-chrome-iron and nickel-copper are sensitive to this defect. Particularly sensitive are the alloys containing chrome and this characteristic must be borne in mind especially when using filler metal of these alloys on parent metal with a high silicon content. The critical silicon content which must not be exceeded if this harmful effect is to be avoided varies from alloy to alloy and is also affected by the welding process used. It has been noticed, for instance, that the harmful effect brought about by silicon in the fusion zone of the weld is less evident in the processes using inert gas. Cracking can also occur in the heat-affected zone of the weld, but to a far less degree. The metallurgical effect of silicon can be counteracted by the addition of niobium in the filler metal.

Also susceptible to cracking in the fusion zone are alloys containing boron in percentages below 0.03%; crack sensitivity in the heat-affected zone appears to be more controllable, with these alloys, if one is careful to use a

welding process with low specific overheating and to plan the structure so as to obtain welded joints with the least rigidity possible. The harmful effect caused by boron is attributable to the formation of intergranular eutectics with low melting point.

A similar effect, hot-crack formation in either the fusion zone or the heat-affected zone, is also noticeable in alloys containing zirconium in small amounts, say 0.1%; fusion welding is not advisable on such alloys because it would be difficult to avoid cracking in the heat-affected zone. The metallurgical reasons for this defect on such alloys is also attributed to the formation of low-melting-point eutectics.

To avoid the incidence of cracking, special care must be taken against pollution by sulphur, phosphorus and lead, which can provoke eutectic reactions at low fusion temperature, thus contributing to hot-crack formation, which is based on the intergranular brittleness of the structure. Sulphur is the most likely of these harmful elements because it is more difficult to guarantee its exclusion as it tends, with its compounds, to form the numerous materials continuously used in industry (thermocolour pencil, chalks, cutting lubricants, grease, paint) and it is also normally contained in the industrial atmosphere to which alloys may be exposed during storage.

In order to prevent, as far as possible, the cracking of nickel alloys in general, the most suitable stage for exploiting, during welding, the best characteristics of ductility of the alloy, is that of annealing or solution treatment. This structural state guarantees also the absence of possible stress from work-hardening caused possibly by previous cold plastic processing. For alloys which can be hardened, welding on material already "aged" is not advisable for various reasons; the aged material offers little ductility, especially at the temperature reached in the heat-affected zone, and could crack under the internal stresses induced by welding; the heat cycle of welding can destroy locally the effect of the treatment already applied to the parent metal; it would be impossible to obtain the desired mechanical properties in the fusion zone without further ageing of the zone itself.

TABLE IV

High-Nickel Alloys Commonly Used in the Aircraft Industry*

Description	*Shielded Metal-Arc*	*Gas Tungsten-Arc*	*Gas Metal-Arc*	*Gas Shorting-Arc*	*Electron Beam*
Inconel alloy 600	X	X	X	X	X
604	X	X	X		X
625		X			
700		X			X
702		X			X
718		X		X	X
722	X	X			X
750	X	X			X
Hastelloy alloy "B"	X	X	X		X
"C"	X	X	X		X
R-235	X	X	X		X
W	X	X	X		X
X	X	X	X		X
M-252 alloy					
René 41		X			X
Udiment 500	X	X			X
700		X			
Incoloy alloy 800	X	X	X	X	X
801	X	X	X	X	X
804	X	X	X	X	X
825	X	X	X		X
901		X			X

Note:

X Weldable by this method. A dash indicates that the process is not usable on the alloy or information has not been developed. Contact the manufacturer for latest information.

* From Welding Handbook, Section Four, fifth edition (Chapter 67), published by the American Welding Society.

4.2.22 TYPICAL WELDING DEFECTS AND THEIR DETECTION BY NON-DESTRUCTIVE TESTING

Of the various defects which can occur during welding some, as previously explained, are characteristic of the type of welding process used and some of the parent metal employed; others are common to both and occur often.

In the general scope of the non-destructive test programme for checking welds, it is advisable to consider together the various types of defects, independently of their origin, and to prescribe appropriate non-destructive test methods to reveal them.

In autogenous welding of butt joints the following defects may occur:

Undercuts are due to limited fusion on the surface of the parent metal near the seam and to incomplete filling of the grooves with filler metal. They are revealed through X-rays and on the screen they appear as dark grooves shading off at the sides of the seam (Fig.1). These defects do not represent real discontinuities and therefore they are not revealed by any other non-destructive method. It must be noted that, at least in larger welds, these defects are not visible to the naked eye and, unless very sharp, they are acceptable.

Porosity and blowholes are caused by gases in the fusion zone which are trapped in it during solidification. These defects, which are fairly round cavities, are usually called blowholes if their diameter is 10 to 15 mm or more and porosity if it is less than this. These defects are usually revealed by X-rays and they appear as dark spots easily distinguishable from other defects. The X-ray screen reproduces their shape and exact location and, in relation to porosity, permits an assessment, albeit a visual one, of their density (number of pores per unit volume). Incidentally, they can also be detected by ultrasonic techniques (especially large blowholes) but in general the sensitivity is lower inasmuch as these defects tend to diffuse, instead of reflect, the beam. Furthermore, not being surface defects, they are not detectable by liquid penetrants.

Wormholes are defects similar to blowholes but oblong. They are clearly visible by X-rays, but only by chance by ultrasonic and other methods.

Herringbones are defects consisting of a group of oriented wormholes (Fig.2). They are typical of welding done in a shielded atmosphere, without proper control of the process. The defects are clearly detectable by X-rays but only incidentally by ultrasonic techniques and then with difficulty. They are never detected by other methods.

Porosity describes groups of pores and areas covered by a large quantity of pores (Fig.3). As already mentioned, these defects are clearly detectable by X-rays but not at all, or only occasionally, by ultrasonic methods. They are not detectable by other methods.

Incomplete root penetration consists of incomplete filling of the weld (Fig.4). Compared with the length of the seam it can be continuous (more often in automatic welding) or discontinuous, with more or less sharply defined sections (in manual welding). It is a defect easily revealed by X-ray and ultrasonic techniques. No other methods are used unless the weld is without reverse pick-up and on components which are not closed, for example tanks or boxes. In such cases the lack of root penetration is detectable by the naked eye.

Lack of fusion is a defect due to insufficient heating or to the local presence of oxide and it can occur at the root of the weld and on both sides of it (Fig.5). It can be detected by X-rays and appears as a thin line if the direction of the X-ray beam is parallel to its plane; if it is not parallel (the most common case), it appears as a very shadowy area, sometimes hardly detectable for lack of contrast. Because of this factor, the usual method is to use ultrasonic techniques with a transducer than can generate inclined beams (45° 80°, according to the plate thickness), inasmuch as the echo reflected is not affected by the thickness of the defect but is sufficient for the defect to create two-dimensional discontinuity. Ultrasonic testing is recommended for use with stainless steels. The tendency shown by many stainless steels to grain enlargement in the welded zone can make difficult or impossible the use of ultrasonic methods, because of the excessive absorption of the ultrasonic beam. However, if the welded section is not too large, it is possible to restrict the attenuation and diffusion of the ultrasonic beam within acceptable test limits by choosing a sufficiently low frequency.

Inclusions are foreign particles which remain trapped in the fusion zone during solidification. These defects are detected either by X-rays or by ultrasonic methods, although with the latter it is not always easy to distinguish them from other defects. Non-metallic inclusions are generally formed by fragmentation of the electrode covering, i.e. by fusible slag. Almost always they are thinner and thus less absorbent than the surrounding metal and, on the X-rays, appear as clear spots of irregular, fairly round, shape. When non-metallic inclusions are refractory, they appear on the X-rays as clear spots of rather jagged shape (Fig.6(a)). If the inclusions are metallic, they may appear as clear spots or dark spots according to their relative density compared to the surrounding metal. An example of such inclusions is given in Figure 6(b), which shows (apart from the two cracks) a tungsten inclusion (shed from the electrode) in a weld made by the T.I.G. process. This type of defect is not considered serious if the dimensions are relatively small; the danger increases when there are more inclusions close together or in line. Similar defects can be caused by inadequate cleaning between one welding run and the next or when particles of the parent metal flake off and form surface inclusions (Fig.7(a), (b)) which, owing to the high temperature during welding, tend to

concentrate on the edges of the filler metal, giving rise incidentally to aligned inclusions. In X-ray testing of very thin welds with "soft" rays (low kV) it is necessary to use very fine grain film and to take appropriate measures (e.g. geometrically) to obtain the best image possible. A distinct image is indispensable in X-ray testing of oxides of aluminium and magnesium, because their densities are quite near to that of the matrix in which they are trapped.

Craters, which are more frequent in normal than in automatic welding, are characteristic defects that may show up when the arc is interrupted along the weld. Rapid local cooling may prevent the release of gas bubbles (with consequent formation of porosity) and/or produce small cracks in the radial direction (Fig.8). These defects are detectable by X-ray testing if the plane in which they lie is parallel to the X-ray beam, and by liquid penetrants (generally the red ones) if they are on the surface. When they are not on the surface they are satisfactorily detected by ultrasonic methods, through inclined-beam techniques (45° to 80°) with appropriate frequency.

Hot cracks are produced during the first stage of solidification of the fusion metal, when the dendrites of solidification form a coherent reticule of grains; in the interstices some liquid remains and the intergranular sections of limited strength can yield under the shrinkage stresses due to the progressive decrease of temperature. These defects are detectable easily with X-rays, fairly easily with ultrasonic techniques, but not at all with liquid penetrant and magnetic methods unless they are on the surface. Hot cracks (which form during heating and successive cooling of the metal) may in fact be considered as three-dimensional defects, with the possibility of producing, when examined by X-rays, a trace of different density (blackening) on the film, even if the orientation is not the most favourable.

Cold cracks may form when the fusion zone has already solidified, owing to high stresses during the cooling process. These defects generally form in the fusion zone, but they can also occur in the heat-affected zone, especially with steel alloys or high-strength steel. Cold cracks generally have a linear or jagged appearance (Fig.9). For thin welds, or in cases when the crack is expected to reach the surface, the methods of detection which appear the easiest and safest are the liquid penetrant and magnetic methods, even though care must be taken to avoid misleading traces, owing to the possibility of penetrants remaining in the interstices of the surface folds after washing, or to variation of magnetic permeability in the interface with the filler metal.

Ultrasonic methods are particularly suitable for detecting cracks which do not reach the surface, because this type of defect forms a discontinuity which is highly reflecting. Generally it is advisable to use techniques with beams inclined at 45° to 80°, according to the thickness of the plate; the basis of the technique is illustrated in Figure 9, where case (a) deals with a crack in the filler metal and case (b) with a crack in the heat-affected zone.

X-ray testing is not altogether suitable for detecting cold cracks inasmuch as it requires that the plane in which they lie should be approximately parallel to the direction of the X-rays. When this condition is obtained they are represented on film as sharp traces; otherwise they appear as shadowy areas, medium dark in colour and with little contrast; cracks which lie in planes very much inclined to the direction of the X-rays are not detected at all. However, if we consider only very thin welds, for which the plane of the cracks is almost perpendicular to the plate, namely parallel to the X-ray beam, the limitations just mentioned are no longer valid. In spot welding the defects which can occur are classifiable into fewer types compared to those in arc welding. The heat cycle of each "nugget" is extremely short and interaction of the liquid metal with the external atmosphere is practically negligible.

The classical X-ray of a spot weld obtained with correct values of the welding machine parameters is that illustrated in Figure 10(a), where the characteristic clear halo surrounding a circle of slightly darker background is noticeable and is due to the forging action exerted by the electrodes (note the variation in thickness as shown in Figure 10(b)). The liquid metal, piled up during the heating phase, cools rapidly through the action of the surrounding material and of the electrodes, and the nuggets produced are characterized by a crystal column structure, as sketched in Figure 10(b). The main types of defects are the following.

Pores are small round cavities filled with gas, generally caused by inadequate cleaning of the surfaces (Fig.11). They are not as a rule regarded as dangerous defects.

Shrinkage cracks are cracks positioned roughly radially and are star-shaped (Fig.12). They appear when there is excessive heating, and they are almost always present in nuggets of excessive size. They are regarded as dangerous defects.

Spattering of fuse material may be due to excessive heating and thermal expansion, interfering with the surrounding solid material. Contact with the plate and imperfect cleanness are other possible causes of this defect (Fig.13).

Lack of fusion appears as spots with minimum mechanical resistance, owing to insufficient heating, and thus without enough nugget volume. They are considered dangerous and generally lead to rejection.

The first types of defects (pores, cracks, spattering) are detectable very easily by X-rays. Lack of fusion, on the other hand, is not directly visible by X-rays because it does not appear as cavities or thickness variations, which can produce variation in the absorption of X-ray beams. However, with certain materials (of low ductility), the

small volume of the melted nugget reduces and eliminates the forging action of the electrodes, so that the white halo does not appear in the X-rays: this can be taken as a sign (even if not absolutely definite) of lack of fusion. Another sign, even though indirect, of the reduced size of the nugget is indicated in X-ray testing of light alloys with high copper content, owing to the tendency of copper to migrate from the exterior to the centre of the nugget. This occurs during the fusion cycle and during solidification of the nugget when the copper tends to segregate and, being subject to heating followed by cooling, forms an outside ring of low copper concentration and a core of higher copper concentration. It is a relatively small variation but, because of the enormous difference between its absorption coefficient and that of aluminium, it is sufficient to show up in X-ray testing as a dark halo (of diameter nearly the same as the light halo of the forging action) and a lighter central zone indicating copper enrichment (Fig.14).

There has recently been developed an ultrasonic technique of high frequency (10 to 15 MHz) suitable for the evaluation, through multiple echoes, of the size of the nugget according to the damping of the ultrasonics. Although it has proved promising, it appears to be too expensive. Some attempts to use ultrasonics applied directly to the electrode of the welding machine have been made, so far without success.

A modern method of test directly applicable on the welding machine or on the part during welding, seems now to be offered by acoustics: during the fusion phase, solidification and forging, both in the nugget and around it. Very strong impulses are produced which free energy in the form of elastic vibration of high frequency. A suitable transducer, set nearby, can capture these signals, which radiate as impulses of various energies and frequencies; such impulses, for each welded spot, are related to the size of the nugget and it is thus possible to distinguish the welded spot with lack of fusion (small acoustic signal) from the large and average one.

4.2.23 DANGER OF DEFECTS AND ACCEPTABILITY CRITERIA

With regard to the strength, both static and dynamic, of the weld, an assessment of the danger of defects and the relevant acceptability criteria is based essentially on the possible effect of fissure and the resultant stress concentration that this can produce. From this point of view a classification of defects implies a division into two main categories:

(a) Defects which are round, or at least three-dimensional, and without sharp corners.

(b) Defects with sharp corners, generally three-dimensional-shaped, with marked effect of fissure.

Category (a) comprises blowholes, porosity, inclusions etc. These defects are not liable to spread under fatigue conditions inasmuch as they do not have sharp corners: they can be accepted if, under the prescribed conditions, they are of dimensions tolerable for static strength.

Defects of category (b), on the other hand, cause stress concentration and are, furthermore, likely to spread. Cold cracks, especially, represent a very serious danger for their tendency to spread under fatigue conditions: they are never tolerated in welds on important components. In addition, defects such as lack of fusion and lack of root penetration, hot cracks and, finally, aligned inclusions belong to this category.

Suitable X-ray standards of defects in welds have been collected and issued by specialised organisations: the numerous defects illustrated are in order of increasing danger and importance. In acceptability definitions these standards are often referred to.

It must always be borne in mind that the criterion of acceptability for defects of the two categories mentioned depends not only on their importance and nature, but also on the position of the weld and thus the influence the defect has on the part or assembly. It is self-explanatory that in areas of low stress some types of defect can be tolerated up to a certain limit, inasmuch as they do not give rise to appreciable stress concentrations or, if they do, there is a considerable margin of safety. Conversely, in highly stressed areas the presence of a defect, however small, can be responsible for initiating a fatigue crack.

In considering the effect on safety, it must be remembered that in an aircraft there are structural components and mechanical parts of primary importance, while there are others of secondary importance by comparison: the acceptability criteria of defects are also related to the function of the particular welded component.

It is obvious that the various types of possible defect in welding can be classified according to their nature and origin, but they differ widely in shape, position, importance and so on. In this respect the personal experience of an inspector entrusted with acceptance is of great help in the interpretation and assessment of defects: but, because of the situation just described, he would find himself compelled to pass judgement based on personal concepts, to decide on very complex requirements not easily assessed solely according to his own specific competence. To give him a chance of being more objective, using generally applicable criteria, the idea has been established of creating classes with a different degree of severity for the acceptability of defects. Referring to X-ray standards, the most severe class will permit the acceptance, for instance, only of defects of minimum order in category (a), excluding absolutely any defect of category (b). The less severe class will permit acceptance (referring always to standards) of defects

progressively greater of both categories. The classification is generally established by the design offices, in cooperation with those responsible for quality control, and can refer to the component or only to its critical zones. The category in which the particular component is placed is shown on the relevant drawing or quality control specification: the inspector responsible for acceptance is now able to judge the defect by comparison with similar defects reproduced in the standard, and referred to by the class in which the part under inspection appears. A simple scheme of classification of components according to their use is now given.

Class 1 This class comprises components whose failure during take-off, flight or landing may cause

(a) structural failure,
(b) loss of control,
(c) engine failure,
(d) inability to actuate the landing gear.

If the failure results only in damage through a second, unlikely event (for instance, the damage to the rudder control cable caused by failure and collapse of a radio antenna) the component does not come within Class 1.

Class 2 This class includes components under specification which do not belong to Class 1.

Class 3 This class includes components not under specification or under slight specification.

The classification just described relates specifically to X-ray testing, but it is applicable (and it is applied) also to other non-destructive methods. In ultrasonic testing, for instance, for each class, reference can be made to prescribed specimens, containing artificially produced defects of different types: the echo of the particular defect is compared with that of various standard specimens.

In addition to what has already been said, it must be emphasized that an acceptability criterion must always consider the deterioration with time of a defective weld.

It is essential that the departments responsible for quality control and acceptance assess the degree of danger of the defect with this in mind, evaluating how much a defective weld can be further weakened in time by in-service conditions (atmosphere, temperature, stress), by the structure of the welded material itself and by the type of defect.

Fig.1 Undercut

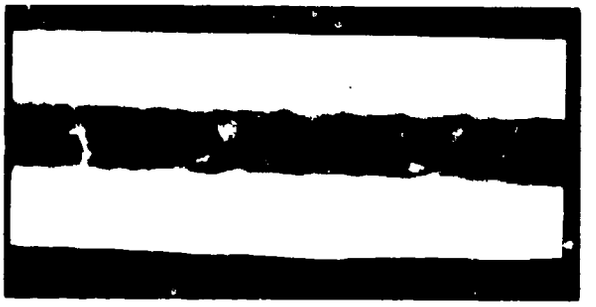

Fig.2 Herringbone

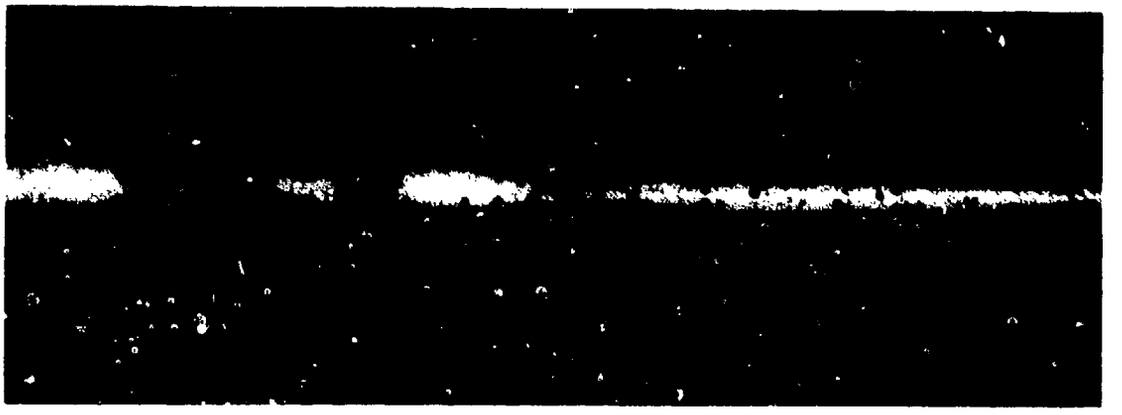

Fig.3 Porosity

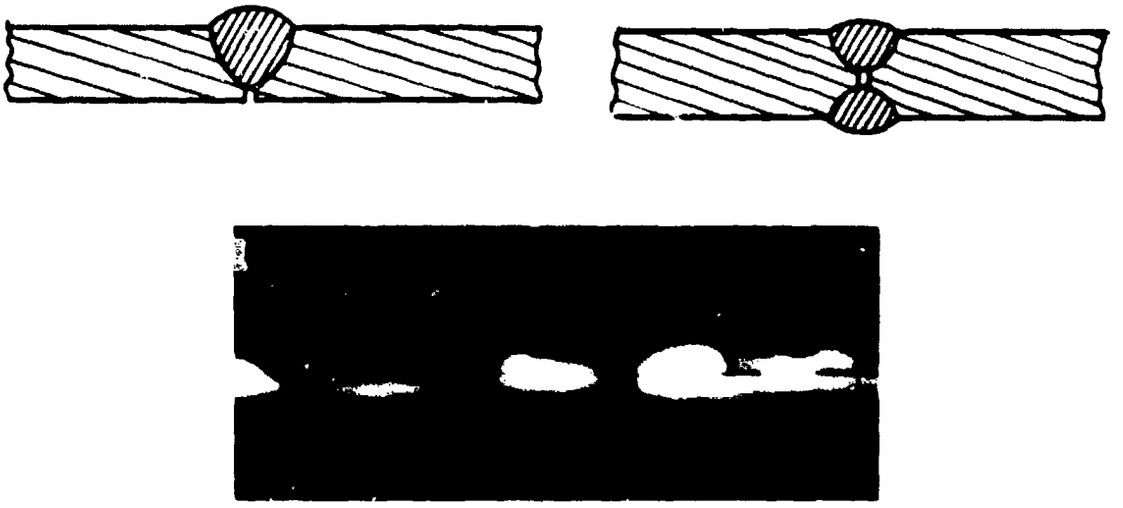

Fig.4 Incomplete penetration

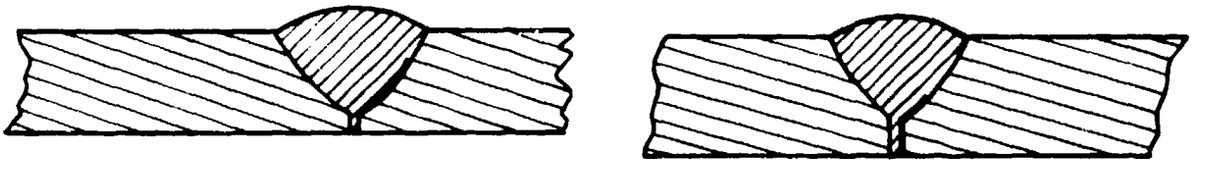

Fig.5 Lack of fusion

Fig.6(a), (b) Inclusions

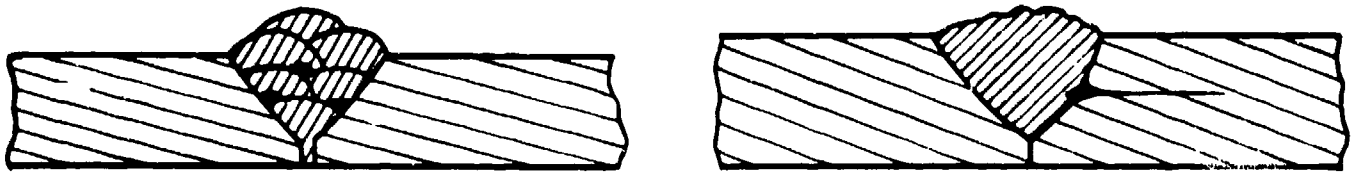

(a) Slag inclusions

(b) Capillary inclusions

Fig.7 Aligned inclusions

Fig.8 Crater

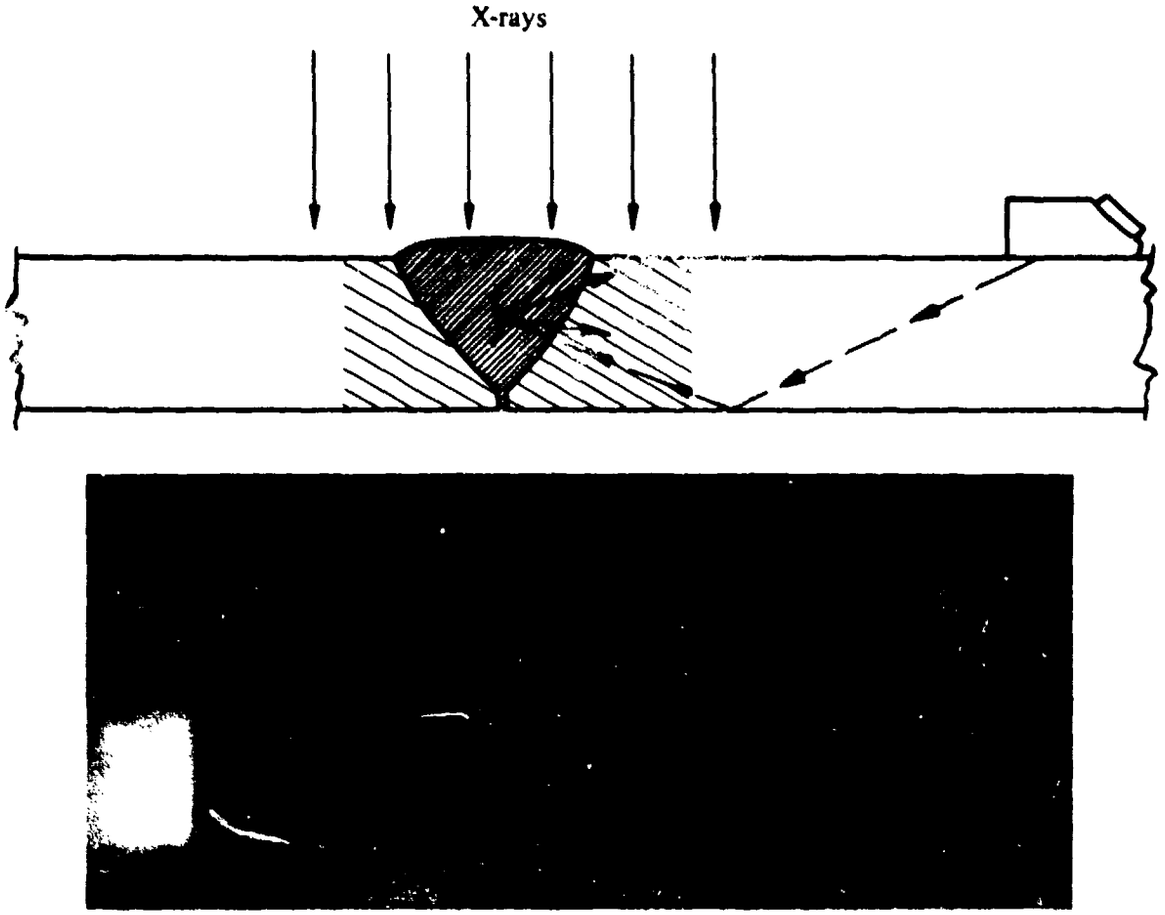

Fig.9(a) A crack in the weld metal easily detected by X-rays

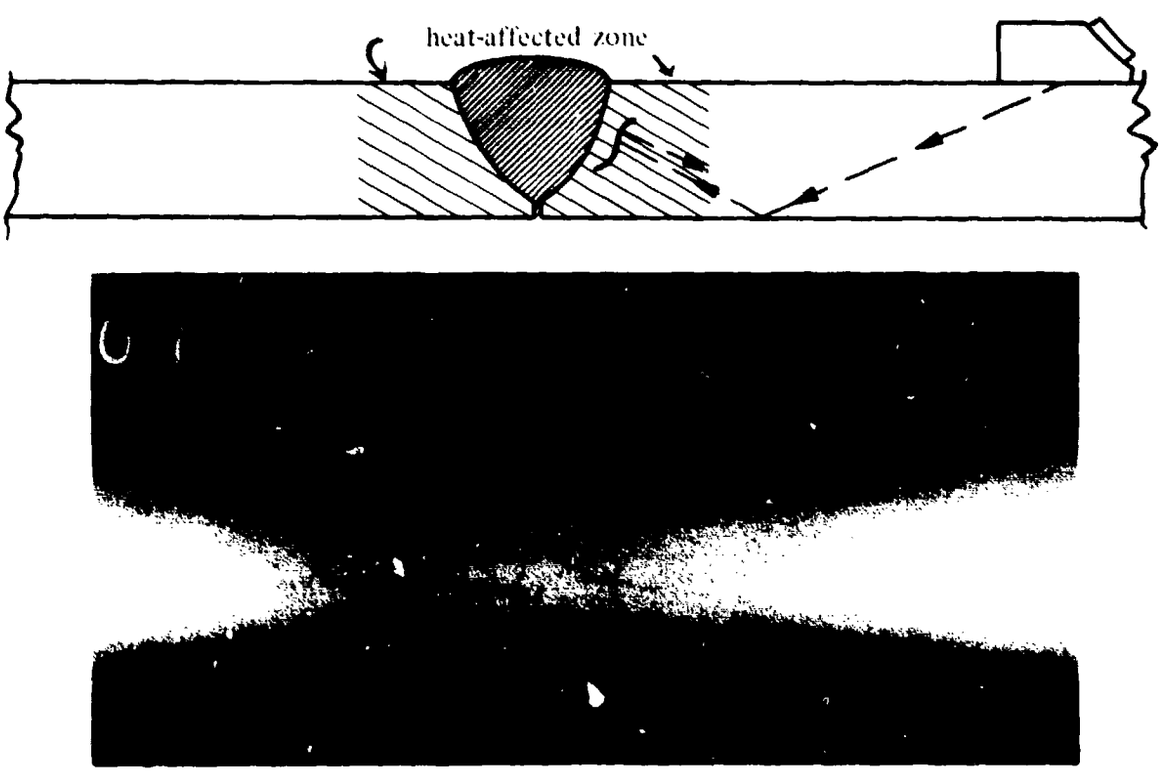

Fig.9(b) A crack in the parent metal in the heat affected zone difficult to detect by X-rays

(a) X-ray photograph of a spot weld

(b) Diagrammatic sketch of a spot weld

Figure 10

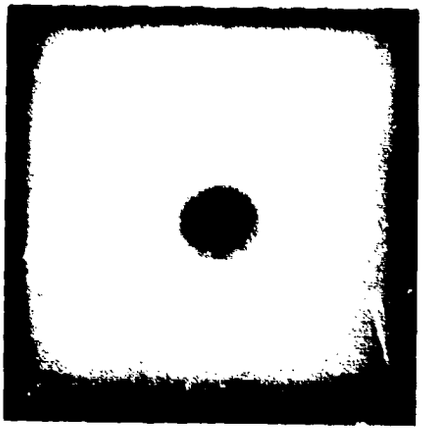

Fig.11 Spot weld showing porosity

Fig.12 Spot weld showing cracks

Fig.13 Spattering of fusion metal

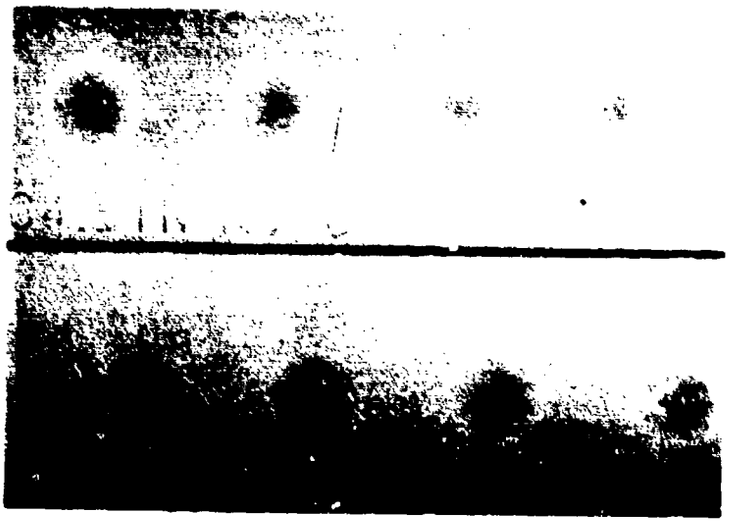

Fig.14 Spot weld on light alloy with high copper content (C4·5 TN·10/40).
Above: normal spot weld with characteristic halo due to copper migration.
Below: imperfect spot weld with halo reduced and indistinct.

CHAPTER 4.3

NDI OF BONDED STRUCTURES

by

M.Tréca

Société Nationale Industrielle
Aérospatiale
Laboratoire Central
3, Quai Leon Blum – B.P. 376
92153 Suresnes
France

CONTENTS

4.3.1 INTRODUCTION
- 4.3.1.1 History
- 4.3.1.2 Advantages of Bonded Structures
- 4.3.1.3 Design Factors
- 4.3.1.4 Materials

4.3.2 BONDING
- 4.3.2.1 Bonding Adhesives
- 4.3.2.2 Honeycomb Core Manufacturing Processes
- 4.3.2.3 Honeycomb Structure Repairs

4.3.3 FLAWS IN BONDED STRUCTURES
- 4.3.3.1 Inspection Process During Manufacturer
- 4.3.3.2 Inspection During Maintenance

4.3.4 INSPECTION PROCESS DURING PRODUCT MANUFACTURE
- 4.3.4.1 General
- 4.3.4.2 Bonding Adhesive Technological Value Evaluation
- 4.3.4.3 In-Process Inspection
- 4.3.4.4 Quality Control Test Pieces

4.3.5 INSPECTION METHODS
- 4.3.5.1 Sonic Inspection Technique
- 4.3.5.2 Vacuum Cup Inspection
- 4.3.5.3 Ultrasonics
- 4.3.5.4 Sonic Resonance
- 4.3.5.5 Eddy Sonic Methods
- 4.3.5.6 Holographic Interferometry
- 4.3.5.7 Thermal Methods
- 4.3.5.8 Radiography

4.3.6 STANDARD BLOCKS AND ACCEPTANCE CRITERIA
- 4.3.6.1 Standards (see Figures 46 and 47)
- 4.3.6.2 Acceptance Criteria

4.3.7 CONCLUSIONS

REFERENCES

NDI OF BONDED STRUCTURES

M.Tréca

4.3.1 INTRODUCTION

4.3.1.1 History

From the beginning of Aviation, adhesives have been used in the construction of wooden aircraft. Aircraft rigid structures were achieved by stacking their bonded wooden sheets (spar flanges, plywood cores, propeller blades etc.) but the actual development dated from the second world war thanks to plastics chemistry improvements and in particular thermo-setting materials (phenolic and later epoxy resins).

At the beginning, sandwich structure cores were made up of low density materials such as balsa wood, cork, rubber foam, plastic foam, etc. Altnough some of these materials are still being used, the great majority of current sandwich structures incorporate honeycomb cores (Fig.1).

4.3.1.2 Advantages of Bonded Structures[1]

Two types of bonded structures are now being used:

Metal-to-Metal bonded structures,
Sandwich structures.

4.3.1.2.1 Metal-to-Metal Bonded Structures

This covers the assembly of two parts by means of a bonding adhesive. Two major groups can be retained:

Stiffener bonding (refer to Figure 2) which makes possible a thin skin stabilization. Such process then replaces riveting or spot welding and helps in improving mechanical and above all, fatigue strength properties as:

(a) the stabilizing reinforcement mating surfaces are evenly and constantly loaded,
(b) the bonded joint stops fatigue crack propagation.

Reinforcement bonding (see Figure 3) by which the use of the lamination method makes possible local reinforcement replacing conventional or chemical machining, thence entailing:

(a) Material saving (sometimes in a most substantial way).
(b) Greater safety capability against crack propagation.

4.3.1.2.2 Bonded Sandwich Structures (see Figure 4)

From the design view point, bonded structure proves to be the best achievement of skin stabilization techniques.

In general, honeycomb cores are used for load carrying structures and withstand shear stresses while skins withstand both compression and tensile stresses.

This results in a significant weight gain as compared to conventional structures with stiffeners, and thanks to component consistency, fatigue strength is improved (mostly acoustic).

Attachment points constitute nevertheless the most critical areas in honeycomb panels and must be particularly well designed.

4.3.1.2.3 Applications

The advantages bonded structures and especially honeycomb sandwich structures offer, are obvious in several fields. Nowadays, there is no aircraft, missile or satellite which do not incorporate bonded structures and notably honeycomb sandwich structures.

Adhesive bonding is increasingly used for the manufacture of components such as: fuselage and wing panels, bulkheads, slats, flaps, airbrakes, landing gear door panels, fairings, tail units components, helicopter blades, floor panels, etc.

4.3.1.3 Design Factors[2]

4.3.1.3.1 Impact Resistance

It is generally admitted that a thin skin panel can successfully take applied tensile and compression stresses. However, in practice much thicker skin panels are being used to withstand impact loads. In effect a thicker panel has a high energy dissipation capability over a larger surface, which decreases the loads applied to the honeycomb.

4.3.1.3.2 Environmental Conditions

Temperature, exposure at such temperature, humidity and resistance to several fluids and gases must be assessed early in the design stage. The effect of loads under all these different environmental conditions must not be underrated.

Table I provides data on material selection according to their working temperature.

TABLE I

Materials Selection According to Working Temperature[2]

Temperature (°C)	*Core*	*Facing material*	*Adhesive*
Up to 175	Aluminium	Aluminium	Resins
Up to 250	Fibreglass	Laminates Steel or Titanium	Resins
From 175 to 500	Steel	Steel or Titanium	Brazing or welding

4.3.1.4 Materials

4.3.1.4.1 Metal Sheet Facings[3]

Till now, the majority of sandwich structures incorporated aluminium alloy or plastic reinforced fibreglass facings. Steel, wood or paper have been used likewise and probably their use will be developed in future. Other materials such as carbon fibre composites are liable to be developed because of the great advantages they offer.

Aluminium facings are mostly from 0.3 to 2 mm thick. Steel and titanium facing thickness ranges from 0.125 to 1 mm.

But there are specific cases, where reinforced plastic facings or plastic cores must be used for the construction of components such as radomes or any other structures requiring electrical transparency properties.

Plastic facings associated with aluminium paper or foam cores can be likewise used for the following reasons: easy forming of complex parts, weight control, insulation and thermal radiation, high temperature resistance and higher impact resistance.

4.3.1.4.2 Honeycomb Core

Honeycomb cores are produced in a great variety of materials including aluminium alloys, stainless steel, "Super Alloys", paper, resin impregnated fibreglass (NOMEX).

Core density may vary with ribbon thickness and cell size. Usually core height ranges from 5 to 25 mm, but may reach 150 mm and even 300 mm (for instance for surface controls). Ribbon thickness ranges from 13 to 130 microns – and regular cell size ranges from 3 to 10 mm.

4.3.2 BONDING

4.3.2.1 Bonding Adhesives

4.3.2.1.1 Different Bonding Adhesives[1]

Bonding adhesives available on the market and intended for aeronautical use are supplied under the following different forms:

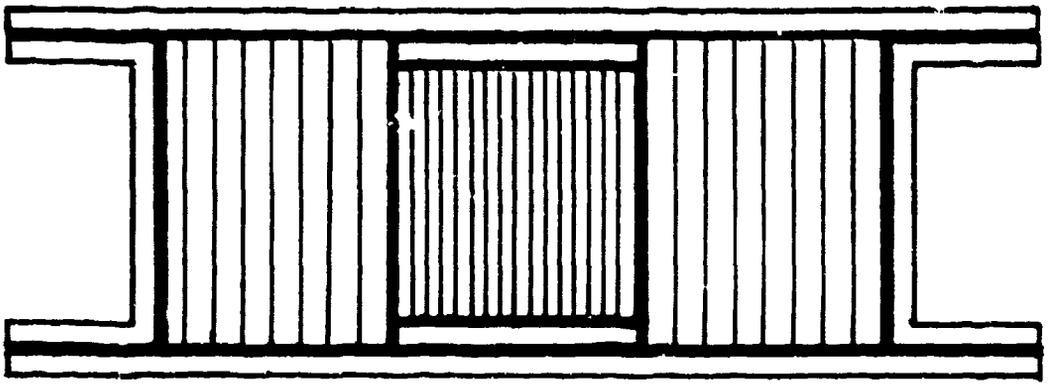

Fig.1 Honeycomb sandwich structure

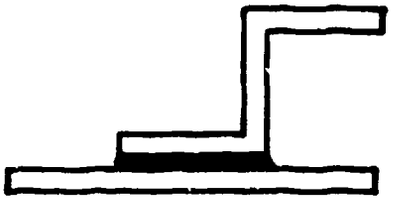

Fig.2 Bonded stiffeners

Fig.3 Bonded reinforcements

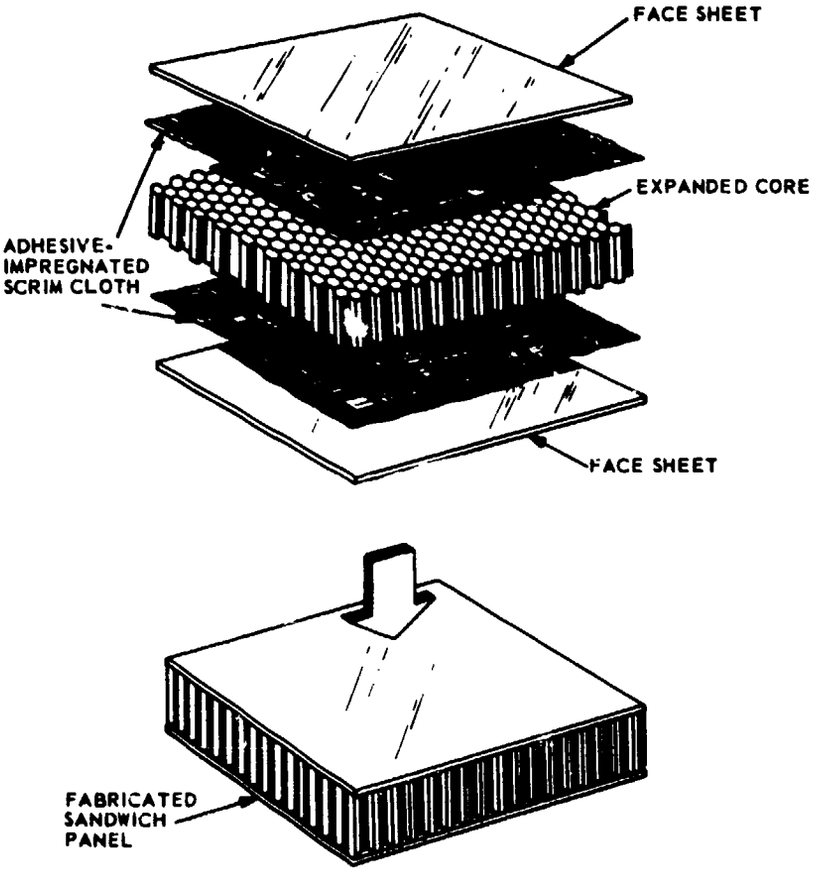

Fig.4 Honeycomb as a sandwich core material

- *Solid*

  As sticks, early solution which is now practically abandoned because of the difficult conditions of application it offers.

- *Powder*

  Again an old solution still in use but requiring special equipment and tools.

- *Paste*

  This solution rather applies to repairs, to tool jig construction and insert bonding in sandwich structures.

- *Film*

  It is the most widely used solution for structural bonding because of the simplicity of preparation and handling it offers. Adhesive films are commercialized in the form of rolls about 1 meter wide and 50 m long.

  A pre-jellified resin generally impregnates a carrier which can be as follows:

  - fibreglass or synthetic fibre fabrics
  - synthetic fibre knitted fabric
  - dispersed fibres
  - glass microbeads

  which results in a relative adhesive film flexibility for contoured structure bonding and entails an acceptable minimum bond thickness.

  There are also other bonding adhesives without carriers which are advantageous for their low density per square metre and can be used for any bonding applications.

- *Foam*

  It is intended for honeycomb/honeycomb adhesion and honeycomb/edge. It is available in the form of sheets.

4.3.2.1.2 Adhesive Curing Conditions

In order to achieve optimum mechanical properties at initial and aged condition, three major parameters must be controlled:

- pressure applied to the glue line,
- curing temperature,
- curing cycle length.

As a rule, adhesive paste hardens at ambient temperature and only requires the application of a simple pressure. On the contrary, structural adhesive films are thermo-setting and require specific cure temperatures (of the order of 120° to 170°C) under a given pressure (1 to 7 bars) for a period of time which generally ranges from 1 to 3 hours.

4.3.2.1.3 Bonding Process

Bonding is an adhesion process by molecular attraction between two parts to be bonded and a third factor: the adhesive which is placed in between in order to transmit mechanical loads.

Bond quality is conditioned by two completely different important factors.

adhesion of the adhesive to metal,
cohesion within the bond (see Figure 5).

4.3.2.2 Honeycomb Core Manufacturing Processes

4.3.2.2.1 Honeycomb Core Manufacturing

Honeycomb structures are made from thin metal foil the gauge of which generally ranges from 13 to 130 microns. There are two basic honeycomb core manufacturing processes as follows:

First process or corrugation process (see Figure 6)

Thin web strips are fed to two corrugated rolls which transform them into corrugation sheets. They are then stacked into a honeycomb block and bonded (or brazed in the case of stainless steel sheets).

Second process or expansion process (see Figure 7) being only applicable to bonded honeycomb.

In this process staggered parallel adhesive ribbons are applied on either side of the web material at regular intervals. Sheets are cut to the required length and stacked layer upon layer, to be cured in hot presses into hobes. Slices are sawed from the hobes and then expanded into honeycomb panels.

For laminated and polyamide paper honeycomb, it is necessary once expanded to dip them into a resin solution followed by a curing operation.

4.3.2.2.2 Lay-Up Process

Lay-up process can be broken down into three major steps:

(a) surface preparation of the components to be bonded,
(b) adhesive application. Lay-up,
(c) pressure application. Curing.

4.3.2.2.3 Surface Preparation

This surface preparation is intended to remove from the component surfaces to be bonded any foreign matters such as grease, oil, dust or carbon composites, etc. and to create on the material surface optimum conditions to ensure a total adhesion of the adhesive to the metal.

As a rule for aluminium alloys, surface preparation is a sulphochromic degreasing or unsealed chromic anodizing.

4.3.2.2.4 Adhesive Application -- Lay-Up (see Figures 8 and 9)

Components are interfayed with adhesive either in the form of film or by brush coating when paste. For adhesive films it is very important to remove protective tapes for they would impede the adhesion of the film.

For bonded sandwich structures, the lay-up operation consists generally in positioning first the lower sheet facing, then the panel edge members and then the assembly is clamped in position. The honeycomb core is then positioned into the edge member thus formed. Finally the panel is closed by positioning the upper sheet facing.

Once clamped the lay-up is placed in the autoclave for curing.

For complex panels, the lay-up operation can be broken down into two phases by bonding firstly the metal-to-metal components and later the honeycomb sandwich sub-assemblies.

4.3.2.2.5 Curing Process

4.3.2.2.5.1 Different methods

Curing of thermosetting adhesive bonded structures can be achieved by several methods

(a) hot press for flat panels,
(b) ventilated oven for flat or contoured panels,
(c) self-heated mould (oil, vapour) by conduction,
(d) autoclave, which is a pressurized oven where both temperature and pressure are controlled; it is nowadays the industrial process which can be considered as most adapted to component bonding carried out in several steps: fuselage panels, wing panels, control surface panels etc

4.3.2.2.5.2 Autoclave bonding (see Figures 10 and 11)

The panel to be bonded is placed in a tool as shown in Figure 11.

It essentially includes:

- an aluminium alloy support plate,
- a synthetic rubber sheet or aluminium foil or polyethylene sheet applied over the panel and acting as a cover for the sealed vacuum bonding chamber,
- a sealing device made up of platens bearing on the sealing joints,
- suction inlets to create a vacuum in the vacuum chamber thus formed,
- thermocouples for temperature checking.

Once the vacuum chamber is operative, a partial vaccum is created to make sure there is no leakage, and then the lay-up is placed in the autoclave for cure.

4.3.2.2.5.3 Curing parameters

To obtain a successful curing, it is necessary to conform to a certain number of parameters:

- temperature rise time, it must not be too rapid in order to avoid high thermal gradients,
- curing temperature,
- pressure.

As a rule, all these parameters are recorded to make sure the required curing conditions are properly met.

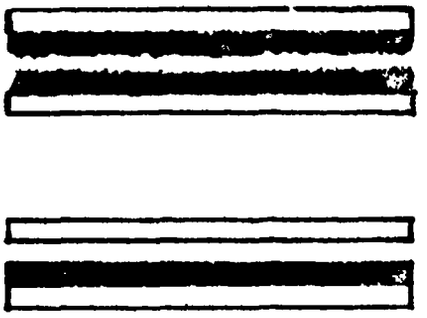

Failure resulting from a lack of adhesion

Failure resulting from a lack of adhesion

Fig.5 Different bonded joint failure types

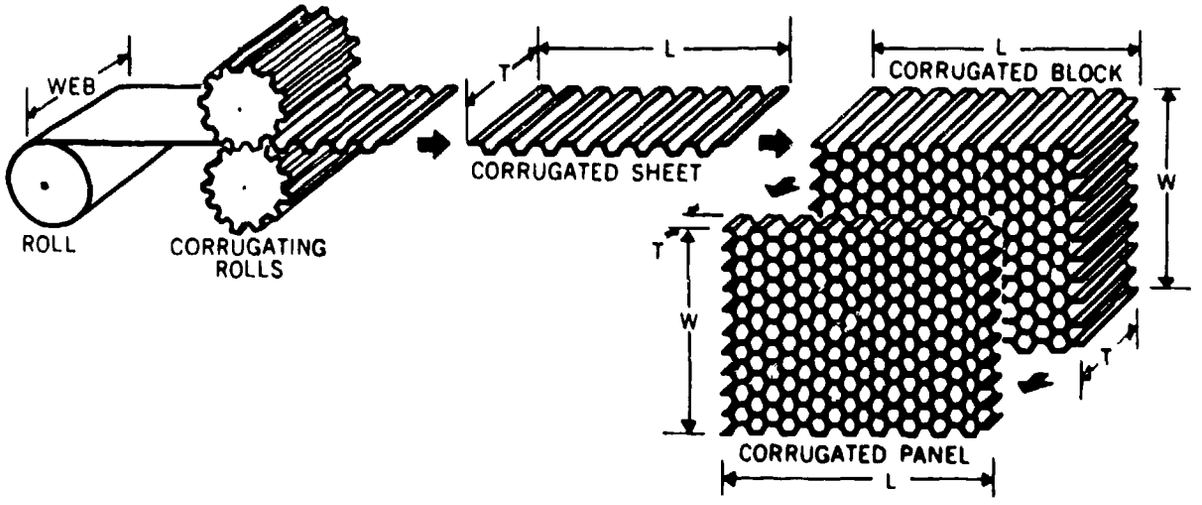

Fig.7 Expansion process of honeycomb manufacture. In this process all bonds are made simultaneously while the corrugation method is essentially a one-layer-at-a-time operation. ("Hobe" denotes "honeycomb before expansion".)

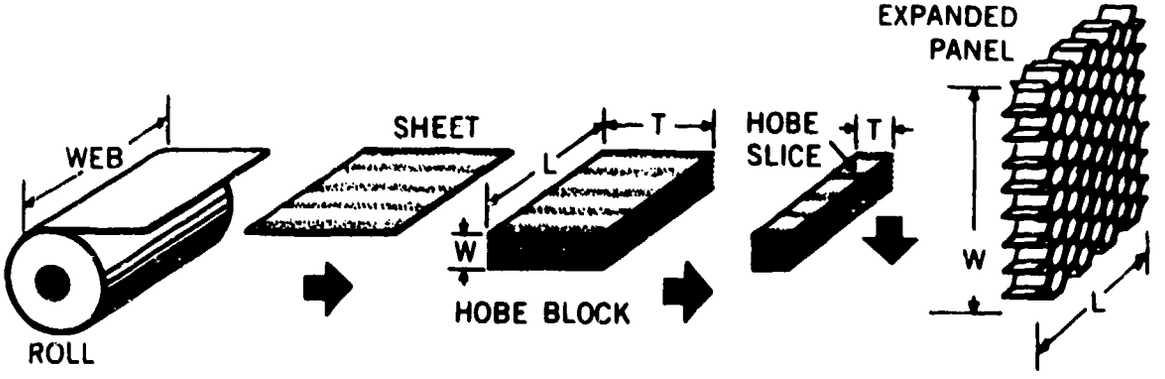

Fig.6 Corrugation process of honeycomb manufacture. Materials which can be converted using this process include metals, plastics, plastic-reinforced glass and paper

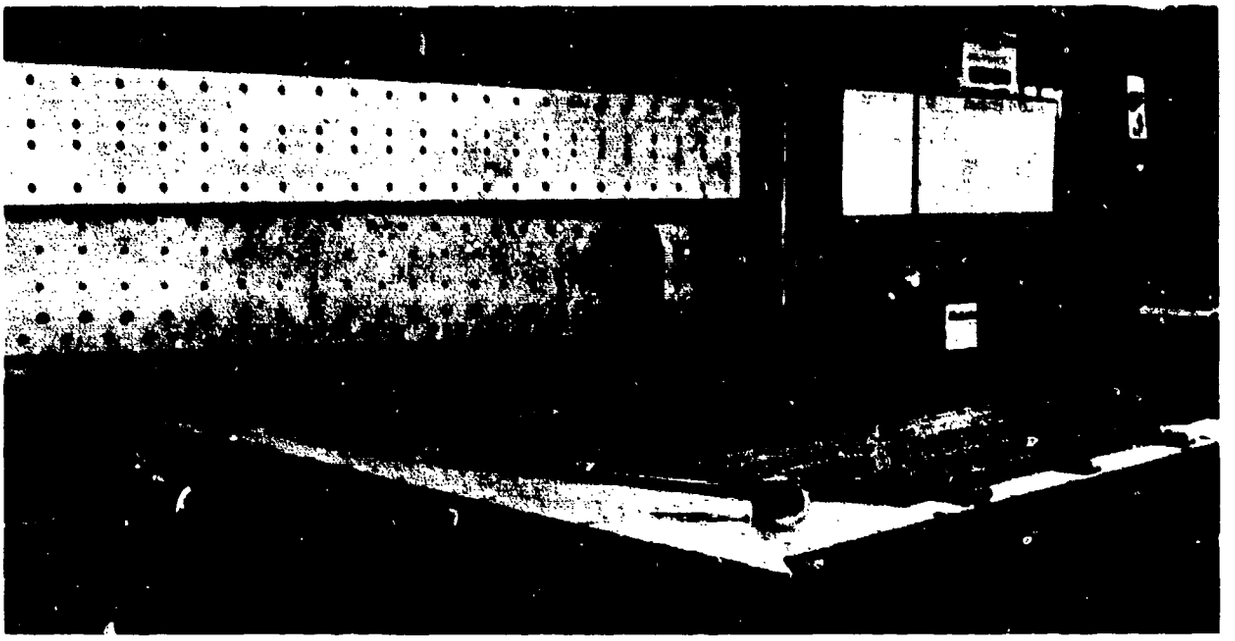

Fig.8 Honeycomb core machining

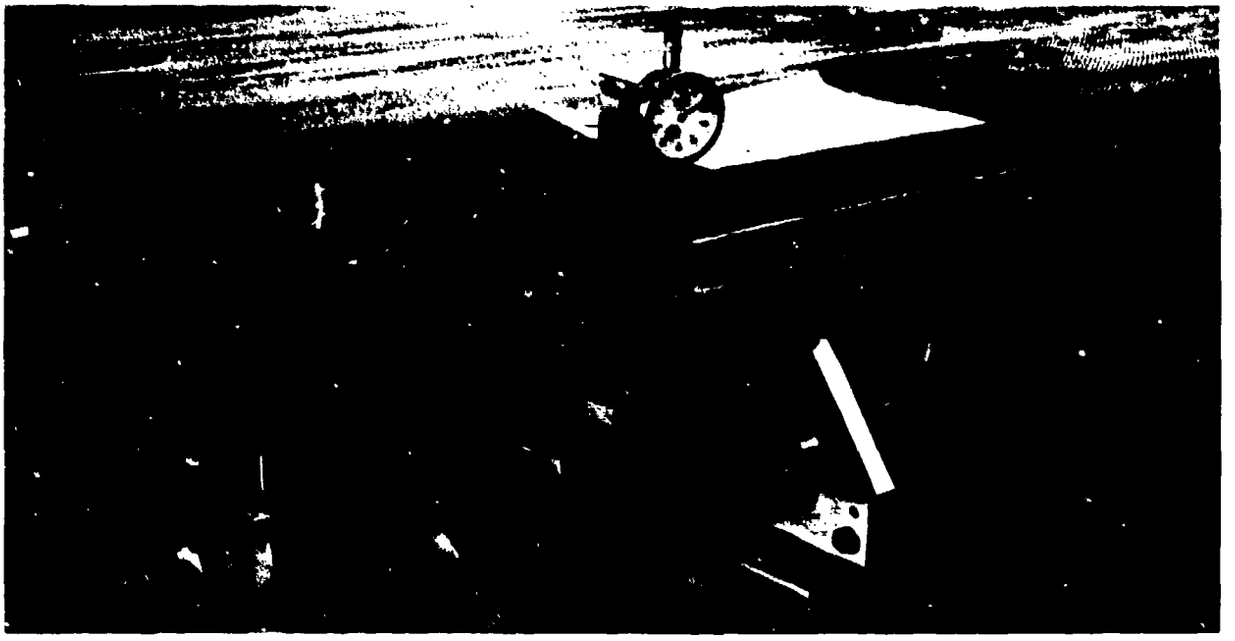

Fig.9 Checking of core protruding out of edgings (from 0.1 to 0.2 mm)

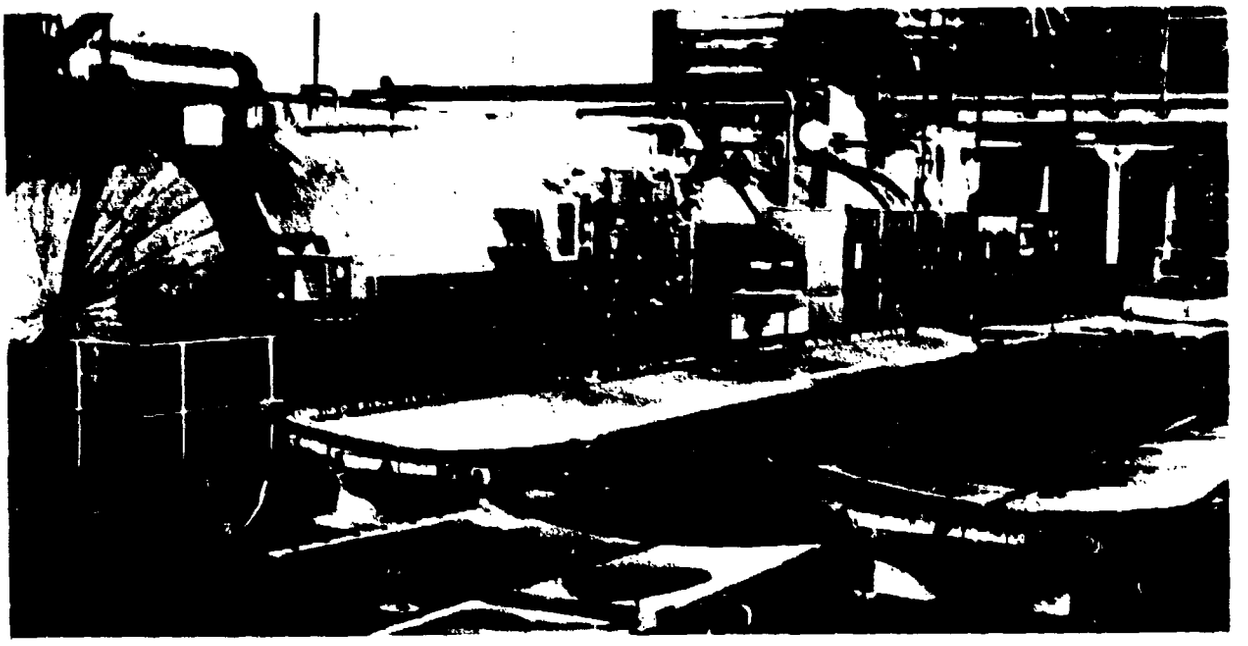

Fig.10 Autoclave of 2.4 m diameter and 14 m long

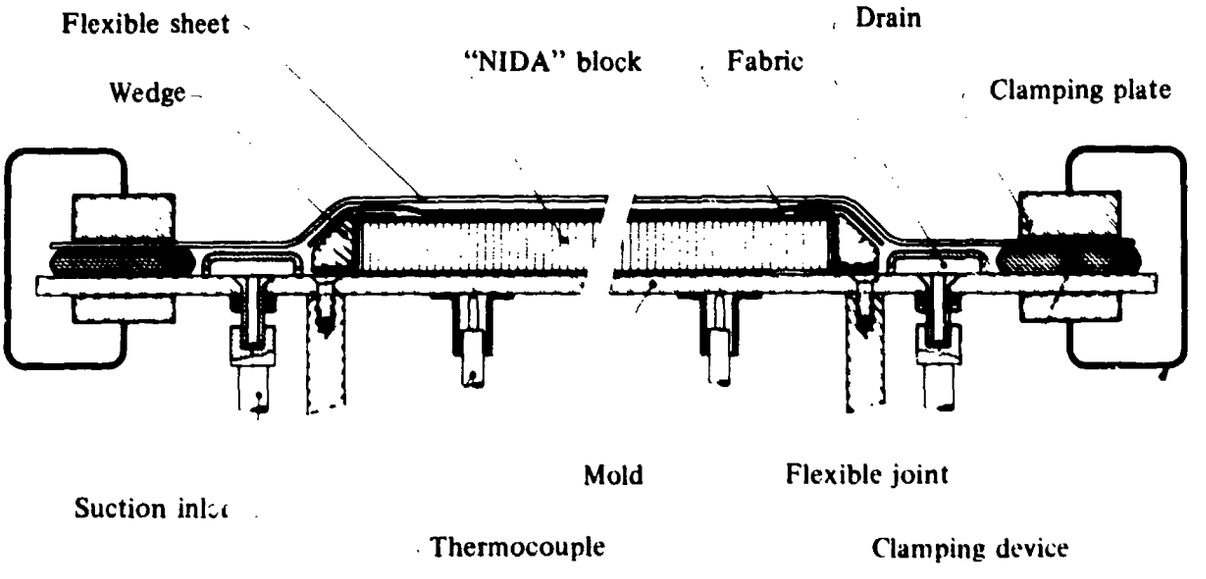

Fig.11 Autoclave bonding tool layout

4.3.2.3 Honeycomb Structure Repairs[4]

Honeycomb structures can be successfully repaired sometimes very easily and simply without in most cases any alteration in strength and rigidity (see Figures 12-15).

The following repairs can be quoted:

- single bonded and riveted reinforcements (Fig.14),
- bonded and riveted reinforcement by resin filling (Fig.12),
- elimination of defective areas replaced by honeycomb blocks with resin pouring (Figures 13 and 15).

4.3.3 FLAWS IN BONDED STRUCTURES

Before discussing the different non-destructive inspection methods which could be applied to bonded structures, it would be advisable to analyse the different types of flaws liable to be encountered and which are typical of this type of construction.

These flaws can be divided into two main groups:

- flaws developing during manufacture,
- flaws developing in service.

4.3.3.1 Inspection Process During Manufacture

Many flaws may appear during manufacture. They are:

4.3.3.1.1 Splicing Flaws

This type of defect occurs when sheet facing and honeycomb core joining is not perfect. During manufacture, the honeycomb core is machined to be inset into the structure formed by the edgings and facings. The honeycomb core depth is generally greater by about 1/10 mm than the edgings in order to ensure a perfect joining with absorption of the adhesive bond. Such condition is easy to achieve. The major problem is in areas where there are sudden variations in honeycomb thickness (edging areas, bonded reinforcements with variable facing thickness (see Figure 16)). Such areas require specific honeycomb core machining to mate with these thickness variations and such processes must be carried out with great care and accuracy.

It may occur sometimes, in order to obtain an excellent joining of the components, to locate these reinforcements or variations in core thickness on the external side of facing (see Figure 17). This technique may slightly decrease the aerodynamic features of the finished component. But on the contrary, they greatly improve joint quality and ease panel construction.

Figure 18 shows examples of the different types of joint which are entailed by these core thickness variations. When machining is satisfactory the honeycomb core and facings mate perfectly. On the contrary, when machining is too deep in the core, as seen in Figure 18(a), an unbonded area exists between the facing and core.

Figure 18(c) shows that when the machined area is unsufficient the facing thicker area bears on the protruding cells resulting in panel distortion.

All these joining flaws are among those most commonly found during manufacturing processes. And they are all the more difficult to avoid as the structure is more complex. These flaws generally are elongated. They may vary more or less in length but their width ranges most of the time from some millimetres to some centimetres. They are generally located along the edgings, along the stiffeners or at the skin thickness variations. When inspecting a finished product, the greatest care will be given to the examination of these areas. As calibration is affected in the greatest part of the currently used techniques by facing thickness variations, it is advisable to check carefully calibration on either side of such thickness variation to determine if the reading provided by the instrument results from thickness variations or from a flaw.

Figure 19 shows the different flaw types to be found in edging areas. If the honeycomb core is too thick, this will result in a defective joint with the edge members. If on the contrary honeycomb core depth is insufficient, defective joining will take place at the sheet facing level, as the structure rigidity in such area impedes any satisfactory adhesion of the sheet facings to honeycomb.

Likewise joining flaws may be found in honeycomb expanded panel assemblies. They may originate from a defective dimensioning of the honeycomb expanded panel or from the effect of adhesive which when curing tends to excessively force apart the two panels.

Repair Examples

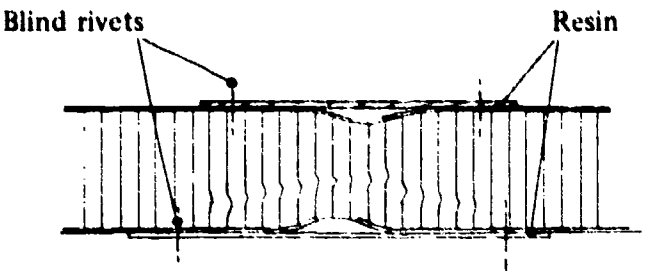

Figure 12

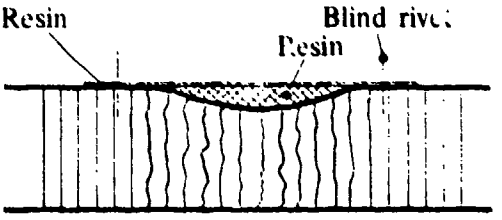

Figure 13

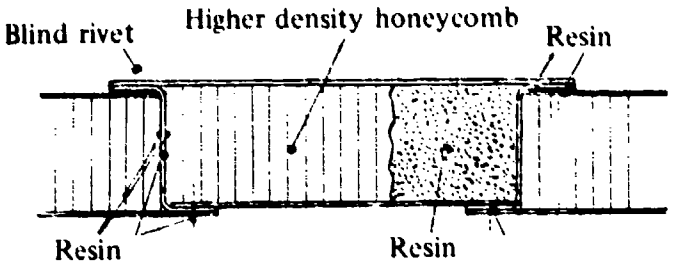

Figure 14

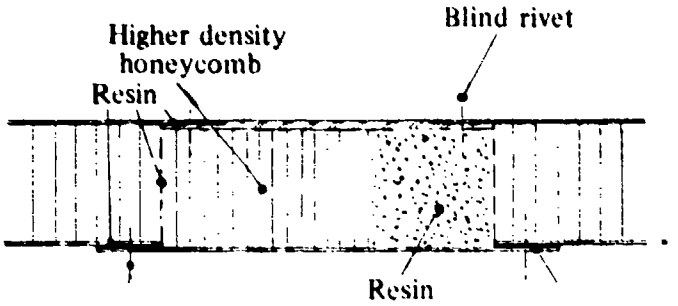

Figure 15

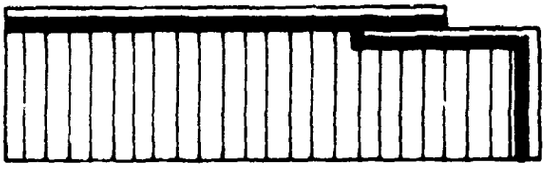

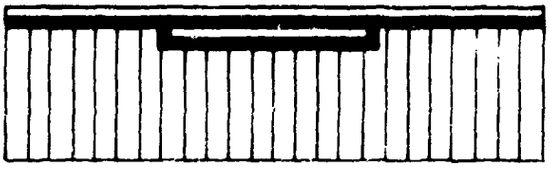

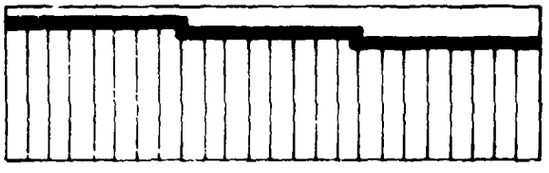

Fig.16 Difficult joining areas

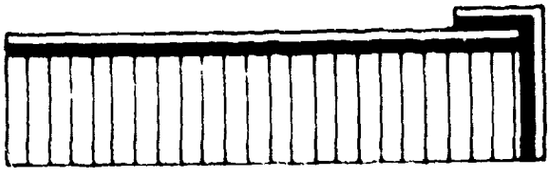

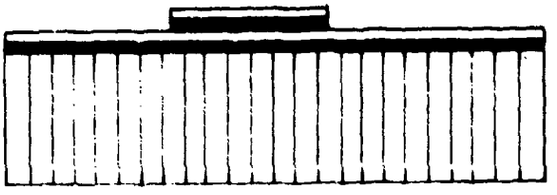

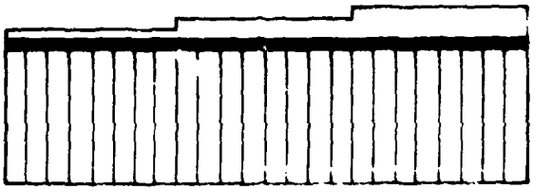

Fig.17 Areas without joining problems

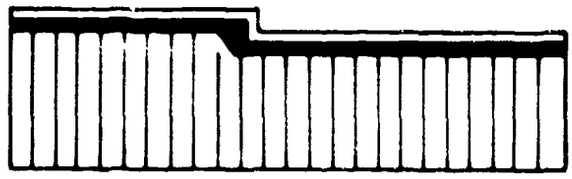

Fig.18(a) Unbonded area (too large a machined area)

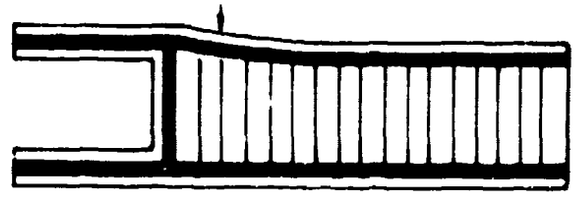

Fig.18(d) Unsufficient honeycomb cell depth

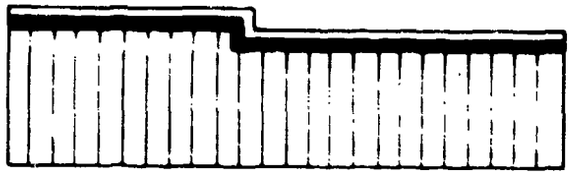

Fig.18(b) Good joining

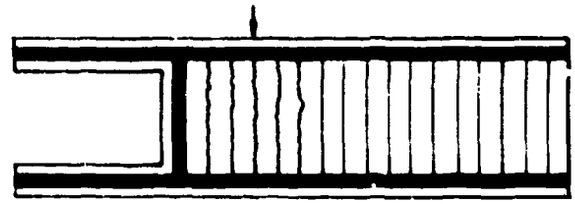

Fig.18(e) Too important honeycomb cell depths

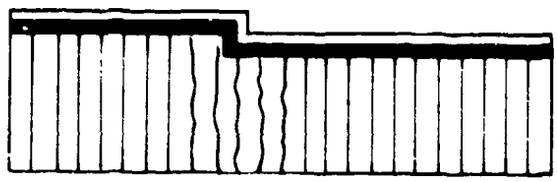

Fig.18(c) Crushed cells (too small a machined area)

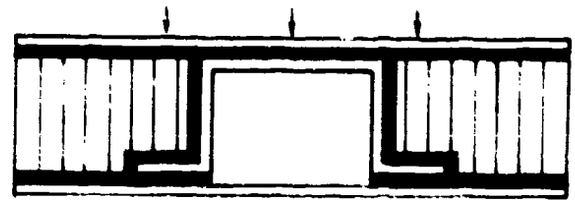

Fig.18(f) Critical areas

Fig.18 Defective facing to honeycomb joining

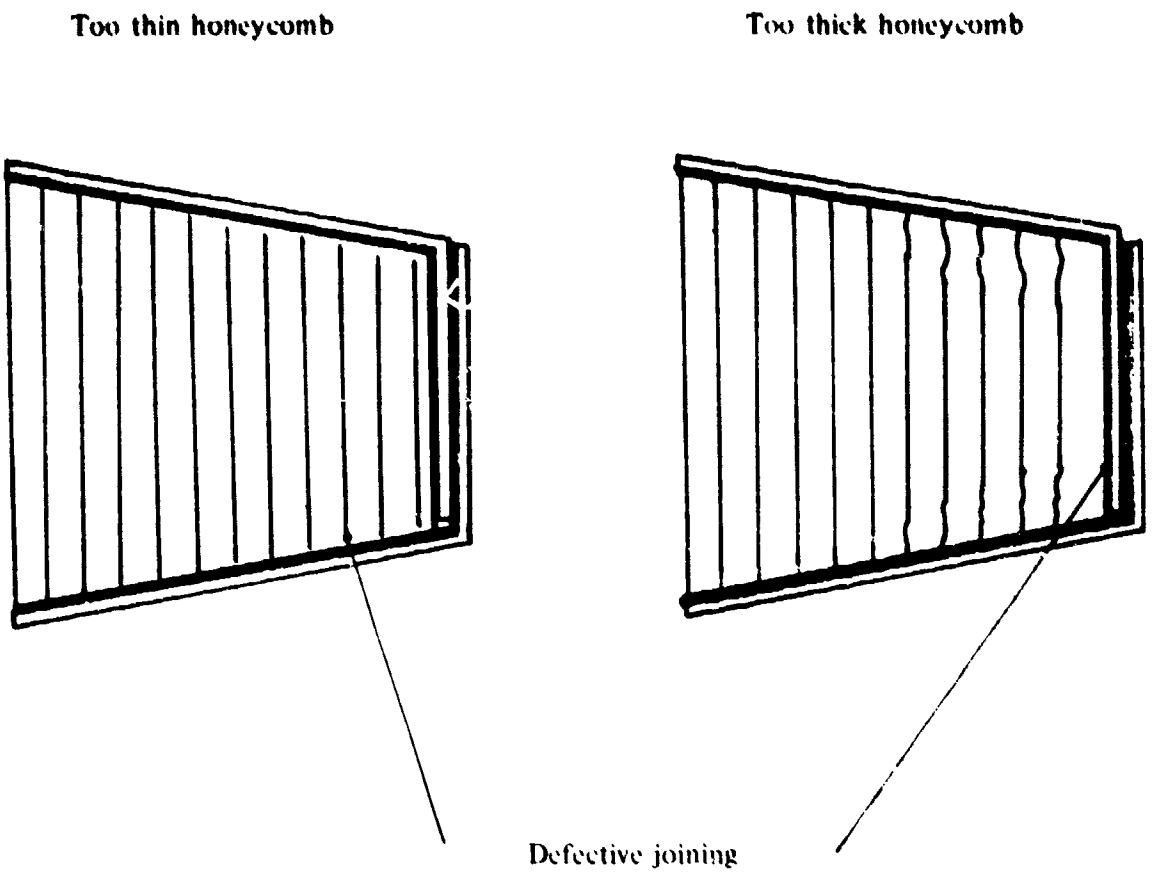

Fig.19 Defective edging to honeycomb joining

4.3.3.1.2 Bonding Flaws

Many other parameters than defective joining may entail bonding defects during manufacture. It can likewise result from the use of a poor quality adhesive, from an insufficient surface protection, from a curing process improperly carried out or from the use of an ill-adapted tool. It is then recommended when bonding a complex structure for the first time to perform a preliminary test on the tool by applying between the tool and the structure facing, a coat of VERIFILM with the appropriate temperature and pressure. At the end of the test, a check of the VERIFILM coating thickness will help in making sure that the structure was properly positioned on the tool.

These parameters being easier to control than the joining itself, this type of flaw is less frequent. On the contrary, they can be found all over the structure surface and there are no preferred areas.

4.3.3.1.3 Other Flaws

Flaws may result from the absence of bonding adhesive (such an omission may occur during manufacture).

Sometimes, the bonding film is correctly positioned but the protective tapes have not been removed. This type of flaw generally is very difficult to detect once the panel is completed.

We must mention likewise honeycomb flaws (crushed cells).

Finally the defective sealing of a completed panel may likewise be considered as a defect for it can entail further flaws found during maintenance such as water entrapment and corrosion.

4.3.3.2 Inspection During Maintenance

Flaws liable to be detected during maintenance are practically the same as these found during manufacture. However, as a rule, they can be easily detected after the structures have been stressed in service. Failed bonds are then obvious and the data provided by the inspection equipment much easier to interpret.

To the above mentioned flaws, can be added:

water entrapment resulting from a defective panel sealing. The presence of water (or of any other fluid, such as jet fuel for instance) in the honeycomb cells increases structure weight. On the other hand, in some moving components such as helicopter blades, water entrapment may cause important blade unbalance.

corrosion that can take place in the honeycomb due to the presence of water. As cell walls are very thin, honeycomb corrosion can result fairly quickly in complete destruction of sandwich structure cores thence considerably decreasing structure strength.

defects resulting from impacts or blows sustained by the panel entailing both skin distortion (or even a tear in the panel) and core damage. Non-destructive inspection carried out at this stage helps in assessing the extent of the existing flaw and defining possible repair action.

Finally it could be necessary to inspect a repaired area to make sure the repair work has been properly incorporated or that the flaws have not further developed.

4.3.4 INSPECTION PROCESS DURING PRODUCT MANUFACTURE

4.3.4.1 General

Although the non-destructive techniques applicable to completed sandwich structures constantly improve, they do not replace in any way inspection processes during manufacture which are the only way to check parameters impossible to evaluate on a finished product. They mainly apply to the evaluation of:

technological value of adhesives,
inter-operation inspection,
quality control test pieces.

4.3.4.2 Bonding Adhesive Technological Value Evaluation

Obviously the inspection must make sure at first that the adhesive quality is satisfactory. To do so, it is necessary to test the adhesive properties by means of an appropriate specific test. On the other hand, before the adhesive is applied it is recommended to make sure that the storage requirements were satisfactorily met and that the limit date is not over.

These tests can be performed with shear metal-to-metal test pieces or honeycomb-to metal peel test pieces.

4.3.4.3 In-Process Inspection

This type of inspection is essentially preventive and is performed at all manufacturing process stages. Among the numerous evaluation operations it implies, let us mention the following they affect:

dimensional inspections and aspect of the constituants,
surface preparation inspection,
bonding inspection,
lay-up (the inspectors making sure that the protective tapes are removed from the adhesive films; they likewise check the adjustments and pinning),
bonding tool inspection,
curing process. This evaluation is mostly performed by recording the various parameters (temperature, vacuum, pressure),
sealing inspection.

4.3.4.4 Quality Control Test Pieces

The test pieces which are usually used are:

shear metal-to-metal test pieces,
tensile metal-to-honeycomb test pieces,
peel metal-to-honeycomb test pieces,
peel metal-to-metal test pieces.

4.3.5 INSPECTION METHODS

4.3.5.1 Sonic Inspection Technique

The oldest and probably the simplest inspection method to detect whether or not a bonding defect exists between the honeycomb and facing is by tapping the part with a coin or a small mallet.

The difference in sound (tone or frequency) between an unbonded area and a bonded area can easily be heard.

Initially, inspectors used a coin but nowadays they generally prefer a nylon stick, one end of which has been rounded off in order to avoid any detrimental indentations in the structure.

The thinner the facing gauge, the lighter the tap.

With such techniques, unbonded areas are directly detected, provided the tested facing is thin enough.

This rudimentary but practical method however requires skilled personnel. This is generally used as an alternative process when an appropriate and sophisticated equipment is not available.

4.3.5.2 Vacuum Cup Inspection[5]

A vacuum cup fitted with dial indicator, the probe of which is applied to the centre of the area under test, is used in this technique.

While the vacuum is created (up to 800 g/cm^2) the dial indicator pointer deviates over some 1/100 mm. But over an unbonded area the deviation is much more important.

This time consuming and nowadays seldom used technique, only applies to thin gauge facings (less than 0.8 mm) and requires a certain glue line width.

4.3.5.3 Ultrasonics

Ultrasonic techniques are largely used for the evaluation of adhesive bonded honeycomb sandwich structures (Fig. 20). Several methods can be retained among which the most generally used are the pulse echo technique (a transducer acting as transmitter-receiver receives the echo signals reflected by the bonded interface) and the through transmission process (the transmitter and receiver transducers are separated and located on either side of the structure).

We shall describe in the present text the ultrasonic pulse echo ringing process for several reasons.

(a) This process is widely used because of its simplicity and flexibility of use. It does not require any advanced equipment and can be directly operated without any problems on-board the aircraft.

(b) The phenomena under investigation are typical of bonded structures, while other processes with focused transducers are much closer to conventional ultrasonic inspection techniques.

Fig. 20 Ultrasonic inspection

4.3.5.3.1 Pulse Echo Ringing Process

4.3.5.3.1.1 Basic principle

This process compares the echo signal envelopes displayed on a screen with calibration standards traces representative of the structures to be inspected.

4.3.5.3.1.2 Metal-to-metal bond[1]

Two cases may arise as follows:

When the sheet facing thickness is important enough with respect to pulse amplitude, it is then possible to discern the signals reflected by each interface (see Figure 21). The parameters to take into account are the echo amplitudes from the metal-to-adhesive interface and in particular from the lower facings. When no lower facing signals are received this almost certainly implies an unbonded area. It is possible to use, in order to obtain short pulses, transducers of 10 MHz frequency.

If the facing sheets are thin, which generally is the case, the echo signal cannot be separated any more on the screen. Signal reflection in the sheet only is obtained. The impedance variation at each interface determines the quantity of energy reflected and the cured bond cohesive properties can be deduced from the study of the oscillogram so obtained. The reflected signals will be the more weak and scarce the higher the bond quality . Figure 22 shows typical oscillograms relative to an unprotected metal sheet, a metal sheet with adhesive film and a perfectly bonded metal-metal assembly.

4.3.5.3.1.3 Methods for inspecting adhesive bonded honeycomb structures

4.3.5.3.1.3.1 Basic principle[6]

In the case of adhesive bonded honeycomb structures, the phenomena under test are much more complex than for metal-to-metal bonds, because of the assembly geometry; out in practice the results can be easily processed and even generally more meaningful than in metal-to-metal bonded assemblies.

Figures 23, 24 and 25 show oscillograms of an adhesive bonded honeycomb structure 25 mm thick and incorporating three typical cases:

correct bond,
facing-to-adhesive unbond,
honeycomb-to-adhesive unbond

The following comments apply to these oscillograms:

(a) Figure 23(a) oscillogram results from a lack of adhesion between the facing sheet and the adhesive film. This phenomenon can be easily explained by the fact that the present case is similar to the case of an unprotected metal sheet having a high reflective surface capability (high acoustical impedance variation at the metal-air interface). Causing the emitted pulse signal to reverberate in the sheet during a relatively long period of time. Figure 23(b) shows the enlarged display of the first third part of Figure 23(a) oscillogram traces.

(b) Figure 24(a) oscillogram results from a lack of adhesion between the adhesive film and the honeycomb. The presence of an adhesive film has eliminated the metal-to-air interface, it being replaced by a somewhat weaker acoustical impedance variation. A great part of the pulse signal energy is, then, transmitted to the adhesive where it vanishes. The pulse signal energy then decreases rapidly with each subsequent reflection out of which only a small number are displayed on the screen.

Figure 24(b) provides an enlarged display of the first third part of Figure 24(a) oscillogram.

(c) Figure 25(a) oscillogram results from a good adhesion of the facing sheet to the honeycomb core. Again the adhesive film damping effect is apparent but additional echo signals appear on the oscillogram caused by the energy transmitted in the honeycomb cell walls and which is later reflected back to the probe.

Figure 26(a) oscillogram is similar to Figure 25 but the delay displayed results from a time scale displacement. This causes the traces to be displaced on the left. Such displacement has been so adjusted to eliminate on the screen multiple signals resulting from multiple reflections in the facing sheet and to retain only the signals generated by the honeycomb structure. Figure 26(b) and 26(c) oscillograms result from transduced tested areas where again there is a lack of adhesion between the adhesive film and the honeycomb and between the facing sheets and the adhesive.

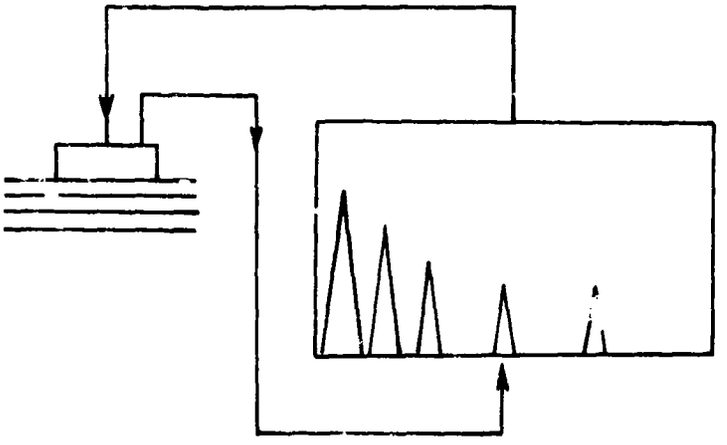

Figure 21

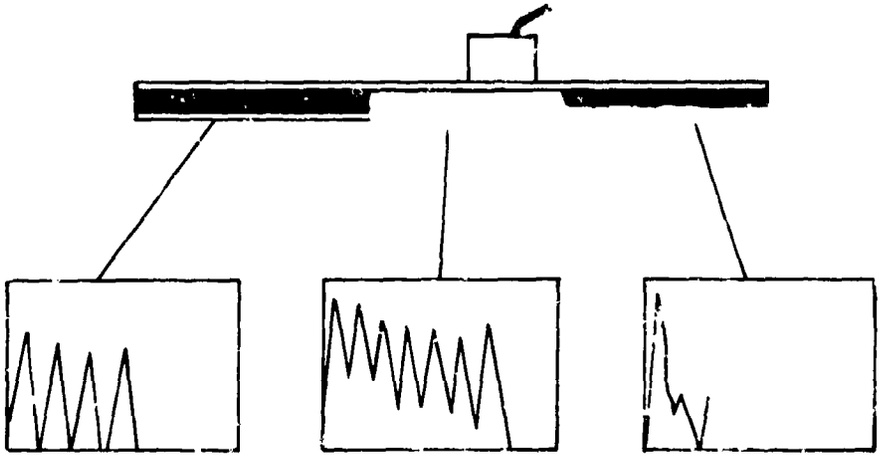

Fig.22 Metal-to-metal bond; three typical oscillograms

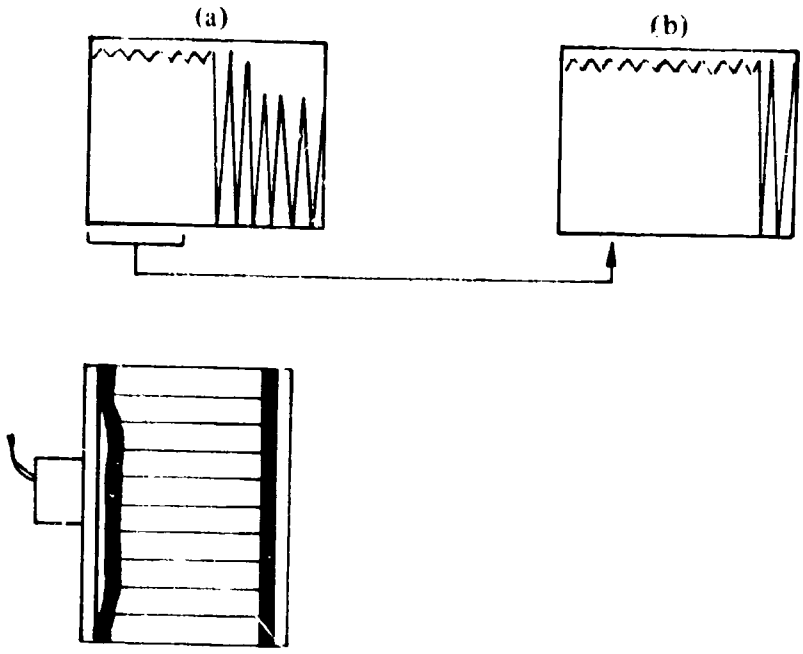

Fig.23 Facing sheet to adhesive unbond

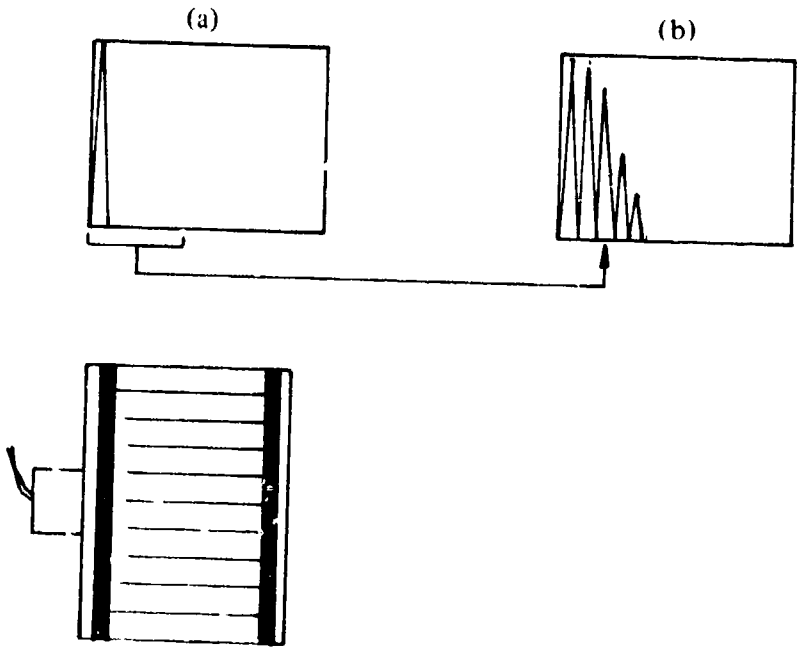

Fig.24 Honeycomb to adhesive unbond

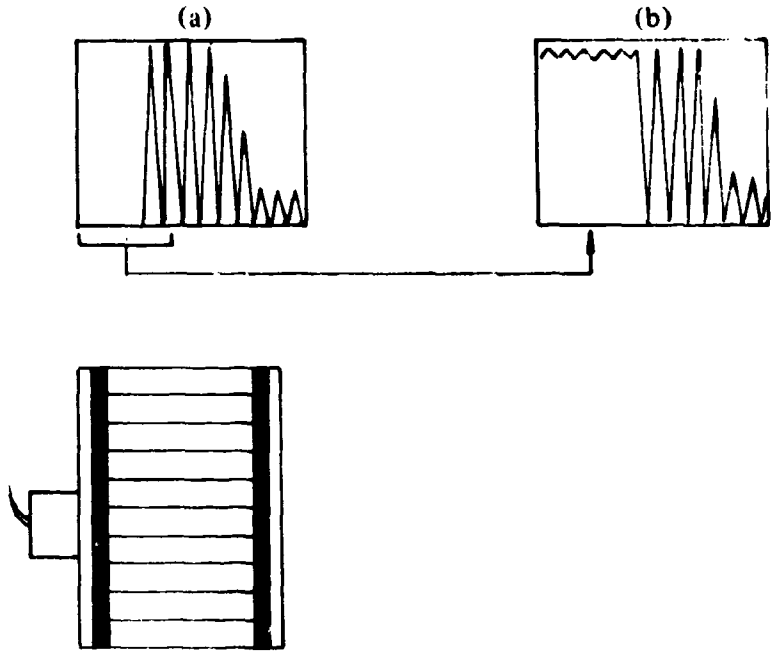

Fig.25 Correct bonded area

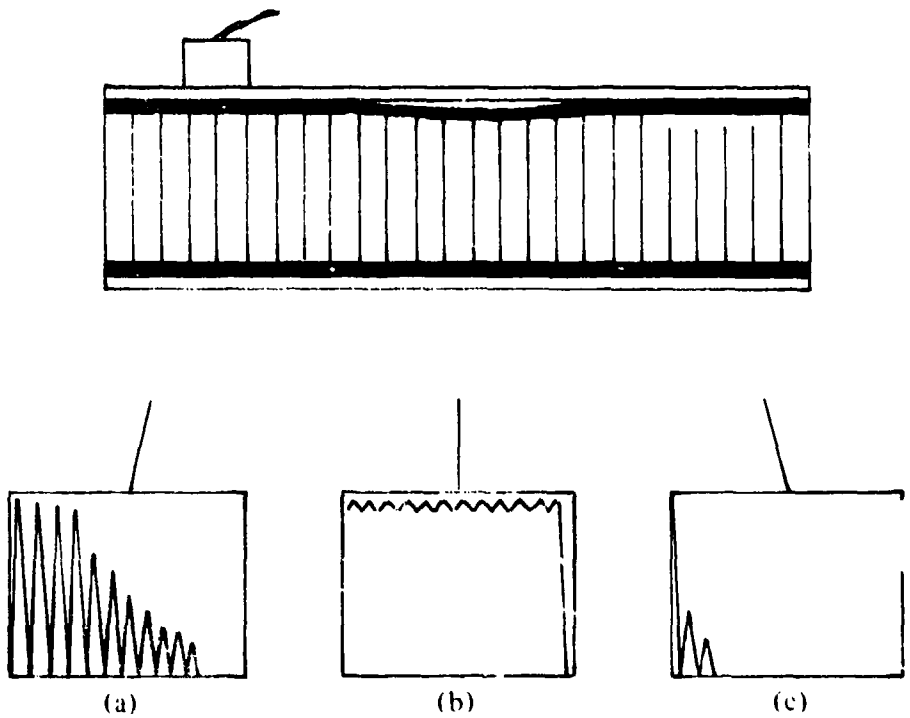

Figure 26

To sum up the situation, the three following cases are liable to be found:

Conditions	*Oscillogram*
Good adhesion of honeycomb to facing.	Signals covering approximately half of the screen.
Lack of adhesion of the adhesive to the honeycomb.	Uniform basic line, important damping.
Lack of adhesion of the facing to the adhesive.	Complete facing sheet signal saturation. No basic line.

The oscillograms recorded may vary from one structure to another. The instrument is adjusted with the help of reference test pieces representative of the structure to be inspected and incorporating typical defects to be found. Such adjustments should generate on the screen the previously described oscillograms.

The exact explanation of the recorded phenomena proves to be quite complex. Nevertheless the general trend seems to be as follows:

- part of the longitudinal wave transmitted to the structure is reflected by the facing sheet generating multiple signals.
- part of the longitudinal wave is transmitted to honeycomb and is propagated in the cell walls and when reaching the cell bottom is sent back to the probe. This wave propagation though the honeycomb is accompanied by wave transformations and it seems that it simultaneously develops into several different wave types. The propagation velocities of these waves may vary from the original longitudinal wave velocity to about 15% of the latter, according to the working frequency and the structure geometry.

4.3.5.3.1.3.2 Effect of honeycomb structure thickness

We previously noted that the received signals are, on the one hand, generated by multiple reflections from the facing sheet and on the other hand by signals which have traversed the honeycomb structure. Now, when the honeycomb panel is thin, these two types of signal cannot be associated. For instance if the inspector wants to evaluate a honeycomb sandwich 20 mm thick, incorporating a facing sheet 1 mm thick, it proves impossible at a frequency of 2 MHz. On the contrary, with the same structure, at a lower working frequency (0.5 MHz) the inspection process is then possible not only because many successive cell bottom signals can be received but also because the waves which are propagated in the honeycomb have lower velocities then at 2 MHz. In effect one can note that at 0.5 MHz the waves are propagated at velocities which might be 12 to 15% of the original longitudinal wave velocity and which probably are Lamb's waves.

As a rule, for panels incorporating facing from 0.5 to 3 mm thick, the working frequency is 2 or 3 MHz for honeycomb core thicknesses higher than 25 mm. For panels from 10 to 15 mm thick, it is often necessary to select a 0.5 MHz frequency, the selection being always made as shown further on, in line with the results obtained on reference test pieces.

The selection of 0.5 MHz frequency may entail sometimes with certain panel configurations, difficulties in the interpretation of signals. In effect at such a low frequency, the discrimination of the saturation case resulting from a defective bond between the facing sheet and the adhesive becomes less easy. Under such circumstances, the evaluation may be conducted in two steps. A first action at 0.5 MHz reveals adhesive to honeycomb unbonds. A second action carried out at 2 MHz reveals facing sheet to adhesive unbonds.

4.3.5.3.1.3.3 Effect of facing sheet thickness

We demonstrated previously that correct bonding evaluation at 2 MHz with the honeycomb cell bottom signals depended upon the presence of the adhesive film which limits the number of multiple reflections in the facing sheet, to the part located on the screen in front of the traces of the first cell bottom signal. As in the case of honeycomb panel thickness decrease, such difficulty can be coped with, by selecting a lower frequency (0.5 MHz for instance).

On very thin facings (lower than 0.6 mm) a lower frequency to the order of 0.5 MHz could be likewise interestingly valuable to frequency selection.

But the tests conducted on a reference test piece are the final factor enabling the inspector to select the appropriate frequency.

4.3.5.3.1.3.4 Effect of facings incorporating several bonded sheets

The difficulties encountered when evaluating areas made up of several bonded sheet facings are due to a combination of two factors: a global facing thickness increase and the presence of adhesive

The global facing thickness increase is comparable to a single sheet facing thickness increase.

The presence of bonds in facings greatly attenuates the transmission of ultrasonic energy to honeycomb. In fact, if we compare the results obtained with a 3 bonded sheet lay-up and with a single sheet whose thickness is identical, we realize that with the same setting, both the amplitude and the number of multiple reflections are much lower in the presence of bonded joints.

However, in spite of the problems met, the pulse echo technique is perfectly valid for an evaluation of areas incorporating several bonded sheets. It is, of course, not so easy as in the case of single sheet facings and it is necessary then to adapt the inspection technique to each particular case.

4.3.5.3.1.4 Operational mode

As previously stated, the pulse echo technique selected for the evaluation of bonded structures is essentially based on comparative data. Result interpretation is in fact a comparison with the oscillogram traces displayed on the instrument, once the latter has been properly calibrated.

Calibration is made with calibration standards representative of the structure to be inspected and including the different defect types liable to be found which are as follows:

- unbond on facing upper side,
- unbond on facing opposite side,
- collapsed honeycomb, etc.

To find defects existing in the facing sheet side tested, the transducer is applied on a correctly bonded area and the "distance" setting knob is adjusted in order to obtain traces corresponding roughly to Figure 25(a) oscillogram. The transducer is then positioned over the reference test piece areas incorporating both honeycomb-to-adhesive and facing sheet-to-adhesive unbonds. It is, then, necessary to make sure that the traces so obtained correspond respectively to Figure 23(a) and Figure 24(a) oscillograms.

By expanding the "distance" scale and delaying the time scale, we are back to Figure 26 traces. The traces corresponding to the different areas of the reference standard are then checked for conformity with the 3 typical traces of Figure 26. It is sometimes necessary to reset the other setting in order to obtain very different traces according to these three typical cases.

Frequency selection is made in conformity with calibration standards in order to obtain the best possible results. It is difficult to assess values as a great number of parameters affect frequency selection. However, as a rule, a frequency to the order of 2 or 3 MHz is retained for panels more than 25 mm thick and sheet facings more than 0.5 mm thick. For thinner facings as well as for honeycomb panels ranging from 10 to 15 mm, it is necessary to adopt as a rule a lower frequency value (of the order of 0.5 MHz).

To evaluate defects existing in the facing opposite the facing on which the transducer is applied, as well as in collapsed honeycomb, a similar process is followed but the transducer is positioned on defective areas corresponding to the reference standard.

There is no general rule for calibrating the units. In any case it is advisable to refer to calibration standards representative of the structure to be inspected and incorporating typical defective areas. Both frequency selection and unit settings are made so as to obtain the most contrasted traces possible corresponding to the sound areas of the component under test and to the defective areas of the reference standard.

It must be noted that the unit frequency setting may not be the same as the transducer frequency. Results prove to be sometimes much more satisfactory at 5 MHz for a transducer frequency of 3 or 2 MHz or vice versa.

4.3.5.3.1.5 Corrosion detection

In sandwich structure, corrosion affecting all walls can also be detected with the pulse echo technique. The traces displayed on a cathode ray tube screen are very similar to the traces generated by a honeycomb to adhesive film unbond.

Calibration is achieved with the help of calibration standard representative of the component to be inspected and incorporating corroded areas. When calibrating, the maximum contrast between traces corresponding to sound areas and defective areas are sought.

Such process generally proves satisfactory with honeycomb structures incorporating a single sheet facing. But with multiple sheet facings, the result interpretation is much more critical.

On the other hand, a certain number of parameters may alter the technique efficiency. One such case, for

It is then necessary to be very careful in the interpretation of results and to always refer to a reference standard perfectly representative of the component to be evaluated.

4.3.5.3.1.6 Detection of water entrapment in bonded honeycomb structures

The presence of water within a honeycomb structure with single sheet facing is easily detected with the ultrasonic technique provided that the entrapped fluid is in direct contact with the facing on which the inspection is made.

It is then necessary, whenever possible, to place the component under evaluation in the most favourable position. Water entrapment in wing upper panels is impossible to detect with ultrasonics as water collects near the facing opposite to the surface on which the transducer is applied.

Water entrapment is then detected with the cathode ray tube technique by an important amplification of echo signals.

Confirmation of the presence of water is made by the X-ray technique. For structures with multiple sheet facings the pulse echo technique does not appear to be able to detect water.

4.3.5.3.1.7 Method limitations

The pulse echo technique can be used to confirm the existence of an acoustic coupling over the bonded structure facing surface.

It can thus be used to detect metal-to-metal unbonds and honeycomb sandwich structure unbonds (lack of adhesion of facing to honeycomb). It can be admitted that the unbonded area extent is more or less equal to the probe diameter.

For corrosion in honeycomb cell walls, the defect size is roughly similar.

This technique proves to be specially valid for light alloy structure evaluation.

For certain types of structures, as for example when the facing sheet is thin, the flaws located near this facing are the only ones which can be detected. But on the contrary in a great number of cases (thicker sheets) flaw detection can be ensured in the bulk of the honeycomb panel.

4.3.5.3.2 Ultrasonics Techniques

4.3.5.3.2.1 Signal damping by finger contact[3]

This technique is a variant of the previous one (see Figure 27). Echo signal damping by finger contact on the lower facing is studied on the cathode ray tube screen. When the bond is satisfactory finger contact with a liquid couplant, substantially damps the echo traces on the screen. If on the contrary the bond is defective, the ultrasonic signal reaches with difficulty the bonded lower surface and finger contact would result in a very minor decrease.

4.3.5.3.2.2 Ultrasonic C-SCAN techniques (see Chapter 3.6)

4.3.5.3.2.2.1 Basic principles

The purpose of these techniques is to develop an increased sensitivity and improved resolution. Either the pulse echo or the through transmission techniques can be used. In either technique, focused transducers are used. Component inspection can be carried out by immersion, but it is very difficult to do this with honeycomb panels; this is why the semi-immersion technique is retained.

4.3.5.3.2.2.2 Pulse echo technique (see Figure 28)

In this technique, the transducer is so positioned as to be focused in the bond to be evaluated.

Each time the ultrasonic beam meets a cell wall, the transmitted signal is slightly damped. An electronic device judiciously positioned allows the signal to be used for recording.

4.3.5.3.2.2.3 Through transmission technique (see Figure 29)

This through-transmission technique requires a transducer support system allowing the transducers to be located on either side of the structure to be inspected

When the bonds are satisfactory, the transducer receives a signal

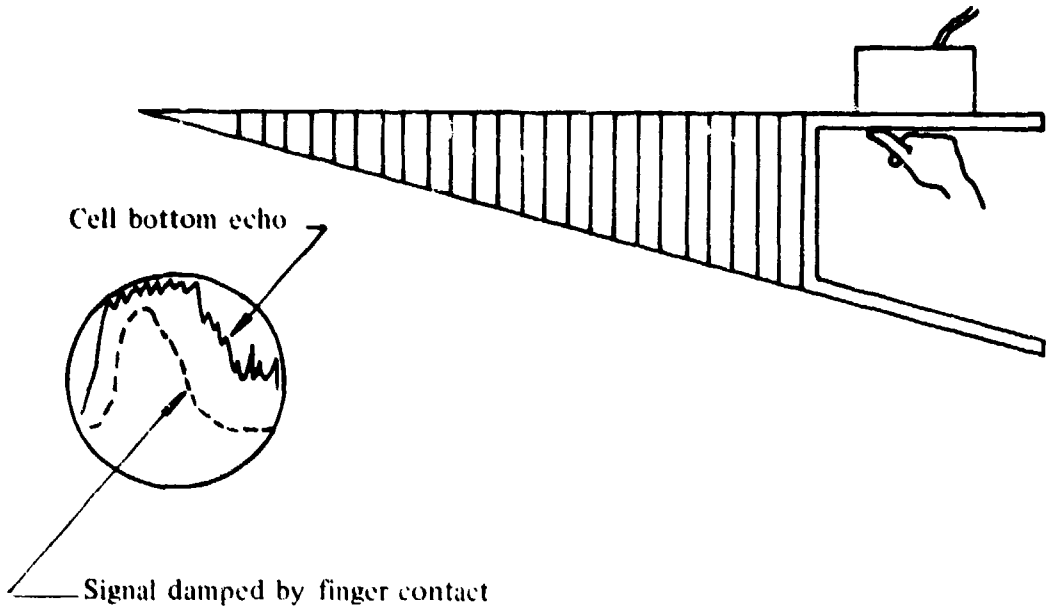

Figure 27

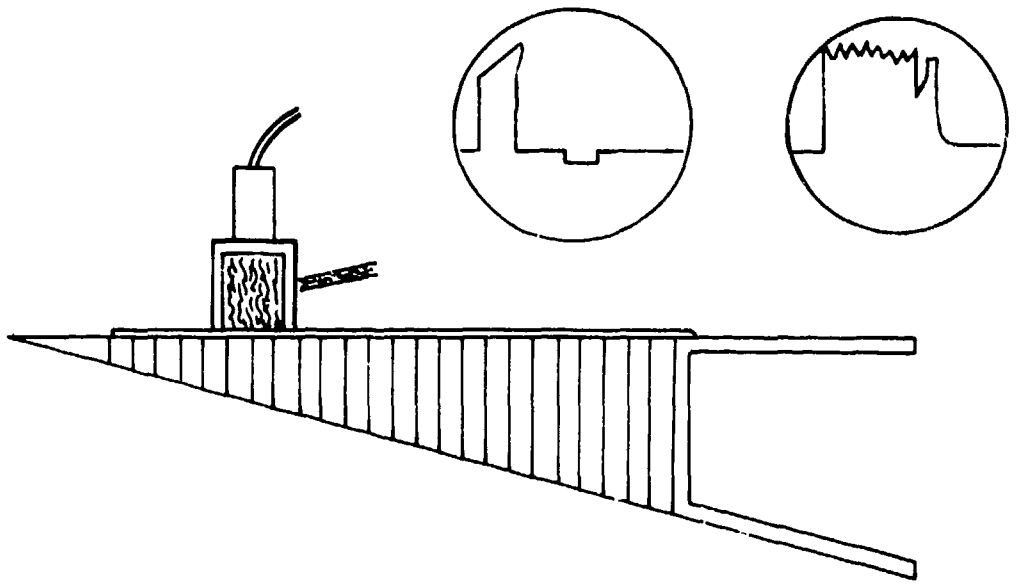

Figure 28

On the contrary when there is a lack of adhesion in one bond, no signal (or rather a very weak one) is received by the transducer.

The advantages of the technique are as follows:

(a) its capability to detect unbonds at both interfaces and in the honeycomb core.

(b) its high sensitivity not requiring too high a frequency.

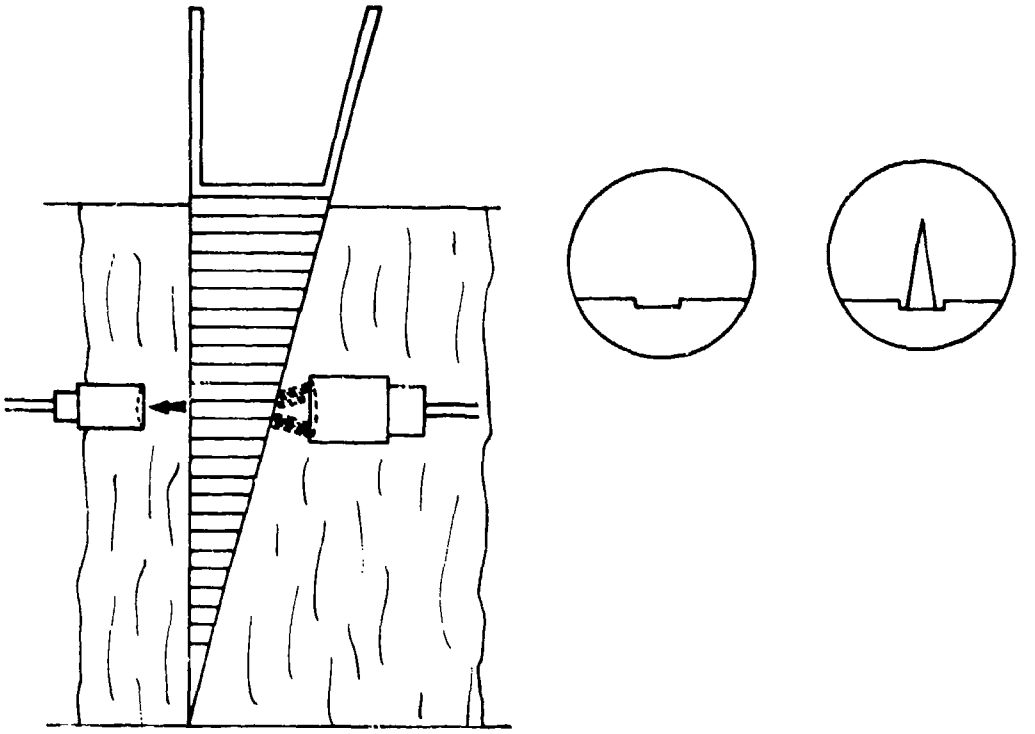

Figure 29

4.3.5.4 Sonic Resonance

4.3.5.4.1 General[3]

A large number of instruments operate on the sonic resonance principle, the best known being the following: Coindascope, Stub-Meter, Fokker Bond Tester, North American Rockwell, Sonic Resonator, Sondicator and Arvin Acoustic Impact Test.

A transducer is used to induce vibrations in the components under test, the local resonance variations being compared to reference standards to evaluate the different flaws. Sound waves are of great interest as they are largely influenced by the structure of the composite structure without creating, however, any excessive attenuation.

All the above instruments allow to a certain extent the determination of the bond quality. By these means joint cohesion may be controlled, but not adhesion.

To obtain suitable accuracy and good reproducibility, it is essential to correctly set the instruments by means of test-pieces representing the structures to be inspected and having typical known flaws.

Disbonded areas are readily detected both in metal-to-metal joints and in honeycomb, which means that any damage appearing in service will always be detected.

4.3.5.4.2 Fokker Bond Tester (Fig.30)

4.3.5.4.2.1 Principle

The description and operation of the Fokker Bond Tester has been widely described in the current literature

A vibrating transducer placed on the structure, transmits to the latter a vibration generally in the ultrasonic frequency range. The principle of the Fokker Bond Tester is totally different from that of conventional ultrasonic inspection instruments, such as the pulse echo system. The only point where the Fokker Bond Tester can be compared to the latter instruments, is in the use of a high vibration frequency, but this has nothing to do with the basic principle.

The vibrating transducer is fitted to the probe so as to avoid being affected by any external influence other than variations in the bonded joint.

Frequency of the transducer excitation current is scanned in a narrow adjustable range in the frequency band frequency scan being synchronized with the C.R.T. display trace.

Vertical deviation on the tube is a function of voltage at the crystal terminals, thus the impedance.

For a crystal having a frequency spectrum identical to that shown on Figure 31(a), the pass band chosen and the centre frequency may be adjusted on the Bond Tester in such a manner that each portion of the spectrum and consequently each resonance, can be displayed on the screen as shown on Figure 31(b).

Following analysis of the signals received from the transducer, the instrument gives the results on two scales (A and B).

Scale A comprises a C.R.T. on which appears a peak, corresponding to the resonance frequency. The vertical graduations enable this resonance frequency shift (see Figure 32) to be measured.

Scale B indication comprises a micro-ammeter for measuring the signal amplitude shown on scale A.

The quality of the glue line can be determined from the readings provided by the two scales. However, in practice, the readings are generally limited to scale A for metal-to-metal joints and scale B for honeycomb.

Metal-to-metal bonded assemblies are generally subjected to shear loads. A vibrating transducer is used in the case in a horizontal plane.

Sandwich structures are usually compression loaded: In this case longitudinal vibrating probes are used. Thus the joints are subjected to vibrations occurring in the same direction as the loads to which they would be submitted in the aircraft.

4.3.5.4.2.2 Operating procedure

For metal-to-metal joints, the probe is placed on a sheet whose thickness is equal to the thickness of the upper sheet of the bonded assembly. The oscillator centre frequency is adjusted so that the lowest point on the impedance curve lies in the centre of scale A. At the same time, scale B is set to 100. Scale A frequency is then calibrated. With older models (model 67 and earlier) this was made by means of a calibration signal giving a series of vertical peaks on scale A at a 10 KHz spacing; scale A can then be calibrated by adjusting the scan length (see Figure 32). If, for example, two peaks are separated by two divisions on the scale, one division corresponds to a frequency shift of 5 KHz. On the Model 70 Fokker Bond Tester, calibration of scale A is far simpler and can be made by using the calibration selector comprising pre-set frequency shift values for each division on the scale.

4.3.5.4.2.3 Result interpretation

The Fokker Bond Tester is sensitive to adhesive cohesion, that is, essentially to the porosity or the thickness of the adhesive. On the other hand, it does not allow the detection of adhesion flaws due essentially to poor surface preparation.

If the inspected structure only shows cohesion flaws and that perfect adhesion exists between the glue line and the sheet, it is then possible to trace a quality diagram giving the strength value of the glue line.

Tracing a quality diagram, for a given adhesive, implies the use of a large number of test pieces of the same metal and type of adhesive and for different t/l ratios.

where t = thickness of skin,
l = width of glue line.

Quality diagrams for metal-to-metal joints and for honeycomb sandwich are shown differently.

4.3.5.4.2.4 Metal-to-metal joints

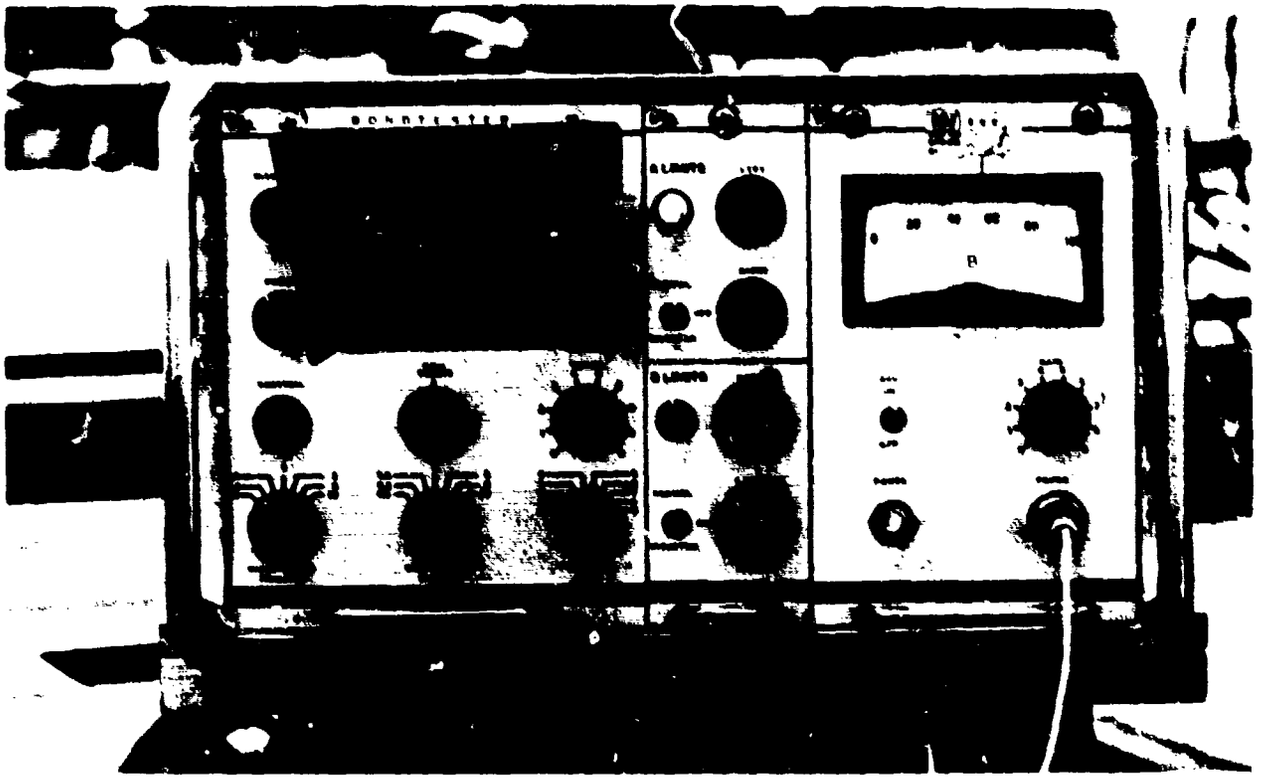

Fig.30 Fokker Bond Tester Model 70

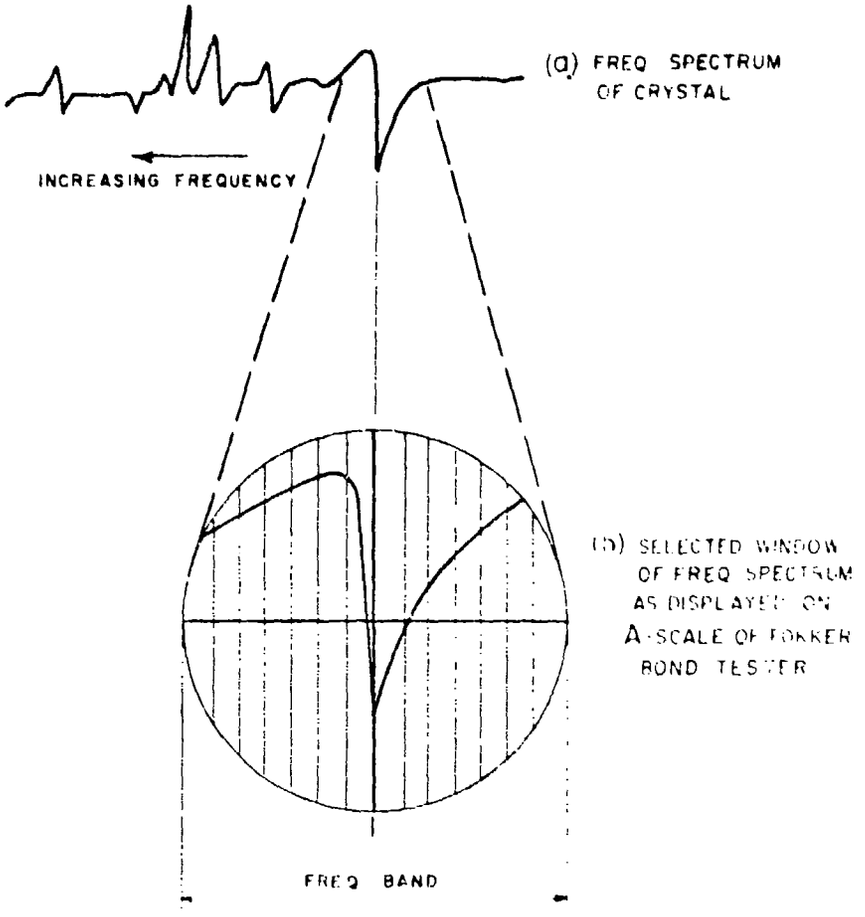

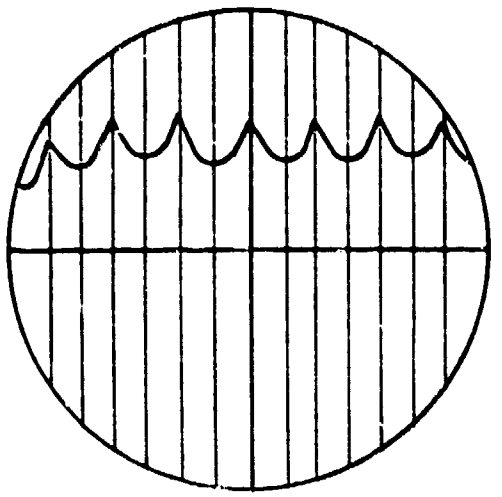

(a) CALIBR' ON

CALIBRATION SIGNAL ON.
DISTANCE BETWEEN PEAKS = 10 QUALITY UNITS.
SWEEP ADJUSTED SO THAT PEAK SPACING
EQUALS 2 SCALE UNITS.
HENCE, EACH SCALE UNIT = 5 QUALITY UNITS.

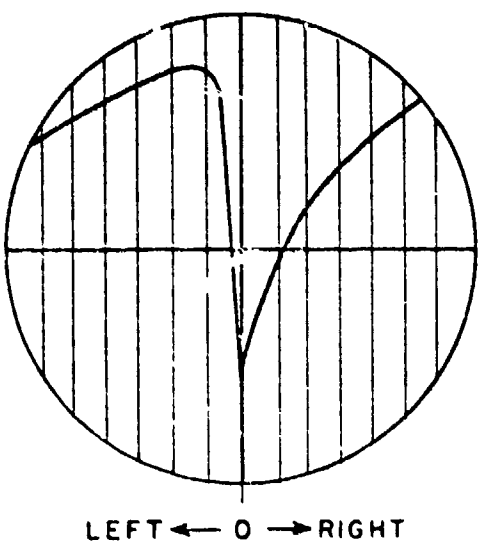

(b) VOID PANEL

CALIBRATION SIGNAL OFF
PROBE ON SINGLE SHEET
PEAK IS CENTRED USING FREQUENCY
SHIFT CONTROL.

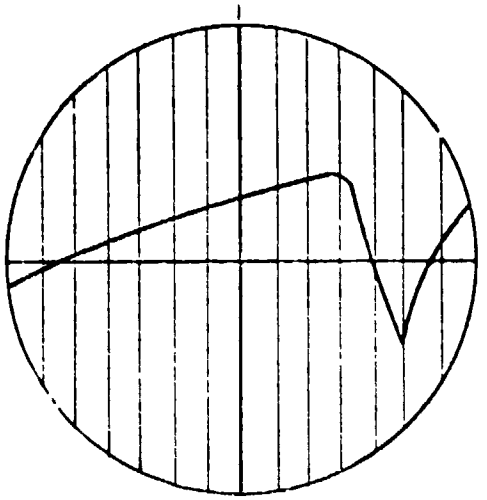

(c) BONDED PANEL

PROBE ON BONDED PANEL.
PEAK SHIFT IS 5 SCALE UNITS TO
THE RIGHT = 25 QUALITY UNITS
FOR SETTINGS OF 4a

Fig.32 Typical A-scale indications for Fokker Bond Tester

If a quality level is set, the diagram allows the definition of the areas on scale A, answering these criteria.

4.3.5.4.2.5 Honeycomb sandwich

The quality diagram depends especially on the density of the honeycomb core and to a lesser extent on the thickness of the facings. This type of diagram (see Figure 34) shows the horizontal portion of the curve representing a break in the honeycomb before failure of the joint. The quality diagrams only relate to the cohesive force of the glue line.

The Fokker Bond Tester is, in fact, insensitive to adhesion flaws between the adhesive and the metal, except when it concerns voids of sufficient size. Flaws due to insufficient surface adhesion due to contamination or to incorrect curing are undetected by the instrument. The quality diagrams thus rarely give the results anticipated.

Experience shows that qualitative detection of cohesion flaws, as well as voids and disbonds, are satisfactorily carried out on metal-to-metal joints by the Fokker Bond Tester. In honeycomb sandwich structures, detecting these flaws becomes more critical.

The Fokker Bond Tester being a comparative method, it calls for the use of standards representative of the structure to be inspected.

A coupling liquid is required.

4.3.5.4.3 The Coindascope

From certain points of view, the Coindascope is similar to the Fokker Bond Tester. A barium titanate crystal is energized by a constant amplitude sinusoidal current. By instrument settings excitation and display of all crystal resonances are ensured on the oscilloscope, in a similar manner to scale "A" on the Fokker Bond Tester.

The main operating difference is that the Coindascope uses a wave form as identification means rather than a measure of frequency shift, and is based on changes in amplitude for identical wave forms.

4.3.5.4.4 The Stub-Meter[7]

The Stub-meter was developed by the Stanford Research Institute, its aim being to make readings as easy as possible (a simple measuring instrument) by showing the adhesive bond quality.

While the basic principle is very similar to that of the Fokker Bond Tester, i.e. one studies the effect of adhesive quality variation on the frequency and amplitude of a given resonance, its operation is entirely different. Early models used a frequency scan oscillator in order to display on a C.R.T. the relation between the bond quality and the transducer resonance mode. In view of simplification, later models use a simple frequency system by which the transducer itself determines the frequency and the oscillation amplitude

4.3.5.4.5 Sonic Resonator (North American Aviation)[8]

4.3.5.4.5.1 Principle

The North American Sonic Resonator makes use of a vibrating crystal to acoustically excite the structure. Disbonds and other flaws modify the elastic properties of this structure thus creating variations in the crystal load

The Sonic Resonator normally operates in the upper region, or nearly, of the audible range and uses a low amplitude signal emitted continuously.

4.3.5.4.5.2 Operating procedure

Frequency is tuned to give stationary waves in the structure, the bridge is then balanced by adjustment of the circuit resistors and capacitors to bring the needle to zero. Any flaw in the structure gives rise to a deviation of the needle according to the nature and position of the flaw in the structure.

Choice of a transducer depends on the structure to be inspected.

Adjusting the Sonic Resonator is fairly critical when one inspects a new structure. For a given structure, adjustment is made easier by knowing in advance the parameters required

4.3.5.4.5.3 Performance and limitations

Figure 35 shows that flaws having a diameter 75% greater than the diameter of the probe can be detected (i.e. 10 mm for ordinary probes) but this is an approximation, and also the sensitivity of the flaws underlying the

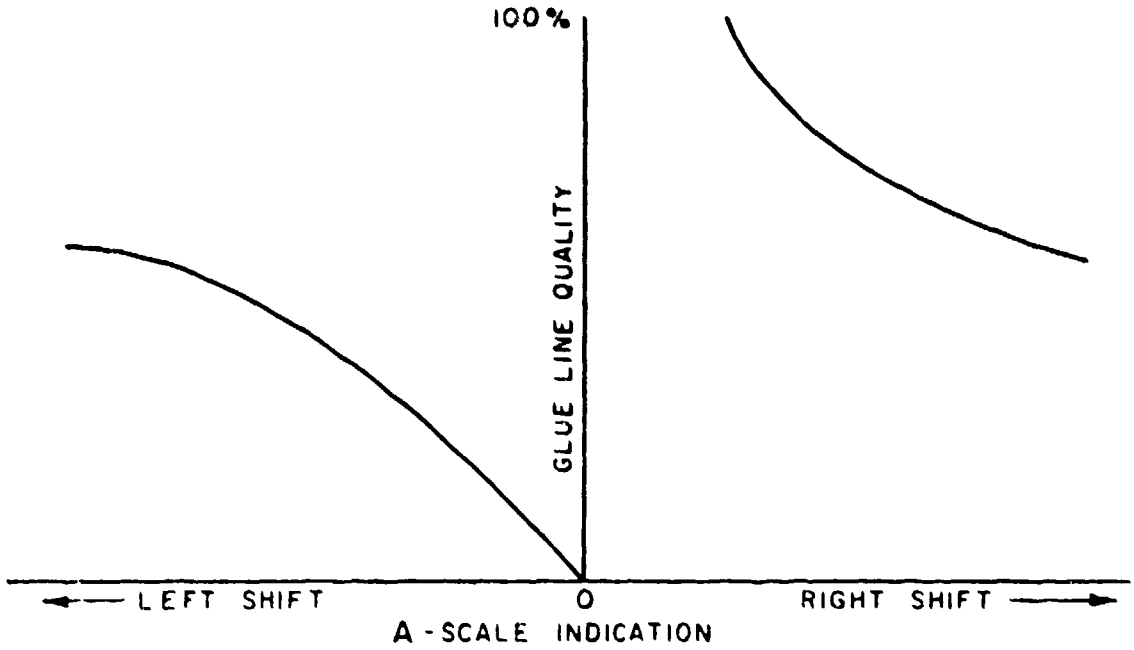

Fig.33 Typical correlation curve for metal-to-metal panels

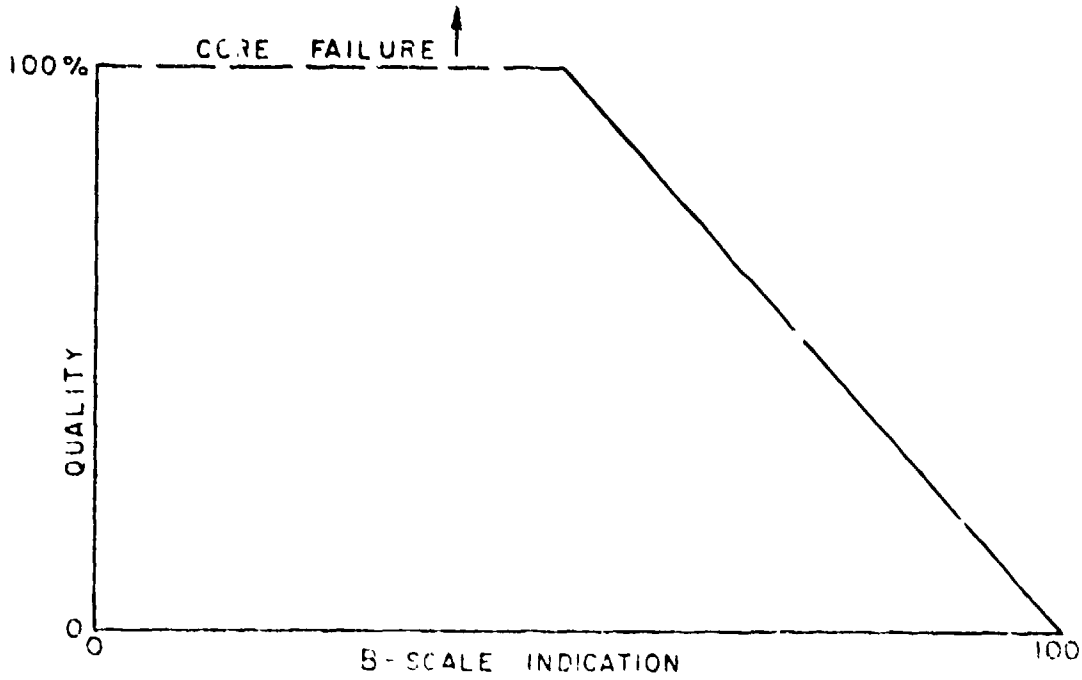

Fig.34 Typical correlation curve for honeycomb panels

The Sonic Resonator can be used to inspect honeycomb structures, assembled by adhesive, brazing or diffusion welding, laminated structures or metal-to-metal joints, etc.

By use of this instrument, flaws can be detected throughout the thickness from one single face. Maximum skin thickness being about 4 mm. It is fairly sensitive to the edge effect and curvature of the part to be inspected.

A coupling liquid is required.

4.3.5.4.6 Sondicator S 2 (see Figure 36)

This very low frequency ultrasonic instrument (20 to 40 KHz) was more particularly designed for inspecting metallic and non-metallic honeycomb and various bonding operations that cannot be inspected by conventional high frequency ultrasonics. Inspection is made by direct contact between the probe and the material to be inspected.

Ultrasonic energy impulses are transmitted in the material by means of a point transducer and cross in a lateral direction the area under the probe; they are received by a second point transducer located at about 20 mm from the transmitter.

Amplitude and the signal phase received are displayed on the unit's measuring instruments.

Any delamination under the probe creates vibrations modifying the transmitted signal, this is shown by deviation of the needles on the instrument dials.

The single probe used with this instrument is fitted with 3 interchangeable Teflon points, one being an application point.

The Sondicator caters for the detection of voids or delaminations in metallic or non metallic honeycomb, in metal-to-metal joints and in reinforced plastics.

Inspection does not require the use of any coupling liquid. Detection is limited to flaws located near the surface and whose minimum dimensions are of the order of 12 mm.

4.3.5.5 Eddy Sonic Methods

4.3.5.5.1 General

In the preceding methods (ultrasonic, sonic resonance) the requirement for using a coupling liquid between the transducer and the structure to be inspected involves various disadvantages:

- complicated equipment (immersion or semi-immersion),
- slower inspection time,
- unpleasant for the operator,
- risk of structure contamination (can hinder an ulterior bonding or protection operation),
- cleaning required after inspection.

In the Eddy Sonic method these disadvantages do not exist since the structure is excited by means of eddy currents. It is not necessary to contact the surface with the probe and no coupling liquid is required.

This method applies to honeycomb and bonded metal-to-metal joints or at least comprising a metal part allowing the flow of eddy currents. When the probe contacts the structure, eddy currents are induced, creating an alternating magnetic field reacting with the probe's magnetic field to produce vibrations in the structure.

In a lightly bonded conductive structure or in disbonded areas, these vibrations give rise to an ultrasonic noise, whose phase and amplitude characteristics depend on the dimension and type of flaw. An ultrasensitive microphone on the probe detects this response, which is then displayed on a dial.

Difficulty in transmitting mechanical vibrations to the structure is, for conventional acoustic methods, a major drawback. In the case of the Eddy Sonic this difficulty is avoided. Coupling variations have here but little influence. The problem of possible sound attenuation due to air coupling is largely solved by the low frequency vibration properties of composite structures.

Consequently, frequencies are generally use in the upper audible range, or just beneath, as the attenuation coefficient of air is then sufficiently low to prevent a too important influence.

Besides ease of operation and short inspection times, coupling with air provides another advantage as it allows the use of a paper or Mylar to be placed between the probe and the surface, giving all the information (e.g. change in [illegible] location of stiffeners, joints, skin thickness variations, etc.). Interpretation of the results is thus

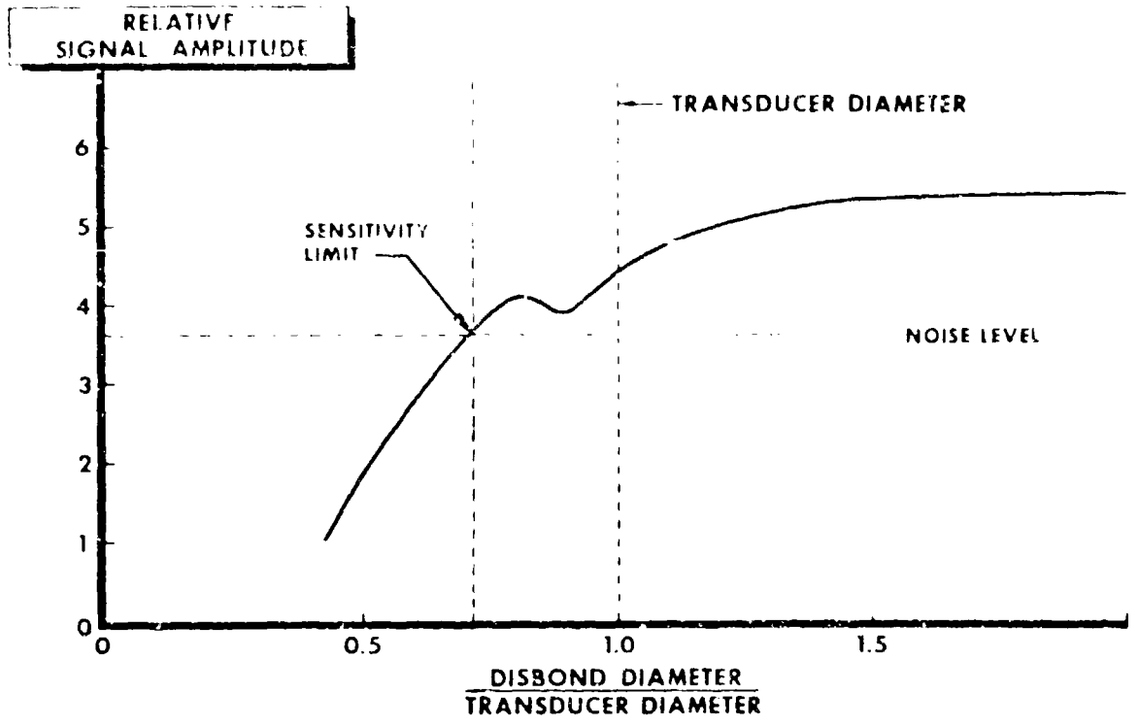

Fig.35 Typical disbond detection sensitivity

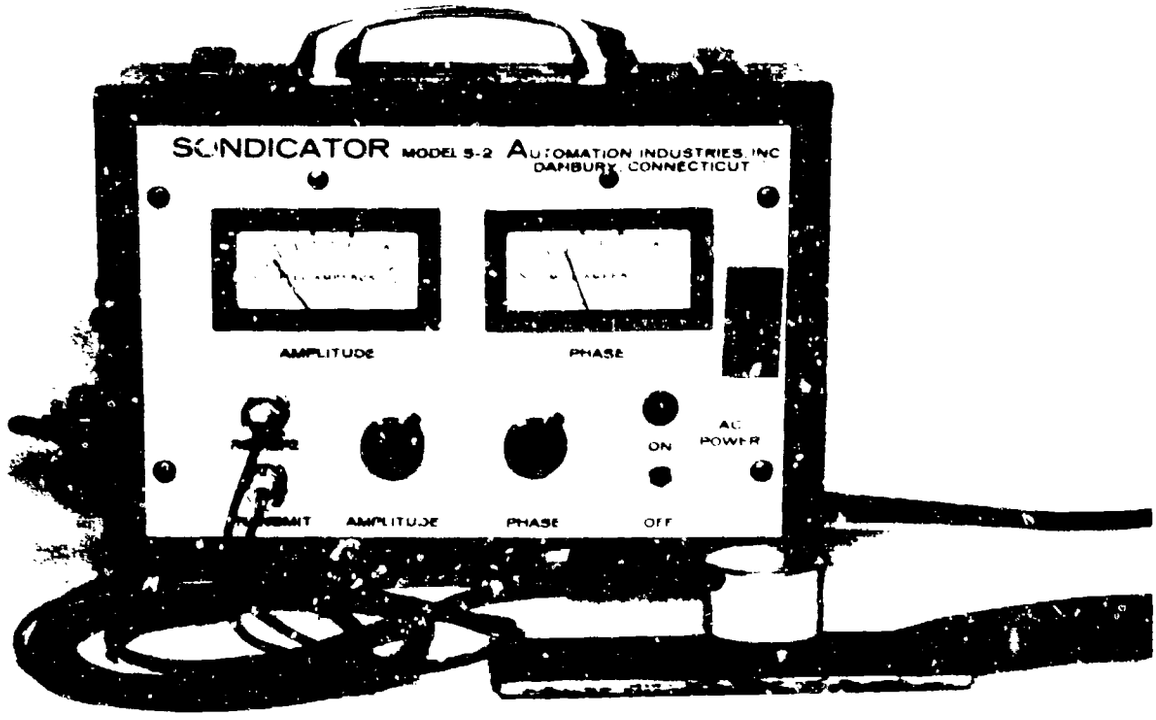

Fig 36 Sondicator S2

Furthermore, the follow-up of a flaw during maintenance can be very easily made by locating the Mylar sheet showing the previous flaw evaluation and by directly tracing the new evaluation.

Eddy Sonic methods are comparative methods, as one searches for received signal variations from the flaws. Instrument calibration requires the use of standards having sound and defective areas representative of the structure to be inspected.

4.3.5.5.2 Eddy Sonic (North American Aviation) (Reference 9)

The North American Eddy Sonic instrument was designed as a complement to the Sonic Resonator described previously. These two assemblies, having certain common parts, are designated "Sonic Test System" (see Figure 37).

In the Eddy Sonic system, acoustic vibrations induced in the material spread throughout the structure thickness and the response is modified by any flaws encountered.

Readings are made on a dial graduated 0 to 100. A special probe is available fitted with a small dial thus enabling the scan speed to be increased during manual inspection and making the method more efficient. This small dial on the probe gives simultaneously the same reading as the main dial located on the instrument. This is an advantage for the operator who needs only to look at the probe without having to constantly refer to the instrument. This system is particularly useful for large size structures.

The Eddy Sonic can also be used for automatic scanning with recording possibilities.

Figure 38 shows a typical example of honeycomb sandwich panel. Flaw detection sensitivity close to the surface to be inspected is greater than that for flaws located on the opposite face. The figure shows a constant section panel, but slight thickness variations have little effect on the readings.

The Eddy Sonic caters for the inspection of brazed or adhesive bonded honeycomb as well as metal-to-metal joints. The type of adhesive used has little effect on the results.

Flaws such as disbonds, voids, crushed or broken cells, disbonds between cells can be detected in a great number of structure types. The minimum dimension of detectable flaws is generally between 12 and 25 mm according to the type of structure and diameter of the probe used. Detection sensitivity depends upon the type of material, the type of flaw and also the type of probe used.

Regarding honeycomb, inspection is feasible if the skin thickness is approximately between 0.05 and 4 mm and for core thicknesses ranging from 3 to 120 mm.

Electrical conductivity and/or magnetic permeability of the material to be inspected have also an appreciable influence on the response of the Eddy Sonic. The ideal material is that whose conductivity is approximately above 12 M S/m (20% IACS) such as the usual types of aluminium alloys. It is sometimes possible to inspect low conductive materials such as diffusion welded titanium honeycomb, whose conductivity is under 3 MS/m (5% IACS). On the other hand, inspection of low conductive austenitic non-magnetic stainless steel honeycomb gives very poor res High permeability magnetic materials such as ferretic stainless steels give perfectly good results. Here, alignment of the magnetic fields appears to be an important mechanism of the transducer in addition to eddy current flow. For instance, inspection sensitivity is very satisfactory in PH15-7Mo stainless steel assemblies.

It can be noted that at certain frequencies, resonant grids (vibration loops) can be produced on the surface of small dimension parts or near edge members. This phenomenon can lead to some confusion in signal interpretation particularly if it gives signal values identical to those given by the structural flaws. Resonant grids produced by certain relations between wave length and part size can be detected by choosing a different control frequency (usually higher) or a different magnetic field intensity. Such resonant grids are not encountered on simple large area assemblies.

4.3.5.5.3 Harmonic Bond Tester (SHURTRONICS) (See Figure 39)

Different to the North American Eddy Sonic which operates on a continuous signal, the Harmonic Bond Tester uses a pulsed signal, thus avoiding the formation of standing waves and thereby making the instrument less sensitive to edge effects.

Frequency of the excitation signal is approximately 15,000 cycles per second, a frequency located at the upper limit of the audible range of the human ear. Since, maximum positive and negative excitation signals produce vibrations in the probe and in the structure under inspection, the resulting mechanical vibrations are around 30,000 cycles per second. A filter in the instrument suppresses all frequencies under 25,000 cycles per second, thus eliminating the effects of signal excitation on the receiver. The majority of ambient noises are suppressed by this filter (see Figure 39).

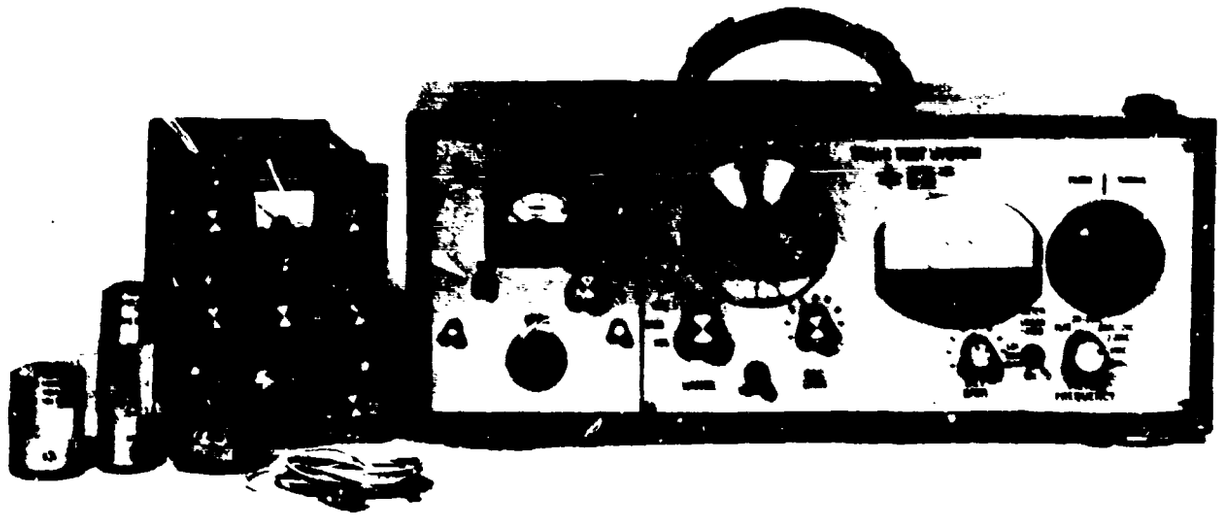

Figure 37

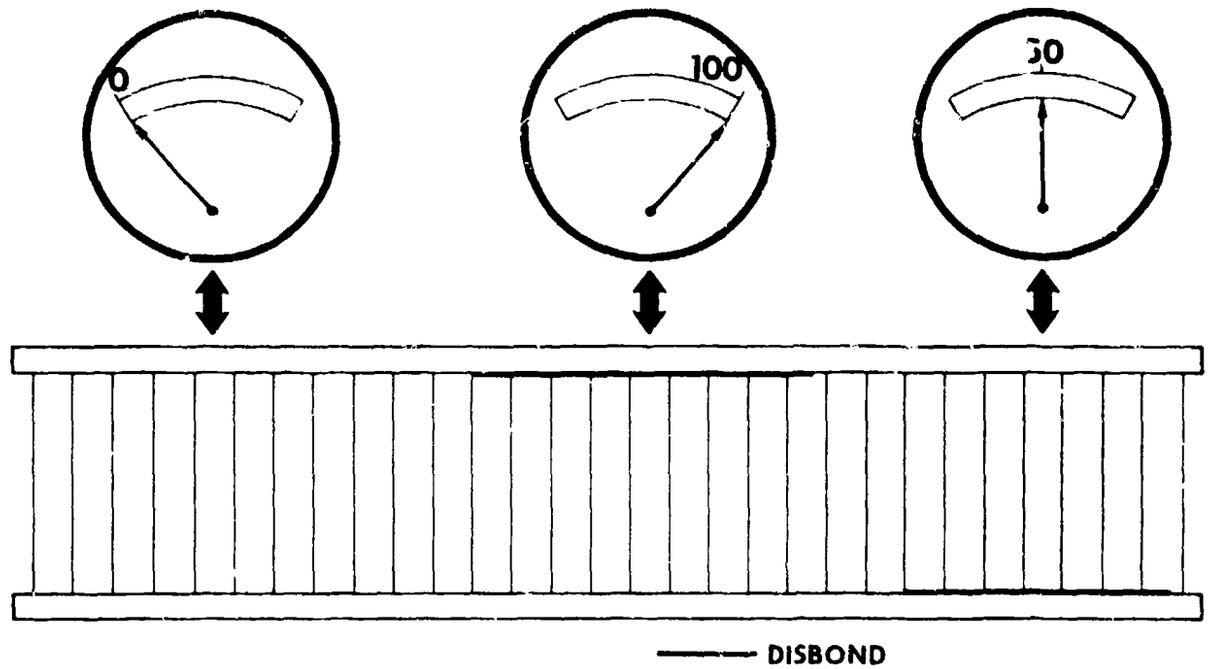

Fig.38 Test response for brazed, stainless steel honeycomb composites

In the Mark III B model, both the phase and amplitude characteristics are detected in the structure under inspection. Amplitude variations are generally used to inspect metallic materials and phase variations for non-metallics

The dial is graduated both in phase and amplitude. A switch is used to display either phase or amplitude values

Response received by the instrument is compared to an adjustable setting. Any value exceeding this basic setting activates an audible warning or a small red light located directly on the probe

Setting the instrument is very simple: a frequency is chosen giving the best sensitivity, the frequency then being adjusted so that the needle shifts to about the 10th graduation in the "sound" area.

The Harmonic Bond Tester gives very good results with all metallic materials, bonded aluminium, bronzed stainless steel and Stress Skin structures.

Skin thickness has an influence on the instrument's sensitivity; results are valid up to a thickness of 3 or 4 mm

The Harmonic Bond Tester is capable of detecting 10 mm diameter disbonds.

Amoag the advantages of the Harmonic Bond Tester, can be stated:

fast inspection due to the fact that no coupler is required and that the probe slides easily,

clear readings,

easily put into operation.

The main disadvantages are:

influence of high frequency ambient noises,

influence of surface curvature, inspection is impossible on concave surfaces. For convex surfaces the curvature radius should be sufficiently large (above 450 mm)

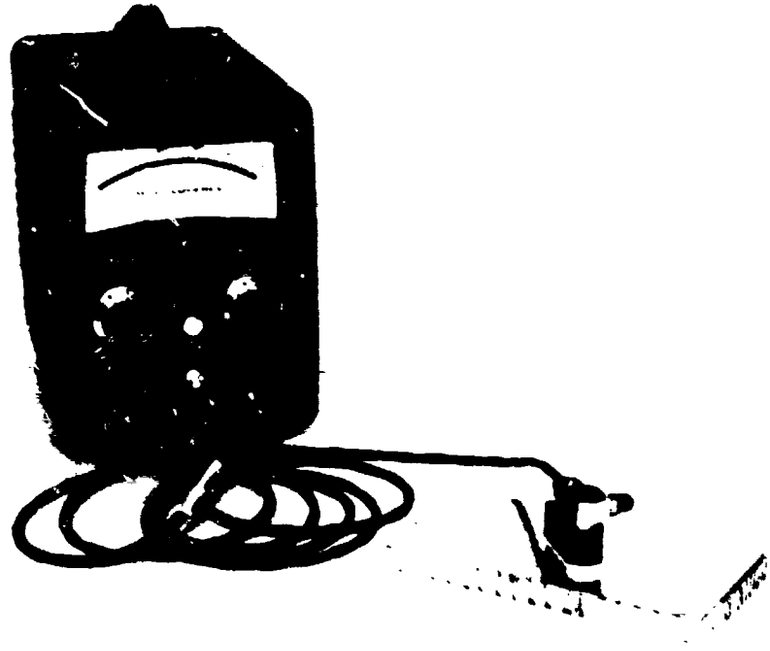

Figure 39

4.3.5.6 Holographic Interferometry

We shall not give here the operating principle of holographic interferometry which has already been described at some length in a previous chapter.

Let us simply recall that it is an optical method by which very small surface displacements are revealed in the form of interference fringes. Where a flaw in a bonded structure can lead to a slight surface deformation, this method will allow its detection.

Fokker has carried out very extensive tests, leading to the following conclusions [12]:

- holographic interferometry of bonded structures offers interesting prospects, as a complement to the usual non-destructive inspection methods.
- for sandwich structures, the thermal deformation technique appears to be sufficiently efficient: the minimum size of flaws that can be detected is 10 x 10 mm for skins under 1.5 mm thick and 5 x 5 mm for skins under 0.6 mm thick.
- for metal-to-metal bonded joints the thermal deformation method does not give valid results.
- the holographic interferometry method is increasingly sensitive as the skin thickness decreases.
- the use of a closed T.V. circuit does not seem to offer any particular help in a holographic interferometry inspection production installation.

4.3.5.7 Thermal Methods

Thermal methods used for the non-destructive inspection of bonded structures mainly amount to 3:

- infrared radiometry
- thermochrome or thermoluminescent coatings
- liquid crystals.

These techniques are described in a chapter dealing with thermal methods. They are especially useful in the case of composite structures. For bonded metal structures, the low thermal conductivity of the adhesive in relation to the metallic areas make the results meaningless.

4.3.5.8 Radiography

Radiography of bonded aluminium alloy honeycomb is more particularly used to inspect the honeycomb core: core deformation, broken cells, edge fillings, splices in honeycomb blocks, honeycomb slippage or shrinkage. Radiographic inspection also allows to a certain extent the measurement of adhesive film regularity - absence of voids or film overlaps. However, this is only possible if the adhesive backing is sufficiently opaque to X-rays and only for thin aluminium facings (See Figure 45)[2].

Radiography can also detect the ingress of liquids in the honeycomb (water or jet fuel) as well as the presence of corrosion or foreign matter.

For honeycomb radiography steps are taken to ensure that the X-rays run parallel to the cell walls. This means that the source be placed at a sufficient distance from the panel (1 to 2 metres) to avoid any excessive cell deformation.

Figure 40 shows what takes place when the X-rays are not in line with the cell walls. In Figure 40(b), the beam angle is too great and the cell images on the film overlap - the results in this case are useless. Size of the inspected area depends upon the distance between the source, the panel and the honeycomb thickness. The greater this thickness, the smaller the inspected area.

For brazed stainless steel honeycomb, it is also possible to inspect the brazing between the skin and the honeycomb. In fact, the brazing metal forms a fillet at each cell during the brazing operation. These fillets are perfectly seen on radiographic points, thus enabling the poorly brazed areas to be detected.

In radiography of metal-to-metal joints, lack of brazing material is shown up on the film as a darker area.

Radiography of metal to-metal joints and edge members are carried out as per Figure 41.

Two special techniques improve the efficiency of radiographic inspection and speed up the inspection operation.

Radioscopy

Radioscopy coupled with an image intensifier is a modern technique, allowing the complete inspection of a honeycomb panel to be made far quicker than by making radiographic prints.

The operator views the part to be inspected on a T V screen. Furthermore, he has at hand the control devices to move the part in relation to the X-ray beam (Figure 42)

This technique offers a number of advantages over conventional radiography

much faster inspection

immediate interpretation

possibility of focussing inspection on a doubtful area by searching for the location and orientation giving the best results.

Figure 43 shows an installation designed for helicopter blade inspection The presence of water in the cells is revealed as light spots In case of doubt on the nature of the flaw, the operator can turn the blade slightly and can thus see the water move inside the cells

It is possible to keep trace of the results of radioscopic inspection by tape recordings or, if only the affected areas are required, prints may be made.

In-Motion Radiography

In the in-motion radiography an X-ray beam is focussed by means of lead plate with a slit opening (see Figure 44). By means of a continuous action, at right angles to the slit, either the focussed beam, the panel or the film can be moved

In this technique, each area of the radiographic film is successively exposed, the X-ray beam direction being beneficial to inspection in the area

Sweep speed is generally between 50 and 300 mm/ min

Beam direction arriving at a given point on the film varies as this point travels under the slit This leads to a fuzzy image that has little effect on the panel face contacting the film,but, can eliminate the opposite face For example, in the case of brazed honeycomb panels where the brazing metal fillets are perfectly revealed on the prints, in-motion radiography only allows one face to be seen One must have access to both sides to inspect the opposite face (See Figure 45)

For large size panels, film strip is generally used, offering several advantages (fast inspection, easy interpretation of the results, film economy by avoiding overlaps)

4.3.6 STANDARD BLOCKS AND ACCEPTANCE CRITERIA

4.3.6.1 Standards (see Figures 46 and 47)

Most of the methods already described are comparative methods, the results being only interpreted by reference to standards

Great care must be taken in the realization of these standards as inspection efficiency depends on the reference used

The first necessary requirement to which the standard must answer is to be representative of the structures to be inspected, i.e. reproduced from the same materials and having the same shape and dimensions The adhesive should be the same as that used in the structure under inspection and should follow the same curing cycle All these parameters are very important, as a variation of one of them can lead to faulty calibration and result, in the end, in inaccurate inspection.

Standards are generally used having artificial flaws introduced during, or after their manufacture.

The four main types of flaws are

Type I Lack of adhesion between the skin and the adhesive.

Type II Lack of adhesion between the adhesive and the honeycomb.

Type III Lack of adhesion between the adhesive and the metal (metal-to-metal joint).

Type IV Break in the core

Local use of grease, Teflon, or foreign materials to reproduce a bonding flaw is inefficient The techniques mostly used for producing the flaws are described below Experience only can dictate the best technique, which can vary according to the type of adhesive used.

1. A blob of pre-cured adhesive may be used during the realization of the standard In this case, the adhesive blob is placed at the location where the flaw is required. An opening is cut into the adhesive film so that the blob may be

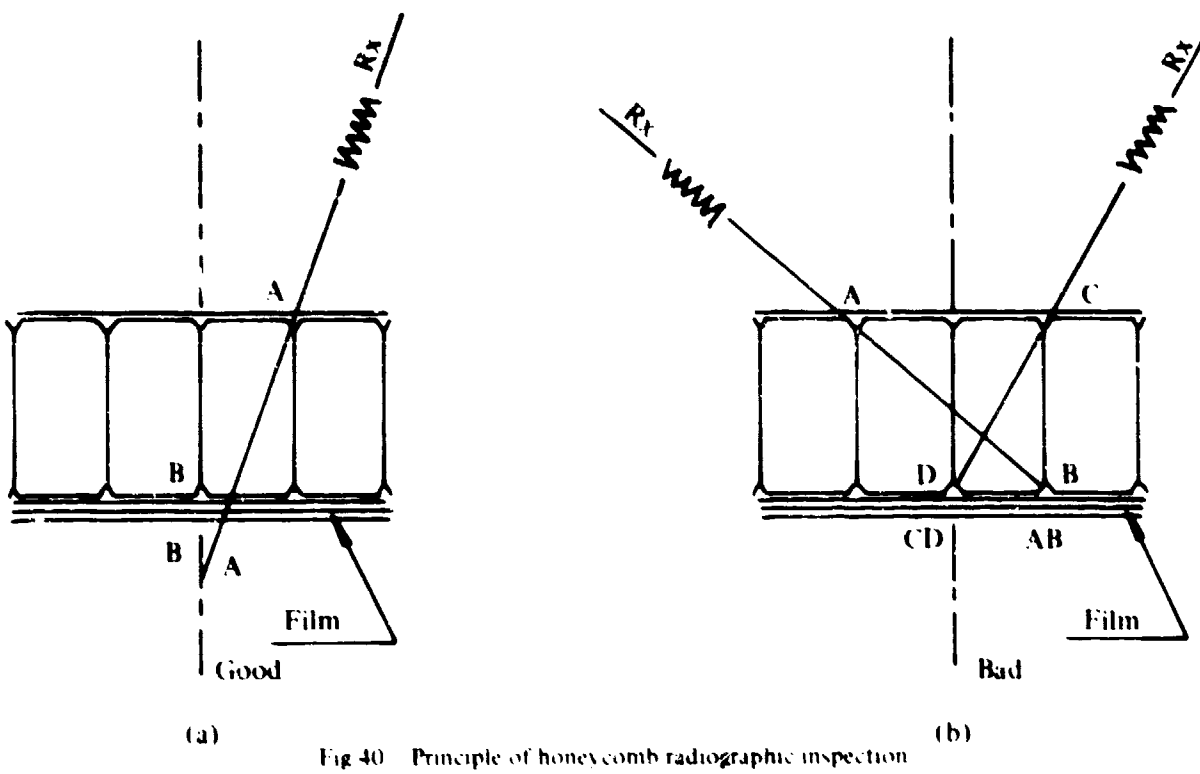

Fig 40 Principle of honeycomb radiographic inspection

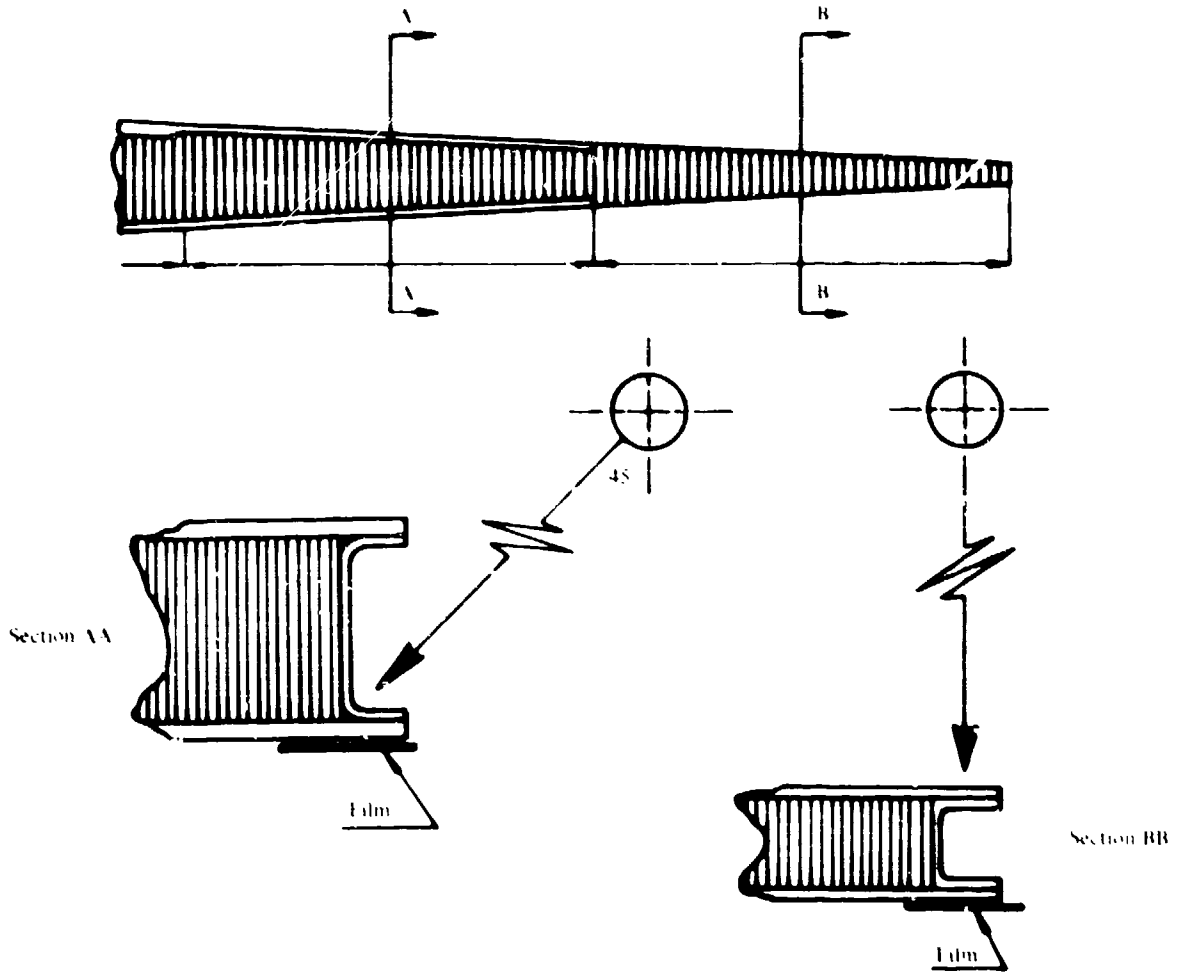

Fig.41 Typical X-ray tube positions for the examination of metal-to-metal bonded edge members

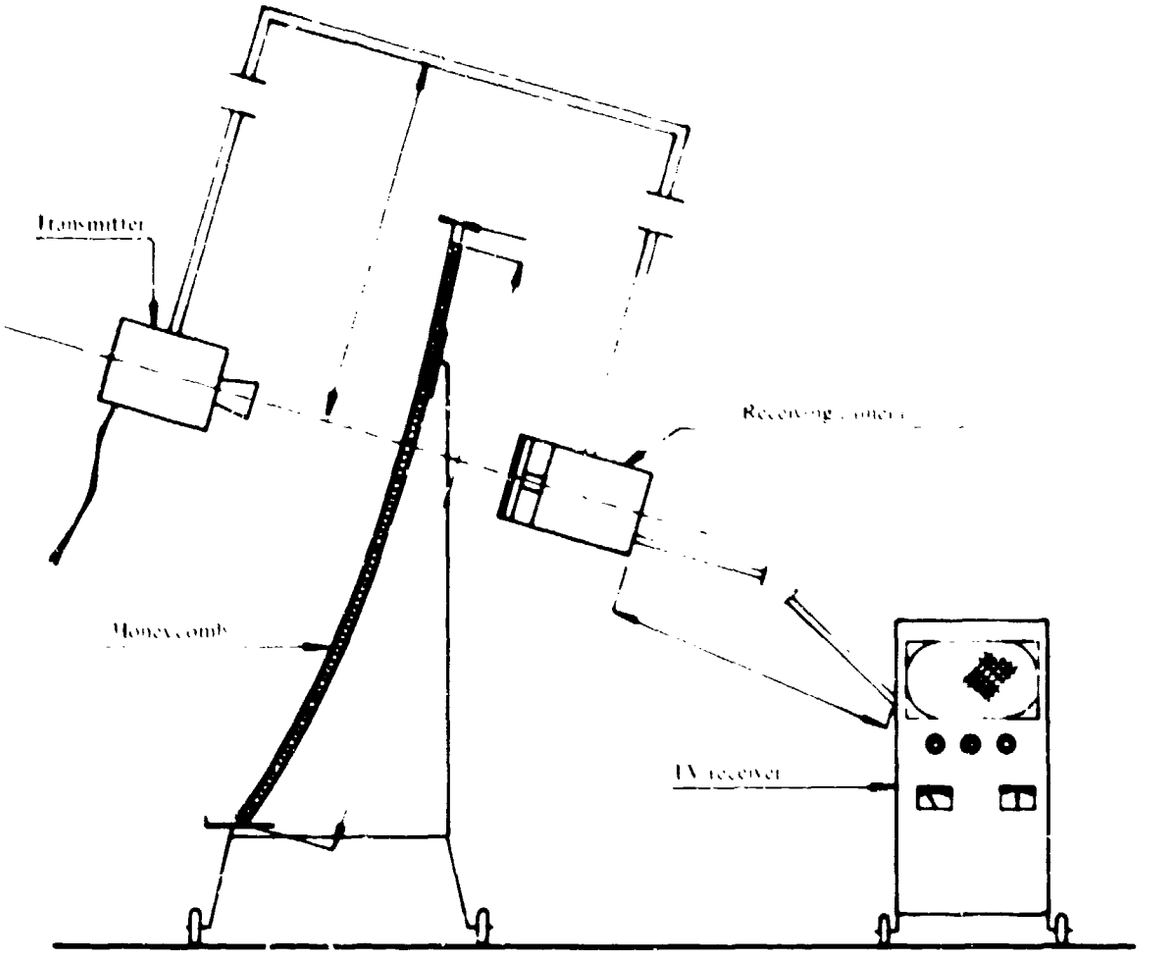

Fig 42 Radioscopy of honeycomb sandwich

Fig 43 Radiography of a helicopter blade

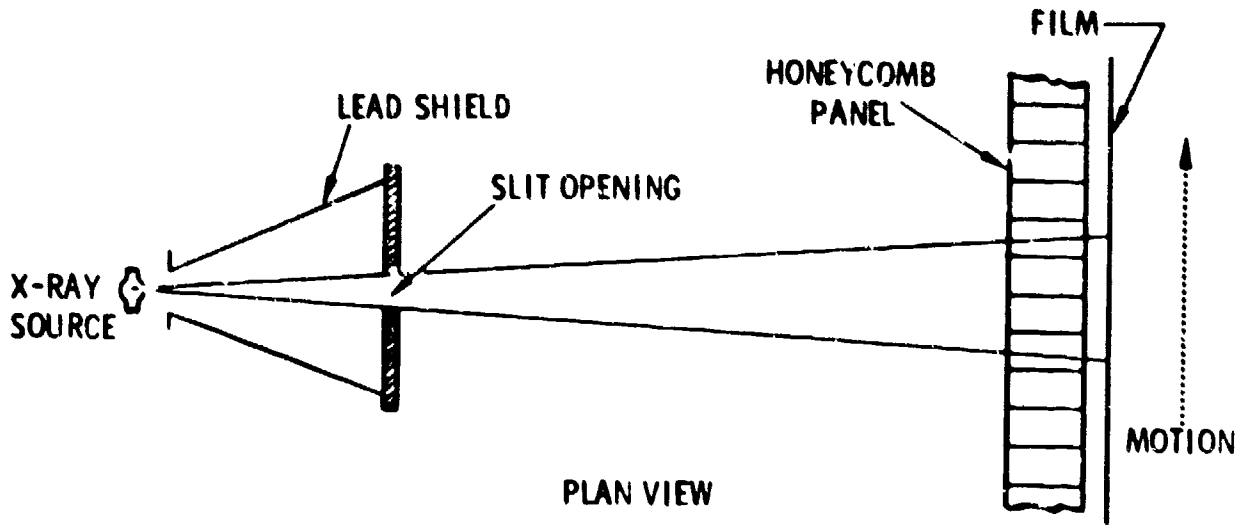

Fig 44 In-motion radiography for brazed honeycomb panels

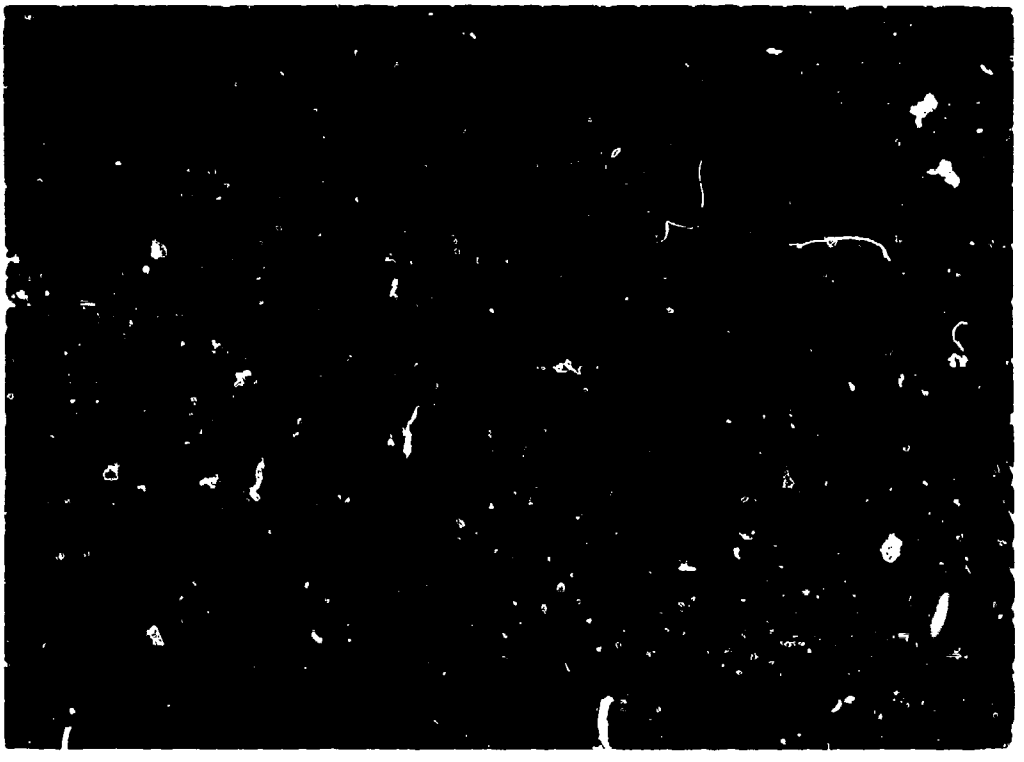

Fig 45 Radiography of a honeycomb

inserted correctly. During the curing operation of the test piece a disbond of known dimension is thus obtained. This method can be used for the fabrication of standards Types I, II and III.

2 Type I, II and III standards can also be produced by fabricating perfectly bonded test pieces. A hole, of given size is then drilled from the opposite face to the interface under inspection.

This method, while being satisfactory for ultrasonic inspection, is not valid for resonance inspection.

3 For Type II standards, flaws between the adhesive and honeycomb can be obtained by machining out an area corresponding to the flaw. This machining can be light (just sufficient to remove the adhesive) or heavier (breaking through the honeycomb). This last case is only used for ultrasonic inspection standards.

4 Lack of bonding in metal-to-metal joints (Type III) can be reproduced by pre-drilling holes in the metal base before bonding. Residual cured adhesive can be removed from the bottom of these holes after curing.

4.3.6.2 Acceptance Criteria

Definition of the acceptance criteria for inspecting bonded structures is very useful:

- it enables the inspector to judge whether he accepts or not a particular flaw.
- choice of the best adapted inspection method depends to a certain extent on the size of the flaw to be detected. If detection is only limited to a flaw of a given dimension, a simple and easily carried out method should be used. If however it is necessary to detect flaws the size of a cell, a more elaborate method should be resorted (such as holography or ultrasonic C-Scan) to the detriment of cost and ease of inspection.

Determination of these acceptance criteria requires a sound knowledge of the harmful nature of the flaws. Very often it will be necessary to carry out non destructive tests to obtain a correlation between the flaws (type and dimensions), non-destructive inspection indications and destructive test results.

Generally, the admitted criteria for sandwich structures are defined as follows:

- all flaw indications shall be compared to the reference standards and it is recommended to confirm the result by at least one other inspection method.
- all assemblies having disbonded areas opening into an edge member shall be rejected.
- assemblies having flaws whose size and number exceed the top limit of the requirements shall be rejected.
- a full scale tracing of these flaws shall be made on Mylar film, after manual inspection.

4.3.7 CONCLUSIONS

Among all the non-destructive inspection methods we have reviewed, none can be considered as universal for inspecting bonded structures. Choice of an inspection method depends upon a number of parameters:

- size of the minimum detectable flaw
- shape of the part, thickness, size
- localization, type and direction of flaw
- material
- instrument availability
- inspection cost
- ease of implementing operation

In the majority of cases, ultrasonics (pulse echo, impedance) give good results. Eddy current or some resonance methods can also be used, being easier to put into operation. In the case where very small flaws are to be detected, holographic or ultrasonic C-Scan techniques can be used.

It is often useful to adopt two different inspection methods so as to ensure that all flaws are identified and detected, while mentioning radiography which allows detection of other types of flaws.

Tables 2 & 3 established by HAGEMAIER show the possibilities of each method.

Table 2 is a list of different non destructive inspection methods together with their advantages and limitations for inspecting honeycomb sandwich structures.

Table 3 sums up the results of a comparison of the merits of each method for the detection of different flaws in bonded honeycomb structures.

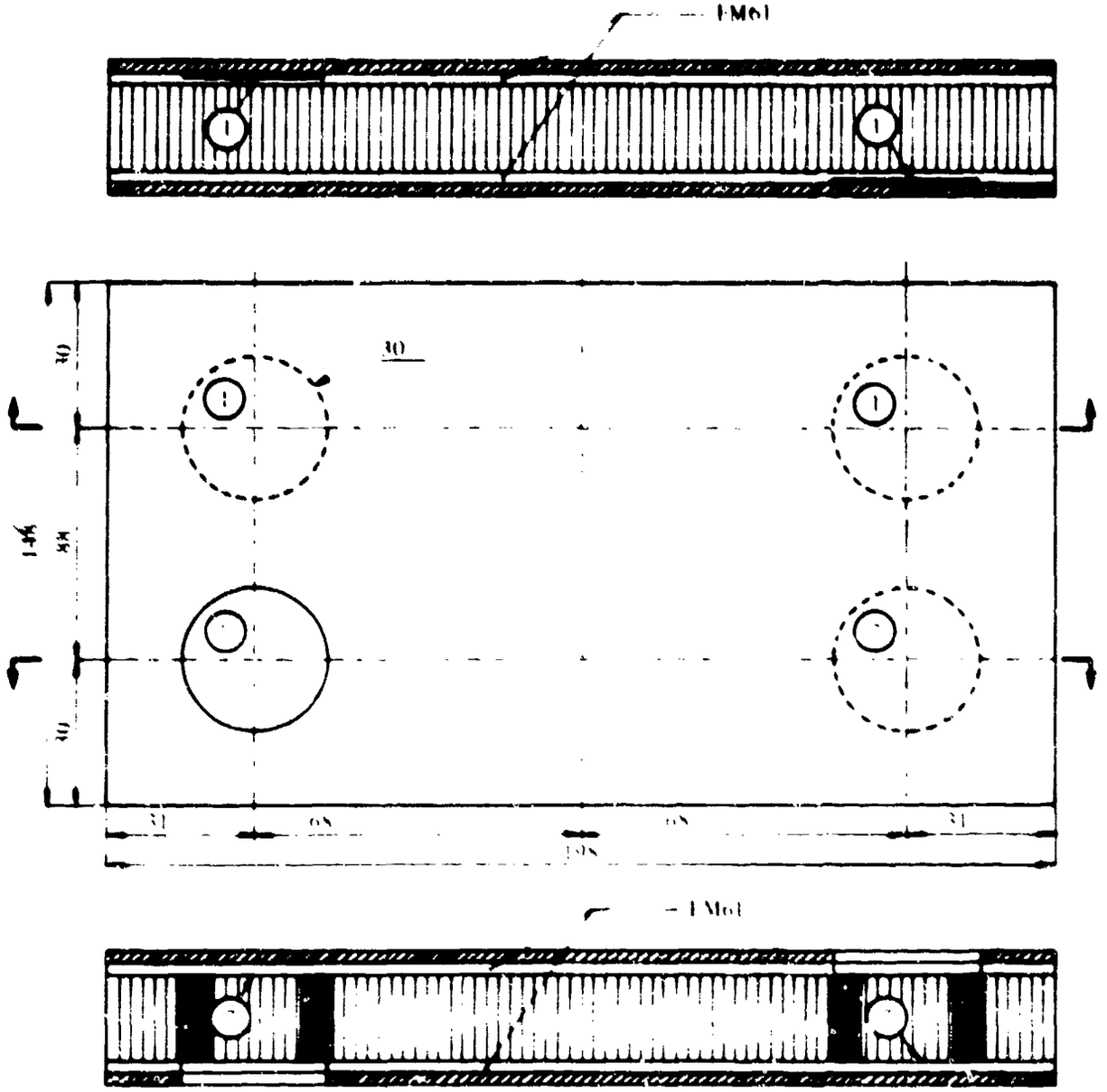

Position of bonding flaws

1 Disbond between skin and film

2 Disbond between honeycomb and film (disbond under load)

Fig 46 Example of calibration standard

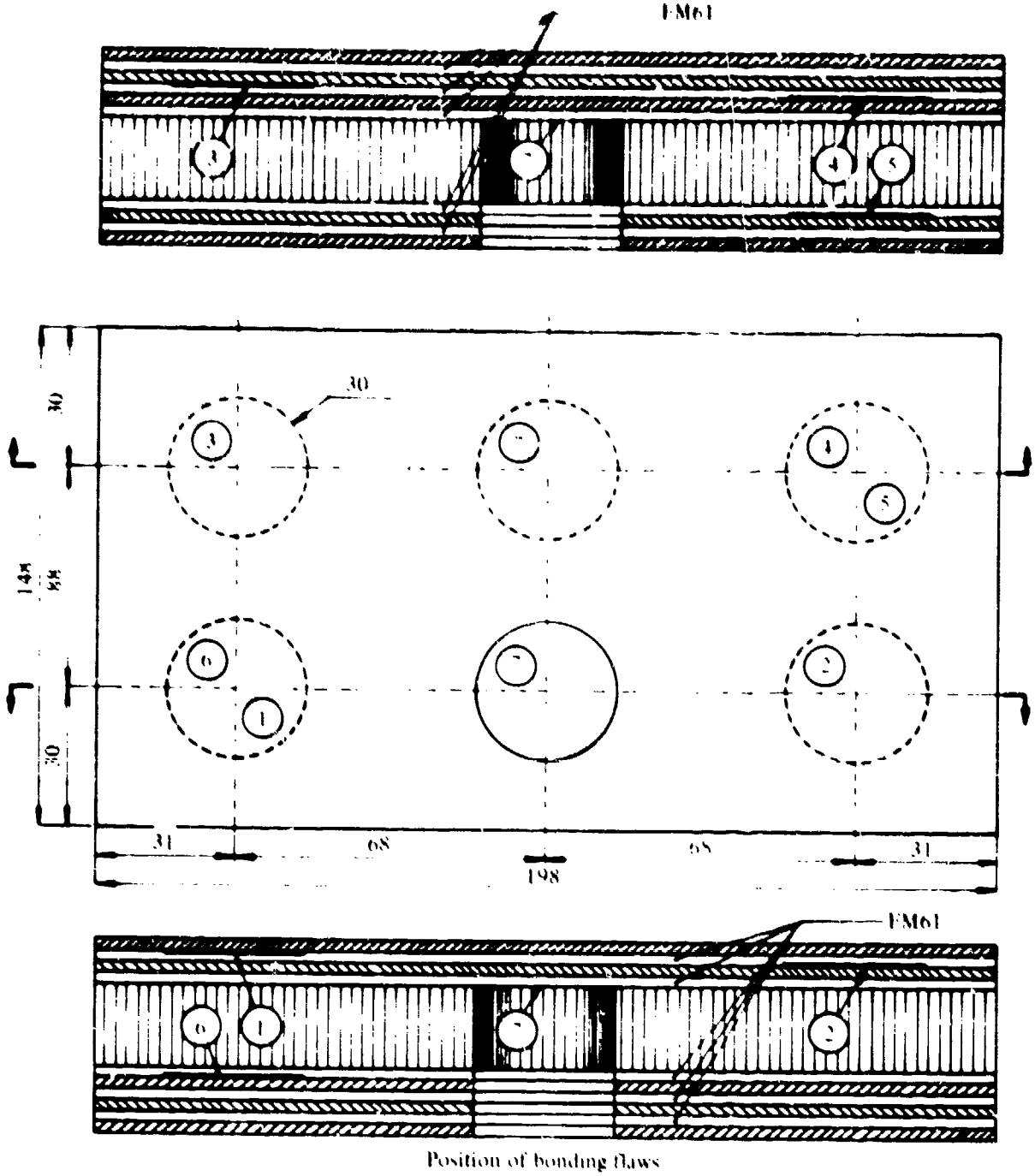

Position of bonding flaws

1 Disbond between skin and film

2 Disbond between film and stiffener

3 Disbond between stiffener and film

4 Disbond between film and 2nd stiffener

5 Disbond between stiffener and film

6 Disbond between 3rd stiffener and film

7 Disbond between honeycomb and film (disbond under load)

Fig 4 Example of calibration standard

TABLE II

NDT Methods for Evaluating Adhesive Bonded Honeycomb Structures[3]

	Ultrasonic C-scan (Through-transmission)	*Ultrasonic C-scan (Pulse-echo)*	*Ultrasonic (Contact pulse-echo or ringing)*
Measures or Defects	1 Skin-to-adhesive unbond (G)* 2 Skin-to-core unbond (G) 3 Metal-to-metal unbond (G) 4 Crushed core (G) 5 Teflon mould release (G) 6 Water entrapment if cells are filled (G) 7 Core splice (G) 8 Contaminated rinse (P–M)	1 Skin-to-adhesive unbond (G) 2 Skin-to-core unbond (P–M) 3 Metal-to-metal unbond (G) 4 Crushed core (M–G) 5 Teflon mould release (G) 6 Water entrapment if cells are filled (M) 7 Core splice (G) 8 Contaminated rinse (P)	1 Skin-to-adhesive unbond (G) 2 Skin-to-core unbond (P–M) 3 Metal-to-metal unbond (G) 4 Crushed core (P–M) 5 Teflon mould release (P–M) 6 Water entrapment (M–G) 7 Core splice (M–G) 8 Contaminated rinse (P–G)
Advantages	1 Permanent record 2 Good defect resolution 3 Plan view of part and defect 4 Detects back-side unbond 5 Can be used to test parts with thick facing sheets	1 Permanent record 2 Good defect resolution 3 Plan view of part and defect 4 Locate defect depth or position 5 Can be used to test parts with thick facing sheets	1 Good defect resolution 2 Locate defect depth or position 3 Portable 4 Moderate scanning rate 5 Can test complex shapes 6 Moderate cost for equipment
Limitations	1 Part immersion or squirter required 2 Access to both sides of part required 3 Reference standards required 4 Trained operator 5 Costly equipment	1 Part immersion or squirter required 2 Panel must be tested from both sides 3 Reference standards required 4 Trained operator 5 Costly equipment	1 Liquid couplant required 2 Panel must be tested from both sides 3 Reference standards required 4 Trained operator
	Infrared (Radiometers)	*Holographic Interferometry (Thermal)*	*Infrared (Thermochromic materials)*
Measures or Defects	1 Skin-to-adhesive unbond (G) 2 Skin-to-core unbond (P–G) 3 Metal-to-metal unbond (G) 4 Crushed core (P) 5 Teflon mould release (P) 6 Contaminated rinse (P) 7 Water entrapment (M–G)	1 Skin-to-adhesive unbond (G) 2 Skin-to-core unbond (G) 3 Metal-to-metal unbond (G) 4 Crushed core (M) 5 Teflon mould release (M) 6 Water entrapment (M) 7 Core splice (G) 8 Contaminated rinse (P–G)	1 Skin-to-adhesive (P–M) 2 Metal-to-metal (P–M)
Advantages	1 Sensitive to 1.5°F temperature variation 2 Permanent record of thermal picture 3 Remote sensing, need not contact part 4 Portable or automated	1 Surface of test object can be contoured 2 No special surface coatings or couplants required 3 No physical contact with test specimen 4 Sensitive to small defects	1 Low initial cost 2 No couplant required 3 Can be performed on complex geometry parts 4 Visual indication of defect
Limitations	1 Costly equipment 2 Liquid nitrogen cooled detector 3 Critical time, temperature relationship 4 Poor resolution for thick or highly conductive facing sheets 5 Reference standards required	1 Vibration free environment required 2 Thermal, sonic, vacuum or pressure required to deform specimen 3 In plate film processing required for real-time holography	1 Thin skin parts only 2 Critical time-temperature relationship 3 Reference standards required 4 Coating needs to be applied to part surface

* See Key in Table III.

TABLE II (Continued)

	Shurtronics Harmonic Bond Tester	*Arvin Acoustic Impact Test*	*NAR Sonic Resonator*
Measures or Defects	1 Skin-to-adhesive unbond (M G) 2 Skin-to-core unbond (P G) 3 Metal-to-metal unbond (G) 4 Crushed core (P) 5 Teflon mould release (P)	1 Skin-to-adhesive unbond (G) 2 Skin-to-core unbond (G) 3 Metal-to-metal unbond (G) 4 Crushed core (M) 5 Water entrapment (M G)	1 Skin-to-adhesive unbond (P M) 2 Skin-to-core unbond (M) 3 Metal-to-metal unbond (G) 4 Crushed core (P) 5 Water entrapment (M G)
Advantages	1 Portable 2 Simple to operate 3 No couplant required 4 Locates back-side unbonds in thin sections 5 Fast scan rate 6 Access to only one side required for thin sections 7 May be automated	1 Portable 2 No couplant required 3 Detects back-side unbonds 4 Moderate scan rate 5 Can be used to test non-metallic assemblies 6 May be automated	1 Portable 2 No couplant required 3 Detects back-side unbonds 4 Can be used to test parts with thick facing sheets 5 Moderate cost equipment 6 Can be used to test non-metallic assemblies
Limitations	1 Assembly must contain conductive material to establish eddy current field, i.e. aluminium 2 Reference standards required 3 Does not work on thick facing sheets 4 Reference standards required	1 Part geometry and mass influence test results 2 Reference standards 3 Test results are subjective 4 Time consuming calibration	1 Requires liquid couplant 2 Time consuming calibration 3 Slow scan rate 4 Reference standards required 5 Geometry and mass of part influences test results
	Fokker Bond tester	*Radiography x-ray*	*Tap Test (Coin, mallet)*
Measures or Defects	1 Skin-to-adhesive unbond (G) 2 Skin-to-core unbond (G) 3 Metal-to-metal unbond (G) 4 Crushed core (P M) 5 Unconfirmed data indicate capable of measuring bond degradation caused by environment and fatigue 6 Bond strength (M G) 7 Teflon mould release (P M) 8 Contaminated rinse (P)	1 Water intrusion 2 Foreign objects 3 Crushed, wrinkled, or spliced core 4 Assembly 5 Presence or absence of skrim cloth 6 Node bond (under ideal conditions) 7 Internal corrosion	1 Skin-to-adhesive unbond (M) 2 Metal-to-metal unbond (G) 3 Crushed core (P)
Advantages	1 Portable 2 Qualitative and quantitative measurements 3 Can be used to test parts with thick facing sheets	1 Permanent record, film 2 Adjustable energy levels 3 No couplant required 4 Geometry variations not a problem	1 Fast scan rate 2 No couplant required 3 Low cost 4 Easy to perform
Limitations	1 Liquid couplant required 2 Incapable of measuring all discrepancies which reduce bond strength caused by lack of adhesion of resin to adherent faying surfaces; improper compounding, overaging, contamination or incomplete cure 3 Calibration standards required 4 Special probes required	1 High initial cost 2 Radiation hazard 3 Access to both sides of part required	1 Limited defect detection 2 No record of test 3 Results are subjective 4 Reference standards required 5 Mars finish on thin facing sheets

TABLE III

Merits of Bond Testing Method for Honeycomb Structures[3]

		Titanium						*Aluminium*							
	Test method	*Skin-to-adhesive*	*Skin-to-core*	*Metal-to-metal*	*Crushed core*	*Teflon mould release*	*Contaminated rinse*	*Skin-to-adhesive*	*Skin-to-core*	*Metal-to-metal*	*Crushed core*	*Teflon mould release*	*Contaminated rinse*	*Water entrapment*	*Remarks*
		VOIDS						VOIDS							
BOND TESTING METHODS	1 Ultrasonic C-scan through transmission	G	G	G	G	G	P	G	G	G	G	G	M		1, 2, 3
	2 Holography (thermal) Real-time	G	G	G	M	M	P	G	G	G	M	M	G	Yes	5, 6
	3 Ultrasonic C-scan Pulse-echo	G	M	G	M	G	P	G	P	G	G	M	G		1, 2, 3
	4 Fokker Bond tester	G	G	G	ND	P	P	G	G	G	M	M	P	No	1, 3, 4
	5 Ultrasonic-manual Pulse-echo	G	ND	G	P	P	P	G	P	G	M	M	G	Yes	1, 2, 3
	6 Shurtronic Harmonic	M	P	G	P	P	ND	G	G	G	ND	P	ND	No	2, 5 6, 7
	7 Infrared Radiometer C-scan	G	G	G	ND	ND	ND	G	P	G	P	P	P	Yes	5, 6, 8
	8 NAR Sonic Resonator	ND	M	G	ND	ND	ND	M	M	G	P	P	ND	Yes	1, 2, 3, 4
	9 Tap	M	ND	G	ND	ND	ND	M	ND	G	P	ND	ND	No	6, 7
	10 Arvin, Acoustic impact test	G	G	G	M			G	G	G	M			Yes	2, 3, 4, 6
	11 NAR Eddy Sonic	ND	ND	ND	ND	ND	ND	M	G	G	P	ND	ND	No	4, 5, 6
	12 Turco-bond check	M			M	P	ND	ND			ND	ND	ND	Yes	5, 6, 7
	13 Coinda scope	M			ND	ND	ND	M			P	P	P	No	1
	14 Sondicator		G	G					G	G				No	1, 3

Key: (G) GOOD (66 to 100) (M) Moderate (33 to 66) (P) Poor (0 to 33) (ND) Not detected (Zero)

Detectability percent

Remarks:

1. Requires liquid couplant.
2. Detects defects in back-side of panel.
3. Detects unbonds in panel having thick facing sheets.
4. Requires time consuming calibration procedures.
5. Electrical conductivity influences system response.
6. Does not require liquid couplant.
7. Easy to set-up and use.
8. Data based on "pitch catch" techniques. Better results are anticipated with "through transmission" techniques.

N.B. With "skin-to-core" defects in aluminium and titanium honeycomb, it has been our experience that such flaws are not detected by the Fokker Bond Tester but, on the other hand, are very clearly shown up by Method 5 (Ultrasonic-manual Pulse-echo).

REFERENCES

1. Briens — *L'Utilisation des Adhésifs dans l'Aéronautique* SNIAS Document interne.
2. Hexcel — *Notices Commerciales.*
3. Hagemaier, D.J. — *Bonded Joints and Non Destructive Testing.* Non Destructive Testing, December 1971 and February 1972.
4. Hericourt — *Le Contôle Eléments Collés.* Breguet-Aviation Document interne.
5. Avions L.Breguet — *Notice de Collage à l'Usage des Bureaux d'Etudes* DT/CA No.3.
6. British Aircraft Corporation — *Development of Inspection Standards for Honeycomb Bonded Parts* Report AL/MAT/3040.
7. Pinkney, H.F.L. Scott, R.F. — *Data from Non-Destructive and Destructive Tests Carried Out in a Program to Evaluate Ultrasonic Devices for the Inspection of Adhesive Bonds*, National Research Council of Canada, NAE Misc.45, Ottawa, February 1967.
8. - Fokker Bond Tester Training Manual.
9. Botsco, R. — *The Eddy Sonic Test Method.* Materials Evaluation, Vol.XXVI, No.2, pp.21-26.
10. Botsco, R. — *Non Destructive Testing of Composite Structures with the Sonic Resonator.* Materials Evaluation, Vol.XXIV, No.11, pp.61 1-623, 1966.
11. Schliekelmann, R.J. — *Non Destructive Testing of Adhesive Bonded Metal-to-Metal Joints* Non Destructive Testing, Vol.5, No.2, pp.79-86, April 1972. Vol.5, No.3, pp.144-153, June 1972.
12. Schliekelmann, R.J. — *Holographic Interference as a Means for Quality Determination of Adhesive Bonded Metals Joints.* The eighth Congress of the International Council of the Aeronautical Sciences, Amsterdam, 1972.

CHAPTER 4.4

NDI OF COMPOSITE MATERIALS

by

W.L.Shelton

Technical Representative Department of the Air Force
Air Force Materials Laboratory (AFSC)
Wright-Patterson Air Force Base
Ohio, 45433
USA

CONTENTS

ABSTRACT

4.4.1 INTRODUCTION

4.4.2 INSPECTION TEST METHODS
- 4.4.2.1 Visual
- 4.4.2.2 Acoustic Techniques

4.4.3 SONIC METHODS
- 4.4.3.1 Sonic Resonator
- 4.4.3.2 Eddy Sonic Technique
- 4.4.3.3 Stress Wave Analysis (SWAT)

4.4.4 RADIATION METHODS
- 4.4.4.1 X-Radiography
- 4.4.4.2 Gamma Radiation Technique

4.4.5 ELECTRICAL METHODS
- 4.4.5.1 Electrical Resistivity
- 4.4.5.2 Corona Discharge

4.4.6 ELECTROMAGNETIC METHODS
- 4.4.6.1 Microwaves

4.4.7 THERMAL METHODS
- 4.4.7.1 Infrared Scan Heating Techniques
- 4.4.7.2 Thermal Coatings

4.4.8 OTHER NONDESTRUCTIVE TEST METHODS

REFERENCES

NDI OF COMPOSITE MATERIALS

W.L.Shelton

ABSTRACT

This chapter presents a review, which includes many of the techniques applicable to the nondestructive inspection of composite materials and structures. Included are subjects covering the general problem areas of composites, the defects which may occur in composite production and fabrication, and the nondestructive tests which are applicable for detection and measurement of such defects. The nondestructive tests are discussed in sufficient detail to give the user an appreciation of the concept of each test, and the limits of its capability.

4.4.1 INTRODUCTION

Nondestructive inspection technology has not advanced to the point where it alone may be relied upon to assure necessary product quality in a given engineering application. There are a number of variables in the materials and processes used in composite structures that must be very carefully controlled. These controls used in combination with nondestructive inspection can go a long way toward assuring product quality. There is not, for instance, any reliable nondestructive technique to measure bond strength. This can only be assured through good process control and a nondestructive inspection for voids and unbonded (disbonded) areas. Bonded sub-assemblies must be nondestructively inspected prior to incorporation into the final assembly. This situation can become a real problem if contamination from other sources is not controlled.

Nondestructive testing (NDT) identifies and measures abnormalities within a material without degrading or impairing the use of the material in any way. Acceptability of the material depends on engineering judgement, and where possible correlation of the "observed" defects with performances.

This chapter presents a brief review of available nondestructive test methods that have been used for evaluating reinforced/composites structures.

TABLE I

Defects Common to Composites[1]

			Metal Components	*Composite Components*
1.	**Adhesive bonded honeycomb assemblies**			
	1.1	**Skin to core**		
		1.1.1 Unbonds	X	X
		1.1.2 Chemical milled land voids	X	
		1.1.3 Doubler step voids	X	
		1.1.4 Porosity	X	X
		1.1.5 Extra adhesive	X	X
		1.1.6 Missing adhesive	X	X
		1.1.7 Inclusions (foreign material)	X	X
		1.1.8 Adhesive gaps	X	X
		1.1.9 Cut adhesive	X	X
		1.1.10 Voids	X	X
		1.1.11 Weak bonds	X	X
		1.1.12 Unremoved protective film	X	X
	1.2	**Skin to structural member**		
		1.2.1 Missing adhesive	X	X
		1.2.2 Unremoved protective film	X	X
		1.2.3 Doubler unbonds	X	
		1.2.4 "Brownies" (resin starved adhesive)	X	X
		1.2.5 Porosity	X	X
		1.2.6 Weak bonds	X	X
		1.2.7 Extra adhesive	X	X
		1.2.8 Inclusions (foreign material)	X	X
		1.2.9 Adhesive gaps	X	X
		1.2.10 Cut adhesive	X	X
		1.2.11 Voids	X	X

TABLE I

Defects Common to Composites[1] (Continued)

		Metal Components	*Composite Components*
1.3	**Splice plate to composite**		
1.3.1	Voids		X
1.3.2	Gaps		X
1.3.3	Unbonds		X
1.3.4	Porosity		X
1.3.5	Resin fills		X
1.3.6	Inclusions (foreign material)		X
1.3.7	Unremoved protective film		X
1.3.8	Porosity		X
1.3.9	Weak bonds		X
1.3.10	Extra adhesive		X
1.3.11	Cut adhesive		X
1.4	**Foaming adhesive (lack of)**		
1.4.1	Core splice	X	X
1.4.2	Core/structural members	X	X
1.4.3	Shear ties	X	
1.4.4	Voids	X	X
1.5	**Core defects**		
1.5.1	Node separations	X	X
1.5.2	Crushed core	X	X
1.5.3	Condensed core (cell nesting)	X	X
1.5.4	Distorted core	X	X
1.5.5	Wrinkled core	X	X
1.5.6	Low core	X	X
1.5.7	Distorted core	X	X
1.5.8	Wrinkled core	X	X
1.5.9	Blown core	X	X
1.5.10	Water in core	X	X
1.5.11	Cut core	X	X
1.5.12	Missing core (short core)	X	X
1.6	**Surface flaws**		
1.6.1	Cracks	X	X
1.6.2	Scratches	X	X
1.6.3	Blisters	X	X
1.6.4	Voids		X
1.6.5	Porosity		X
1.6.6	Protrusions	X	X
1.6.7	Indentation (dents/dings)	X	X
1.6.8	Wrinkles		X
1.6.9	Pits		X
1.6.10	Pinholes		X
1.6.11	Cuts and abrasions		X
1.7	**Lack of sealant at fasteners**	X	
1.8	**Poor fit-up**	X	X
1.9	**Double drilled or irregular holes**	X	
1.10	**Thick adhesive bond joint**	X	X
1.11	**Foreign materials**	X	X
1.12	**Adhesives**		
1.12.1	Voids	X	X
1.12.2	High and low density areas	X	X
1.12.3	Non-uniformity	X	X

TABLE I

Defects Common to Composites[1] (Continued)

	Metal Components	*Composite Components*
1.13 Composite tape/laminate flaws		
1.13.1 Tape		
1.13.1.1 Missing filaments		X
1.13.1.2 Broken filaments		X
1.13.1.3 Misaligned filaments		X
1.13.1.4 Spliced filaments		X
1.13.1.5 Filament spacing		X
1.13.1.6 Filament cross-overs		X
1.14 Laminate		
1.14.1 Fractures		X
1.14.2 Delaminations		X
1.14.3 Voids		X
1.14.4 Porosity		X
1.14.5 Resin fills		X
1.14.6 Resin rich/starved		X
1.14.7 Inclusions (foreign material)		X
1.14.8 Off angle lay-up		X
1.14.9 Bridging		X
1.14.10 Blisters		X
1.14.11 Cuts and abrasions		X
1.14.12 Pre-preg butt joints		X
1.14.13 Pre-preg overlaps		X
1.14.14 Pre-preg gaps		X

TABLE II

Available NDT Techniques for Composites

Techniques	*Detection Capability*	*Limitations Disadvantages*
Visual	Blisters, Porosity, Cracks, Discoloration, Surface Defects	Limited to surface defects in opaque material
Ultrasonics		
1. Pulse Echo	Delamination, Porosity	Requires immersion in water. Requires expert interpretation
2. Transmission	Delamination	Limited to access to both sides. Geometry of the part sensitive
3. Resonance	Composition, thickness	Sensitive to geometry of the part
4. Velocity	Modulus, density	Requires immersion in water
5. Fokker Bond Tester	Void detection in metal-to-metal and metal to honeycomb structures	Requires liquid coupling, must test both sides of honeycomb panel separately
6. Shear Wave	Defects in complex shapes	Requires immersion in tank of water
Sonics		
1. Coin tap	Lack of bond	Requires expert interpretation
2. Sonic resonator	Unbonds and other gross defects	Requires liquid coupling, difficult to use when inspecting tapered structures
3. Eddy-Sonic	Cracks	Limited to surface or near surface defects

TABLE II

Available NDT Techniques for Composites (Continued)

Techniques	*Detection Capability*	*Limitations Disadvantages*
4. SWAT	Crack crazing	Requires trained personnel to apply and interpret results
Radiation		
1. X-ray	Inclusions, cracks	Limited to crack size, must have access to both sides of the structure
2. Gamma radiation	Density variations	Must have access to both sides of the structure
Electrical		
1. Electrical Resistivity	Degree of cure, composition, moisture	Limited to flat surfaces
2. Corona Discharge	Voids	Limited to flat surfaces
Electromagnetic		
1. Microwaves	Voids, delaminations, porosity, resin variables	Difficult to interpret, requires specialized personnel
Thermal		
1. Infra Red	Voids, delaminations, unbonds	Sensitive to geometry of the part
2. Liquid Crystals	Voids, delaminations, unbonds	Not useful for aluminum metals-to-aluminum honeycomb structures
3. Photo Chromic Coating	Voids, delaminations, unbonds	Very insensitive to small defects, useful for surface and near surface defects only

4.4.2 INSPECTION TEST METHODS

4.4.2.1 Visual

Visual inspection is the most commonly and widely used NDT method. Defects which are observed include foreign inclusion, crazing cracks, scratches, nicks, blisters, pitting, air bubbles, porosity, resin rich and resin starved areas, discoloration, wrinkles, voids and delaminations. Visual aids such as intense light or magnifying glasses are used to increase detection capability. Reflected light is used for observing surface irregularities and other defects, transmitted light is often used when both surfaces of the material are accessible to reveal defects within the material. Visual examination is limited to the detection of rather large defects even though inspected by a trained operator.

The use of reinforced composites in sandwich construction requires further inspection. Visual inspection immediately after cure and upon removal of adhesive-bonded honeycomb sandwich parts from the heat source often can reveal blisters which may disappear when the part cools and the internal pressure is reduced. Where void-free laminate facings are used, visual examination can be accomplished by special lighting to detect defects within the structure.

4.4.2.2 Acoustic Techniques

4.4.2.2.1 Ultrasonics

Ultrasonics includes a number of different techniques. These techniques utilize sound energy at frequencies generally at 100 KHz to 25 MHz. In the two most basic methods a beam of ultrasonic energy is directed into the material, and either the energy transmitted through the material or the energy reflected from interfaces within the material is indicative of the characteristics of the material[2]. Ultrasonics has demonstrated its ability to detect defects within composite materials. Figure 1 shows a C-scan recording of a graphite epoxy test specimen. Unbonded or delaminated areas and voids of 1/8in. or larger can be readily detected. The dark areas indicate defects.

When the ultrasonic wave reaches an interface or a discontinuity, part of the energy is reflected. The amount of reflected energy depends on the acoustic impedance of each medium. The energy transmitted through the material is reduced by energy reflections and attenuations within the sample. Thus, the variations in reflected and transmitted energy can serve to locate defects, i.e., discontinuities in the path of the ultrasonic beam.

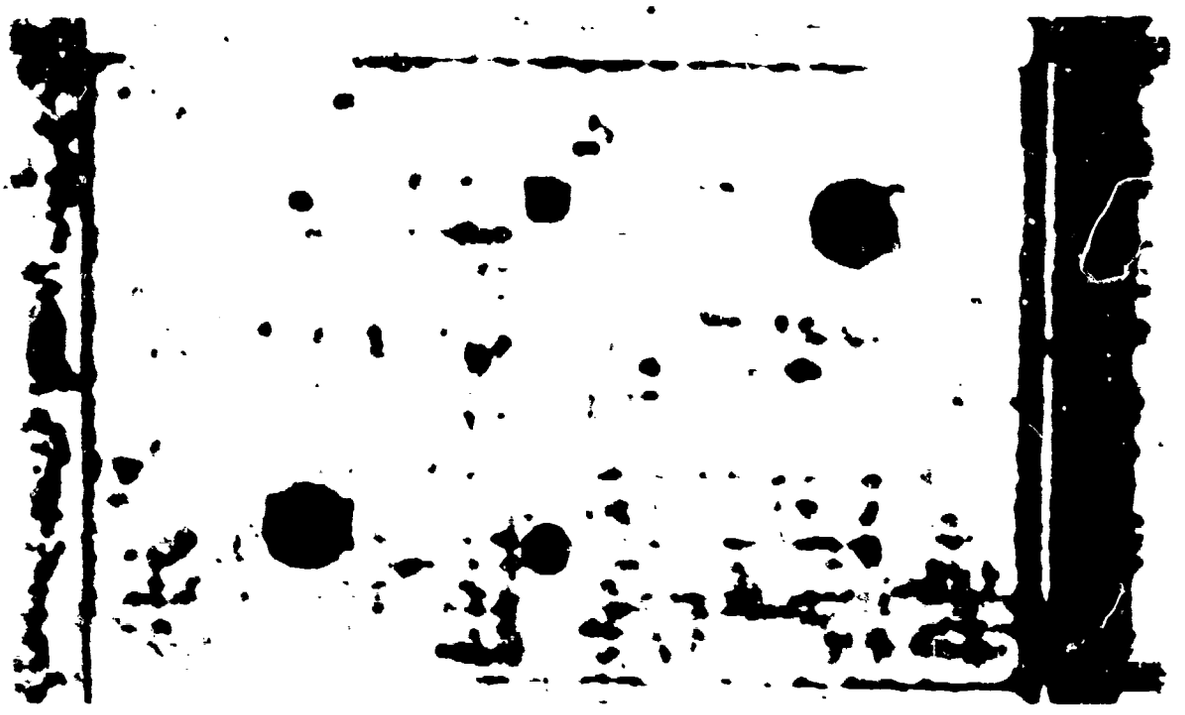

sens 0.7"
index .015" Thorn-transmission C scan 5 MHz

Fig.1 Ultrasonic C-scan of graphite epoxy reference standard showing areas of unbond
This is a grey scale recording by G.F. Evendale

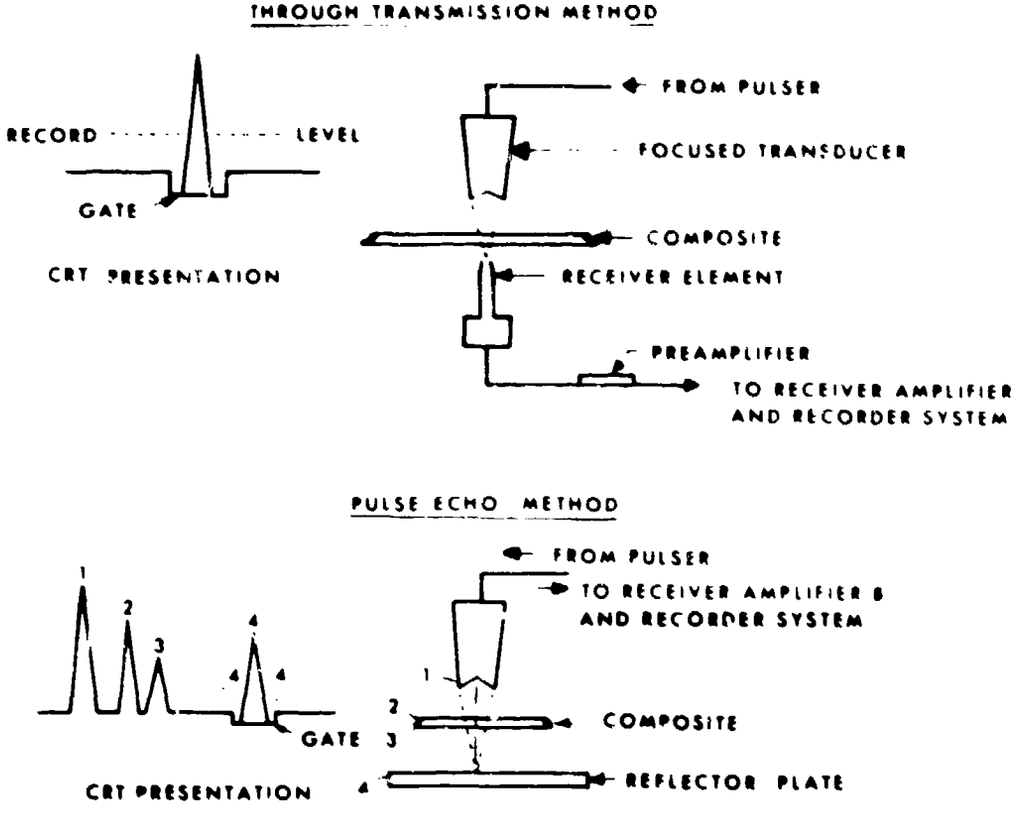

Fig.2 Ultrasonic inspection techniques

The ultrasonic method involves the electrical pulsing of a crystal of piezoelectric material which converts the electrical pulse to mechanical energy. The mechanical energy is thus fed into the test material with the use of a coupling medium (couplant), e.g., water oil, glycerine, and water gel. The sound energy reflected by or transmitted through the system is picked up by a transducer that converts would to electrical energy, which is then analyzed and displayed on a cathode ray tube (CRT) or scanning tape recorder. Figure 2 is a schematic diagram of a typical ultrasonic system.

4.4.2.2.2 Pulse-Echo Technique

In the pulse-echo technique the reflections or echoes from interfaces and anomalies provide the measurement information from one side of the material. A defect is determined to be present if the transmitted energy is reflected before it reaches the back surface. This can be observed as a peak on the CRT between those pulses corresponding to the initial pulse or the front surface reflection and the back surface reflection. The approximate location of the defect is determined to be relative to the position of the resulting peak with respect to the peaks of the initial pulse or front surface reflection and the back-surface reflection.

4.4.2.2.3 Through-Transmission Technique

The through-transmission technique utilizes the ultrasonic energy that passes through the material. The received energy is reduced by defects and results in reduced amplitude of the peak on the CRT.

The two basic ultrasonic techniques pulse-echo and through-transmission are useful for locating large delaminations which are perpendicular to the direction of the ultrasonic transmission. Smaller defects such as delaminations, voids, resin starved areas, and porosity are more difficult to detect.

4.4.2.2.4 Shear Wave Technique

Complex shapes are difficult to test with ultrasonics, as are rough surfaces, large grained materials and fiber reinforced composites. For complex shapes a shear-wave ultrasonic technique has been used[3]. The ultrasonic signal is sent into the part at a predetermined angle from the normal (15° ± 30 deg). Where defects are present the signal is reflected and an echo will be received by the transducer. If no defects are present, the sound wave is reflected between the surfaces of the part until attenuated, and there is no return signal.

4.4.2.2.5 Resonance Technique

Ultrasonic resonance techniques utilize the change in resonant frequency or the energy decrease at the resonant frequency as indications of the presence of a defect in a reinforced composite part. The resonant frequency of the part must be determined, this depends on the type of material and its physical dimensions[4]. Inherent variations in compositions or dimensions of the material reduce the sensitivity and resolution of defects.

4.4.2.2.6 Velocity Technique

The ultrasonic velocity technique can be used to indicate variability in density and elastic modulus in the material. Changes in the velocity provide the measurement information[4]. Figure 3 is a block diagram of the ultrasonic velocity measuring apparatus.

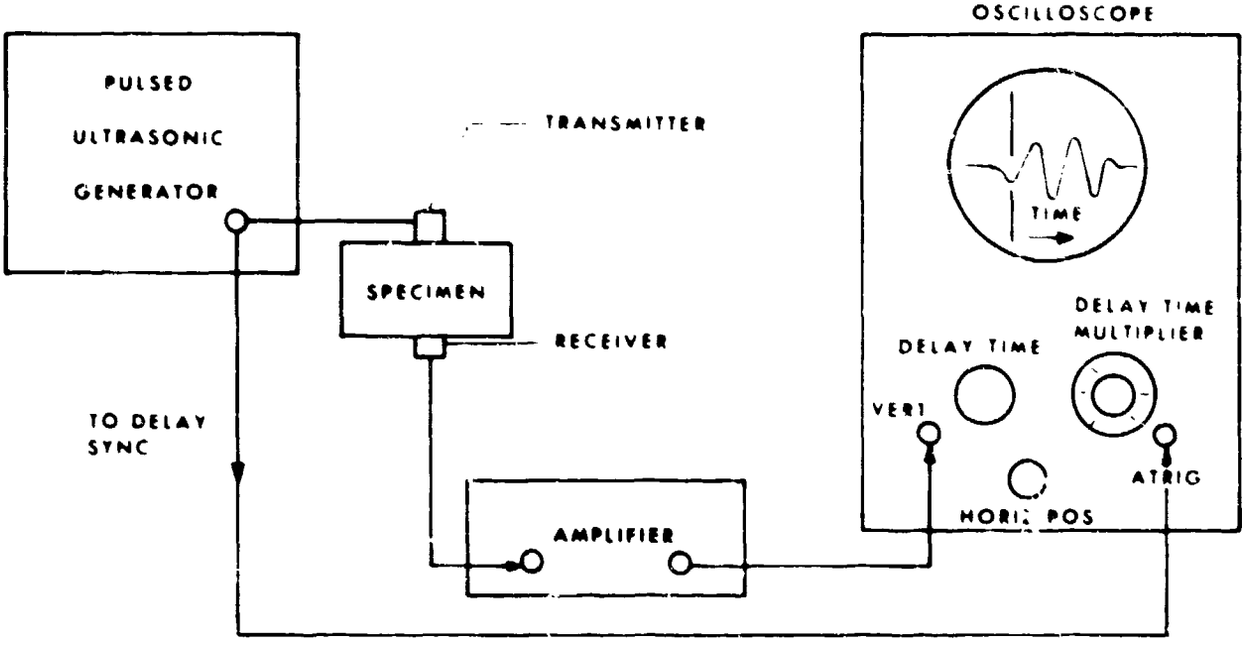

Fig. 3 Diagram of ultrasonic velocity measuring apparatus

4.4.2.2.7 *Fokker Bond Tester*

One of the most commonly used acoustical NDT techniques for evaluating the quality of adhesively bonded metal assemblies is the Fokker Bond Tester. The Fokker Bond Tester is an ultrasonic-resonance type instrument which utilizes as its sensing element a piezoelectric crystal vibrating at ultrasonic frequencies[8]. When the transducer is placed in contact with the material being inspected, its vibration is influenced by the characteristics of the material. A voltmeter (B-scale) indicates the amount of damping of the transducer vibration, and a CRT (A-scale) indicates the shift in resonant frequency. The tester is calibrated with bonded specimens of known quality. The quality of the bonded specimen under test is then determined from the magnitude of the resonance frequency shift (A-scale) on the damping of the peak amplitude (B-scale).

4.4.3 SONIC METHODS

Sonic testing utilizes frequencies from the audible to the lower ultrasonic region in the range of from 20 Hz to 100 KHz. Tapping a structure with a coin or other metallic objects is a common technique for detection of gross conditions such as cracks and delaminations. A well defined ringing sound is indicative of a well-bonded structure. A dull sound or thud indicates a delamination or relatively large void area.

4.4.3.1 Sonic Resonator

In addition to manual tapping, automated apparatus can be used to facilitate the operation and improve sensitivity. The Sonic Resonator[8] developed by North American Rockwell Inc. has been employed to locate unbonded areas and other gross defects in laminated and honeycomb-sandwich structures. This instrument utilizes a vibrating crystal to excite the structure acoustically. Resonance occurs when the frequency of the applied force corresponds to the natural frequency of the structure under inspection. As with ultrasonics, the sonic resonator requires a liquid couplant in order to transmit adequate acoustic energy into the test part. The instrument is capable of detecting large voids within the accuracy of 20% of its probe diameter, and has demonstrated its capability to detect fractured honeycomb core at any depth throughout a composite. Only one surface of the structure need be accessible for the technique. One of the limitations of the technique is because of the periodic nature of acoustic impedance the reading from the instrument varies as a function of bond laminate or honeycomb core sandwich part thickness. This variation requires that the sonic resonator be retuned when testing along a tapered honeycomb section.

4.4.3.2 Eddy Sonic Technique

The Eddy Sonic Technique[8] utilizes electromagnetic means to energize the material with eddy currents. Monitoring of the resulting acoustical responses locates defects. Contact between the structure and the transducer is not required, liquid or oil couplants are not used. However, in order to produce the eddy currents, an electrically conductive material must be present in the material to be inspected.

4.4.3.3 Stress Wave Analysis Techniques (SWAT)

Noise generated during proof loading of a reinforced composite structure can be used as an indicator of the formation of crazing or cracks. A change in the sound level accompanies the formation or extension of cracks within the structure. With the use of suitable equipment, the areas of suspect can be located. The technique is not nondestructive in nature, since it requires the application of a proof load to the part being tested, since such loads can and do frequently degrade the strength of the part. The Stress Wave Analysis Technique (SWAT) developed by Aerojet-General Corp. utilizes accelerometers to record noises during hydro testing. This technique was used to detect noises produced at lower stress levels for correlation with ultimate strength in pressure vessels.

4.4.4 RADIATION METHODS

4.4.4.1 X-Radiography

X-ray radiography is the most widely used penetrating radiation method of NDI. The detection of defects depends upon variations in thickness or density of a material in the path of the radiation. Areas of lower density within the material will absorb less radiation, so that the detector (film) will receive a greater intensity of radiation in the corresponding area. Because composites such as fiber glass epoxy, carbon-carbon epoxy, and graphite epoxy are of lower density than most metals, the presence of inclusions of higher densities are readily seen by this method. Figure 4 is a print of a radiograph showing sensitivity to disbonds, crack, fiber gaps, and voids, the smallest of which is 0.03 inches.

X-ray radiography has been employed for locating large voids, delaminations and cracks in reinforced composite parts. Such a defect can be detected provided the defect is sufficiently large with respect to the direction of the X-ray beam. Defects oriented normal to the radiation often are difficult to detect (e.g., tight surface cracks normal to a material's surface).

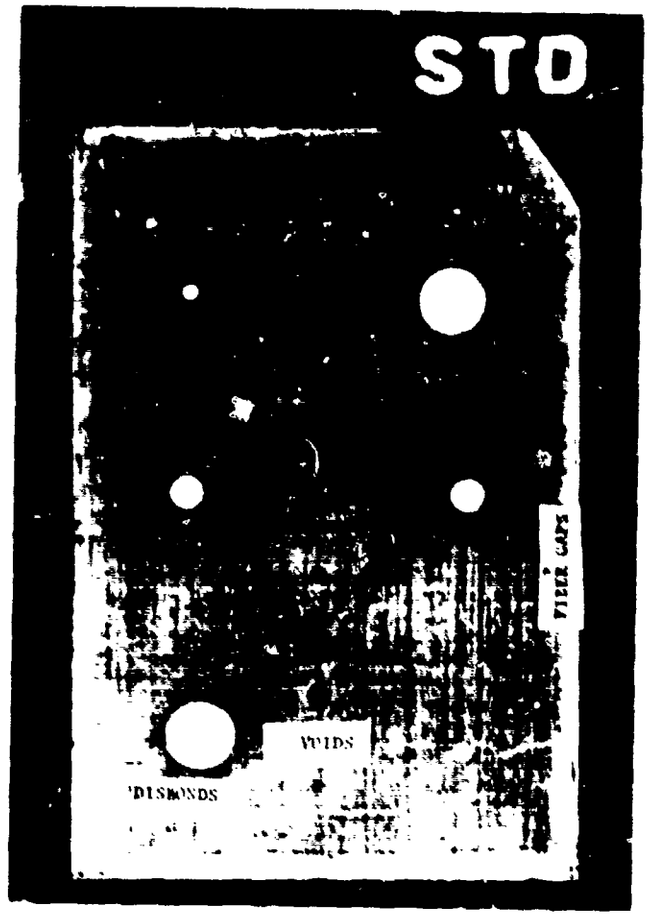

Fig.4 Radiograph of graphite epoxy reference standard

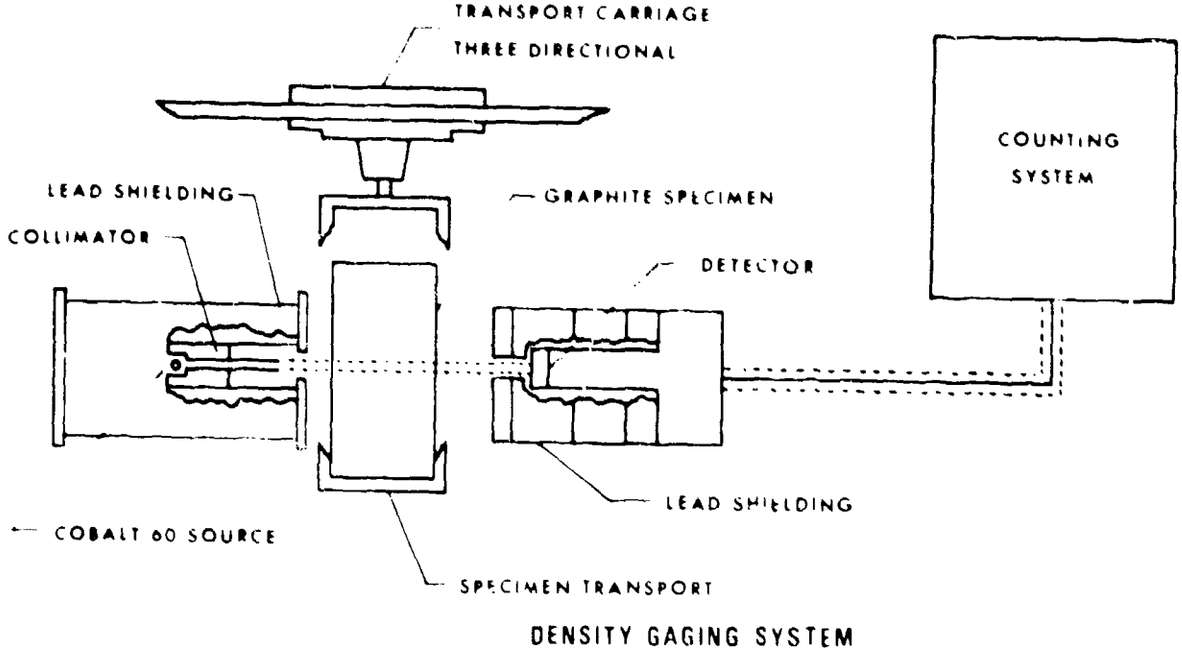

Fig.5 Diagram of radiation density gage

4.4.4.2 Gamma Radiation Technique

Gamma radioisotopes are available from sources such as Cobalt 60, Cadmium 109, and Cesium 137. A through transmission gamma-radiation technique is being currently used to indicate variation in material density. Figure 5 is a diagram of a radiation density gage system.

4.4.5 ELECTRICAL METHODS

Electrical properties such as the dielectric constant and dissipation factor (or loss tangent) can be used as indicators for nondestructively determining variations in reinforced-plastic composite materials[9]. For a given thickness and composition, changes in degrees of cure can be evaluated by dielectric constant and dissipation factor measurements, the values for these parameters decreasing as the resin is cured. Similarly, moisture content can be determined with an accuracy of approximately ±1%.

4.4.5.1 Electrical Resistivity

Electrical resistivity has been used to determine optimum curing cycles, uniformity of composition, and the presence of moisture. Continuous resistivity measurement has been investigated for monitoring the cure of reinforced-plastic composites. Because electrical resistance of plastics is highly sensitive to changes in temperature, the temperature during the test must be carefully controlled. Volume resistance measurements require that the probe have access to both surfaces of the part.

4.4.5.2 Corona Discharge

Corona discharge is being used for determining the presence of voids within plastic laminates. When the material is subjected to a high potential (electrical), the gas (air, moisture from the resin) within a void ionizes, causing acceleration of electron to the wall of the void[10]. The presence of voids can be detected and evaluated by measurement of the resulting voltage charge, the light produced, or the noise emitted. The high voltage that produces the corona discharge must be of a short duration to prevent burning the part.

4.4.6 ELECTROMAGNETIC METHODS

4.4.6 1 Microwaves

Microwaves are electromagnetic radiations of very high frequencies ranging from about 50 KMHz to 100 KMHz. Microwave techniques can be used to detect defects and for measuring thickness, moisture content, and dielectric properties for nonmetallic materials[10]. For composites, defects that can be detected by these techniques include voids, delaminations, porosity, foreign inclusions, resin-rich and resin-starved areas and variations in degree of cure and moisture content. Because of the high frequencies used, the microwave radiation beam can be focused on small areas, providing high resolution in locating defects.

A microwave source (horn) directs the radiation at the test material. The energy reflected or transmitted by the specimen can be used for the evaluation. A crystal detector converts the resultant wave into an electrical response. Figure 6 is a block diagram of a typical microwave system.

Voids have been detected at the core-to-skin interface of honeycomb ablative material that were adhesive bonded to metallic face sheet. Scattering of the microwaves by the voids causes a reduction in signal amplitude, which was observed on a cathode ray tube. Microwave signals at 3 to 4 KMHz have been used to detect bond separations of about 1/16 sq.in. in areas in complex, reinforced-plastic honeycomb-sandwich structures.

Microwaves can be used to monitor the curing process and to indicate the degree of cure. The dielectric properties of a material change as the resin cures, the microwave reflections respond to these changes. The dielectric properties of a reinforced plastic depend on chemical compositions, composition variables and impurities can be detected by microwave techniques.

Microwaves strongly interact with water, and therefore may be used as a means to measure moisture in plastics. In addition to signal attenuations due to microwave energy loss, phase shifts in the standing waves can also be used for NDT measurements. A phase shift will occur if the dielectric properties of the material are varied. Part thickness and geometry can influence the results of NDT measurements for both signal attenuation and phase shift.

4.4.7 THERMAL METHODS

4.4.7.1 Infrared Scan Heating Techniques

The difference in heat flow caused by defects within a material can be used as a nondestructive test indicator. In order to study heat flow in a material it is necessary that the part contain either an excess or a deficiency of heat with

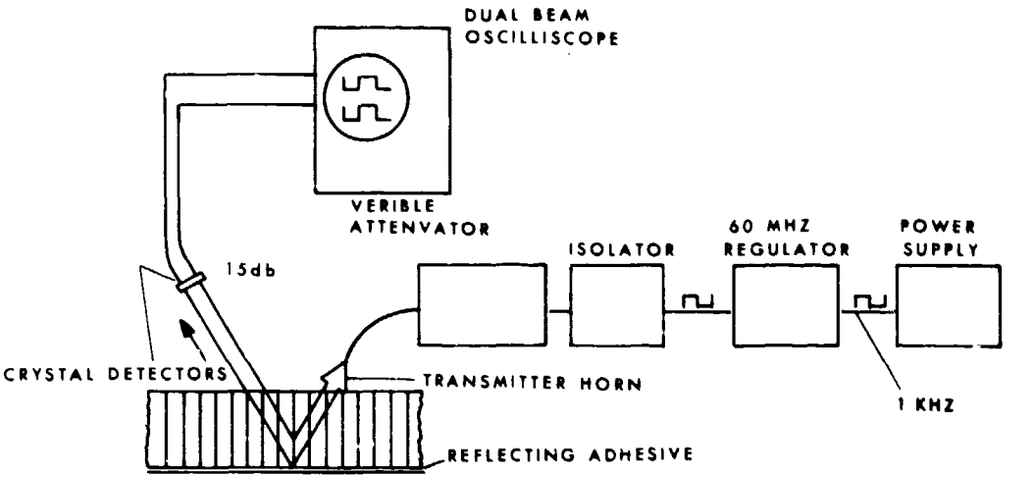

Fig.6 Microwave void detection system

50 KMHz to 100 KMHz microwave energy is transmitted from a single horn and part of this incident energy is reflected and part refracted into the test sample. This refracted wave is totally reflected from the conducting adhesive and is received by one or the other of the two receiver horns. The angle which the transmitter and receiver horns make with the surface of the sample is critical for proper operation of the system. For a system without voids a maximum signal is reflected from the conducting adhesive. When a void exists there is a drop in the received signal amplitude in comparison to that from a normally bonded area. The wave reflected from the top surface is neglected since it does not interfere with the receiver horns and passes out of the system path.

respect to its surroundings[11]. The more conventional methods of thermal NDT employ scan heating or fixed large area heating methods of introducing heat into a material. The scan heating technique is shown schematically in Figure 7. Once the material is heated, as it heats further or cools, the surface temperature is observed with a sensitive infrared radiometer.

4.4.7.2 Thermal Coatings

Another thermal NDT approach utilizes the temperature and color sensitivities of liquid crystals[12] and Photo Chromic dyes. Applied from aqueous solutions, these coatings can be removed by solvents or simply stripped off. The coated part is heated uniformly; a defect is indicated by the color change at the surface (coating) nearest to the defect as the materials heat or cool. Because this method is based on thermal flow, defects can be seen during heating as well as during cooling. The simplicity and low cost of these thermal coating techniques make them very attractive.

In general, thermal methods of NDT can detect only separations (gross-size voids, delaminations or unbonded areas), and are not suitable for weakened areas. Defects near the surface are more readily detected, and sensitivity decreases as part thickness increases.

4.4.8 OTHER NONDESTRUCTIVE TEST METHODS

Those methods described above are the more common methods being used for the NDT inspection of composites. In addition to these methods, there are a variety of other approaches for NDT of composites that have been used or are still under development. Many of these methods are not unique to composites and a detailed discussion will not be presented here.

Methods for detecting surface defects include liquid penetrants (fluorescent and dye); strain gages to measure dimensional changes or distortions when a load is applied to the material; strain-sensitive "brittle" coatings to indicate stress distribution over the surface of the part when a load is applied; and photoelastic stress measurements. This latter technique uses a birefringent plastic coating or film bonded to the surface of the material being evaluated. Upon application of a load, one can see the stress distribution by noting fringe patterns (changes in color) in the coating under polarized light. This technique has been used to detect and measure the effects of strength reducing factors in filament wound pressure vessels.

A recent technique developed for the NDT of bonded assemblies is differential laser holography. This technique provides a means for precise measurements of displacement of deformation within a structure. Holography is basically a two step process that permits the reconstruction of three-dimensional images. In holographic NDT, displacement of

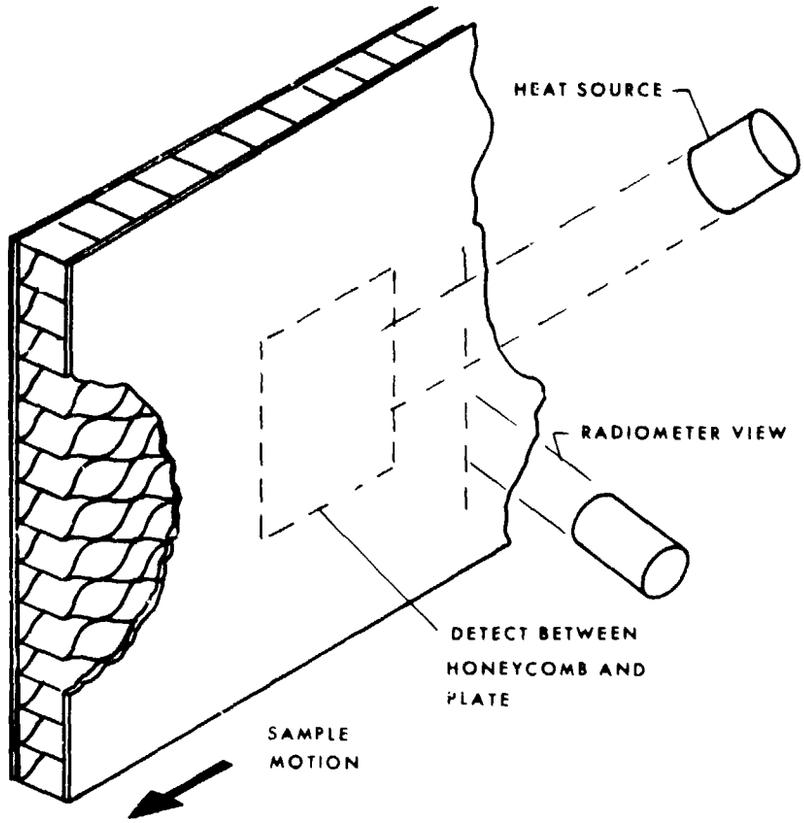

Fig.7 Scan heating technique

the structure or a portion thereof results in an interferometric fringe pattern that depends on the extent of the displacement, and can be visually observed or recorded on film. This technique is reported capable of being able to detect surface and subsurface cracks, voids, delaminations, and inclusions.

Nuclear resonance techniques hold some promise in the nondestructive inspection of reinforced plastic/composites. Nuclear magnetic resonance (NMR) and nuclear quadruple resonance (NQR) are valuable in evaluation of the molecular structures of material components of composites to define and measure abnormal conditions and structural changes.

REFERENCES

1. Roehrs, R.J. — Private communication compiled from the Table developed at McDonnell Douglas Corporation, St.Louis, MO, 1972.

2. McGonnagle, W.J. — *Nondestructive Testing*. McGraw-Hill Book Co., Inc., New York, 1961.

3. Kramer, J.M., Nuzzo, A.F., Epstein, G. — *Large Plastic Moldings OK'd by Ultrasonic Inspection*. Material Design Eng., 55, 13-16, 1961.

4. McMaster, Robert C. — *Nondestructive Testing Handbook*. Vol.II, The Ronald Press Co., 1959.

5. Zurbrick, J.R. — *Development of Nondestructive Methods for the Quantitative Evaluation of Glass Reinforced Plastics*. TR-66-269, AFML, W-PAFB, Ohio, June 1966.

6. Miller, N.B., Boruff, B.H. — *Adhesive Bonds Tested Ultrasonically*. Adhesive Age, 6, June 1963.

7. Arvin, M.J., Howell, W.D. — *Development of General Specifications for a Device for Inspecting Helicopter Bonding*. Federal Aviation Agency, Bureau of Research and Development, Test and Experiment Division, Final Report, AD257-989, Office of Technical Services, U.S. Dept. of Commerce, Washington, D.C., November 1959.

8. – *North American Aviation Sonic Test System.* Brochure STS203, North American Aviation, Inc., Los Angeles Division, 1967.

9. Warfield, R.W. *Studying the Electrical Properties of Coating Resins.* SPE J. 14 (11) 39, 44, 46, 1958.

10. Henderson, J.A. et al. *Corona and Microwave Methods for the Detection of Voids in Glass-Epoxy Structures.* Materials Evaluation, 22 (7) 311-314, 1964.

11. Gericke, O.R. Vogel, P.E. *Infrared Bond Defect Detection Systems.* Material Evaluation, 22 (2) 65-68, 1964.

12. Woodmansee, W.E. *Cholesteric Liquid Crystals and Their Application to Thermal Nondestructive Testing.* Materials Evaluation 24 (10) 564-572, 1966.

CHAPTER 4.5

DETECTION AND MEASUREMENT OF CORROSION BY NDI

by

A.R.Bond

Assistant Quality Control Superintendent
British European Airways
P.O.Box No.6
Engineering Base
London (Heathrow) Airport
Hounslow
Middlesex
UK

CONTENTS

4.5.1 THE SUBJECT CORROSION

4.5.2 THE PROBLEM

4.5.3 THE IDEAL SOLUTION
4.5.3.1 History

4.5.4 REVIEW OF NDI METHODS
4.5.4.1 The Evaluation
4.5.4.2 Conclusions

4.5.5 THE PREFERRED METHOD
4.5.5.1 Eddy Currents
4.5.5.2 Use in Service - Single Skins
4.5.5.3 Use in Service - Multiple Skins

4.5.6 NOTES ON OTHER METHODS
4.5.6.1 Radiography
4.5.6.2 Thermovision
4.5.6.3 Ultrasonics

4.5.7 THE SELECTION AND TESTING OF EDDY CURRENT PHASE SENSITIVE DETECTORS
4.5.7.1 Discussion
4.5.7.2 Tests

4.5.8 TEST PROCEDURES USING EDDY CURRENT PHASE SENSITIVE DETECTORS

DETECTION AND MEASUREMENT OF CORROSION BY NDI

A.R.Bond

4.5.1 THE SUBJECT – CORROSION

Corrosion is the breaking down of a homogeneous metal into oxides either in localized areas for a specific reason or generally spread over the surface of the metal.

The factors which contribute to this degeneration in dissimilar parts are the introduction of an electrolyte, e.g. impure water and the formation of a circuit in the particular assembly. The chemical action at the faces is the driving force and the whole process is self generating when it starts. The part which is less noble becomes the anode and dissolves away.

In the light alloy metals, used in aircraft structure fabrication, this electrochemical action occurs easily in one part because the supposed homogeneous material used to make it is in itself made up of discrete particles and as in the case of composite parts the discrete particles can locally become the start points of corrosion and form self generating areas.

Differing concentrations of the electrolyte can cause different attacks of corrosion in similar areas.

4.5.2 THE PROBLEM

When corrosion is on the visible side of aircraft structure it can be identified, and removed. Estimates of the remaining material thickness can be made quite quickly and repairs and/or fitness for service deemed quickly.

When corrosion takes place on the sides of aircraft skins which are not visible then the problem can assume a greater financial and/or safety problem than is obvious when the onset is noticed, i.e. at the first sign of corrosion the concealed area could, after a very expensive strip, be classed as fit for further service or without any sign (or a very minute sign) could be found to be in a dangerous condition.

Background to Inspection

With all the best will in the world it would be quite wrong to imagine that all protective paint schemes will remain perfect for ever. In a structure which is moving, however minimal, *washed* by condensation and sometimes rubbed by debris a good protective finish is bound to suffer through the years.

As soon as a small path appears the electrolyte, ready to form the final factor in the mechanism of corrosion, will creep along it and start the corrosive process off. The primary method for corrosion detection is of course Visual examination and Inspectors examine the visible surfaces for the symptoms. They look for localised discolouration, faint powder lines or pimples on the paint showing that underneath the paint something is going wrong. Also they are looking for paint damage which thereby leaves the metal unprotected. Symptoms are investigated and action taken to open up suspected areas in order to ensure that the reason for the indication is revealed and any corrosive origins are laid bare for remedial action. All areas are not equally prone to attack because of differing conditions in some areas so there are more particular searches in certain areas. It is often found necessary for a variety of reasons to examine structure by extra means and devices ranging from the simple mirror to very expensive optical viewing aids are used to look in dark corners.

Anything about an aircraft in service is interlocking when you find a flaw; how significant is it, how long have you got to get the spares, how much of the original structure can you save by thoroughly cleaning out and reprotecting, can you repair or must you order a new panel? The combinations are numerous and greater accuracy in our findings means a longer time to study the situation coldly, order the parts, and bring the aircraft in before the situation in the specified area becomes critical financially and certainly much, much earlier than any technically critical state. Around fuselage cut-outs, such as doors, it is common practice to reinforce the cut-out with doublers bonded to the skin. Corrosion starts up in the surface of one of the joined plates and this, of course, releases the bonding film and in some areas a large area of disbond occurs without corresponding tell-tale signs at the edge of the doubler or bulging of the surface. It is therefore most important to examine double and triple joints whether there are any visible signs or not.

So, although these practices have been shown to give satisfactory service in the past, in view of the minute indications of concealed corrosion it is necessary to make better inspections and be sure of the results. Such inspections are done by the use of applied physics, i.e. NDI.

4.5.3 THE IDEAL SOLUTION

The method most suitable for the examination has to take into account all factors and produce answers which will permit Inspection and Design Personnel to evaluate the situation correctly and produce a solution that will allow the safe operation of the aircraft in an economical manner.

4.5.3.1 History

As the NDI methods were tried out in service it was possible to identify all of the factors which had to be overcome in the best solution.

The factors that make the examination of concealed faces difficult are now determined to be as follows:

(a) Paint films of varying thickness over outer faces.

(b) Corrosion products entrapped between faces.

(c) Bonding and bonding spew.

(d) Interfaying and sealing compounds.

(e) Water and contaminants in corroded areas.

4.5.4 REVIEW OF NDI METHODS

There is no ideal solution at the moment but one method is shown to be of superior potential to all the others and gives better and consistent results at this time. In fact, for most general assessments of conditions, it can be classed as adequate for the purpose.

4.5.4.1 The Evaluation

Penetrant Testing was considered as a means for detecting the voids or paths by which the electrolyte could enter. One were sure that the path was dry and clean and would permit the penetrant to enter it is obviously visible as a path. If the path is not visible and is full of electrolyte the penetrant cannot enter, so the path would not be detected. These contrary answers show that this is no valid test.

Ordinary *Radiography* has only ever been certain of detecting gross corrosion consequently it has been a pointer to when the structure should be opened up to clear up a corrosive situation. There have been many ideas and many processes on this system but it still remains a fairly coarse filter. It can be used for certain inspections where it is not possible to use a more sensitive method.

Neutron Radiography and Colour Radiography, using both Film or T.V., were discarded for expense, time and general impracticability.

Thermography, in particular thermovision, was thought to hold some promise but tests showed that the heat absorption in thin skins was insufficient to give a stable picture.

Ultrasonic resonance methods and transmission methods were tried. The first mentioned required a flat surface away from the interrogating face and corroded surfaces are, of course, not flat. The latter type of test required that the area of examination be immersed in water.

The pulse echo method of interrogation of one skin from the good side was the only method that showed promising results but unfortunately it measured the paint and gave incorrect answers when the corrosion products and or a liquid was present.

Full reports on these methods are shown in 4.5.6.

In *Eddy Current* testing there are a variety of ways of applying the phenomena to the object under test. The right method for corrosion detection was determined to be in referencing the phase of the eddy currents in the test area. Evaluations showed that all of the factors, that interfere with the detection of corrosion in thin skins, had minor effects on the method if the instruments were used correctly.

The system measures the volume of metal under the influence of the probe so must be considered a quantitative system; nevertheless, by a system of plotting, it is found that certain qualitative results can be obtained. In the same way multiple skins can be tested out there is a reduction in the best sensitivity available.

Early detection of concealed corrosion by this method allows inspecting staff to maintain control of any defective areas without fear that the corrosion has reached a dangerous condition; always, providing that the detectors used are stable and have good lift-off characteristics.

Full report in 4.5.5.

4.5.4.2 Conclusions

Eddy Current Phase Sensitive Detectors give readings which result in better evaluation of the conditions of the faces of aircraft skins which cannot be viewed directly. It is not envisaged that the method will ever be accurate to the same degree in all situations because it is already clear that older structures, where adjoining faces are not parallel, because of inconsistent rivetting practice, only give results of a lower sensitivity. Nevertheless, providing that the instruments are of sound design, the accuracy of the method is much better than anything attained hitherto.

See 4.5.7.

The method takes time in training staff in the accurate use of the instruments and in the idiosyncrasies of individual structures, but, in the end, gives good service in the evaluation of aircraft skin condition.

See 4.5.8.

Also, in certain circumstances, the use of a combination of one of the methods described in 4.5.6 and the Eddy Current Phase Sensitive Detector can give added information for assessment purposes.

4.5.5 THE PREFERRED METHOD

As described in 4.5.4 the method of inspection which gave the best results was deemed to be the Phase Sensitive Eddy Current Method.

4.5.5.1 Eddy Currents

A coil is excited with an a.c. current and when it is placed near a metal component, eddy currents oscillate in the metal at close proximity to the coil (probe). Anything disturbing the eddy currents, such as a crack, is detected electrically and displayed on a scale.

These currents penetrate into the metal to a depth which is dependent on frequency and various techniques were tried out to determine whether a thickness change could be detected by using this phenomenon. It was proved that there was a phase shift and that it could be displayed. In use, a coil close to the skin is referenced against one above it (i.e. more distant from the skin); when the lower coil passes over a thin (corroded) area the phase change is identified.

This phase shift when electronically converted into a scale reading was found to be linear, that is that when the probe is placed over a good piece of material and the meter adjusted to zero and with the probe placed over a piece of material which is 10% thinner and the needle adjusted to the maximum position on the scale, the other positions on the scale were relative to intermediate losses of material.

History

Investigation was carried out as to the suitability of eddy current techniques for the detection of corrosion beneath aircraft skin panels.

The first test was to examine whether the method was able to detect loss of cladding from the underside of skin panels, this cladding loss represents 5% thickness reduction. The primary trials carried out showed that a phase sensitive eddy current technique was suitable for detecting thickness reductions of this amount, experimental results having actually detected a 2% thickness loss.

After the first production instrument came into use, the method was found to be capable of detecting corrosion as little as 0.5% in aluminium alloy panels from 22 SWG to 14 SWG provided that the area was greater than that of the probe cross section. Lesser areas could also be found but with lower sensitivity. It was also found capable of detecting corrosion between two panels with the same sensitivity provided that the panels were each thicker than 18 SWG. Thinner panels gave spurious indications due to buckling, but this problem was overcome by technique improvements.

Accurate corrosion depth measurement was found to be awkward to achieve but the instrument still gave viable results. If the instrument indicates say 1% corrosion it could be 1% over a large area or 20% over a very small area. It is really indicating the volume of the missing metal, but by approaching corroded areas using different techniques the test engineers were able to estimate depth and area. The instrument was five times more sensitive to corrosion than to rolling tolerance; lift-off compensation was such, that a variation in paint thickness of 0.2 mm caused no loss in sensitivity. The instrument worked equally well on mains and internal battery.

The use of Eddy Current Phase Sensitive Detectors for corrosion detection was shown to be quite accurate in its estimation of the volume of metal under the probe. With careful assessment of results and with experience in the use of the system, better evaluation of the condition of aircraft skins was deemed to be possible.

4.5.5.2 Use in Service Single Skins

In service use the method performed in the manner predicted and the results obtained throughout three years were used to produce graphs, which are of practical use as explained herein

Discussion

The estimation of corrosion depth on a single skin is not straightforward because the meter indication is a function of both depth and area. If the corrosion is evenly distributed over an area greater than that of the probe cross-section then the method can be quite accurate even when measuring corrosion as little as 1%, see Figure 1. Smaller areas can, however, introduce considerable errors as shown in Figure 2 where it can be seen that at 2 KHz the accuracy starts to fall before the corroded area was reduced to the size of the probe (16 mm)

These errors can be reduced by using a higher frequency as shown by the 7 KHz and 15 KHz curves in Figure 2 The upper test frequency is limited by the skin thickness.

Operation

The way to estimate the depth of large evenly corroded areas is to note the maximum change in meter reading as the probe passes over the suspect area. This reading is converted into depth using a graph like Figure 1.

The measurement of small areas or pits is carried out by a different technique. This is to traverse the suspect area and increase the frequency to each traverse until the defect indication reverses on the meter. This frequency can be converted into corrosion depth using a graph similar to the one shown as Figure 3 This technique gives depth estimations which are within 10% of actual depth of corrosion.

Graphs must be made up for each instrument probe panel combination and are simple to produce. The graphs shown in Figures 1 and 3 are produced by accurately milling the material in areas greater than the probe size and then taking a series of readings using a part cular probe; repeat for other probes. The graph shown in Figure 2 is produced by accurately milling different diameter areas of constant depth and taking a series of readings.

Conclusion

The method is capable of detecting corrosion of 1% on single skin panels provided that the corroded area is greater than the diameter of the probe. With care good estimates of small areas of corrosion can be made.

4.5.5.3 Use in Service Multiple Skins

During the use of the instrument on aircraft, appraisal of results on multiple skins was maintained and a variety of tests conducted under laboratory conditions. These results were used to produce graphs and these graphs proved that the use of the method had greater potential on multiple skins than expected.

Discussion

Aircraft skins are assembled in a variety of ways and any reference to single, double or multiple skins are to combinations of skins as depicted in Figure 4

Double skins make corrosion measurement more difficult because the meter indication is also a function of skin separation. When corrosion occurs, the skins are forced apart because the volume of the corrosion products is greater than the metal they replace. Even under conditions of no corrosion, the separation is not constant Fortunately there is a frequency at which the effect of this is negligible Figure 5 shows the effect of using this frequency compared with two frequencies, one too high and the other too low. At 7 KHz the meter indication will be due to the combined effects of corrosion and separation. At 26 KHz it will be due to the effect of corrosion less the effect of separation and at 18 KHz it will be due to the effect of corrosion only (see Figure 6). So, the technique on multiple skins is to use the lower frequencies and in suspect areas use the optimum frequency to measure the corrosion remembering that both skins may have to be accessible. Each optimum frequency depends on the conductivity and nominal thickness of the near skin in each case, and is also a function of the probe.

The method of inspecting the outer skins in a multiple situation is the same as for double skins, if only the outer skins are to be measured accurately Should the skin further from the probe have to be tested from the near side, a frequency should be selected which will penetrate all skins In this case, due to the possible varying gap at the interface, one could only expect an overread of corrosion of as much as 100% In the multiple skin situation one could expect an overread of 15% to 100% on the inspection of a middle skin.

In all combinations of skins the particular set-up should be reproduced so that the optimum frequency can be determined and the expected sensitivity proven to be possible

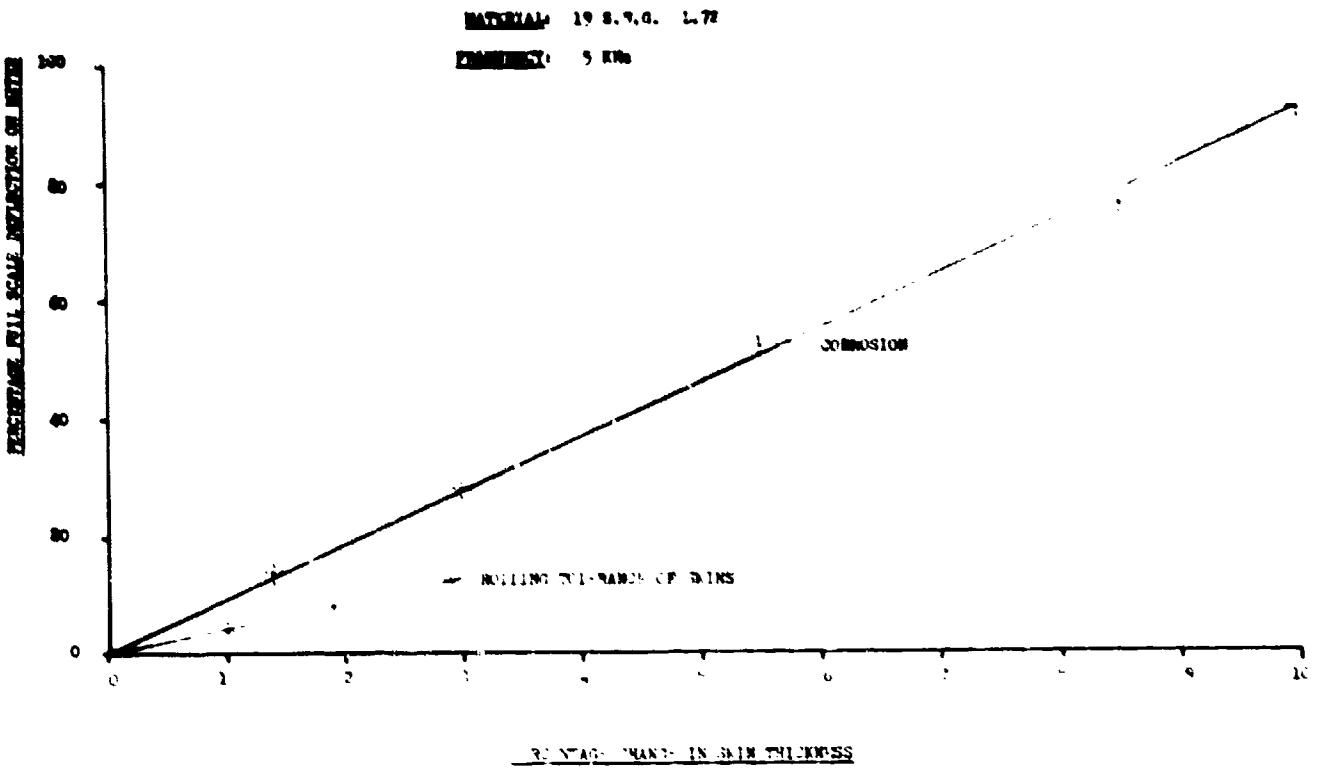

Fig 1 Conversion graph for large areas of evenly distributed corrosion

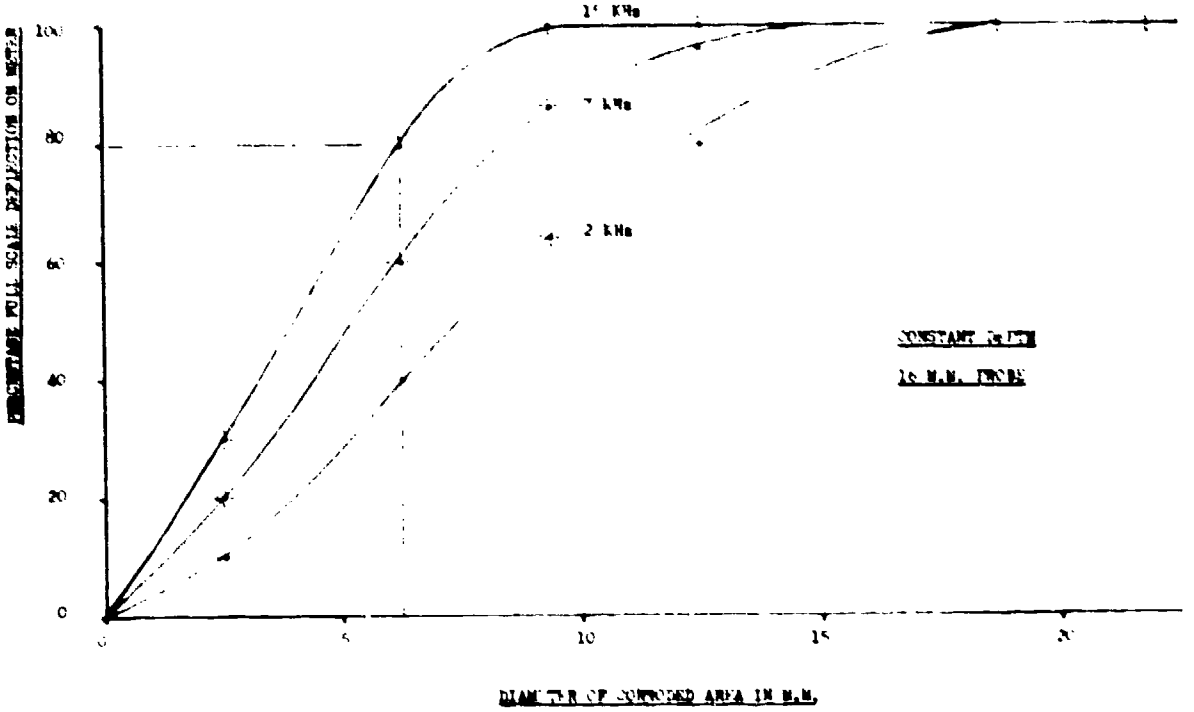

Fig 2 Effect of size of corroded area and frequency

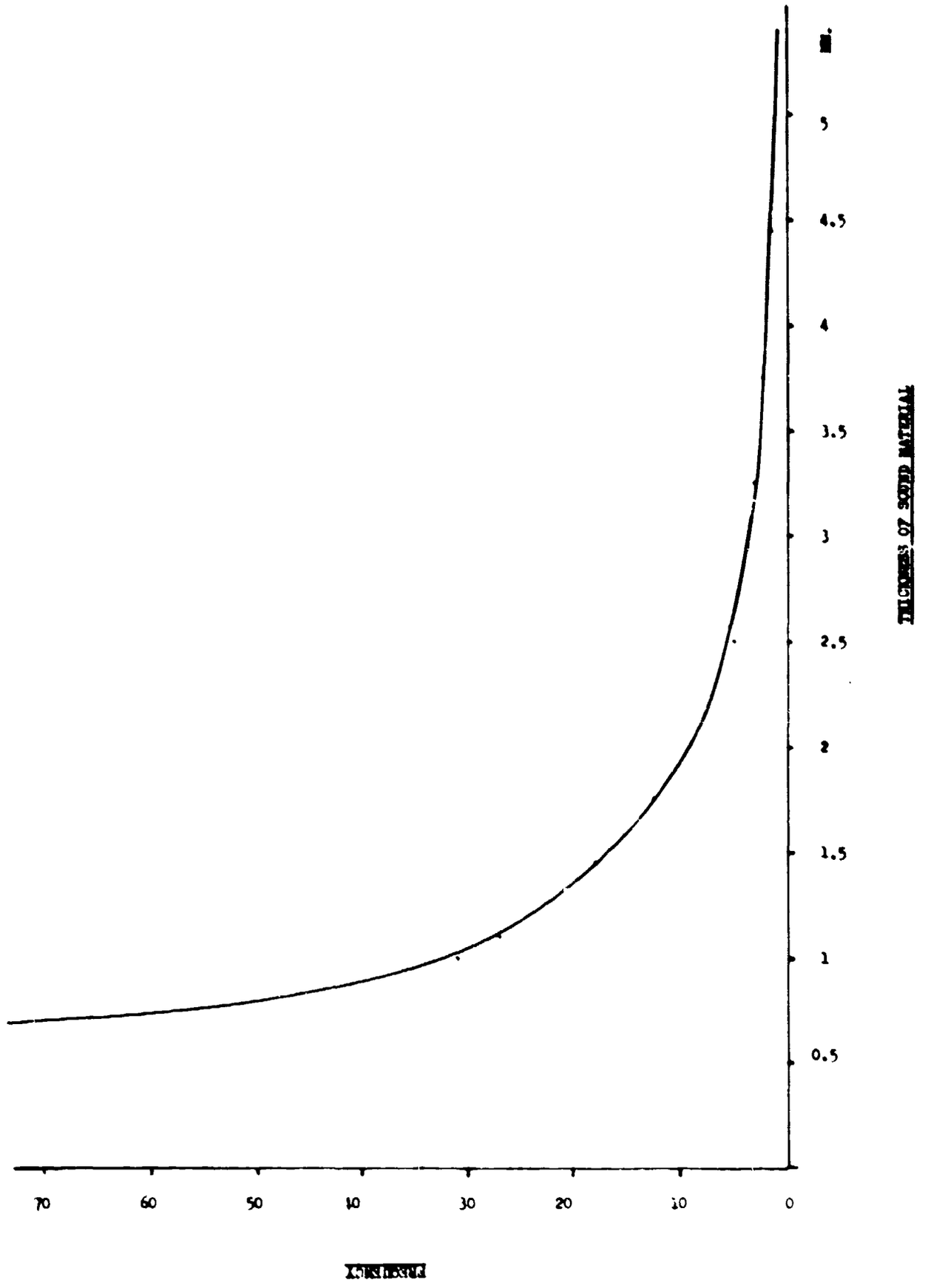

Fig 3 Frequency/thickness of sound materials

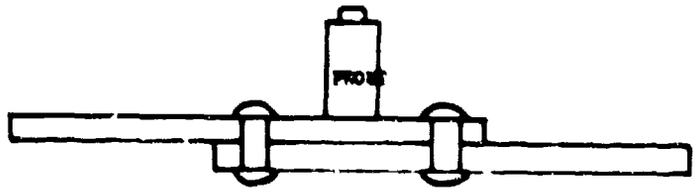

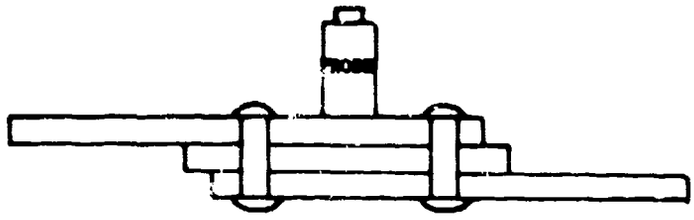

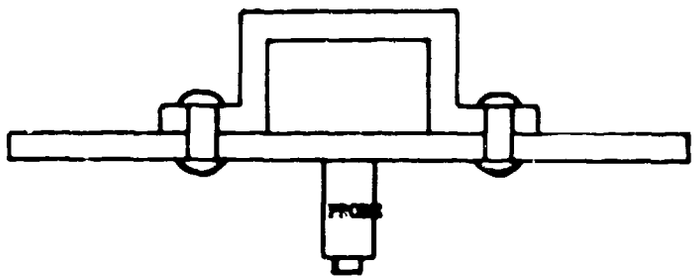

Fig 4 Typical structural composition

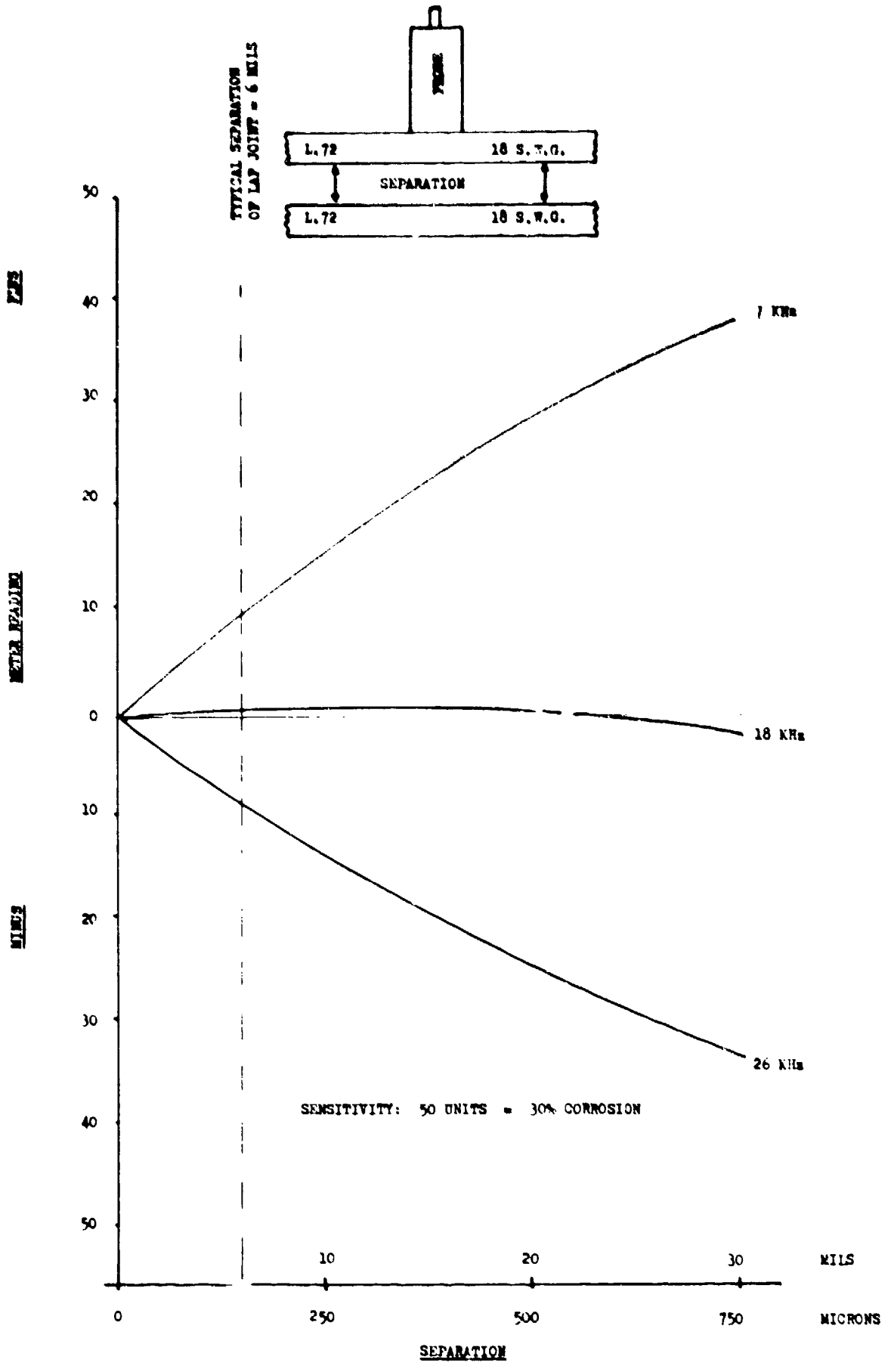

Fig 5 Effect of frequency and separation on meter reading

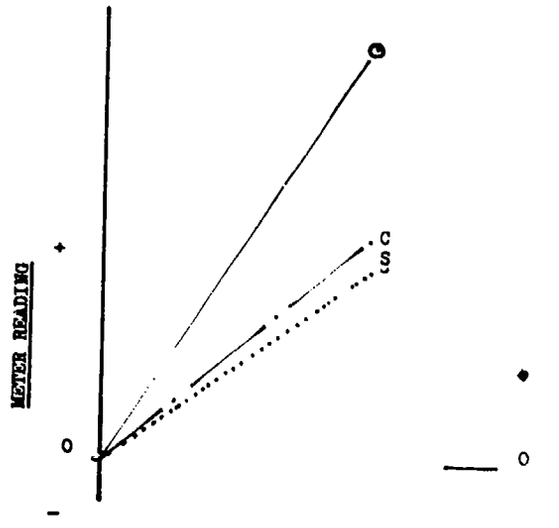

7 KHz 500 MICRON GAP
20% CORROSION

CAUSE	READING
CORROSION (C)	+33
SEPARATION (S)	+29
C + S	+62

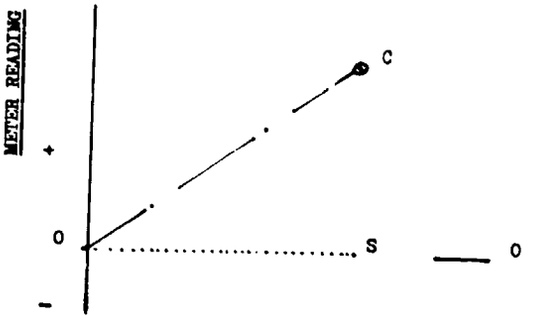

18 KHz 500 MICRON GAP
20% CORROSION

CAUSE	READING
CORROSION (C)	+28
SEPARATION (S)	0
C + S	+28

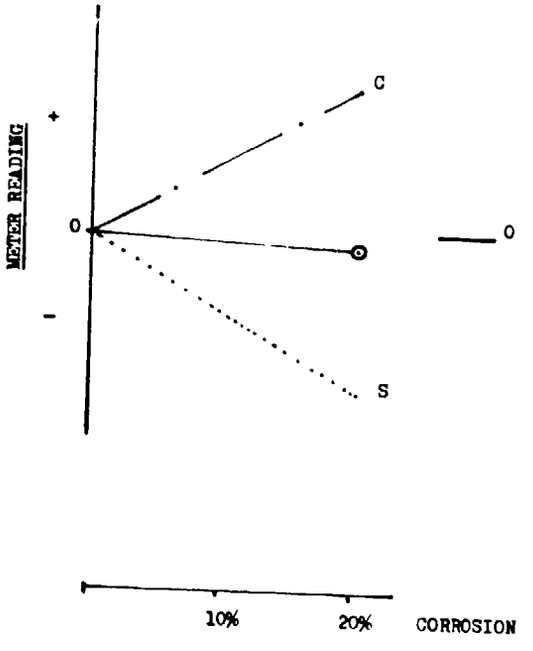

26 KHz 500 MICRON GAP
20% CORROSION

CAUSE	READING
CORROSION (C)	+22
SEPARATION (S)	–24
C + S	– 2

Fig.6 Separation – Typical readings with change in frequency

Conclusion

Providing a test piece is made up which is representative of the area to be tested and the optimum frequency and sensitivity is selected to suit the inspection requirements it is possible to examine multiple skins to varying degrees of accuracy.

4.5.6 NOTES ON OTHER METHODS

The other methods which were thought to have the potential to test aircraft skin panels are described herein; they failed certain tests. To assist inspection staff, the inherent problems particular to such methods are explained in this chapter and, provided their failings are noted, may assist in some corrosion assessments.

4.5.6.1 Radiography

Radiography has been used to survey skins for corrosion for some years.

Radiographic Method

Radiography is actually radiation striking a film or other recording medium after passing through an object. The radiation is modified by the object and the varying shape of the object causes changes in the quantity of radiation passing through the object. The film etc. records the varying quantities of radiation by corresponding varying densities on its surface.

It can be seen thus, that the loss of metal in a corrosion pit on a skin will allow more radiation to pass to the film, causing an area of increased density on the film, which should be visible to the radiologist.

History

When radiography was first started on aircraft the determination of corrosion was not considered to be possible, but the introduction of low kilovoltage radiography allowed a certain amount of success by NDT staff in some areas. Unfortunately, this success plus outside pressure to enlarge the scope further has brought the use of the method into disrepute with some engineers. Primarily such disrepute is because these people consider the method by measuring specific (bad) results instead of total performance and they certainly do not fully appreciate the physical problems that exist in the process.

4.5.6.1.2 Steps in the Method

Radiation quantity converted by object to varying quantity at film.

Radiation at film converted to latent image in film.

Latent image in film converted into visible halides by chemistry.

Visible halides on film converted to visible image by light transmission.

Visible image on film converted to words by radiologists.

Even with these conversions it is possible to see a 2% variation in object thickness and this is termed the sensitivity of the exposure. In the case of an aircraft structure there are several items that are interposed in the line of radiation and these items are the cause of the bad performances of the method and the consequent disrepute.

4.5.6.1.3 Interferences to Radiography

All materials absorb radiation to varying degrees and they can usually be seen on the radiograph if they are in the line of radiation. Further if such materials have high absorption rates they seriously interfere with the radiography.

Paint

External paint may tend to run down to the area under examination giving differential absorption at changes of thickness. Internal paint can be of varying grades and thickness with the same result.

Sealant

This is applied in the form of a bead at the junction of the stringer and skin. This is the point where there is not only a change of density because of the change in thickness of metal but the favourite starting point of corrosion. Sealants absorb a lot of radiation and thiokol is the worst sealant in this respect.

Interfaying Compounds

These have a little effect by their absorption but are not of great significance as they tend to be well squeezed out.

Dirt

There are sometimes areas of paint (usually where the paint scheme has been patched) which have had dirt swept on to it when tacky and this gives some interference to the radiation, with resulting loss of sensitivity.

Corrosion Products

In the case of corrosion pits in open or box structure, the products of the corrosion process fall out of the centre and the ring of products on the edge enhance the detection of the pit.

In the case of corrosion trapped between surfaces, the corrosion products and the good metal offer the same absorption to radiation if there has been no movement of the products and there are times when nothing is visible on the film to signify that corrosion is present.

Water or Other Liquid

These generally have the same effect as of overlaying another piece of metal over the whole area, thereby reducing the sensitivity.

Bonding Spew

This is by far the worst item in the list of offenders, in that the holes in this rough material have ragged edges and when viewed with other interposing factors have a very similar appearance to corrosion pits.

Upholstery and Soundproofing

These items are normally in areas where dust etc. fall away and, although there is a minor loss of sensitivity, corrosion is usually detectable. Lead Vynil, when introduced, completely eliminates any possible radiography.

All the items mentioned above have the effect of making viewing and interpretation difficult for the radiologist.

4.5.6.1.4 Mathematical Consideration of Interposing Structure

If we consider a piece of structure mathematically, as per Figure 7, we find that in the case of a skin supported by other structure, which is four times thicker, a 4% sensitivity can actually represent a defect size which corresponds to 20% of the outer thickness. Even when the structure behind is equal in thickness to the skin; Figure 8 demonstrates that the 4% sensitivity can represent 10% of the outer skin.

4.5.6.1.5 Summary

All of the facts may, or may not, be present and the interpretation of the radiographs can present a decision problem for the radiologist.

A faint indication with a ragged edge can mean severe corrosion being concealed by interference, very light corrosion or just a hole in Redux or paint

All in all, there are more things interfering with the radiologist than helping him, but considering these problems there has been considerable financial advantage in the use of the method to date. It can still be used to great effect in many areas, but in the lower half of the fuselage where these interference items abound, one can only expect some degree of error.

4.5.6.1.6 Conclusion

Although corrosion can be detected on the inside faces of an open box structure, it must not be assumed that a similar loss of metal is easily detected in any structure.

The items that contribute most to radiological errors are always present in certain areas (e.g. lower fuselage) and improvement in performance is most unlikely.

4.5.6.2 Thermovision

History

In recent years Thermography has successfully been applied in Medical Research, fault detection in power lines and in heat distribution in steel manufacturing equipment.

RADIOGRAPHIC LIMITATION

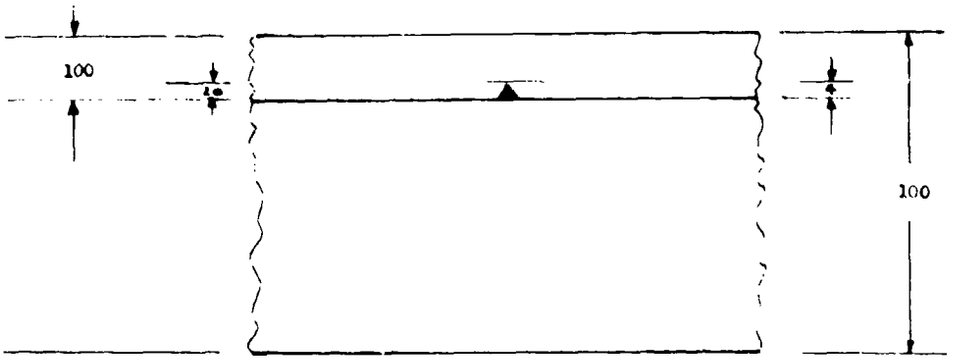

CONSIDER SECTION SHOWN, THICKNESS - 100

RADIOGRAPHIC SENSITIVITY - 4% (4 UNITS/100)

BUT IF THESE FOUR UNITS ARE TOTALLY IN THE TWENTY UNIT THICKNESS, THE SAME DEFECT BECOMES 20% OF THIS ONE SKIN WHICH MEANS THAT RADIOGRAPHY CAN ONLY BE CLASSED AS A ROUGH POINTER TO THE CORROSION STATE OF THE JOINT IN THIS CASE.

Fig.7 Radiographic sensitivity thin skin thick stringers

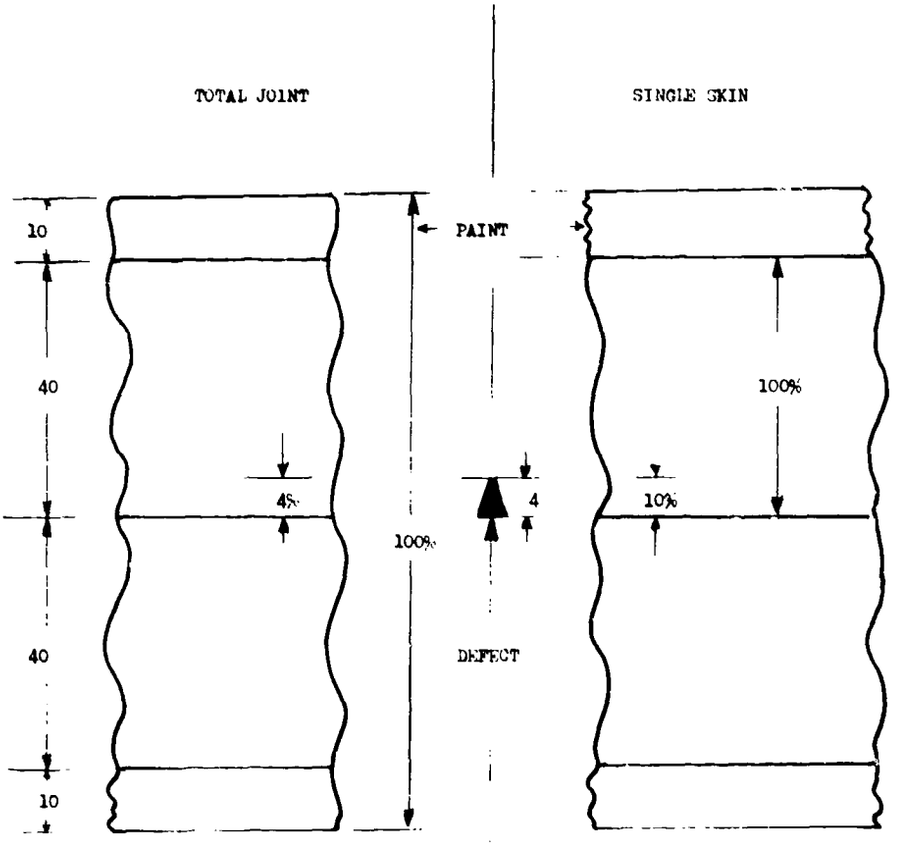

DEFECT SENSITIVITY RELATIVE TO TOTAL JOINT AND SINGLE SKIN

Fig.8 Radiographic sensitivity joint of equal thickness skins

It was proposed that Thermographic techniques could also be used in the detection of corrosion on aircraft structures. The proposal was based on the idea that with the provision of a suitable heating method, a reduction in thickness, or void, would result in a distinctive thermal distribution on the surface of the structure, which could be detected by a Thermal-Vision Camera.

Three methods of heating the specimens were tried:

(1) Infra-red and photo flood lamps.

(2) Hot air.

(3) Heat soaking in an oven.

As the camera detects the intensity of infra-red radiation which depends not only on the temperature, but also the emissivity of the specimen it was found necessary to ensure a uniform surface emissivity. Covering the surface of a specimen with a material which would ensure uniform emissivity was barely possible in the laboratory and is considered to be totally prohibitive on service aircraft.

Conclusion

The tests were not as successful as had been hoped because definite patterns of heat cycling could not be repeated to give similar indications, also none of the heating methods would give uniform heating, which is essential.

4.5.6.3 Ultrasonics

High frequency sound waves have been used to probe metal for defects for some years; the same phenomena have also been utilised to gauge the thicknesses of milled sheets.

Ultrasonic Method

A crystal excited by means of an electric current, rapidly expands and contracts sending sound waves through the metal and the relative time of return of the sound shows the relative thickness of good metal.

History

The display of the returned signal was usually on a Cathode Ray Tube and the speed of the tubes in use precludes use on thin light alloy skins. Equipment with a fast digital display had the potential to detect thickness of thin skins so it was tested.

The tests were divided into two series: those designed to check the accuracy of the instrument against the machined calibrated panels, and those designed to check the effect on the instrument of double layers, actual corrosion, corrosion products and moisture.

A sample of unmachined sheet 29.5 mil. thick consistently gave a reading of 27.0 (an error of 8.5%), but on machined panels the accuracy of the instrument was good with an error of not more than 0.1 mm. As a check of the instrument's sensitivity to area change, a number of different diameter steps were machined to the same depth in skins. The diameter varied from 31.25 mm down to 6.25 mm and the instrument gave correct depth readings for all diameters without difficulty.

Spurious Effects

The result of the tests on panels containing actual corroded areas were not so encouraging. The readings obtained for the test panels were optimistic, the error being as high as 9.25% and 21%. These panels were measured with the corrosion products left undisturbed to simulate actual aircraft conditions, and it is probable that these corrosion products, being well coupled to the aluminium, gave extra transmission to the ultrasonic pulse. This was borne out by additional readings made on one panel with the same corroded areas moistened with water. This tended to increase the readings still further and similar effects were noted with oil and fresh jointing compound.

It was also found that at the edges of some corroded areas readings as high as 80.6 (dry) and 82.9 (wet) were obtained, although the uncorroded thickness of this panel was only 79.5 mils. Again, this effect is probably due to the presence of corrosion products outside the actual corroded area.

The test on a panel did not indicate corrosion at two areas where it was known to be present. In fact one area gave an indication of increased panel thickness. However, on visual examination of the corrosion after separating the panel from the stringer, it was found to be very slight — less than 1%. Similar spurious indications were obtained with a Redux-bonded panel. Readings showing up to 0.05 mm deep corrosion in several areas between skin and stringer were not borne out by examination.

Conclusion

The system is extremely accurate (providing care has been taken with initial calibration) for determining the thickness of material with clean, dry and parallel surfaces. It is evident however, that the effects resulting from the presence of contaminants such as corrosion products and/or moisture make this instrument unsuitable for the purpose of the detection of corrosion on aircraft skin panels. N.B. One must also allow for varying added thickness of external painting.

4.5.7 THE SELECTION AND TESTING OF EDDY CURRENT PHASE SENSITIVE DETECTORS

Phase Sensitive Detectors could have inbuilt faults affecting accuracy and in order to determine the freedom of the instrument from such inaccuracies certain tests have been devised and are laid out herein.

4.5.7.1 Discussion

There are varying paint thicknesses on skin surfaces and these are not obvious to the Inspector. The paint which is in contact with the probe "lifts off" the probe from the metal and consequently any lift-off compensation in the instrument which interferes too much with the sensitivity is dangerous every time the paint thickness changes.

In evaluating some instruments it has been found that sensitivity can drop to zero with the introduction of as little as a 100 micron gap (lift-off) between the probe and the metal surface. The lift-off results from a good instrument have been plotted on Figure 9 and it can be seen that the sensitivity is not affected by reasonable changes in lift-off.

So, when the lift-off compensation has been set the introduction of paint should not affect the zero.

If the instrument has a tendency to drift it will not consistently give a correct zero and without continual checking and rechecking the settings would thus not give accurate measurements of corrosion.

The instrument should be clearly indicative of changes in thickness of all the particular skins required to be tested. Testing the instrument for a particular sensitivity at one thickness of skin is not indicative of its performance across all frequencies and metal thicknesses.

If critical inspection of metal to metal joints have to be done the instrument should be capable of measuring the thickness of the near skin by selecting the optimum frequency. If the optimum frequency cannot be selected there must be a fall-off in accuracy because the readings will be affected by the farther skin. The varying gap between the skins varies the interference from the other skin hence there are unknown changes in sensitivity, i.e. accuracy.

Tests to evaluate an instrument are tabulated below.

4.5.7.2 Tests

(1)	Lift-off	(a)	Set up instrument to makers instructions.
		(b)	Apply probe to unpainted skin specimen of specific thickness and obtain zero meter reading.
		(c)	Apply probe to unpainted skin area 10% thinner than specific thickness and obtain full scale meter reading
		(d)	Apply probe to first area of test (b) interposing a non-metallic film of 300 microns thick. Zero should not be affected.
		(e)	Apply probe to second area of test (c) interposing the non-metallic film. The meter reading should be at least 95% full scale deflection.
(2)	Drift	(f)	Set up instrument to makers instructions.
		(g)	Apply probe to areas of test and obtain readings as per (b) and (c).
		(h)	Lay probe on non-metallic surface and leave instrument switched on for 30 minutes.
		(i)	Apply probe to the areas of test and check for readings as in (g). The alterations to the readings should not be more than 2% full scale deflection on the meter.
(3)	Sensitivity	(j)	Set up instrument to makers instructions.
		(k)	Apply probe to areas of test as in (b) and (c) on all thicknesses of metal to be tested. Accuracy should be within 1% on all the specimens.
(4)	Battery Life	(l)	Set up instrument as per (f), (g), and (h) leave for 6 hours and test battery level. Battery level indicator should show that the battery power is above the minimum usable level.

4.5.8 TEST PROCEDURES USING EDDY CURRENT PHASE SENSITIVE DETECTORS

The testing of aircraft skins with the Phase Sensitive Detectors can be carried out using the manufacturers instructions providing,

(a) the instrument has been accepted under the test requirements in 4.5.7,
(b) the particular material and combination of specimens has been tested to prove the sensitivity of the method and the necessary graphs have been evolved,
(c) the sensitivity of the method matches the sensitivity required by the stress engineers for the area under test,
(d) due care is taken to observe and investigate odd results.

Fig.9 Lift-off characteristics of a good instrument

APPENDIX 5.1

SUBJECT INDEX

SUBJECT INDEX

Acceptance
- criteria (1.4) p.58

Acoustic emission (2.2) p.119; (3.7) p.389
- amplitude (3.7) p.391
- application (2.2) p.120
- burst (2.2) p.120
- continuous (3.7) p.390
- correlation, extent of cracking (3.7) p.416
- correlation of A.E. and ductility of material (2.2) p.120
- correlation with size of crack and crack growth rate (3.7) p.436
- count (3.7) p.391
- definition (3.7) p.389
- differ from other NDI technique (3.7) p.389
- dislocation (3.7) p.389
- electrical disturbances (3.7) p.440
- emission source location (2.2) p.120
- extraneous noise (3.7) p.428, p.440
- in weld (3.7) p.413
- Kaiser effect (2.2) p.120; (3.7) p.390
- precursor of plane strain instability (3.7) p.424
- rate (3.7) p.391
- system (3.7) p.408
- theoretical and experimental limitations (3.7) p.435
- white noise (3.7) p.440

Acoustical and ultrasonical (3.6) p.333
- acoustic impedance (2.2) p.126
- coin tapping (2.2) p.114
- methods (2.2) p.113

Adhesives, type of (4.3) p.532

Austenite
- residual, x ray diffraction (3.4) p.273

Beta-ray
- backscatter method (for thickness of coatings measurements) (2.2) p.104

Blister (1.4) p.68

Bond
- bonding spew (4.5) p.605
- disbond, corrosion (4.5) p.595
- Fokker, tester (2.2) p.118; (4.3) p.555; (4.4) p.587
- harmonic tester (4.3) p.563
- strength in composites (4.4) p.581

Bonded structures
- acceptance criteria (4.3) p.571
- flaw in (4.3) p.540
- inspection methods (4.3) p.545; (3.6) p.345
- inspection processes during manufacturing (4.3) p.545
- metal to metal (4.3) p.531
- sandwich (4.3) p.531

Bubble air (1.4) p.68

Burned (1.4) p.68

Burst (1.4) p.62, p.64

Calibration blocks (1.4) p.70

Carbon (1.4) p.62

Carburizing (4.1) p.479

Castings (1.4) p.62

Ceramic (1.4) p.62

Characterization
- of materials (1.4) p.58
- of materials defect (1.4) p.59

Chip (1.4) p.69

Cleavage (1.2) p.14

Cold shuts (1.4) p.60, p.62

Composite (1.4) p.63; (4.4) p.581
- available NDI technique (4.4) p.583
- defects common to (1.4) p.68; (4.4) p.582
- interface (4.4) p.584
- laminate (4.4) p.583
- observed defects in (4.4) p.581
- product quality in (4.4) p.581
- surface flaws (4.4) p.582
- testing of structures, liquid crystal (3.8) p.452

Compton scattering (3.5) p.300

Conductivity (3.8) p.452

Contaminants, corroded area (4.5) p.596

Contamination, Fokker-VFW tester (2.2) p.127

Contrast (3.3) p.250
- radiographic and thickness sensitivity in gammagraphy (3.5) p.303

Core (1.4) p.67
- honeycomb (4.3) p.532, p.535

Corona discharge (4.4) p.589

Correlation (2.1) p.85

Corrosion (1.4) p.14; (4.5) p.595
- concealed area (4.5) p.595
- degeneration, electrolyte (4.5) p.595
- detection by E.C. (3.2) p.217; (4.5) p.597
- detection in sandwich structure (4.3) p.552
- multiple echo with, wall thickness (3.6) p.333
- NDI, review methods (4.5) p.596
- paint films (4.5) p.596
- penetrant testing (4.5) p.596
- pimples (4.5) p.595
- products (4.5) p.596, p.605
- radiographic detection (3.3) p.258; (4.5) p.604

S.F. technique (3.6) p.334, p.338
start points (4.5) p.595
stress (3.7) p.389
stress cracking (3.7) p.405
visual examination (4.5) p.595

Crack (2.1) p.86; (3.3) p.256
arrest element (1.2) p.13
coalescence (1.2) p.14
cold (4.2) p.521
correlation acoustic emission extent of (3.7) p.416
crater (1.4) p.67; (4.2) p.521
critical equilibrium state (1.2) p.16
critical size (3.7) p.389; (1.2) p.13
delayed weld (3.7) p.412
detection by E.C. (3.2) p.189
embedded flat elliptical (1.2) p.14
embrittlement (1.4) p.61
fatigue (1.4) p.61
fatigue growth rate (3.7) p.395
grinding (1.4) p.61, p.67
growth rate (1.2) p.17
heat treating (1.4) p.61
in composites (1.4) p.69; (4.4) p.582
in non metallic (1.4) p.62
in parent metal (1.4) p.62
instability (1.2) p.14; (3.7) p.389
in welding (1.4) p.62
micro (1.4) p.67; (3.7) p.396
minimum detectable by A.C. (3.2) p.200
nucleation subcritical (1.2) p.13
opening (3.3) p.256
potential (1.4) p.67
shrinkage (1.4) p.67; (4.2) p.521
size and growth rate acoustic emission (3.7) p.392
sporadic growth (3.7) p.396
stopper (1.3) p.32
stress (1.4) p.67
stress corrosion (3.7) p.405, p.406, (4.1) p.474
subcritical growth (3.7) p.389
surface (1.4) p.62, p.69
thermal (1.4) p.62
x-ray detection (3.3) p.256

Crazing (1.4) p.69

Creep (3.7) p.396

Cupping (1.4) p.61

Curing process (4.3) p.536

Cyaniding (4.1) p.480

Damage
during service life (1.1) p.3
initial (1.2) p.18
tolerant structures (1.1) p.3, (1.2) p.13

Decarburizing (4.1) p.480

Defects (1.1) p.4, (1.4) p.59, p.69
design requirements (1.4) p.59
discontinuities incorrect diagnoses (1.3) p.30
in castings (3.6) p.341
in forgings (3.6) p.342
inhomogeneity (2.1) p.86
initial determination (1.1) p.6
in wrought material (3.6) p.343
limit between flaw and (1.4) p.69
material requirement (1.4) p.60
observed in composites (4.4) p.581
quantitative detection by E.C. (3.2) p.202

Degradation (1.4) p.57; (2.1) p.86

Delamination (1.4) p.62, p.63, p.69

Delta ultrasonic method (1.1) p.5

Demagnetization (3.1) p.162

Design
detail (1.3) p.30
fracture safe (1.2) p.13

Die Mark (1.4) p.61

Diffractometer, method (4.1) p.490

Dry spot (1.4) p.69

Dynamic condenser
kelvin method (2.2) p.127

Eddy current (3.2) p.183; (4.5) p.597
accessibility (3.2) p.199
airframe holes inspection (3.2) p.208
conductivity (3.2) p.189
corrosion detection (3.2) p.217, (4.5) p.595
drift (4.5) p.608
edge effect (3.2) p.191
effect of permeability magnetic (3.2) p.189
equipment (3.2) p.192
impedance (3.2) p.184
in field (3.2) p.204
lift-off (3.2) p.191, (4.5) p.608
penetration (3.2) p.184
phase sensitive detection (4.5) p.596
probes (3.2) p.194
probe coil design (2.2) p.126
sensitivity of (3.2) p.200; (4.5) p.608
signascope instrument (2.2) p.124
surface preparation (3.2) p.199
wheels (3.2) p.212

Eddy sonic techniques (2.2) p.119, (4.3) p.561; (4.4) p.587

Elastomer (1.4) p.62

Electrical methods (2.2) p.124

Electromagnetic methods (4.4) p.589

Electrolyte (4.5) p.595

Electronical components inspection (2.2) p.109

Embrittlement (3.7) p.389
crack (1.4) p.61
cryogenic temperature (3.7) p.392
hydrogen (3.7) p.405
strain-aging (3.7) p.410

Engineering
design (1.4) p.60
material (1.4) p.59
product assurance (1.4) p.60

Environment (1.1) p.6

Examination (1.4) p.58
x-ray (3.3) p.255

Extrusions (1.4) p.64, p.67

Fail safe philosophy (1.1) p.3, p.4, p.6; (1.2) p.13; (1.3) p.29

Fatigue
crack-growth rate (3.7) p.395
effect of mean stress (4.1) p.474
life (3.7) p.395
variable amplitude loading (1.2) p.18

Film, radiographic (2.2) p.102; (3.3) p.250; (4.1) p.489

Fish eye (1.4) p.69

Flake (1.4) p.61, p.62

Flaw (1.1) p.5; (1.2) p.18, (1.4) p.58, p.68
artificial (1.4) p.70
crack, like (3.7) p.391
detectability limits (1.1) p.5
embedded (1.2) p.14
environmentally induced, growth (3.7) p.394
finishing processing (1.4) p.62
forging (1.4) p.62
growth (1.4) p.70
in bonded structures (4.3) p.540
in field detection acoustic emission (3.7) p.433
inherent (1.4) p.62
initial (3.7) p.393
in service (1.4) p.67
in welding (4.2) p.511
limit between flaw and defect (1.4) p.69
maximum size allowable (1.2) p.13
presence of holography (3.9) p.461
primary processing (1.4) p.62
shrinkage (1.4) p.61
subcritical (3.7) p.394
surface in composities (4.4) p.582
volume length ratio (1.1) p.5

Fokker bond tester (2.2) p.118, (3.6) p.346, (4.3) p.555; (4.4) p.587

Foreign object
metallic (1.4) p.69
non metallic (1.4) p.69
radiographic examination (3.3) p.259

Fractography
electron (3.7) p.396

Fracture (1.4) p.69
analysis diagram (1.2) p.13
brittle (1.2) p.13
instability (1.2) p.23
mechanics (1.1) p.4, p.5, p.6, p.8
processes and flaw size (1.2) p.13
ratio analysis diagram (1.2) p.13
resistance (1.2) p.24
safe (1.2) p.13
safe design (1.2) p.13

Fusion
lack of (1.4) p.61, p.62; (4.2) p.520

Galling (1.4) p.67

Gammagraphy
application in civil aeronautics (3.5) p.308
definition (3.5) p.295
equipment (3.5) p.305
exposure times (3.5) p.304
films (3.5) p.303
in inspection of A/C tires (3.5) p.312
penetrameters (3.5) p.303
photography (3.5) p.301
safety rules (3.5) p.306
sharpness (3.5) p.301

Gammarays (2.2) p.102, (3.5) p.295
absorption (3.5) p.298
Compton scattering absorption (3.5) p.299
energy (3.5) p.296
properties (3.5) p.295
radiation quantity (3.5) p.297
secondary radiation (3.5) p.300
sources (2.2) p.102; (3.5) p.295
source activity decay (3.5) p.297
specific activity (3.5) p.296
specific radiation intensity (3.5) p.297

Gas
pocket (1.4) p.61, p.62
inclusions (3.6) p.342
porosity (1.4) p.61, p.62

Glass (1.4) p.62

Gouge (1.4) p.67

Grain
boundary interfaces (3.7) p.389
residual stress (4.1) p.501
size, x-ray (3.3) p.251

Graphite (1.4) p.62

Hardening
induction (4.1) p.479

Herring bone (4.2) p.520

Heat treatment (4.1) p.477

Holes
blow (4.2) p.520
bushed (1.3) p.30

Holography (2.2) p.107, (3.9) p.461, (4.3) p.566
acoustical (2.2) p.123
acoustic applications (2.2) p.123
as a NDI technique (3.9) p.461
behaviour of bodies surface (3.9) p.461
correlation methods (3.9) p.463
double exposure technique (2.2) p.107
interferometry (3.9) p.461; (4.3) p.566
laboratory investigation (3.9) p.463
loading technique (3.9) p.462
pulsed laser (3.9) p.462
real time technique (2.2) p.107
recording materials (3.9) p.464
structures (3.9) p.461
time average technique (2.2) p.107
ultrasonic (3.9) p.462

Honeycomb
comparison table among different types of NDI methods for (4.3) p.574
core (4.3) p.532, p.535
curing process (4.3) p.536
defects in (4.4) p.581
foaming adhesive (4.4) p.582
inspection method (4.3) p.547
lay-up (4.3) p.536
manufacturing (4.3) p.535
plate, holography (3.9) p.461
structures (2.2) p.119
water entrapment detection (4.3) p.553
x-ray examination of (3.3) p.259

Hot cracks (4.2) p.521

Hot tears (1.4) p.62

Hydrogen embrittlement (3.7) p.405

Impedance measurement (2.2) p.126

Inclusion (1.4) p.61
accidental (1.4) p.62
in welding (4.2) p.520
natural (1.4) p.62
non metallic (1.4) p.63
sand (1.4) p.62
slag (1.4) p.67
tungsten (1.4) p.67

Incomplete penetration (4.2) p.520

Infrared
cameras (2.2) p.111
radiation technique (2.2) p.108
spectrometry (3.4) p.291
scan heating techniques (4.4) p.589
temperature measuring device (2.2) p.110

Ingots (1.4) p.63

Inspection (1.4) p.57
on bonded structures (4.3) p.545
conventional NDI (3.7) p.395
design for (1.3) p.29
inspectability (2.1) p.86
gammagraphy inspection of A/C types (3.5) p.312
in process (1.4) p.76
internal (1.3) p.29
processed materials (1.4) p.76
visual (2.2) p.95
x-ray (3.3) p.255

Inspectors, NDI certified (2.1) p.87

Instability, plane strain (3.7) p.426

Interference
methods (2.2) p.106
pattern (2.2) p.105, p.107

Joints, brazed (3.6) p.345

Kaiser effect (2.2) p.120; (3.7) p.390

Knopp hardness, stress measuring method (4.1) p.502

Lack
of fill out (1.4) p.69
of fusion (4.2) p.520
of wetting (1.4) p.63

Lamination (1.4) p.61

Laps (1.4) p.61
forging (1.4) p.62, p.64

Laser, pulsed, holography (3.9) p.462

Level, trigger (3.7) p.428

Life cycle
management system (1.4) p.73

Liquid crystal (2.2) p.111, (3.8) p.451
application from solution (3.8) p.452
birefringence (3.8) p.451
experimental technique (3.8) p.452, p.453, p.454
film application (3.8) p.453
holography (3.9) p.462
optical rotation (3.8) p.451
scattering of white light (3.8) p.451
testing of electronic components (3.8) p.453

Magnetization techniques (3.1) p.152

Magnatest (3.2) p.192

Magnetic
inks (2.2) p.99
method sensitivity (2.2) p.99
methods of inspection (3.1) p.158
particles (2.2) p.98, (3.1) p.145
rubber inspection (3.1) p.162

Maintainability (1.4) p.74
inspection in service (1.4) p.76
planning for (1.3) p.31
planning for structural integrity (1.3) p.29

Material
ferromagnetic (3.1) p.145

metallurgical state evaluation, x-ray diff. (3.4) p.287
processed (1.4) p.75
raw (2.1) p.86
raw receiving (1.4) p.75

Microscope (2.2) p.95
electron (2.2) p.95; (3.4) p.291

Microscopy scanning (2.2) p.97

Misruns (1.4) p.64

Moire, technique (2.2) p.107

Monitoring (2.3) p.131

Multiple echo, method (3.6) p.333

NDI
as a tool (1.1) p.5, p.8
correlated to destructive (1.1) p.7
current methods (1.1) p.8
interpretation (1.1) p.7
methods (2.1) p.86; (4.4) p.590
of welding (4.2) p.509
philosophy (1.1) p.3
programme (1.1) p.6; (1.4) p.74
specifications (1.1) p.7
team work (1.1) p.7
test engineer (2.3) p.131
test inspector (2.3) p.132
test operator (2.3) p.132

Neutron radiography (3.8) p.454
applications and limitations (3.8) p.455
sources (2.2) p.103
scattering (3.4) p.290

Nitriding (4.1) p.480

Operational readness (1.4) p.57

Optics
fiber (2.2) p.99
viewing aids, corrosion (4.5) p.595
visual aids, in composites (4.4) p.584

Orange peel (1.4) p.69

Organization policy (2.3) p.131

Penetrants
adverse effect of low temperature (1.3) p.32
liquid (2.2) p.97, (3.1) p.171
liquid crystal (3.8) p.453
Q.C. test for (2.2) p.98
removal process (2.2) p.98, (3.1) p.172
sensitivity (2.2) p.99, (3.1) p.171
test corrosion (4.5) p.596
types of liquid (3.1) p.172

Penetration, incomplete (1.4) p.61, p.62

Personnel qualification (2.3) p.131
records (2.3) p.134

Piezoelectric material (4.4) p.586

Pile-ups dislocation (3.7) p.389

Pimple (1.4) p.69
corrosion (4.5) p.595

Pin hole (1.4) p.62, p.69

Pipe (1.4) p.61, p.67

Porosity (1.4) p.63, p.64, p.69; (2.1) p.86; (2.2) p.116

Preform (1.4) p.68

Pregel (1.4) p.69

Prepreg-yarn (1.4) p.68
butt joints (4.4) p.583
gaps (4.4) p.583
overlaps (4.4) p.583

Process
environment certification (2.3) p.131
in (1.4) p.74
order (2.3) p.131
special (2.3) p.131

Procurement document (1.4) p.59

Programs NDI (1.4) p.74

Proof test (3.7) p.391, p.393, p.395

Property
chemical (1.4) p.59
configuration (1.4) p.59
critical (1.4) p.59
mechanical (1.4) p.59
metallurgical (1.4) p.59
physical (1.4) p.59

Pulse-echo technique (2.2) p.114

Pulse transit time (3.6) p.335, p.338

Qualification
certificates (2.3) p.134
expiration (2.3) p.133
requalification (2.3) p.133
requirements (2.3) p.131
validity period (2.3) p.133

Quality
assurance (1.4) p.70
product (1.4) p.75
product in composites (4.4) p.581

Radiation
effects (3.3) p.235
energy (3.3) p.233
intensity (3.3) p.233
maximum permissible doses (3.3) p.234
monitoring (3.3) p.235
personal dose matters (3.3) p.234
protection (3.3) p.235
shielding (3.3) p.235

- sources (3.3) p.232
- tank (3.3) p.234
- units (3.3) p.233

Radiography (2.2) p.99
- in motion (4.3) p.567
- interference, corrosion (4.5) p.604
- limitation (4.5) p.606
- neutron (2.2) p.103; (3.8) p.454
- on aircraft structures (3.3) p.255
- radioscopy (4.3) p.566
- reference (1.4) p.70
- sensitivity of (2.2) p.102
- test corrosion (4.5) p.604
- x-rays (2.2) p.100; (3.3) p.232
- x-rays diffraction (2.2) p.93, p105; (3.4) p.271
- γ-rays (2.2) p 100; (3.5) p.295

Reliability (1.4) p.57, p.74

Resin
- pocket (1.4) p 69
- rich edge (1.4) p.69

Resistivity, electrical (4.4) p.589

Resonance measurements (2.2) p.117

Rolled products (1.4) p.64

Rolling - **cold** (1.4) p.63

Safe
- fail (1.2) p.13
- life (1.1) p.3, p.4, p.6

Safety (1.4) p.74
- flight (1.3) p.32

Sandwich
- acceptance criteria (4.3) p.571
- corrosion detection (4.3) p.552
- non metallic panels defect detection (4.3) p.559

Scale (1.4) p.61

Scratch (1.4) p.69

Sealing, compound (4.5) p.596

Seams (1.4) p.61

Segregation (1.4) p.61, p.62
- in composite (1.4) p.63
- macro (1.4) p.63

Short (1.4) p.69

Shrink (1.4) p.61
- cavities (1.4) p.64
- internal (1.4) p.62
- micro (1.4) p.64
- mark or sink (1.4) p.69

Skin
- double (4.5) p.598
- multiple (4.5) p.598

Slag (1.4) p.62
- inclusions (1.4) p.67

Slug (1.4) p.67

Sonic
- application limits of FBT (4.3) p.559
- coindascope (4.3) p.559
- Eddy, method (2.2) p.119; (4.3) p.561
- Fokker bond tester (4.3) p.556
- resonance principle (4.3) p.555
- resonator (4.3) p.559
- results interpretation using FBT (4.3) p.556
- stub-meter (4.3) p.559
- test, system (4.3) p.563

Spattering (4.2) p.521

Specifications (1.4) p.70, p.71
- acceptance (1.4) p.70
- company (1.4) p.70
- requirement (1.4) p.71
- standard (1.4) p.59, p.70

Speckle (3.9) p.463
- correlation fringes (3.9) p.463
- interferometry pattern (3.9) p.463

Spot heating
- residual stress (4.1) p.477

Standards (2.1) p.87; (1.4) p.71
- codes (2.1) p.87
- correlation (1.4) p.71
- of acceptance (1.1) p.6, p.7, p.8
- reference (1.1) p.7; (1.4) p.70
- testing (1.1) p.6

Strain
- aging (3.7) p.389
- peening (4.1) p.475
- measurement (2.2) p.106

Stress
- coining (1.4) p.63
- comprehensive residual (4.1) p.474, p.480, p.483
- distribution, residual (4.1) p.501
- effect on corrosion (4.1) p.474
- electroplating, residual (4.1) p.480
- factors affecting accuracy of residual measurement (4.1) p.499
- intensity (1.2) p.23
- intensity factor (1.2) p.16
- macro (4.1) p.473
- mean (4.1) p.474
- micro (1.4) p.67; (4.1) p.473, 499
- relieving heat treatment (4.1) p.473
- residual (1.4) p.67; (4.1) p.473, p.475
- residual calculation (4.1) p.475
- residual, x-ray diffraction (3.4) p.275
- tensile residual (4.1) p.474
- threshold, corrosion (4.1) p.474
- ware analysis (SWAT) (4.4) p.587

Stringer (1.4) p.62; (1.2) p.13

Structures
damage tolerant (1.2) p.13
fail safe (1.1) p.4
safe life (1.1) p.4

Surface
flaws in composites (4.4) p.583
roughness, holography (3.9) p.463
roughness, residual stress (4.1) p.499

System
final evaluation (1.4) p.75
management (1.4) p.74

Tape
narrow continuous (1.4) p.68

Team work (2.1) p.87

Tears
flash line (1.4) p.61
hot (1.4) p.61
machining (1.4) p.61, p.62

Temperature
cryogenic embrittlement (3.7) p.392
influence on measurement pulse echo (3.6) p.335
NIL ductility transition (1.2) p.13
residual stress (4.1) p.477
transition (3.7) p.392

Test
cryogenic test temp. (3.7) p.428
curved surface (2.2) p.126
destructive (2.1) p.86
direct (1.4) p.71
environmental (3.7) p.409
equipment qualification and procedures (1.4) p.72
for conductivity (3.2) p.218
indirect (1.4) p.71
NDI task (2.3) p.134
of electronic components, liquid crystal (3.8) p.453

Thermal
coatings (4.4) p.590
methods (4.3) p.566; (4.4) p.589
sensitive materials (2.2) p.113

Thermography, test corrosion (4.5) p.596

Thermovision (4.5) p.605

Thickness
material, and wave length ultra sonic (3.6) p.333
measurement (2.2) p.117
wall pulse-transit method (3.6) p.335, p.338
wall, resonance method (3.6) p.337

Tow (1.4) p.68

Through transmission technique (2.2) p.116; (4.4) p.589

Tubular members (1.3) p.31

Ultrasonic method (4.5) p.607
angle beam technique (3.6) p.340
calibration standards (echo pulse technique) (4.3) p.552
continuous surveillance (3.6) p.347
corrosion detection on sandwich structure (4.3) p.552
Fokker bond tester (2.2) p.118; (4.3) p.555; (4.4) p.587
holography (3.9) p.461
honeycomb structures inspection (4.3) p.547
immersion technique (2.2) p.116; (3.6) p.339, p.346
laminates inspection (3.6) p.345
metal to metal bond inspection (4.3) p.547
piezo electric transducer (2.2) p.116
pulse echo (2.2) p.114; (4.3) p.547; (4.4) p.586
pulse echo method, corrosion (4.5) p.596
pulse transit time (3.6) p.335, p.338
resonance method (3.6) p.337, p.339
spurious effect, corrosion (4.5) p.596
stress measuring method (4.1) p.501
terms used (3.6) p.355
test corrosion (4.5) p.596
transmission technique (2.2) p.116
water detection honeycomb structures (4.3) p.553

Unbonds
metal to metal (4.3) p.547, p.561, p.566

Undercuts (4.2) p.520

Upholstery (4.5) p.605

Variable measured (1.4) p.59

Void (1.4) p.61, p.62, p.68; (2.2) p.116

Volta, potential measurement (2.2) p.126

Wash (1.4) p.69

Water in corroded area (4.5) p.596

Wave
coherent (3.9) p.461
micro (4.4) p.589
shear, technique (4.4) p.586
sound holography (3.9) p.462

Weld
acoustic emission (3.7) p.413
cruciform (3.7) p.413
electric arc (3.6) p.343
electrobeam (3.6) p.345
delayed cracking (3.7) p.412
friction (3.6) p.345
laser (3.6) p.345
suitability of testing (3.6) p.343

Welding (4.2) p.509
defects (4.2) p.520
defects acceptability (4.2) p.522
gas-shielded (3.6) p.344
flash (3.6) p.344
in aeronautical industry (4.2) p.509
materials employed in aeronautical industry (4.2) p.511, p.514, p.516, p.517
oxi-acetylene (3.6) p.344
submerged arc (3.6) p.344
resistance pressure LF and HF (3.6) p.344
plasma (3.6) p.344
projection, spot, roll resistance (3.6) p.344
electro slag (3.6) p.345

Whiskers (1.4) p.63

Worm hole (1.4) p.69, p.520

Wrinkle (1.4) p.69

X-ray (2.2) p.99; (3.3) p.232
angle of emergence (3.3) p.241
beam configuration (3.3) p.238
diffraction (3.3) p.238
equipment (3.3) p.236
exposure techniques (3.3) p.241
focal spot size (3.3) p.238, p.246
high energy (3.3) p.243
low energy (3.3) p.243
material absorption (3.3) p.248
radiation filtration and intensification (3.3) p.248
radiation intensity (3.3) p.245
radiation quality (3.3) p.242
scattered radiation (3.3) p.244
stress measurement (4.1) p.484
voltage (3.3) p.238

APPENDIX 5.2

CROSS REFERENCE TABLE SHOWING WHICH NDI METHODS MAY BE USED FOR INVESTIGATING VARIOUS TYPES OF DEFECTS

CROSS REFERENCE TABLE SHOWING WHICH NDI METHODS MAY BE USED FOR INVESTIGATING VARIOUS TYPES OF DEFECTS

1. THIS TABLE IS INTENDED TO PROVIDE A SELF-EXPLANATORY GUIDANCE FOR PRACTICAL ORIENTATION FOR USE OF "NDI PRACTICES".

2. THIS TABLE SHOULD ALWAYS BE USED IN CONNECTION WITH THE SUBJECT INDEX FOR COMPLETENESS.

3. THE NUMBER IN THE TABLE GIVES REFERENCE TO CHAPTERS WHERE THE DEFECT TO BE INVESTIGATED AND/OR THE AVAILABLE METHODS ARE EXTENSIVELY EXPLAINED.

4. THE CROSSES IN THE MATRIX INDICATE THE METHODS AVAILABLE, WITHOUT ANY ATTEMPT TO RATE DIFFERENT METHODS.

5. IT IS POINTED OUT THAT SOME METHODS HAVE LIMITATIONS DEPENDING ON THE MATERIAL AND THE APPEARANCE OF THE DEFECT.

6. WHEN PARTS TO BE INSPECTED ARE NOT ACCESSIBLE ONLY RADIOGRAPHIC METHODS (X RAY, γ RAYS, NEUTRON) CAN BE USED.

APPENDIX 5.2

CROSS REFERENCE TABLE SHOWING WHICH N.D.I. METHODS MAY BE USED FOR INVESTIGATING VARIOUS TYPES OF DEFECTS

DEFECTS		TEST METHODS CHAPTERS	NORMAL METHODS										ADVANCED METHODS								
			Liquid penetrants	Magnetic particles	X-rays	Gamma rays	Pulse echo techniques	Through transmission techniques	Resonance measurements	Cointapping	Eddy currents	Impedance measurements	X-ray diffraction	Beta ray backscatter	Neutron radiography	Holography	Infrared radiation techniques	Liquid crystals	Eddy sonic	Acoustic emission	Volts potential measurements
			2.2; 3.1.2	2.2; 3.1.1	2.2; 3.3	2.2; 3.5	2.2;4.3;3.6	2.2;4.3;3.6	2.2	2.2; 4.3	2.2; 3.2	2.2	2.2; 3.4	2.2	2.2; 3.8	2.2; 3.9	2.2	2.2	2.2; 4.4	2.2; 3.7	2.2
General	In no accessibility parts				X	X															
	engine missing parts	3.5; 3.6			X	X															
	thickness measurement	3.6					X		X		X										
	in electronic components	3.8			X												X	X			
	in castings	1.4	X				X	X	X		X			X							
	fire damage	5.4									X										
	tube, internal organic residues	3.8													X						
Castings 1.4 3.6	gas porosity	1.4	X		X	X															
	cold shuts	1.4	X	X	X	X	X				X										
	voids	1.4			X	X	X														
	slag	1.4			X	X	X														
Forgings 1.4 3.6	laps	1.4									X										
	inclusions	1.4					X														
	burst	1.4			X	X	X	X													
	cracks	1.4	X	X			X														
Rolled products 1.4	seams	1.4	X	X			X														
	roll marks	1.4	X	X			X														
	inclusions	1.4	X	X			X														
	lamination	1.4	X	X			X														
	pipe	1.4	X	X			X														
Welds 1.4 3.6 4.2	lack of fusion	1.4; 4.2		X	X	X	X	X													
	incomplete penetration	1.4; 4.2		X	X	X	X	X													
	cracks	1.4; 4.2	X	X	X	X	X	X													
	slag	1.4; 4.2	X		X	X	X	X													
	porosity	1.4; 4.2	X		X	X	X	X													
Finished products 1.4	machining tears	1.4	X	X			X	X	X		X										
	heat treatment cracks	1.4	X	X			X	X			X	X									
	grinding cracks	1.4	X	X				X			X										
	embrittlement cracks	1.4	X	X				X			X										
	plating cracks	1.4	X	X	X						X				X						
Service 1.4	fatigue cracks	1.4	X	X	X		X	X	X		X	X								X	
	stress	1.2	X	X	X						X									X	
	corrosion	1.4;3.6;4.5			X		X	X			X	X									
Composite structures 3.6 4.3 4.4	core splice	4.3					X	X													
	composition, thickness	.6; 4.4							X												
	crushed core	4.3						X													
	delamination	1.4;3.6;4.4						X										X			
	density variations	4.3; 4.4				X															
	inclusions, cracks	1.4; 4.4			X														X		
	metal-to-metal unbond	4.3					X	X		X											
	skin-to-adhesive unbond	4.3					X	X		X											
	skin-to-core unbond	4.3						X													
	voids	1.4;4.3;4.4								X											
	water entrapment	4.3					X	X													X

APPENDIX 5.3

NON-DESTRUCTIVE INSPECTION PROCEDURES, USAF

(T.O. 1F-104A-365 4/5)

The following pages are reproduced directly
from the relevant technical manuals.

T.O. 1F-104A-36S-4

OPERATIONAL SUPPLEMENT

TECHNICAL MANUAL

NONDESTRUCTIVE INSPECTION PROCEDURES

USAF SERIES

F-104A, B, C, D
F, RF AND TF-104G (MAP)

AIRCRAFT

THIS PUBLICATION SUPPLEMENTS T.O. 1F-104A-36 DATED 17 APRIL 1970. Reference to this supplement will be made on the title page of the basic manual by personnel responsible for maintaining the publication in current status.

COMMANDERS ARE RESPONSIBLE FOR BRINGING THIS SUPPLEMENT TO THE ATTENTION OF ALL AFFECTED AF PERSONNEL.

PUBLISHED UNDER AUTHORITY OF THE SECRETARY OF THE AIR FORCE

10 JANUARY 1973

1. PURPOSE.

To add new procedures for inspection of the vertical stabilizer front and rear beam mounting pads.

2. INSTRUCTIONS.

a. In Section III, page 3-35, new paragraphs 3-105 through 3-110 are added as follows:

3-105. F-104 NDI PROCEDURE - Vertical Stabilizer Lower Beams.

3-106. General. Both the forward and rear beams of the vertical stabilizer are susceptible to stress corrosion cracking in the lower beam section, commonly referred to as the mounting pad section. See figure 1 (Sheet 1 of 6). This inspection procedure outlines ultrasonic and eddy current techniques to detect cracks without removal of the stabilizer from the aircraft, and without paint removal which is required when using the present T.O. 1F-104A-36 procedures.

3-107. Description of Defects. Refer to figure 1 (Sheet 2 of 6).

1. Cracks initiating from or extending into the four attaching fastener holes - Inspect using the eddy current bolt hole probe technique.

2. Cracks initiating from or extending into the four counterbore areas of the fastener holes – Inspect using the eddy current pencil probe technique.

3. Cracks extending in the forward-aft direction between the four fastener holes and large cracks extending from steps 1 and 2 – Inspect using the ultrasonic technique.

3–108. Equipment Materials Required.

1. Ultrasonic Requirements.

a. Detector-ultrasonic flaw, FSN 6635–018–5829.

b. Transducer-Type SFZ, 10 MHz, Part No. 57A2279, Automation Industries, Inc., or equivalent. FSN 6635–945–1220.

c. Calibration Block – 1-inch block of aluminum, see View A, figure 1 (Sheet 3 of 6) or aluminum shear wave test block. FSN 6635–018–5832.

d. Couplant-Light Grease.

2. Eddy Current Requirements.

a. Detector, ED–520 Magnaflux Corp or equivalent. FSN 6635–167–9826.

b. Probe – Bolt hole expandable 1 ⅞ – 11 16-inch. FSN 6635–018–5839, or equivalent.

c. Probe – Pencil. FSN 6635–409–8845, or equivalent.

d. Calibration Blocks – See Views A and B, figure 1 (Sheet 3 of 6).

3–109. Inspection Procedures: The order of inspection operation is recommended as follows:

1. Ultrasonic Inspection Procedure.

NOTE

Ultrasonic inspect both front and rear beams for large defects. No fastener removal is required except to confirm "suspect" crack indications.

a. Remove fillets to expose lower portions of both front and rear stabilizer beams.

b. Clean and remove rough or loose paint of areas coming in contact with the ultrasonic transducer. Area identified by "U" on figure 1 (Sheet 1 of 6).

c. Ultrasonic instrument calibration – Position the 10 MHz longitudinal wave transducer on the calibration block directing the sound beam through the one inch thickness. See View A, figure 1 (Sheet 3 of 6). Adjust the sweep length and sensitivity controls to display 10 back reflections on the cathode ray tube (CRT). See View A, figure 1 (Sheet 4 of 6).

d. Adjust the marker controls or use a grease pencil to show 6 inches of material thickness.

e. Apply couplant to the transducer face and place it on the area to be inspected. See View B, figure 1 (Sheet 4 of 6). Adjust the sensitivity control to obtain a 2 inch high signal at the 0.5 inch material thickness marker. This signal will be obtained by moving the transducer slightly until a maximum reflection is received from one of the two fastener holes on the opposite side of the mounting pad. See View B, figure 1 (Sheet 4 of 6), beam No. 1.

f. Scan all inspection areas as indicated on both right and left sides of the mounting pads. Note figure 1 (Sheet 5 of 6), which shows the areas to be scanned. Inspection results will be analyzed as follows:

(1) Defect signals less than 2 inches in amplitude should be disregarded unless there is a complete loss of back reflection from the opposite side of the mounting pad.

(2) Disregard defect signals outside the 6 inch marker position on the CRT.

(3) Disregard signals from the small diameter holes located on the aft edge of the rear beam mounting pad flange. These signals will appear at the 3 inch marker position. Note small diameter holes in View B, figure 1 (Sheet 4 of 6).

CAUTION

Scanning outside of indicated inspection areas will produce false indications. Also, occasional signals may result from fillet areas of base that may appear to be defects. Evaluate these carefully. Note fillet position in View B, figure 1 (Sheet 4 of 6).

(4) Confirm all defect indications by visual (10X), eddy current, or penetrant methods. Stabilizer may have to be removed if defect indications do not come to any exposed surfaces.

2. Eddy Current Inspections – If no defects have been confirmed as a result of the ultrasonic inspection, continue to inspect using eddy current techniques.

NOTE

Remove one attach fastener at a time and inspect for cracks using both the eddy current pencil and bolt hole probes. Confirm cracks by visual or penetrant inspections.

a. Calibrate the pencil probe according to the instructions contained in T.O. 33B2-9-1 using the flat eddy current test block shown in View B, figure 1 (Sheet 3 of 6). This block is an accessory of the ED-520 eddy current tester. Obtain at least a 50 microampere deflection from the 0.020-inch deep slot in the test block. Record equipment settings for ease in resetting equipment when pencil probe and bolt hole probe are used alternately for each hole and counterbore inspection.

b. Calibrate the 9/16-inch diameter bolt hole probe (used for front beam holes) according to instructions contained in T.O. 33B2-9-1 using the test block shown in View A, figure 1 (Sheet 3 of 6). An alternate and easier technique is to insert the probe in the 5/8-inch diameter test hole and press the tip of the probe away from the hole wall and note deflection of needle. Adjust lift-off control until there is no needle deflection when the tip of the probe is moved away from the hole wall. During this operation the needle is brought on scale with the balance control. Adjust sensitivity controls (both function control and screwdriver adjustment) until at least a 50 microampere deflection is obtained from the slot in the hole. Again, record equipment settings for ease in resetting between alternate inspections with the pencil probe.

The 5/8 and 11/16-inch diameter holes in the test block are used if probes other than the 9/16-inch diameter probe is used for the rear beam inspections. Record equipment settings if more than one eddy current bolt hole probe is used.

c. Remove one of the four fasteners from the front beam mounting pad and clean all foreign material from the hole and counterbore. Do not remove paint.

d. Using the pencil probe, scan the fillet radius and all surface areas inside the counterbore. Scan all accessible radii and internal surfaces on exposed areas of the mounting pads. (See View A, figure 1 (Sheet 6 of 6).)

CAUTION

Scanning near sharp outside radii or steel such as fasteners will produce edge effect, resulting in sharp downscale deflections resembling defect indications.

e. Remove pencil probe and replace with 9/16-inch diameter bolt hole probe. Position controls to previously recorded positions. Check operation using test standard hole.

f. Adjust the collar on the probe to inspect for defects at the edge of the hole at the counterbore. Rotate in a 360° circle and note any sharp downscale deflections. (See View B, figure 1 (Sheet 6 of 6).)

g. Continue to inspect the entire length of the fastener hole in 0.100-inch increments.

h. Confirm indications detected using eddy current inspections by visual (10x) or penetrant inspections.

i. Reinstall the fastener after proper corrosion protection and remove second fastener. Inspect with bolt hole probe and pencil probe (counterbore area) after proper cleaning.

j. Complete inspection of front beam inspection by removing and inspecting one fastener at a time.

k. Repeat inspection of rear beam holes, counterbores, and adjacent areas similar to the front beam inspection.

l. Record and report all cracks for proper disposition.

b. Figure 1 (Sheets 1 through 6) of this supplement is figure 3-19 (Sheets 1 through 6) of the basic manual.

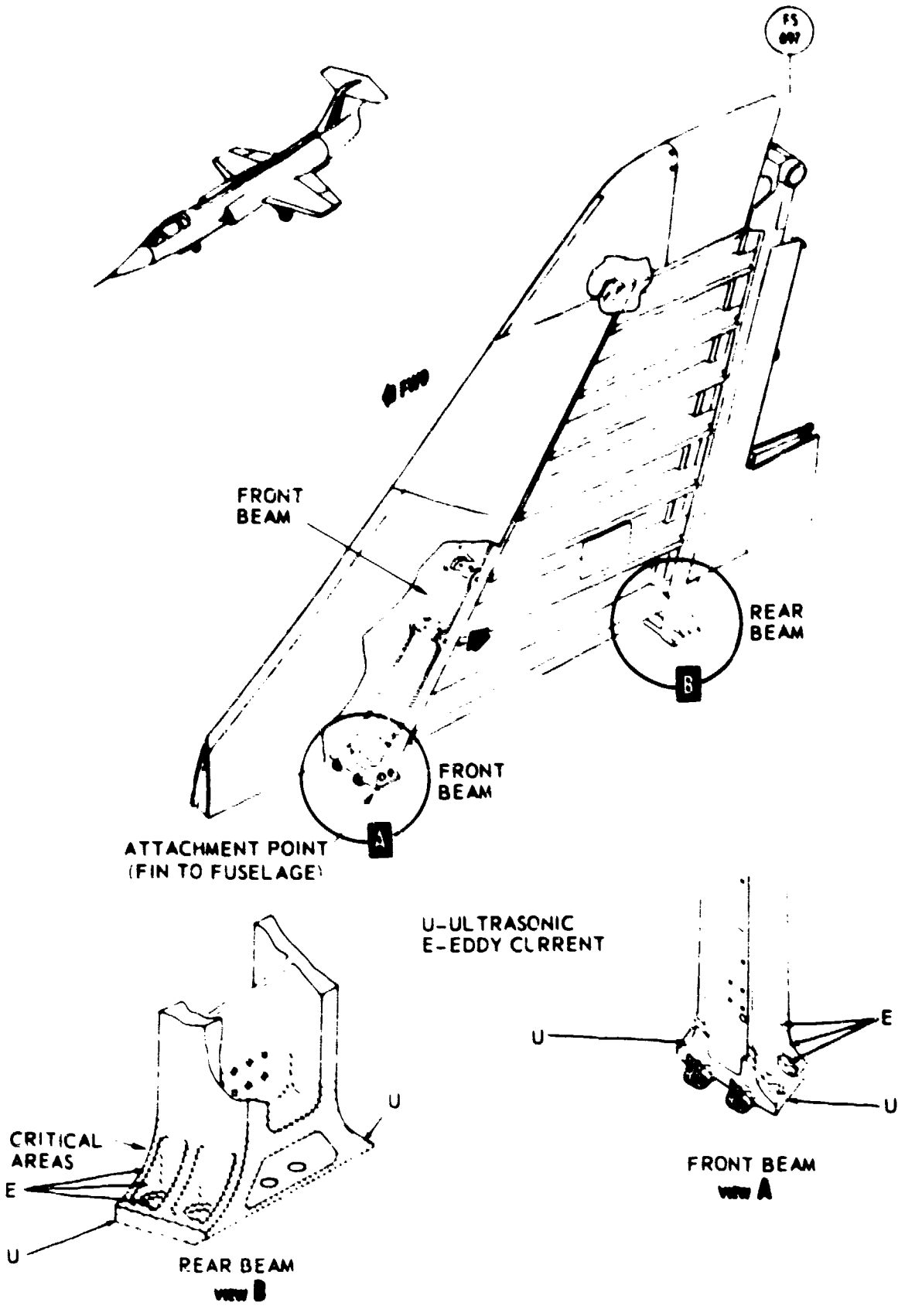

Figure 1. Forward and Rear Beams (Sheet 1 of 6)

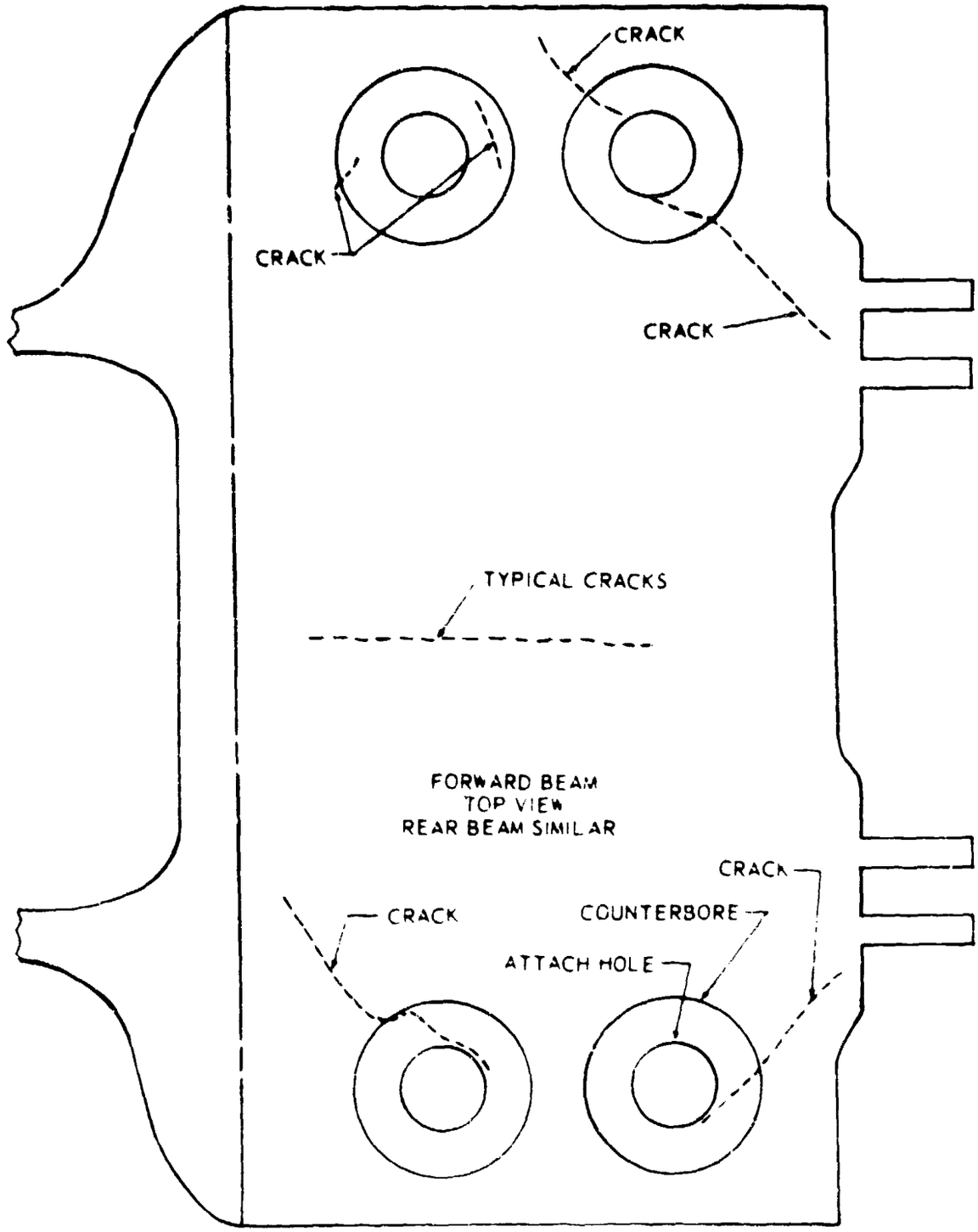

Figure 1. Forward and Rear Beams (Sheet 2 of 6)

STANDARD ULTRASONIC & EDDY CURRENT BOLT HOLE

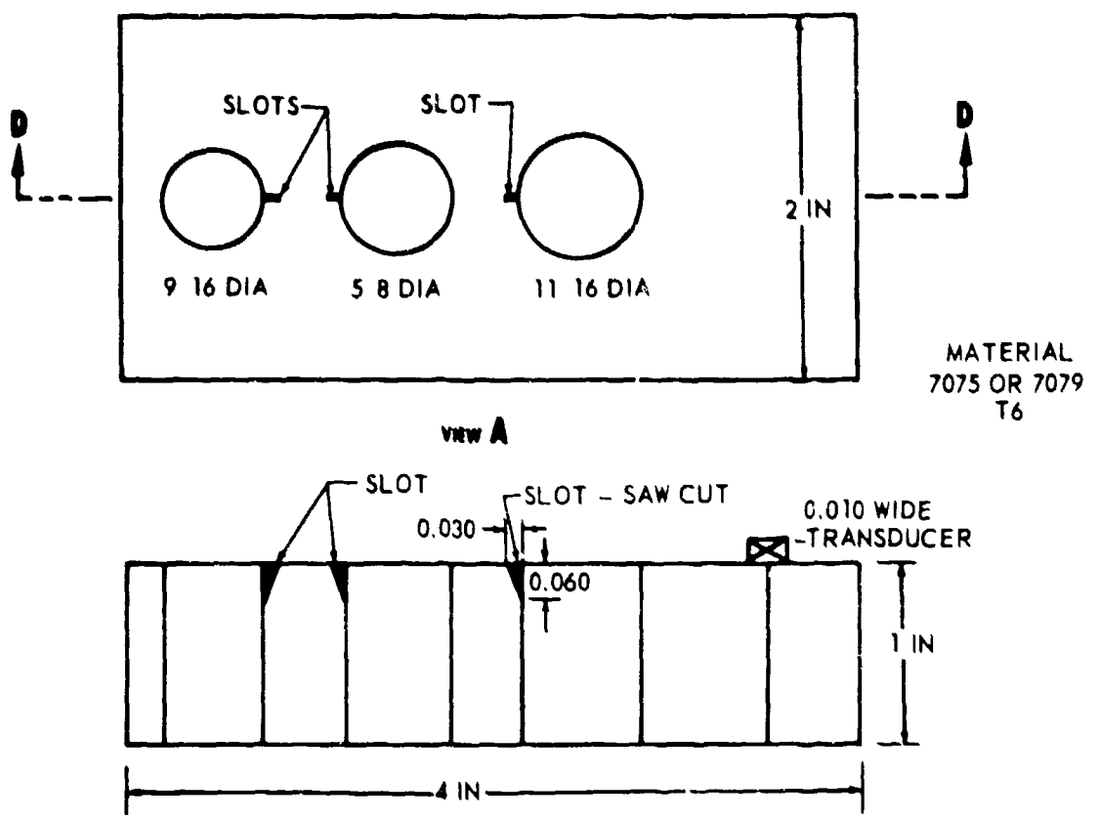

TEST BLOCK-EDDY CURRENT PENCIL

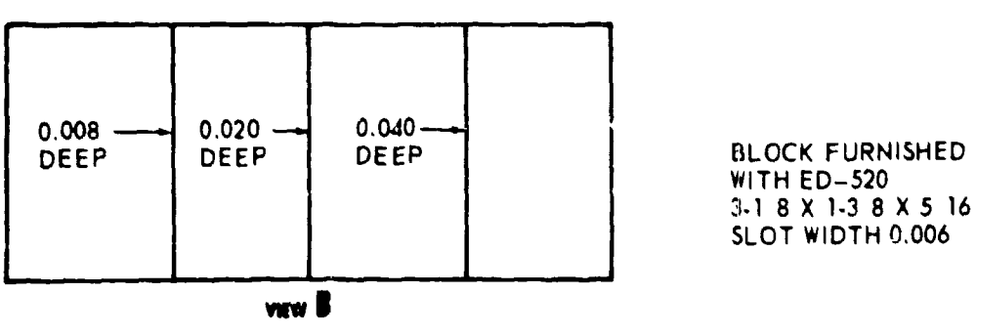

Figure 1. Forward and Rear Beams (Sheet 3 of 6)

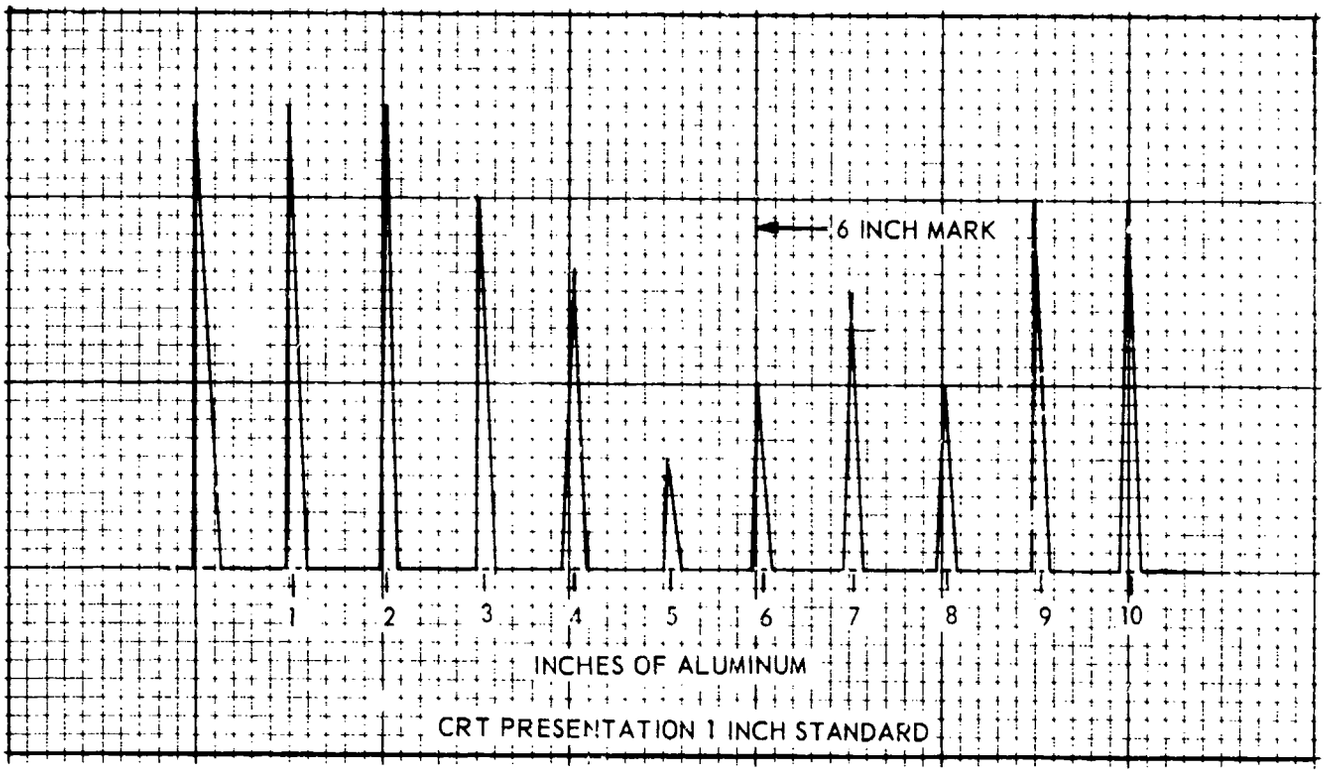

VIEW A

ULTRASONIC CALIBRATION

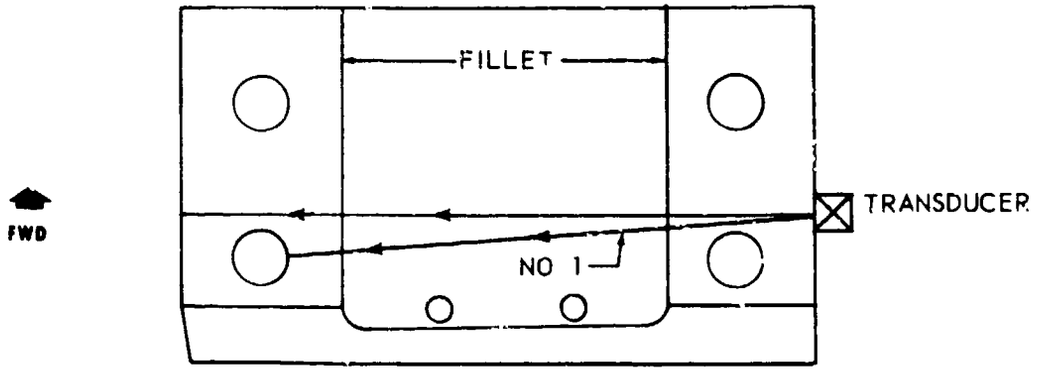

VIEW B

REAR BEAM (FORWARD BEAM SIMILAR)
LOOKING AT BOTTOM

Figure 1. Forward and Rear Beams (Sheet 4 of 6)

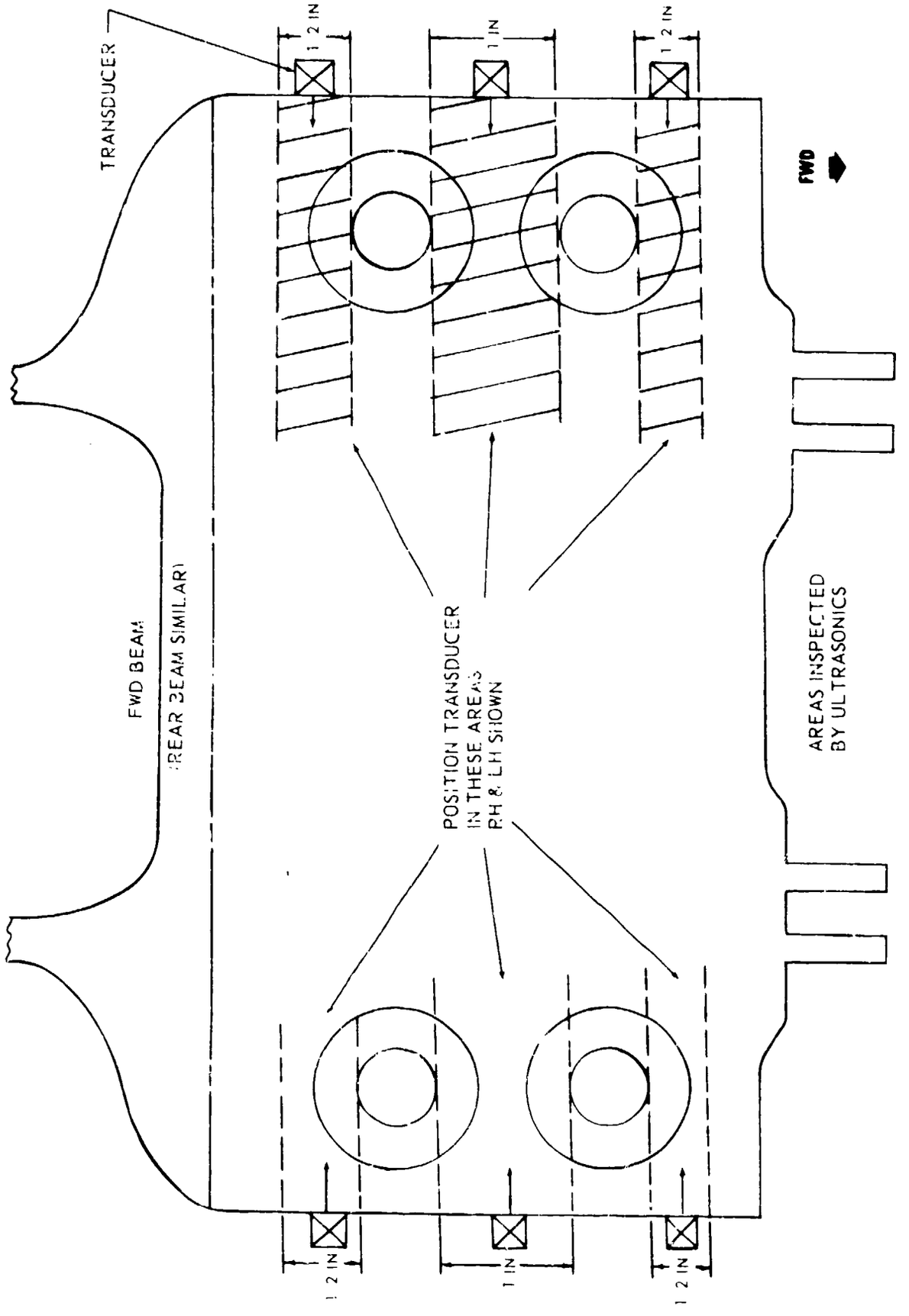

Figure 1. Forward and Rear Beams (Sheet 5 of 6)

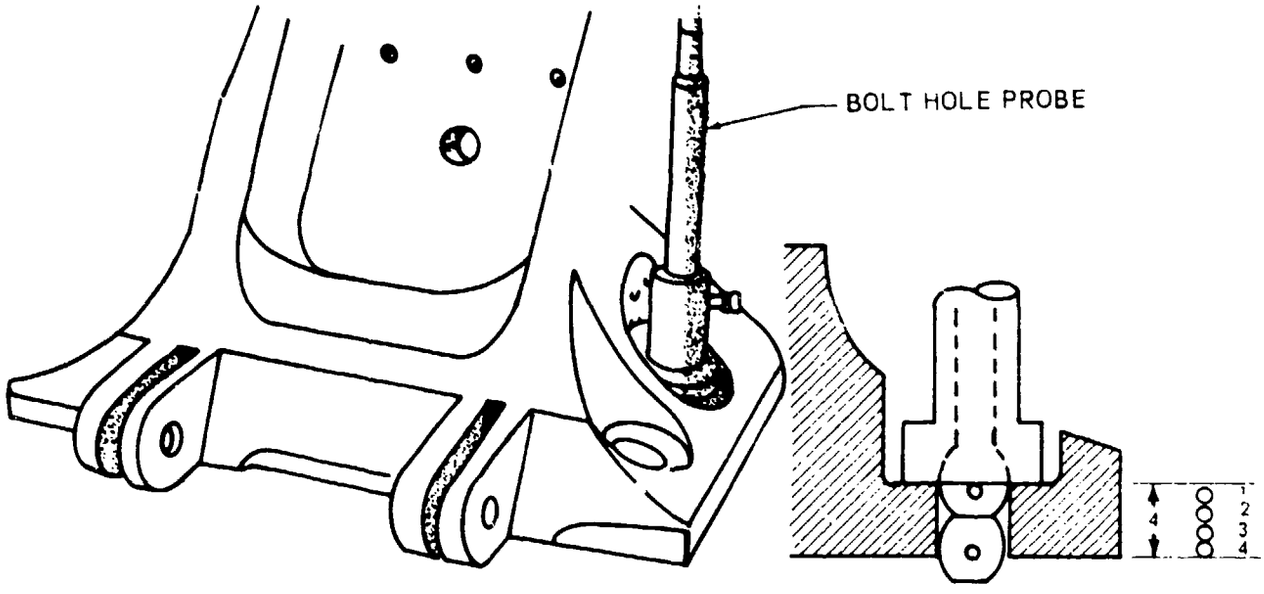

VIEW B

ATTACH HOLE INSPECTION – FWD BEAM
(REAR BEAM SIMILAR)

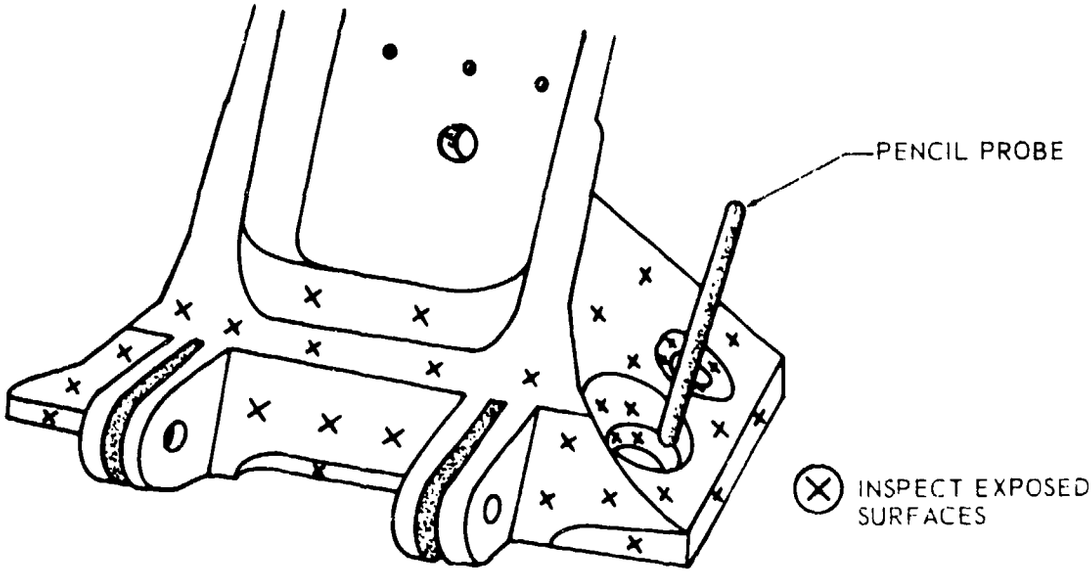

VIEW A

PENCIL PROBE INSPECTION – FWD BEAM
(REAR BEAM SIMILAR)

Figure 1. Forward and Rear Beams (Sheet 6 of 6)

THE END

T.O. 1F-104A-36S-5

OPERATIONAL SUPPLEMENT

TECHNICAL MANUAL

NONDESTRUCTIVE INSPECTION PROCEDURES

USAF SERIES

F-104A, B, C, D

F, RF, AND TF-104G (MAP)

AIRCRAFT

THIS PUBLICATION SUPPLEMENTS T.O. 1F-104A-36. Reference to this supplement will be made on the title page of the basic manual by personnel responsible for maintaining the publication in current status.

COMMANDERS ARE RESPONSIBLE FOR BRINGING THIS SUPPLEMENT TO THE ATTENTION OF ALL AFFECTED AF PERSONNEL.

PUBLISHED UNDER AUTHORITY OF THE SECRETARY OF THE AIR FORCE

8 MARCH 1973

1. PURPOSE.

To add a new eddy current procedure for the knob installed on the tip tank and to improve the existing magnetic particle inspection procedure.

2. INSTRUCTIONS.

a. The existing TIPTANK LATCH KNOB procedure, paragraphs 2-122 through 2-128 are replaced as follows:

2-122. TIPTANK LATCH KNOB, Part No. 704825, Models F-104A, B, C, D and Part No. 776640-1, Models F/RF/TF-104G.

2-123. DESCRIPTION. (See figure 2-26.) The tiptank latch knob is attached to the tip tank as indicated in the figure. The latch knob is made from 4340 steel. Two inspection procedures are provided - - An eddy current procedure for the installed knob, and a magnetic particle inspection for the knob removed from the tip tank.

2-124. DEFECTS. In-service cracks have been developing at the 6 and 12 o'clock positions of the knob. Complete failure of the knob at the intersection of the 0.500-inch diameter shank and the knob has occurred on a number of occasions.

2-125. PRIMARY NDI PROCEDURE FOR KNOB INSTALLED IN TIPTANK - EDDY CURRENT.

1. NDI equipment.

   a. Crack detector, Magnaflux ED-520, or equivalent, Stock No. 6635-167-9826.

   b. Probe, specially designed Magnaflux probe, Part No. 209199. Magnaflux Corp., 7300 W. Lawrence Ave., Chicago, Illinois 60656. Note design of probe in figure 2-26.

   c. Test standard, tiptank knob with circumferential slot as shown in figure 2-26.

2. Preparation of airplane. Remove tiptank in accordance with applicable technical procedures.

3. Preparation of part. Clean tip of knob as necessary to permit good contact between part and probe.

4. Instrument calibration.

   a. Connect probe to ED-520 and check battery condition.

   b. Slide probe onto tip of test standard. Orient coil in probe away from the slotted portion of the standard.

   c. Rotate function switch to "LO" position. Starting at the zero position of the "LIFT-OFF/FREQ" control rotate dial until the needle changes direction, e.g., changes from up-scale direction to downscale. During this operation the needle is kept on scale by using the "BALANCE" control.

   d. To correct for lift-off (minimum movement of needle due to coil-test piece distance variations) wiggle the probe slightly while adjusting the "LIFT-OFF/FREQ" control. Lift-off correction is extremely important and must be done very carefully.

   e. Rotate probe slowly around the tip of the knob and note the deflection from the test standard slot. Adjust the "SENSITIVITY INC" control for a maximum of 50 ± scale units. (Refer to figure 2-26.)

5. Inspection. (Inspect with knob in vertical position, see figure 2-26.)

   a. Slide probe onto knob taking care to seat it properly.

   b. Wiggle probe to minimize lift-off. This operation is required for each knob inspected because of physical differences between knobs.

   c. Slowly rotate probe 360° and note deflections. Small needle movements of 20 or 30 units may occur throughout the rotation due to surface variations on the knob or probe wobble. Upscale deflections in excess of 50 units shall be interpretated as "suspected" crack indications. Crack indications will appear at the 6 or 12 o'clock knob positions.

   d. To confirm defect indications remove tip tank knob in accordance with technical manuals and inspect by magnetic particle inspection method. See below.

2-126. PRIMARY PROCEDURE FOR TIP TANK LATCH KNOB REMOVED FROM TIP TANK AND CONFIRMATION OF EDDY CURRENT INDICATIONS.

1. NDI equipment.

   a. Magnetic inspection unit, portable hand probe DA 200, Stock No. 6635-022-0372, or equivalent.

   b. Magnetic particle solution, fluorescent, Stock No. 6850-841-1347, or equivalent.

   c. Light unit, test, portable (black light), Stock No. 6635-611-5617, or equivalent.

   d. Indicator, field, magnetic variation, 0-6 Oersted range, Stock No. 6635-391-0058, or equivalent.

   e. (Alternate magnetic inspection unit). Stationary type MB-3, Stock No. 6635-055-6596, or equivalent.

2. Preparation of airplane. Remove tip tank from aircraft and remove knob in accordance with technical manuals.

3. Preparation of part. Remove any paint, corrosion, grease, or dry film lubricant from the entire tip tank latch knob.

4. Inspection procedure.

   a. Portable hand probe.

      (1) Position Pulse 'AC switch to AC.

      (2) Position sensitivity control to maximum sensitivity.

      (3) Place tip tank latch knob between probe legs as indicated by figure 2-26.

      (4) Press test switch and spray magnetic particle solution on part. Keep test switch pressed for at least 5 seconds after application of solution.

      (5) In a darkened area using the black light, inspect in the critical areas for cracks. Service cracks have occurred at either the 6 or 12 o'clock positions at the intersection of the 0.500-inch diameter shank and the knob. Also, inspect for deep or sharp grooves in this area. Cracks or grooves are not acceptable in the knob area.

      (6) Evaluate defect indications by examining the part with optical devices. Mark and report indicated defects.

      (7) Demagnetize the part after inspection.

   b. Stationary or portable magnetic particle systems, 7500-10,000 ampere turn capability.

      (1) Position the knob in the magnetizing coil as noted in figure 2-26.

      (2) Apply current for one second while spraying the part with magnetic particle solution.

      (3) Observe for defect indications and evaluate suspect indications similar to that described for the portable hand probe technique.

2-127. SYSTEMS SECURING. Clean areas inspected, restore finishes, recoat the knob with dry film lubricant per MIL-L-46010, Stock No. 9150-142-9309, and reinstall, in accordance with applicable technical orders.

b. Figure 1 of this supplement is figure 2-26 of the basic manual.

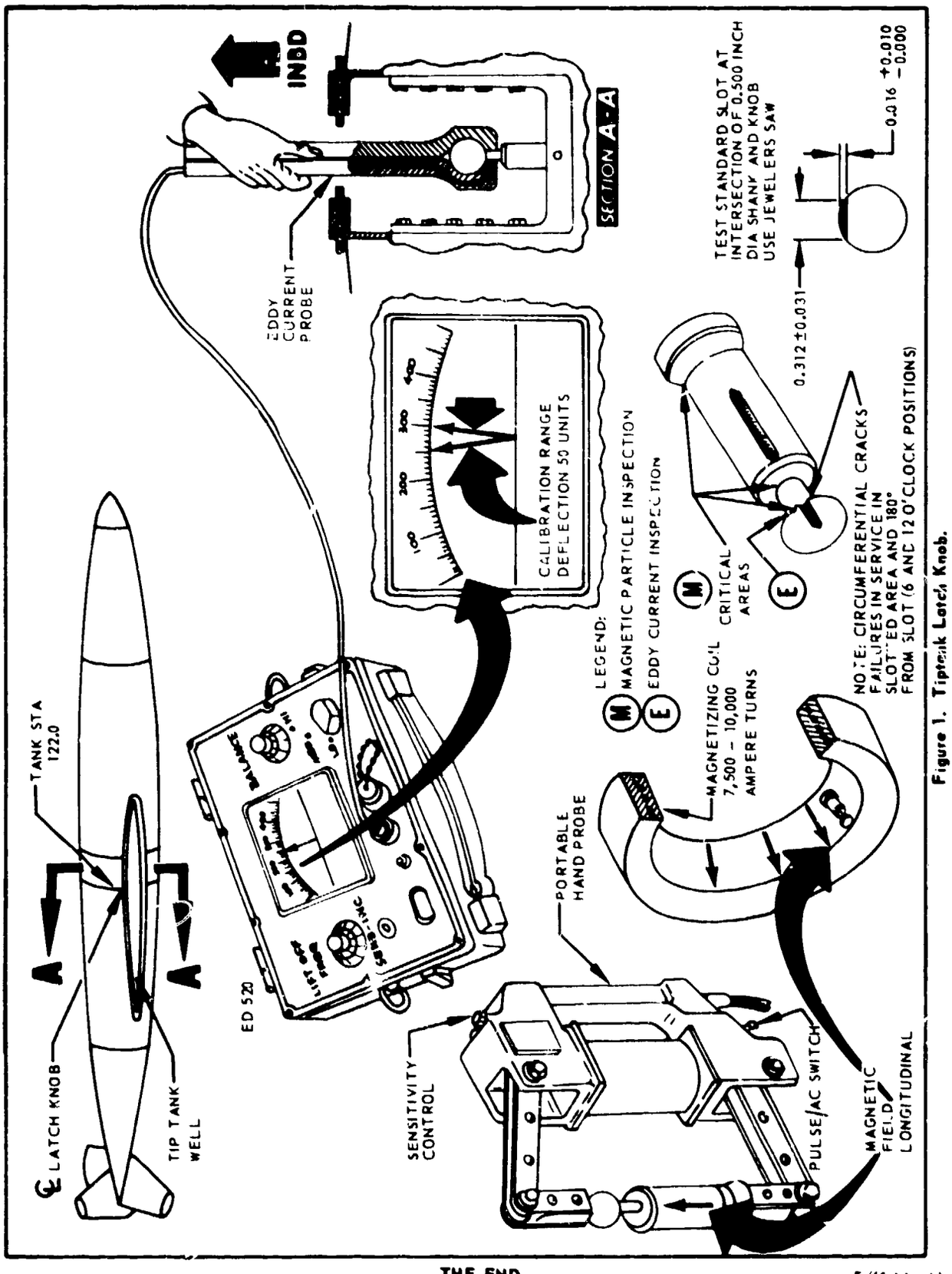

Figure 1. Tiptank Latch Knob.

THE END

APPENDIX 5.4

NON-DESTRUCTIVE TEST MANUAL

Inspection Procedures for Boeing Jet Transports
Boeing Document D6-7170

(T.O. 1F-104A-365-4/5)

The following pages are reproduced directly
from the relevant test manuals.

EFFECTIVITY
MODEL: ALL 707 AND 720 SERVICE BULLETIN REFERENCE: 2330

Commercial Jet

NONDESTRUCTIVE TEST MANUAL

PART 4 - ULTRASONIC

HORIZONTAL STABILIZER

1. Purpose

   A. Service experience shows that cracks can occur in top and bottom lugs of horizontal stabilizer spar terminal fittings, P/N 65-3409-5 or -6. The cracks originate at the bolthole and propagate along the flash line. This longitudinal wave technique is recommended for detecting these cracks.

      NOTE: Cracks cannot be distinguished from inclusions with this procedure.

2. Equipment

   A. Any ultrasonic equipment which satisfies the requirements of recommended procedure may be used.

      (1) Transducers

         (a) 5-mc/s, 1/4-inch diameter crystal, mounted in 3/8-inch diameter case

      (2) Crack comparison standard, fabricated as shown in detail I

      (3) Transducer positioning fixtures, fabricated as shown in details II and III

      (4) Couplant. Light oil or grease is satisfactory

3. Preparation for Inspection

   A. Clean surface of terminal fitting thoroughly to ensure good contact between transducer positioner and fitting.

   B. If painted surface is rough, smooth lightly with abrasive cloth.

   C. Coat inspection area with couplant.

Horizontal Stabilizer Outboard Front Spar Terminal Fitting
Figure 1 (Sheet 1)

4. Instrument Calibration

A. Calibration for Inspecting Inboard Side of Bolt Hole

(1) Place transducer in positioning fixture. Place fixture on comparison standard so as to direct sound beam into artificial crack area. (See detail IV.)

(2) Move fixture forward and aft to obtain maximum signal response from crack.

(3) Identify position of maximum response on oscilloscope. Hold transducer in this position.

(4) Adjust sensitivity of instrument until vertical response indication on oscilloscope is approximately 70 percent of saturation.

(5) Note position of transducer on standard at which maximum response is obtained.

B. Calibration for Inspecting Outboard Side of Bolt Hole

(1) After inspecting inboard side of bolt hole, calibrate instrument for inspecting outboard side using same procedure used for calibrating inboard side.

5. Inspection Procedure

A. Inspection of Inboard Side of Bolt Hole

(1) Place transducer in positioning fixture. Place positioning fixture on lug so as to direct sound beam toward inspection area. (See detail IV.)

(2) Scan area by moving fixture in a forward and aft pattern to a distance of approximately 1/2-inch on each side of maximum scan position established in calibration procedure.

(3) If a crack indication is detected, a response will appear on the oscilloscope similar to the response received from the simulated crack in the comparison standard. Lateral movement of crack response occurs as transducer is moved back and forth on the lug.

(4) Compare indications with those of standard for determination of cracks. Any indication up to or greater than that obtained from standard is positive indication of crack.

Horizontal Stabilizer Outboard Front Spar Terminal Fitting
Figure 1 (Sheet 2)

(5) Verify crack indications by removing pin, cleaning area, and checking by visula or other means.

B. Inspection of Outboard Side of Bolt Hole

(1) After calibrating instrument, repeat procedure on outboard side of bolt hole.

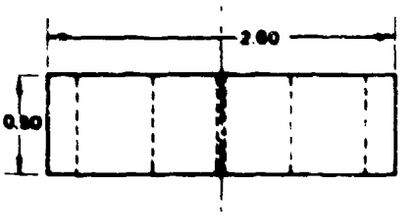

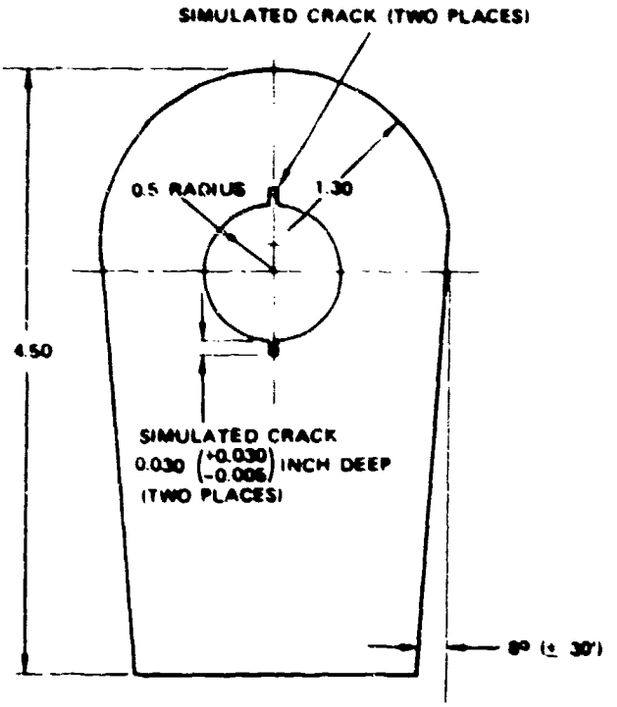

NOTE
1. ALL DIMENSIONS IN INCHES
2. FABRICATE FROM ALUMINUM
3. TOLERANCE ± 0.030 ON ALL DIMENSIONS EXCEPT AS NOTED

COMPARISON STANDARD
DETAIL I

Horizontal Stabilizer Outboard Front Spar Terminal Fitting
Figure 1 (Sheet 3)

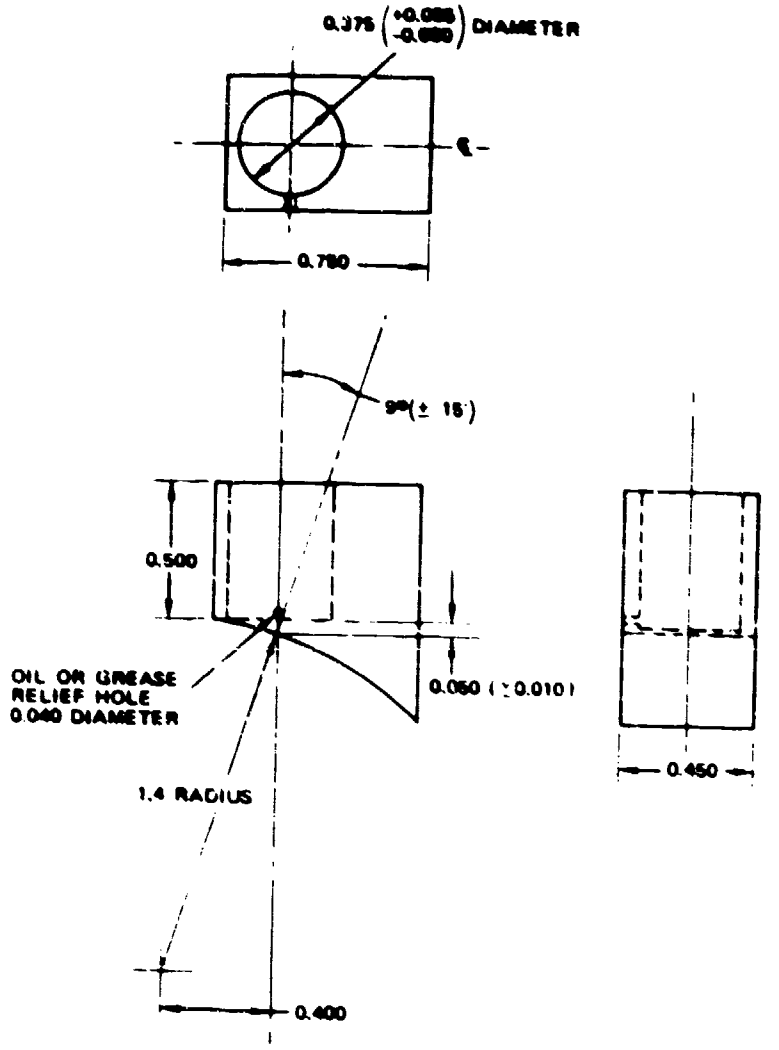

NOTE 1 MAKE FROM LUCITE

2 ALL DIMENSIONS IN INCHES

3 ± 0.030 TOLERANCE ON ALL DIMENSIONS EXCEPT AS NOTED

TRANSDUCER POSITIONING FIXTURE
DETAIL II

Horizontal Stabilizer Outboard Front Spar Terminal Fitting
Figure 1 (Sheet 4)

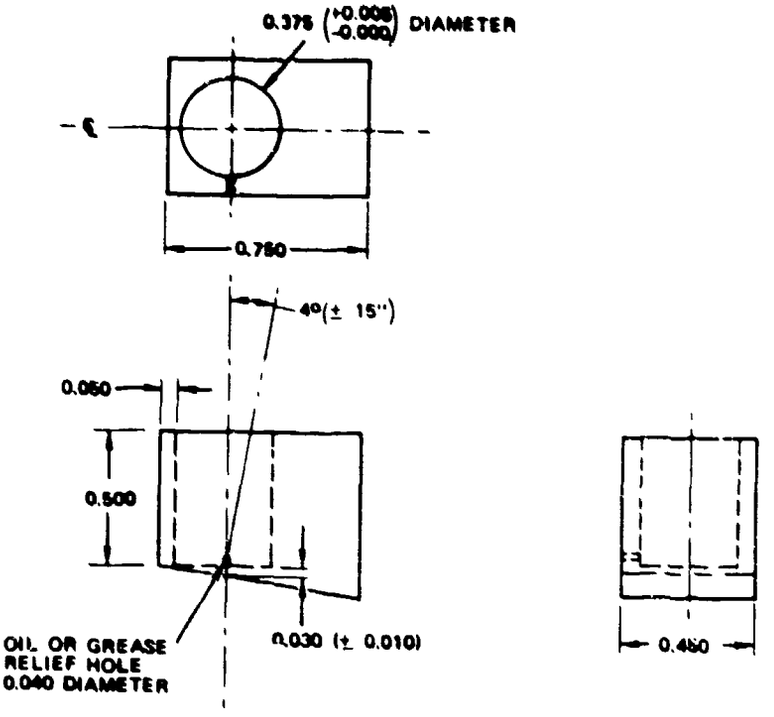

TRANSDUCER POSITIONING FIXTURE

DETAIL III

Horizontal Stabilizer Outboard Front Spar Terminal Fitting
Figure 1 (Sheet 5)

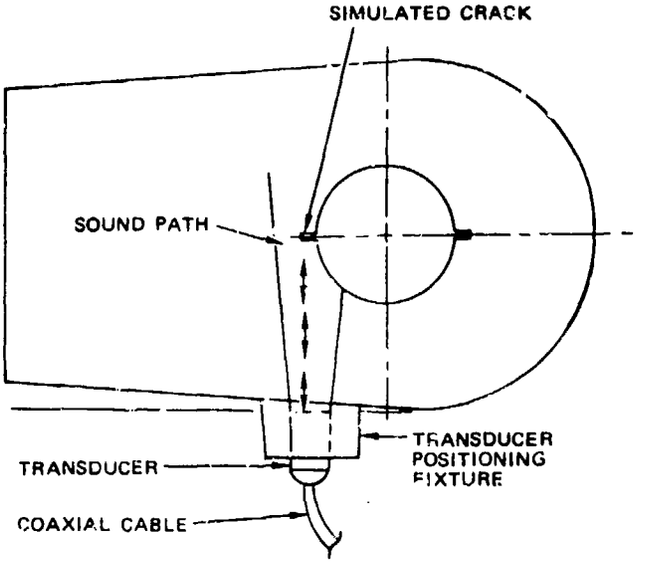

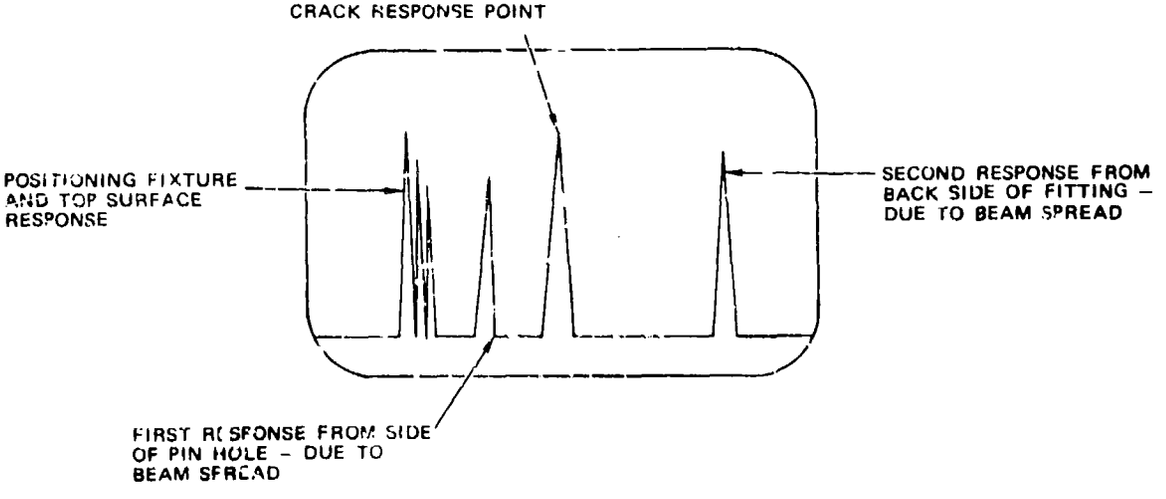

CALIBRATION OF EQUIPMENT
DETAIL IV

Horizontal Stabilizer Outboard Front Spar Terminal Fitting
Figure 1 (Sheet 6)

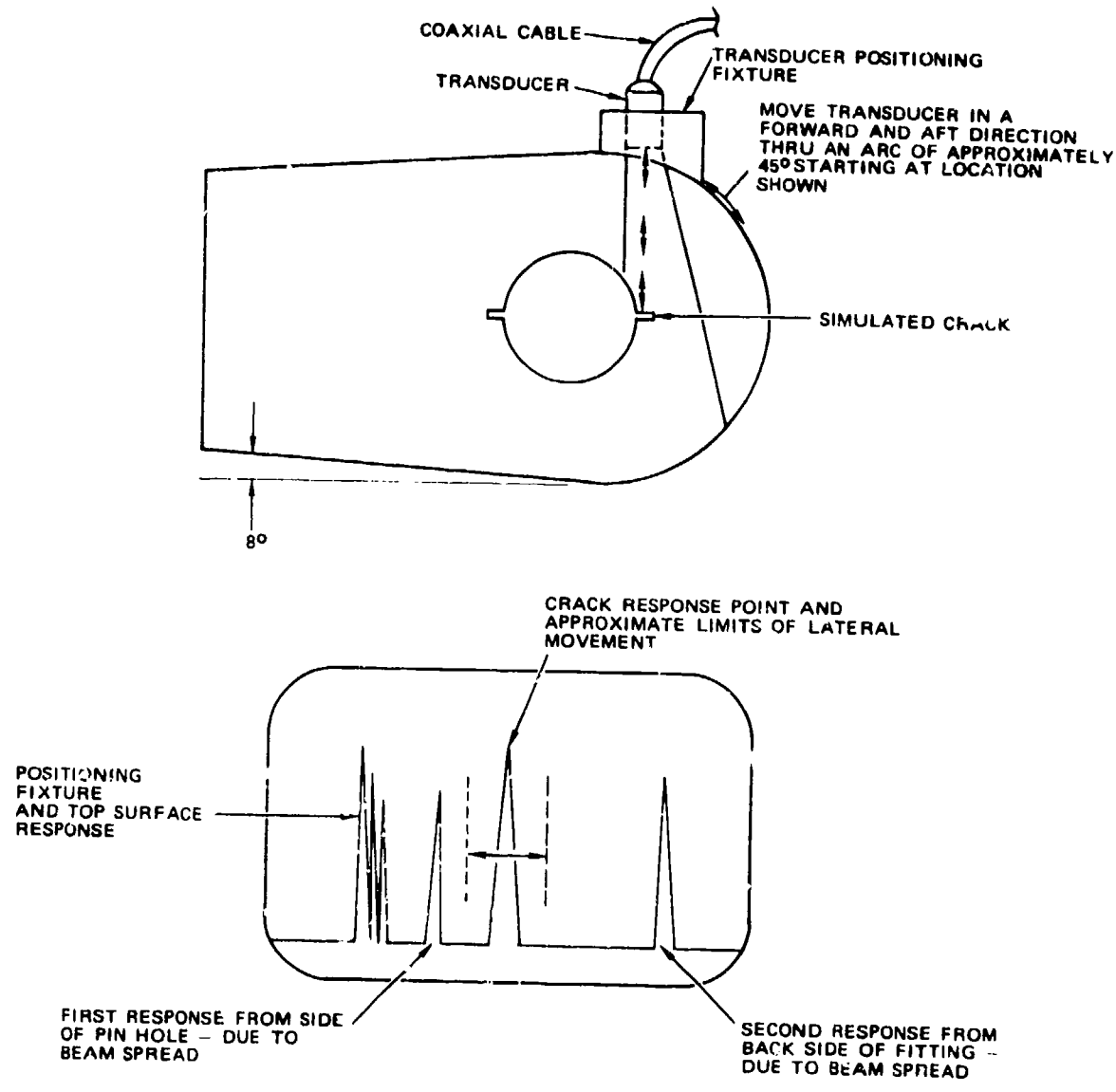

CALIBRATION OF EQUIPMENT
DETAIL IV (CONTINUED)

Horizontal Stabilizer Outboard Front Spar Terminal Fitting
Figure 1 (Sheet 7)

EFFECTIVITY
MODEL: ALL

PART 6 - EDDY CURRENT

STRUCTURES - GENERAL

1. General

A. The technique for inspecting fastener holes in aluminum parts was developed from data derived with Boeing-built probes and equipment specified in following procedure.

2. Equipment

A. Instrument Set - Any eddy-current unit designed for crack detection which is comparable to those listed below.

(1) Magnaflux, Magnatest ED-500, ED-510, ED-520

(2) Uresco FC-2001

(3) Foerster, Defectometer 2.154

B. Probes - Probes used in this procedure should have the following characteristics:

(1) Diameter should be adjustable to obtain a snug fit in the hole.

(2) Probe should be adjustable to permit depth penetration into hole to be adjusted.

(3) Movement of the coil area perpendicular to the axis of the hole from its set depth must be minimal in order to reduce edge effect interference. Axial probe movement should not produce edge effect interference greater than 20 percent of the meter response from the calibrating crack in the test block.

(4) Probe should not give interfering responses from normal handling pressures or manipulation, or from normal operating pressure variations on the sensing coil.

Hole Diameter	Probe Diameter
3/16	0.1875 inch
1/4	0.2500 inch
5/16	0.3125 inch
3/8	0.3750 inch
7/16	0.4375 inch
1/2	0.5000 inch

Fastener Holes in Aluminum Parts
Figure 1 (Sheet 1)

C. Test Blocks - Test blocks with suitable natural cracks or artificial notches to simulate cracks in each of the hole sizes being tested. A Standard test block should meet the following requirements:

(1) Block should be of aluminum alloy similar to the material being tested. Aluminum having conductivity within 5 percent of that of the part being tested is satisfactory.

(2) Block should contain a suitable range of hole diameters to permit calibration of instrument for diameter of each hole to be tested.

(3) The crack or notch in the block must give an eddy-current instrument calibration comparable to that obtained from the recommended Boeing test block. Recommended test blocks with applicable diameters are as follows:

Hole Diameter	Probe Diameter
3/16	0.1875 inch
1/4	0.2500 inch
5/16	0.3125 inch
3/8	0.3750 inch
7/16	0.4375 inch
1/2	0.5000 inch

NOTE: See detail I for details of calibration test blocks.

3. Preparation for Inspection

A. Clean loose dirt and paint from inside and around fastener hole.

B. Remove buildup of paint, sealant, etc., from around outside of hole where probe will bear.

NOTE: If surface of hole is extremely rough, a 1/64-inch cleanup ream may be necessary.

4. Instrument Calibration

A. Attach appropriate probe to instrument.

B. Turn instrument on and allow to warm up per manufacturer's instructions.

C. Select appropriate test block and place probe in hole. Probe should fit snugly but not so tight as to cause excessive wear of probe. Expand loose probe to obtain snug fit.

Fastener Holes in Aluminum Parts
Figure 1 (Sheet 2)

D. Adjust instrument for lift-off.

(1) Place sensitive (coil) part of probe on a flat surface of material to be inspected. Because of edge effect interference, place coil at least 1/4 inch away from edge of part.

(2) Manipulate probe to obtain maximum eddy-current effect.

(3) Place a single sheet of ordinary writing paper (approximate thickness 0.003 inch) between probe and material.

(4) Remove paper and note direction and amount of deflection of needle.

(5) Adjust lift-off control to obtain minimum needle movement when shim is removed. When no needle movement is noted, instrument and probe have been calibrated.

E. Insert probe in hole in test block, and adjust depth in hole to obtain maximum needle deflection on meter from edge crack (center of coil approximately 0.025 inch deep for 0.030-inch edge crack).

F. Adjust sensitivity to obtain a minimum of 10% full scale meter deflection from standard crack. Instrument is now calibrated for detection of edge cracks in hole to be inspected.

G. Insert probe in test block, and adjust depth in hole to obtain maximum needle deflection from crack located between ends of hole in test block. Tighten setscrew on collar of probe.

H. Repeat step F. Instrument is now calibrated for detection of cracks between ends of hole.

5. Test Procedure

A. Adjust collar on probe to set depth of penetration into hole at 0.250 inch from top end of hole.

B. Tighten collar on probe and insert probe into hole. Adjust balance control to bring needle approximately to midscale.

C. Slowly scan entire circumference of hole. Note position of any needle deflection of 10% of full scale or greater, giving a positive crack response.

NOTE: A positive crack response is characterized by rapid deflection of the meter needle over a short scan distance. Deflection occurs as the coil moves over the crack. This movement is equivalent to an arc of approximately 40 degrees in a 1/4-inch fastener hole, and 20 degrees in a 1/2-inch hole.

Fastener Holes in Aluminum Parts
Figure 1 (Sheet 2)

D. Note locations of any questionable indications, i.e., crack-like indications causing needle deflection of less than 10% of full scale, or indications not conforming to a positive crack indication. Perform a 1/64-inch cleanup ream and repeat test, paying particular attention to areas where indication was noted. Note location and response of all positive crack indications.

E. Repeat steps B through D at incremental depths of 0.050 inch and 0.025 inch from bottom end of hole. Calibrate instrument as directed in calibration procedure for each step.

F. When hole is reamed to clean up or remove cracks, perform eddy-current test after each increase in hole diameter.

G. Recheck calibration of instrument with test block periodically to ensure proper sensitivity of instrument.

H. Repeat procedure for each hole in area to be inspected.

Fastener Holes in Aluminum Parts
Figure 1 (Sheet 4)

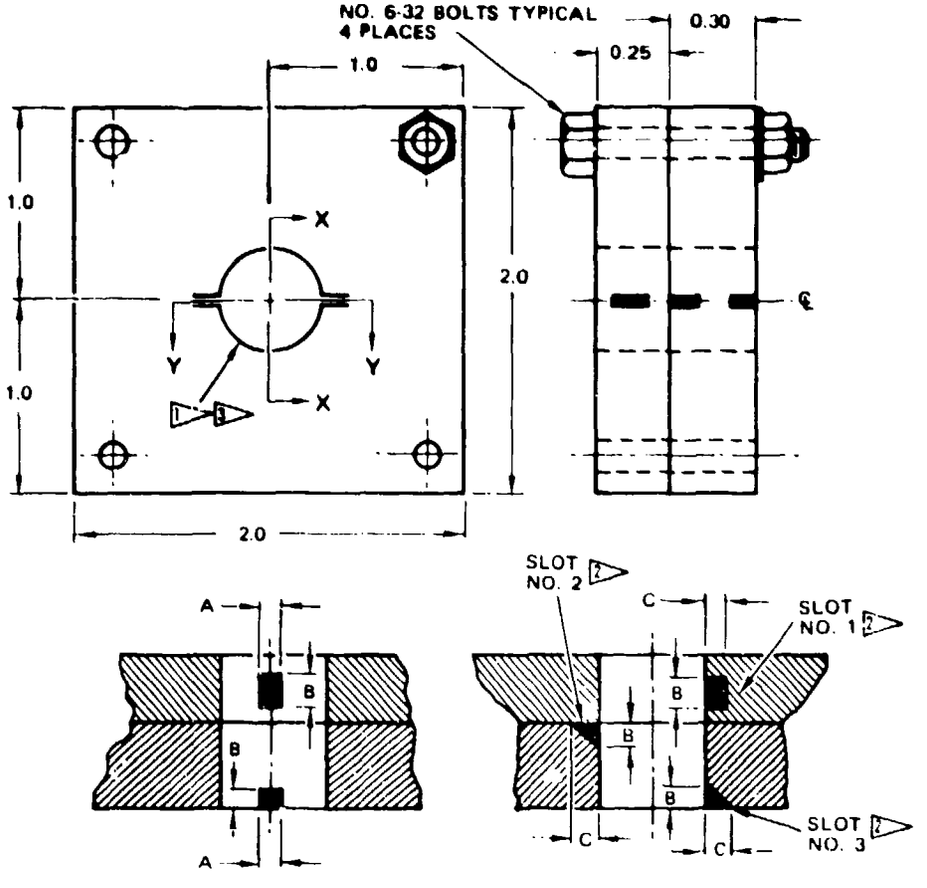

SECTION X X

SECTION Y Y

NOTES:

TOLERANCE ON ALL DIMENSIONS ±0.050 INCH EXCEPT AS NOTED

ALL DIMENSIONS IN INCHES

SLOT NUMBER	A WIDTH	B LENGTH	C DEPTH
1	0.005	0.060	0.030
2	0.005	0.030	0.030
3	0.005	0.030	0.030
TOLERANCE	+0.000 -0.001	± 0.001	± 0.001

1. FINISH REAM HOLE AND DO NOT DEBURR
2. ELECTRIC DISCHARGE MACHINE PER GIVEN DIMENSIONS
3. HOLE DIAMETER (6 STANDARD)
   0.1875 0.2500 0.3125
   0.3750 0.4375 0.5000
   TOLERANCE +0.005 −0.000 ON ALL HOLES

CALIBRATION TEST BLOCK DATA
DETAIL I

Fastener Holes in Aluminum Parts
Figure 1 (Sheet 5)

PART 6 - EDDY CURRENT

STRUCTURES - GENERAL

1. General

A. The technique for inspecting bolt holes in steel parts was developed from data derived by experiment with Boeing-built probes and equipment specified in following procedure.

2. Equipment

A. Instrument Set - Magnaflux ED-510 or ED-511

B. Hole Probes - Probes to suit diameter of holes

Hole Diameter	Probe Diameter
3/16 inch	0.1875 inch
1/4 inch	0.2500 inch
5/16 inch	0.3125 inch
3/8 inch	0.3750 inch
7/16 inch	0.4375 inch
1/2 inch	0.5000 inch

C. Test Blocks - Use test block to establish sensitivity of system for each size hole. Fabricate blocks of low carbon steel (4130, 4140, or 4340) to dimensions shown in detail 1.

3. Preparation for Inspection

A. Clean loose dirt and paint from inside and around fastener hole.

B. Remove buildup of paint, sealant, etc., from around fastener hole where probe will bear.

NOTE: If surface of hole is extremely rough, a 1/4-inch sleeve, reamed may be necessary.

4. Instrument Calibration

A. Turn instrument on and allow to warm up 5 minutes.

B. Select proper probe to be used.

C. Adjust instrument controls.

(1) Set frequency selector at (9).

(2) Adjust liftoff control to about midrange.

(3) Adjust sensitivity to maximum.

(4) Adjust instrument for liftoff.

(a) Place sensitive (coil) part of probe on a flat surface of material to be inspected. Because of edge effect interference, place coil at least 1/4 inch away from edge of part.

(b) Manipulate probe to obtain maximum eddy-current effect.

(c) Place a single sheet of ordinary writing paper (approximate thickness 0.003 inch) between probe and material.

(d) Remove paper and note direction and amount of deflection of needle.

(e) Adjust liftoff control to obtain minimum needle movement when shim is removed. When no needle movement is noted, instrument and probe have been calibrated.

D. Place probe in proper hole in test block.

NOTE: Probe should fit snugly in hole of test block as well as in holes of part to be tested. A folded paper shim may be inserted into slot of the probe to expand probe and make a snug fit.

E. Adjust penetration depth of probe so that center of coil crosses middle of notch in test block. Tighten setscrew on collar of probe.

F. Bring needle to center of scale by means of balance control.

G. Rotate probe slowly in test hole. Note meter deflection as probe crosses notch. Deflection should be 150 microamperes (MA) or greater, reduce sensitivity to obtain approximately a 150-MA deflection from the center-scale position. Instrument and probe are now calibrated for inspection.

NOTE: Unsatisfactory steel, fastener hole probes - Occasionally, a probe may be selected which is extremely sensitive to the notch in the test block. This probe may cause a deflection of 400 MA or more. Minimum instrument sensitivity adjustment may not reduce this deflection to the specified 150 MA. This probe must be discarded; it is too sensitive to be used for inspection of steel holes.

Fastener Holes in Steel Parts
Figure 2 (Sheet 2)

5. Test Procedure

A. Adjust collar on probe to set depth of penetration of probe into hole at 0.05 inch. Slowly scan the complete circumference of the hole first at a depth of 0.05 inch from top of hole; then readjust collar and scan at incremental depths of 0.050 inch, measured along axis of hole, and 0.050 inch from bottom of hole.

B. Note position of each indication giving positive response of approximately 1/2 inch deflection or greater.

NOTE: A positive response is characterized by the rapid deflection (swing) of the meter needle over a short travel distance. The deflection occurs as the probe coil travels over the crack, a distance of approximately 1/4 inch. In fastener hole inspection, this movement is equivalent to an arc of approximately 45 degrees for a 1/4-inch fastener hole and 90 degrees for a 1/2-inch fastener hole.

C. Note location of questionable indications, i.e., "shoulder" indications, or indications not conforming exactly to a positive crack indication. Perform a cleanup ream of hole and repeat eddy current test, paying particular attention to area where crack indication was noted. Perform a cleanup ream of hole if an irregular response is obtained which interferes with a proper eddy current hole inspection. Note location and response of all positive eddy current indications.

D. After reaming hole to remove crack, perform eddy current check after each increase in hole diameter.

E. Recheck test block periodically to ensure proper instrument sensitivity.

F. Repeat procedure for each hole in fastener area.

Fastener Holes in Steel Parts
Figure 2 (Sheet 3)

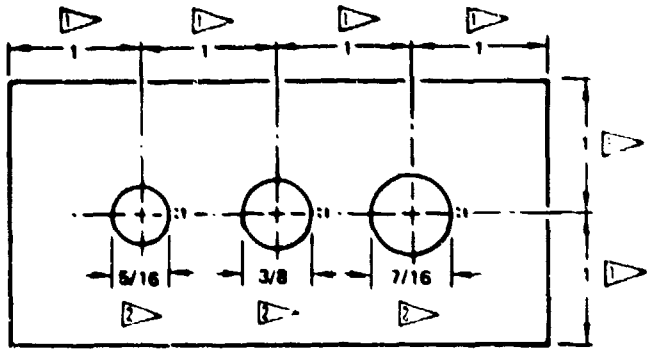

PLAN VIEW

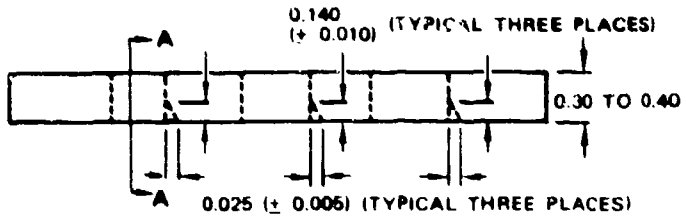

TOLERANCE ON ALL DIMENSIONS ± 0.050

REAM HOLES FOR SMOOTH FINISH

NOTE ALL DIMENSIONS IN INCHES

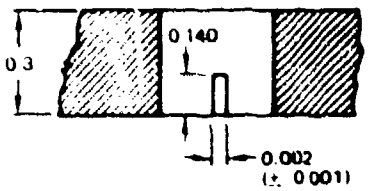

SECTION A–A
(TYPICAL)

CALIBRATION TEST BLOCK DATA

DETAIL 1

Fastener Holes in Steel Parts
Figure 2 (Sheet 4)

EFFECTIVITY
MODEL: ALL

PART 6 - EDDY CURRENT

STRUCTURES - GENERAL

1. General

A. When aluminum alloys are subjected to high temperatures, hardness of the metal decreases and conductivity values increase. The extent of damage to a structural area can be determined accurately by using an eddy current instrument to measure conductivity of the material.

B. Aluminum structure can withstand moderate heat (up to 500°F) for short periods of time without significant loss of strength. Structure that exhibits an increase of conductivity without discoloration of the green or yellow primer (excluding surface smut) may be considered as meeting the design minimum properties providing the conductivity does not exceed the following limits. Values are for bare material. Clad material will have higher readings dependent upon thickness of the surface coating.

Alloy and Condition	%IACS (International Annealed Copper Standard)
2024-T3, T4	33.5%
7079-T6, T611	34.0%
7075-T6	35.0%
7075-T73	42.0%
7178-T6	34.0%
201-T6	40.0%

NOTE: The above limits are applicable only to structure that does not exhibit primer discoloration.

C. Structure exhibiting primer discoloration must be considered as having been exposed to temperatures in excess of [illegible]°. Conductivity readings are not recommended for predicting strength [illegible] an conductivity change above or below the [illegible] considered suspect.

2. Equipment

A. Instrument - Magnatest FM-[illegible], FM-[illegible], or FM-[illegible], [illegible]. The FM-[illegible] is portable; therefore, it is most practical [illegible] structures because of accessibility problems.

B. Probe - Flat, surface type

Investigation of Fire Damage on Aircraft Structure
Figure 3 (Sheet 1)

3. Preparation for Testing

A. Thoroughly clean area to be inspected to ensure good contact between probe and surface.

4. Instrument Calibration

A. Attach probe to instrument.

B. Turn instrument on and allow to warm up according to manufacturer's instructions.

C. Adjust instrument for lift-off according to manufacturer's instructions.

5. Inspection Procedure

A. If area to be inspected is large, a grid system may be used to ensure complete coverage of the area. It is suggested that the area be laid out in a manner which will allow rechecking of test results.

B. Identify material to be tested. Refer to the appropriate Structural Repair Manual.

C. Make test readings on unaffected material to obtain comparative data.

NOTE: If different types of material are used in inspection area, make sample readings from each type. Take sample readings on unaffected portion of structure periodically during test to ensure proper calibration of the instrument.

D. Having established the normal readings to be expected from the unaffected structure, make inspection readings from the suspected area, starting on what appears to be satisfactory material, and working toward the center of the suspected area. Any rapid change in readings from those obtained on the unaffected material is reason to believe that the material under probe has been affected by heat.

NOTE: It is possible for the meter needle to deflect rapidly to either side of the scale when damaged material is encountered. This deflection is caused by a rapid change in the material conductivity.

E. By working the probe back and forth over the area, it is normally possible to determine a definite demarcation line between affected and unaffected material. This should be drawn on the airframe and rechecked in order to verify that all of the affected material has been detected.

6. Conversion Factors

A. To convert N% IACS to conductivity units in meters/ohm-mm squared, perform the following operation:

(1) N X 0.58 = Conductivity unit in meters/ohm-mm squared

(a) Example: Given 31% IACS

N = 31
31 X 0.58 = 17.98 meters/ohm-mm squared

B. To convert conductivity units in meters/ohm-mm squared to % IACS, perform the following operation:

(1) $\frac{\text{meters/ohm-mm squared}}{0.58}$ = % IACS

(a) Example: Given 17.98 meters/ohm-mm squared

$\frac{17.98}{0.58}$ = 31% IACS

C. To convert N% IACS to resistivity units in micro ohm-cm, perform the following operation:

(1) $\frac{1}{N}$ X 172.41 = Resistivity units in micro ohm-cm

(a) Example: Given 100% IACS

N = 100

$\frac{1}{100}$ X 172.41 = 1.7241 micro ohm-cm

D. To convert resistivity units in micro ohm-cm to % IACS, perform the following operation:

(1) $\frac{172.41}{\text{micro ohm-cm}}$ = % IACS

(a) Example: Given 1.7241 micro ohm-cm

$\frac{172.41}{1.7241}$ = 100% IACS

REPORT DOCUMENTATION PAGE

1. Recipient's Reference	2. Originator's Reference	3. Further Reference	4. Security Classification of Document
	AGARD-AG-201		UNCLASSIFIED

5. Originator Advisory Group for Aerospace Research and Development
North Atlantic Treaty Organization
7 rue Ancelle, 92200 Neuilly sur Seine, France.

6. Title Non-Destructive Inspection Practices

7. Presented at

8. Author(s) Editor Enrico Bolis

9. Date October 1975

10. Author's Address

11. Pages 678 in two volumes

12. Distribution Statement This document is distributed in accordance with AGARD policies and regulations, which are outlined on the Outside Back Covers of all AGARD publications.

13. Keywords/Descriptors

Nondestructive tests
Maintenance
Inspection
Aircraft
Design criteria
Aviation safety

14. UDC 620.179.1:629.73.083.02

15. Abstract

Comprises 21 chapters, written by international specialists, on the various methods and aspects of Non-Destructive Inspection (NDI). The importance of NDI is stressed in improving reliability and maintenance and in its contributions to the economy of aircraft operations and to design philosophy and safety. The aim was to provide common ground for designer and maintenance engineer by

(i) presenting a comprehensive collection of current knowledge on NDI practices for all engineers and management concerned with aircraft maintenance and inspection, with emphasis both on the capacity and limitations of the various methods and on major problems describing the relevance of flaws to aircraft safety.

(ii) informing the designer about the capabilities of NDI, explaining the procedures which are used to meet his requirements for quality of the structure during fabrication and the means which exist for detection of flaws and cracks in service, how exact and reliable they are and to what extent he can base his design assumptions on them.

This AGARDograph is published in two volumes and sponsored by the Structures and Materials Panel of AGARD.